



universität
wien

DISSERTATION

Titel der Dissertation

„Phytochemical Investigation and Bioactivity-guided
Isolation of Cytotoxic Compounds
from *Metaxya rostrata*“

Verfasserin

Mag.rer.nat Kerstin Kainz

angestrebter akademischer Grad

Doktorin der Naturwissenschaften (Dr.rer.nat.)

Wien, 2011

Studienkennzahl lt. Studienblatt: A 091 474

Dissertationsgebiet lt. Studienblatt: Ernährungswissenschaften

Betreuerin: ao. Univ. Prof. Mag. Dr. Liselotte Krenn

Acknowledgements

I would like to thank all the people who contributed to the success of my thesis:

I would like to thank Prof. Verena Dirsch for giving me the opportunity to perform my research at the Department of Pharmacognosy.

With sincere gratitude I would like to acknowledge my supervisor Prof. Liselotte Krenn for her help and patience, for her scientific feedback and support and for the great team.

I am deeply thankful to my co-supervisor Prof. Brigitte Marian for passing on valuable knowledge, for her excellent assistance, for encouraging and motivating me and for the best atmosphere in the lab.

My appreciation goes to Dr. Hanspeter Kählig for performing the NMR experiments and to Dr. Martin Zehl and Mag. Oliver Donath for the MS analysis. I am grateful to Mag. Johann Schinnerl for his assistance in performing the anti-fungal and insecticidal assays and to Prof. Simon Gibbons and his group for the anti-bacterial tests. I would like to thank Prof. Andreas Hensel and his group for performing the anti-viral assay and Dr. Werner Huber for collecting the plant material. Furthermore, I am grateful to Dr. Daniela Schuster for performing the *in silico* screening and to Dr. Irene Herbacek for FACS analysis.

I also would like to acknowledge the students Johanna Bleier, Natalie Schmidt, Barbara Merkingner and Teresa Pemmer, I had the pleasure to work with.

Many thanks to my colleagues at the Department of Pharmacognosy, especially to Judith Singhuber, Sylvia Vogl, Paolo Picker, Oliver Donath and Hamid Adhami for a great working atmosphere, their friendship and lots of funny hours during and after work.

I am very thankful to my colleagues at the Institute for Cancer Research, especially to Christine Heinzle and Xenia Hudec for creating a fantastic working (and after-working) atmosphere. I was very lucky having two such great labs to work at.

Finally, I am deeply thankful to my family and friends for their love and support, who have always been there for me during this time.

Table of Content

1	INTRODUCTION	1
1.1	EPIDEMIOLOGY OF CANCER	1
1.2	EPIDEMIOLOGY OF COLORECTAL CANCER.....	3
1.3	DEVELOPMENT OF CANCER – CARCINOGENESIS	5
1.4	HALLMARKS OF CANCER.....	8
1.4.1	<i>Sustained proliferative signaling</i>	<i>8</i>
1.4.2	<i>Evading growth suppressors.....</i>	<i>8</i>
1.4.3	<i>Resisting cell death</i>	<i>9</i>
1.4.4	<i>Inducing angiogenesis</i>	<i>9</i>
1.4.5	<i>Enabling replicative immortality.....</i>	<i>9</i>
1.4.6	<i>Activating invasion and metastasis</i>	<i>10</i>
1.4.7	<i>Enabling characteristics and emerging hallmarks of cancer</i>	<i>10</i>
1.5	CARCINOGENESIS OF COLORECTAL CANCER	11
1.5.1	<i>Anatomy of the colon</i>	<i>11</i>
1.5.2	<i>Histopathology of the colon.....</i>	<i>12</i>
1.5.3	<i>Development of colorectal cancer</i>	<i>12</i>
1.5.3.1	Hereditary colorectal cancer	13
1.5.3.1.1	Hereditary non polyposis colorectal cancer (HNPCC)	14
1.5.3.1.2	Familial adenomatous polyposis (FAP)	14
1.5.3.1.3	MYH associated polyposis (MAP).....	14
1.5.3.1.4	Hamartomatous polyposis syndromes	15
1.5.3.2	Inflammation and colorectal cancer.....	15
1.5.3.2.1	Morbus Crohn	15
1.5.3.2.2	Ulcerative colitis.....	15
1.5.3.3	Nutrition and colorectal cancer.....	15
1.5.4	<i>Staging of Colorectal Cancer.....</i>	<i>17</i>
1.5.5	<i>Genetic alterations in colorectal cancer</i>	<i>18</i>
1.5.5.1	Adenomatous polyposis coli (APC) gene	19
1.5.5.2	Kirsten – Ras (K-Ras) gene	20
1.5.5.3	p53 gene.....	21
1.5.5.4	Deleted in colorectal cancer (DCC) gene	22
1.5.5.5	Transforming growth factor beta (TGF- β)	22
1.6	THE CELL CYCLE	22
1.6.1	<i>Cell cycle regulation</i>	<i>23</i>
1.6.2	<i>Cell cycle and cancer.....</i>	<i>25</i>

Table of Content

1.7	CELL DEATH	26
1.7.1	<i>Apoptosis</i>	27
1.7.2	<i>Mitotic catastrophe</i>	29
1.8	TRADITIONAL MEDICINE	30
1.9	NATURAL PRODUCTS AS SOURCES OF NEW DRUGS	31
1.9.1	<i>Natural products as sources of new anti-cancer therapeutics</i>	32
1.9.1.1	Alkaloids	33
1.9.1.2	Lignans.....	34
1.9.1.3	Flavonoids	34
1.9.1.4	Xanthones.....	35
2	AIMS OF THE THESIS	37
3	MATERIALS AND METHODS	39
3.1	PHYTOCHEMISTRY	39
3.1.1	<i>Plant Material</i>	39
3.1.2	<i>Extraction and Fractionation</i>	40
3.1.3	<i>Chromatographic Methods</i>	41
3.1.3.1	Thin layer chromatography (TLC)	41
3.1.3.2	Column chromatography.....	42
3.1.3.3	HPLC	43
3.1.4	<i>Removal of chlorophyll</i>	44
3.1.5	<i>Solid phase extraction (SPE)</i>	44
3.1.6	<i>Spectroscopic and spectrometric methods</i>	45
3.1.6.1	Mass-spectrometry (MS)	45
3.1.6.2	Nuclear magnetic resonance (NMR).....	45
3.1.6.3	Infrared spectroscopy (IR)	45
3.1.6.4	UV / VIS Spectroscopy	46
3.1.7	<i>Crystallography</i>	46
3.1.8	<i>Histone deacetylase (HDAC) assay</i>	46
3.1.9	<i>Antibacterial assay</i>	46
3.1.10	<i>Antiviral assay</i>	47
3.1.11	<i>Insecticidal assay</i>	47
3.1.12	<i>Antifungal assay</i>	48
3.1.13	<i>In Silico screening</i>	48
3.1.14	<i>Chemicals and Solvents</i>	48
3.2	CELL BIOLOGY	49
3.2.1	<i>Cell lines</i>	49
3.2.1.1	SW480	49
3.2.1.2	HT29	49
3.2.1.3	Caco-2.....	49

Table of Content

3.2.1.4	LT97	50
3.2.1.5	F331.....	50
3.2.2	<i>Passaging of cells</i>	50
3.2.3	<i>Materials used for cell culture</i>	51
3.2.4	<i>Measurement of cell viability</i>	51
3.2.4.1	MTT assay – EZ4U.....	51
3.2.4.2	Neutralred uptake	51
3.2.5	<i>Fluorescence activated cell sorting (FACS)</i>	52
3.2.5.1	Cell cycle distribution	52
3.2.5.2	Quantification of apoptosis: JC-1-FACS	53
3.2.6	<i>Detection of apoptosis: Hoechst-Staining</i>	53
3.2.7	<i>Lactatdehydrogenase (LDH)-assay</i>	53
3.2.8	<i>FoxM1-staining</i>	54
3.3	PROTEIN CHEMISTRY	55
3.3.1	<i>Western blotting</i>	55
3.3.1.1	Protein isolation	55
3.3.1.2	Evaluation of protein concentration with Coomassie	56
3.3.1.3	SDS-polyacrylamid gel electrophoresis (PAGE)	56
3.3.1.4	Western blot	57
3.3.1.5	Ponceau S staining	57
3.3.1.6	Immunological detection of protein	58
3.4	STATISTICS	59
4	RESULTS	61
4.1	PHYTOCHEMICAL INVESTIGATIONS OF METAXYA ROSTRATA	61
4.1.1	<i>Isolation and structure elucidation of compound KK1</i>	62
4.1.2	<i>Isolation and structure elucidation of compound KK5</i>	66
4.1.3	<i>Isolation and structure elucidation of compound KK7</i>	68
4.1.4	<i>Isolation and structure elucidation of compound KK6</i>	69
4.1.5	<i>Isolation and structure elucidation of compound KK3</i>	71
4.1.6	<i>Isolation and identification of compound KK4</i>	73
4.1.7	<i>Overview over the isolation of the pure compounds from Metaxya rostrata</i>	74
4.1.8	<i>Biological Testing of Compound KK1</i>	75
4.1.8.1	Bioviability assay of compound KK1 and KK1 aglycon.....	75
4.1.8.2	HDAC assay of compound KK1	75
4.1.8.3	<i>In silico</i> screening of compound KK1	76
4.1.8.4	Antiviral activity of compound KK1	77
4.1.8.5	Insecticidal activity of compound KK1.....	77
4.1.8.6	Antifungal Activity of compound KK1.....	78
4.1.8.7	Antibacterial activity of compound KK1	80
4.1.8.8	Hydrolysis of compound KK1.....	80

Table of Content

4.2	BIOACTIVITY-GUIDED FRACTIONATION AND ISOLATION OF THE ACTIVE COMPOUNDS FROM <i>METAXYA ROSTRATA</i>	81
4.2.1	<i>Extraction of plant material with solvents of different polarity</i>	81
4.2.2	<i>Pretesting of the extracts</i>	83
4.2.2.1	Time-dependence of effects for selected fractions.....	85
4.2.3	<i>Extraction, fractionation and testing of the CH₂Cl₂-extract from the rootlets of Metaxya rostrata</i>	88
4.2.4	<i>Extraction, fractionation and testing of the EA extract from the rootlets of Metaxya rostrata</i>	89
4.2.5	<i>Extraction, fractionation and testing of the EA extract from the leaves of Metaxya rostrata</i>	92
4.2.6	<i>Extraction, fractionation and testing of the MeOH extract from the rhizomes of Metaxya rostrata</i>	95
4.2.7	<i>Bioassay of the most active CH₂Cl₂-fractions of CC-9</i>	98
4.2.8	<i>Isolation and structure elucidation of the active compounds of the most active CH₂Cl₂-fractions of the rootlets of Metaxya rostrata</i>	98
4.2.8.1	Reextraction and refractionation of the CH ₂ Cl ₂ -extract of the rootlets from Metaxya rostrata ...	99
4.2.8.2	Bioassay of the fractions from CC-13	101
4.2.8.3	Bioassay of selected fractions of CC-13.....	103
4.2.9	<i>Fractionation of the most active fractions from CC-9 and CC-13 by solid phase extraction</i>	104
4.2.9.1	Fractionation of fraction CC-13/5 by solid phase extraction (SPE-1).....	104
4.2.9.2	Fractionation of fraction CC-13/6 by solid phase extraction (SPE-2).....	106
4.2.9.3	Fractionation of fraction CC-13/7 by solid phase extraction (SPE-3).....	107
4.2.9.4	Fractionation of fraction CC-13/8 by solid phase extraction (SPE-4).....	109
4.2.9.5	Fractionation of fraction CC-13/14 by solid phase extraction (SPE-5).....	110
4.2.9.6	Fractionation of fraction CC-13/15 by solid phase extraction (SPE-6).....	111
4.2.9.7	Fractionation of fraction CC-9/3 by solid phase extraction (SPE-7).....	112
4.2.9.8	Fractionation of fraction CC-9/4 by solid phase extraction (SPE-8).....	114
4.2.9.9	TLC comparison of the active SPE fractions with methylated flavonoids	115
4.2.10	<i>Investigation of the selected SPE-fractions by high performance liquid chromatography</i>	116
4.2.10.1	Investigation of SPE-3/4 by HPLC	116
4.2.10.2	Investigation of SPE-3/3 by HPLC	118
4.2.10.3	Investigation of SPE-7/3 by HPLC	119
4.2.10.4	Investigation of SPE-8/4 by HPLC	120
4.2.10.5	Investigation of SPE-5/2 by HPLC	121
4.2.10.6	Investigation of SPE-6/2 by HPLC	122
4.2.11	<i>Isolation of 2-deprenyl-rheediaxanthone B by semipreparative HPLC</i>	124
4.2.12	<i>Biological effects of 2-deprenyl-rheediaxanthone B</i>	127
4.2.12.1	Effect of 2-deprenyl-rheediaxanthone B on cell viability	127
4.2.12.2	Effect of 2-deprenyl-rheediaxanthone B on the cell viability of different cell types	128
4.2.12.3	Effect of 2-deprenyl-rheediaxanthone B on the cell cycle.....	129
4.2.12.4	Expression of specific cell cycle signaling proteins	130

Table of Content

4.2.12.5	Microscopic analysis of SW480 cells treated with 2-deprenyl- rheediaxanthone B.....	130
4.2.12.6	Effect of 2-Deprenyl-rheediaxanthone B on apoptosis	131
4.2.12.7	Effect of 2-deprenyl-rheediaxanthone B on apoptosis related proteins.....	132
5	DISCUSSION	139
5.1	PHYTOCHEMICAL INVESTIGATIONS OF <i>METAXYA ROSTRATA</i>	139
5.2	BIOACTIVITY-GUIDED FRACTIONATION AND ISOLATION OF THE ACTIVE COMPOUNDS OF <i>METAXYA ROSTRATA</i>	142
5.3	EFFECT OF 2-DEPRENYL-RHEEDIAXANTHONE B ON CELL GROWTH.....	146
5.4	EFFECT OF 2-DEPRENYL-RHEEDIAXANTHONE B ON CELL CYCLE	146
5.5	EFFECT OF 2-DEPRENYL-RHEEDIAXANTHONE B ON APOPTOSIS.....	147
5.6	EFFECT OF 2-DEPRENYL-RHEEDIAXANTHONE B ON CHECKPOINT KINASES	150
6	CONCLUSION	153
7	SUMMARY	155
8	ZUSAMMENFASSUNG	157
9	BIBLIOGRAPHY.....	159
10	SUPPLEMENTARY INFORMATION	
11	CURRICULUM VITAE	

List of Tables

Table 1: Yields (in mg) of the extracts for pretesting	41
Table 2: Yields (in g) of selected extracts	41
Table 3: Stationary phases in thin layer chromatography.....	41
Table 4: Mobile phases in thin layer chromatography	42
Table 5: Detection reagents in thin layer chromatography.....	42
Table 6: Stationary phases in column chromatography	42
Table 7: Mobile phases in column chromatography	43
Table 8: Methods for HPLC	44
Table 9: Food for <i>Spodoptera littoralis</i>	48
Table 10: Passaging of cells	50
Table 11: Density of cells in different culture dishes.....	50
Table 12: Pipette schemata for the evaluation of protein concentration	56
Table 13: Schemata for sandwich preparation.....	57
Table 14: Primary antibodies	59
Table 15: Secondary antibodies.....	59
Table 16: Conditions for CC-1	62
Table 17: Conditions for CC-2	64
Table 18: Conditions for CC-3	68
Table 19: Conditions for CC-4	69
Table 20: Conditions for CC-5	71
Table 21: Conditions for CC-6	71
Table 22: Conditions for CC-7	73
Table 23: Conditions for CC-8	74
Table 24: Conditions and results of the insecticidal assay of compound KK1.....	77
Table 25: MICs of KK1 and norfloxacin against six strains of <i>Staphylococcus aureus</i>	80
Table 26: Yield (mg) of extracts from ASE	83
Table 27: Conditions for CC-9	88
Table 28: Conditions for CC-10	90
Table 29: Conditions for CC-11	94
Table 30: Conditions for CC-12	97
Table 31: Conditions for CC-13	101
Table 32: Yield (mg) of the most active fractions of CC-9 and CC-13	104
Table 33: Yield (mg) of the fractions of SPE-1	105

List of Tables

Table 34: Yield (mg) of the fractions of SPE-2.....	107
Table 35: Yield (mg) of the fractions of SPE-3.....	108
Table 36: Yield (mg) of the fractions of SPE-4.....	109
Table 37: Yield (mg) of the fractions of SPE-5.....	110
Table 38: Yield (mg) of the fractions of SPE-6.....	112
Table 39: Yield (mg) of the fractions of SPE-7.....	113
Table 40: Yield (mg) of the fractions of SPE-8.....	114

Table of Figures

Fig. 1: Incidence and mortality of the most common cancer types in women and men worldwide	2
Fig. 2: Cause of deaths in men and women in Austria, 2010	2
Fig. 3: Incidence and mortality of the most common cancer types in women and men in Austria	3
Fig. 4: Incidence and mortality of the colorectal cancer in women and men worldwide	4
Fig. 5: Incidence and mortality of colorectal cancer in men and women in Austria	5
Fig. 6: Carcinogenesis	5
Fig. 7: The interaction of initiation and promotion	7
Fig. 8: The multistage concept of carcinogenesis	7
Fig. 9: The hallmarks of cancer	8
Fig. 10: The emerging hallmarks of cancer	10
Fig. 11: Anatomy of the large intestine	11
Fig. 12: Depiction of colorectal stem cells and crypts	12
Fig. 13: Benign to malignant tumor progression	13
Fig. 14: Incidence of types of colorectal cancer	13
Fig. 15: Comparison of the colon of a FAP patient (1) and a healthy colon (2)	14
Fig. 16: The role of genes and environment in the development of cancer	16
Fig. 17: Dukes' classification (Astler-Coller modification)	17
Fig. 18: TNM classification of malignant tumors	18
Fig. 19: Comparison of the TNM classification with the Dukes' classification	18
Fig. 20: Genetic alterations during the colorectal cancer progression	19
Fig. 21: The biology of colonic crypts and APC/ β -catenin	20
Fig. 22: The regulation of Ras activity	21
Fig. 23: The transforming growth factor β (TGF- β) signalling pathway	22
Fig. 24: The cell cycle and cell cycle regulation	23
Fig. 25: Overview of some essential steps in cell cycle regulation	24
Fig. 26: Different types of cell death	26
Fig. 27: Comparison of apoptosis and necrosis	27
Fig. 28: The intrinsic and extrinsic pathway of apoptosis	28
Fig. 29: Summary of several pathways of cell death	30
Fig. 30: Drugs developed from natural sources	31
Fig. 31: All new chemical entities	32
Fig. 32: All available anti-cancer drugs from 1940-2006	32
Fig. 33: Plant derived anti-cancer agents	34
Fig. 34: Voucher specimen of the plant material	39
Fig. 35: Plant material	40

Table of Figures

Fig. 36: SW480	49
Fig. 37: HT29	49
Fig. 38: CaCo-2	49
Fig. 39: LT97	50
Fig. 40: F331	50
Fig. 41: Principle of the LDH-assay	54
Fig. 42: Extraction and fractionation scheme of the rhizomes of <i>Metaxya rostrata</i>	61
Fig. 43: TLC of the combined fractions of CC-1	62
Fig. 44: TLC of the combined fractions of CC-2	63
Fig. 45: Crystallization of compound KK1	63
Fig. 46: TLC of compound KK1 in 5 fractions	63
Fig. 47: TLC comparison of KK1 with different sugars	64
Fig. 48: Compound KK1 - (2E)-2-(6-hydroxyhexyliden)cyclopropyl- β -glucopyranoside	65
Fig. 49: ORTEP plot (ellipsoids 50% probability) of compound KK1	66
Fig. 50: Compound KK5 - (6E)-6-[2-(β -glucopyranosyloxy)cyclopropylidene]hexanoic acid	67
Fig. 51: TLC comparison of compound KK1 and KK5	67
Fig. 52: TLC of the combined fractions of CC-4	68
Fig. 53: Compound KK7 - methyl- α -fructofuranosid	69
Fig. 54: TLC of combined fractions of CC-5	70
Fig. 55: Compound KK6 - 4-O- β -D-glucopyranosyl-p-trans-coumaric acid	70
Fig. 56: TLC of the combined fractions of CC-6	71
Fig. 57: TLC of combined fractions of CC-7	72
Fig. 58: Crystallisation of KK3	72
Fig. 59: Compound KK3 - 4-O- β -D-glucopyranosyl-caffeic acid	72
Fig. 60: TLC of the combined fractions of CC-7	73
Fig. 61: TLC comparison KK4 with JV-1	73
Fig. 62: Compound KK4 - mixture of cinnamtannin B-1 and aesculitannin B	74
Fig. 63: Isolation scheme of the compounds from <i>Metaxya rostrata</i> isolated in this study	74
Fig. 64: Viability of SW480 treated with KK1	75
Fig. 65: HDAC inhibition by KK1	76
Fig. 66: Fitting of compound KK1 into the α -glucosidase inhibitor pharmacophore model	76
Fig. 67: Cell viability and antiviral activity of compound KK1	77
Fig. 68: Insecticidal activity of compound KK1	78
Fig. 69: Antifungal Activity of different compounds	79
Fig. 70: Application of the fungus in growth medium	79
Fig. 71: TLC of different fractions tested for antifungal activity	79
Fig. 72: Antifungal activity of different fractions	79
Fig. 73: Aglycon of KK1 - (2E)-2-(hydroxyhexyliden)cyclopropanol	80

Table of Figures

Fig. 74: TLC of the CH ₂ Cl ₂ -extracts.....	81
Fig. 75: TLC of the EA-extracts.....	82
Fig. 76: TLC of the MeOH-extracts	82
Fig. 77: Viability of SW480 cells treated with the CH ₂ Cl ₂ -extracts	83
Fig. 78: Viability of SW480 cells treated with the EA-extracts	84
Fig. 79: Viability of SW480 cells treated with the MeOH-extracts	85
Fig. 80: Viability of SW480 cells (1) and LDH assay (2) after 24h	86
Fig. 81: Viability of SW480 cells (1) and LDH assay (2) after 48h	86
Fig. 82: Viability of SW480 cells (1) and LDH assay (2) after 72h	87
Fig. 83: TLC of the combined fractions of CC-9	88
Fig. 84: Viability of SW480 cells treated with the fractions of CC-9	89
Fig. 85: TLC -1 of the combined fractions of CC-10	89
Fig. 86: TLC-2 of the combined fractions of CC-10	90
Fig. 87: Viability of SW480 cells treated with the fractions of CC-10.....	91
Fig. 88: Viability of SW480 cells treated with the fractions of CC-10.....	91
Fig. 89: Viability of SW480 cells treated with the selected fractions of CC-10	92
Fig. 90: TLC of the fractions after removal of chlorophyll	93
Fig. 91: TLC of the combined fractions of CC-11	93
Fig. 92: Viability of SW480 cells treated with the selected fractions of CC-11	94
Fig. 93: Scheme of detannification of the MeOH-extract of the rhizomes of <i>Metaxya rostrata</i>	95
Fig. 94: TLCs of detannification of the MeOH-extract of the rhizomes from <i>Metaxya rostrata</i>	95
Fig. 95: TLC of the combined fractions of CC-12	96
Fig. 96: TLC of the combined fractions of CC-12	96
Fig. 97: Viability of SW480 cells treated with the fractions of CC-12.....	97
Fig. 98: Bioviability assay of selected fractions of the CH ₂ Cl ₂ -extract of the rootlets of <i>Metaxya rostrata</i>	98
Fig. 99: TLC of the most active fractions of the CH ₂ Cl ₂ -extract of the rootlets from <i>Metaxya rostrata</i>	99
Fig. 100: TLC comparison of the two CH ₂ Cl ₂ -extracts of the rootlets.....	100
Fig. 101: TLC of the combined fractions 1-7 of CC-13	100
Fig. 102: TLC of the combined fractions 8 to 16 of CC-13	101
Fig. 103: Viability of SW480 cells after treatment with fractions 1-7 of CC-13.....	102
Fig. 104: Viability of SW480 cells after treatment with fractions 8-16 of CC-13.....	102
Fig. 105: Viability of SW480 cells after treatment with the selected fractions of CC-13	103
Fig. 106: TLC comparison of CC-9 and CC-13.....	103
Fig. 107: TLC comparison of the active fractions of CC-13 with methylated flavonoids.....	104
Fig. 108: TLC of the fractions of SPE-1.....	105
Fig. 109: Viability of SW480 cells treated with the fractions of SPE-1	106
Fig. 110: TLC of the fractions of SPE-2.....	106
Fig. 111: Viability of SW480 cells treated with the fractions of SPE-2	107

Table of Figures

Fig. 112: TLC of the fractions of SPE-3	108
Fig. 113: Viability of SW480 cells treated with the fractions of SPE-3	108
Fig. 114: TLC of the fractions of SPE-4	109
Fig. 115: Viability of SW480 cells treated with the fractions of SPE-4	110
Fig. 116: TLC of the fractions of SPE-5	110
Fig. 117: Viability of SW480 cells treated with the fractions of SPE-5	111
Fig. 118: TLC of the fractions of SPE-6	111
Fig. 119: Viability of SW480 cells treated with the fractions of SPE-6	112
Fig. 120: TLC of the fractions of SPE-7	113
Fig. 121: Viability of SW480 cells treated with fractions of SPE-7	113
Fig. 122: TLC of the fractions of SPE-8	114
Fig. 123: Viability of SW480 cells treated with the fractions of SPE-8	115
Fig. 124: TLC comparison of the active SPE fractions with methylated flavonoids	115
Fig. 125: HPLC analysis (1) of fraction SPE-3/4	116
Fig. 126: HPLC analysis (2) of fraction SPE-3/4	117
Fig. 127: TLC comparison of SPE-3/4 with ursolic and betulinic acid.....	117
Fig. 128: Betulinic acid	117
Fig. 129: HPLC analysis (1) of fraction SPE-3/3	118
Fig. 130: HPLC analysis (2) of fraction SPE-3/3	118
Fig. 131: HPLC analysis (1) of fraction SPE-7/3	119
Fig. 132: HPLC analysis (2) of fraction SPE-7/3	120
Fig. 133: HPLC analysis (1) of fraction SPE-8/4.....	120
Fig. 134: HPLC analysis (2) of fraction SPE-8/4	121
Fig. 135: HPLC analysis (1) of fraction SPE-5/2	121
Fig. 136: HPLC analysis (2) of fraction SPE-5/2	122
Fig. 137: 2-deprenyl-rheediaxanthone B	122
Fig. 138: HPLC analysis (1) of fraction SPE-6/2	123
Fig. 139: HPLC analysis (2) of fraction SPE-6/2	123
Fig. 140: TLC comparison of fraction CC-9/5 and CC-13/14.....	124
Fig. 141: Semipreparative HPLC of fraction CC-9/5	125
Fig. 142: HPLC analysis of fraction 4	125
Fig. 143: HPLC analysis of fraction 4	126
Fig. 144: Viability of SW480 (1) and LDH assay (2) of 2-deprenyl-rheediaxanthone B after 24, 48 and 72h.	127
Fig. 145: Viability of SW480, CaCo-2, LT97 and F331 after treatment with 2-deprenyl-rheediaxanthone B	128
Fig. 146: Effect of XB on cell cycle distribution of SW480 after 48h (1) and 72h (2)	129
Fig. 147: Influence of XB on cell cycle signaling proteins.....	130
Fig. 148: Light microscopy analysis of control (1) and XB treated cells (2)	130
Fig. 149: Fluorescence microscopy analysis of control (1) and XB treated cells (2)	131

Table of Figures

Fig. 150: JC-1 FACS analysis after treatment with XB after 48h (1) and 72h (2)	132
Fig. 151: Influence of XB on apoptosis signaling proteins I	133
Fig. 152: Influence of XB on apoptosis signaling proteins II	133
Fig. 153: Influence of XB on PARP	134
Fig. 154: Influence of XB on Caspase 2	134
Fig. 155: Influence of XB on DNA-damage markers	135
Fig. 156: Influence of XB on FoxM1	135
Fig. 157: Fluorescence microscopy analysis of control (1) and XB treated cells (3) with Höchst staining and analysis of control (2) and XB treated cells (4) with FoxM1 staining	136
Fig. 158: Influence of XB on ATR and ATM	137
Fig. 159: Influence of XB on phospho Histone H3 (Ser ¹⁰)	137

List of Abbreviations

A. bidest	water two times distilled
ACS	American Cancer Society
AJCC	American Joint Committee of Cancer
ATCC	American Type Culture Collection
ATM	Ataxia telangiectasia mutated
ATR	ATM and Rad3-related
APC	Adenomatous Polyposis Coli
APS	Ammoniumperoxodisulfat
ASE	Accelerated Solvent Extraction
BAX	BCL 2-Associated X Protein
BSA	Bovine Serum Albumin
CC	Column Chromatography
CDK	Cyclin dependent kinase
CH ₂ Cl ₂	dichloromethane
CHK	Checkpoint kinase
cm	centimeter
COSY	correlation spectroscopy
DCC	Deleted in Colorectal Cancer
DNA	Desoxyribonucleic Acid
EA	Ethylacetate
EDTA	Ethylenediaminetetraacetic Acid
EtOH	Ethanol
FACS	Fluorescence Activated Cell Sorting
FAP	Familiar Adenomatous Polyposis
FCS	Fetal Calf Serum
FIA	Flow Injection Analysis
XIV	

List of Abbreviations

FOXM1	forkhead transcription factor M1
g	gram
h	hour
HDAC	Histone deacetylase
HMBC	Heteronuclear Multiple Bond Correlation
HMQC	Heteronuclear single-quantum correlation spectroscopy
HNPCC	Hereditary Non Polyposis Colorectal Cancer
HPLC	High performance liquid chromatography
HSV-1	Herpes Simplex 1 virus
IL	Interleukin
IR	Infrared spectroscopy
kDa	kilo Dalton
K-Ras	Kirsten-Ras
LDH	Lactate dehydrogenase
LOH	Loss of Heterozygosity
m	meter
M	molar
MAP	MYH Associated Polyposis
MEM	Minimum Essential Medium
mg	milligram
MIC	Minimal Inhibitory Concentration
min	minute
ml	milliliter
mm	millimeter
mM	millimolar
MRSA	Methicillin-resistant staphylococcus aureus
NCI	National Cancer Institute
NOESY	Nuclear Overhauser effect spectroscopy
NS	Naturstoff

List of Abbreviations

PEG	Polyethylenglycol
µg	microgram
µl	microliter
µm	micrometer
NCI	National Cancer Institute
MeOH	methanol
nm	nanometer
NMR	Nuclear magnetic resonance
MS	Mass spectrometry
PARP	Poly (ADP-ribose) polymerase
PAGE	Polyacrylamid Gel Electrophoresis
PBS	Phosphate Buffered Saline
rpm	revolutions per minute
SDS	Sodiumdodecylsulfate
SFM	Serum Free Medium
SPE	Solid phase extraction
TBS	Tris-Buffered Saline
TEMED	Tetramethylethylenediamine
TGF-β	Transforming Growth Factor Beta
TLC	Thin layer chromatography
WHO	World Health Organization
XB	2-deprenyl-rheediaxanthone B

1 INTRODUCTION

1.1 Epidemiology of cancer

There are several approaches for the definition of cancer. Cancer is defined by the American Cancer Society (ACS) as a „group of diseases characterized by uncontrolled cell proliferation, loss of function and spread of abnormal cells, which can lead to death“ (www.cancer.org). The World Health Organisation (WHO) defines cancer as „a generic term for a group of more than 100 diseases that can affect any part of the body and one feature of cancer is the rapid creation of abnormal cells which grow beyond their usual boundaries“ (www.who.int/cancer). The National Cancer Institute (NCI) describes cancer as „a term for diseases in which abnormal cells divide without control and can invade nearby tissues“ (www.cancer.gov). The NCI also differentiates between the main types of cancer. *Carcinoma* originates in the skin or in tissues that cover intestinal organs, *Sarcoma* begins in connective or supportive tissue and *Leukemia* starts in blood forming tissue. Another main cancer types are *Lymphoma* and *multiple myeloma* which originate in cells of the immune system. *Central nervous system cancers* begin in brain or spinal cord tissues (NCI 2011).

Cancer is one of the major causes of death worldwide, second after cardiovascular disease in developed countries and third after cardiovascular and diarrheal diseases in developing countries (Garcia *et al.*, 2007). Each year cancer is diagnosed in about 11 million people worldwide and was responsible for over 7.9 million deaths in 2008 (WHO) and so the search for new therapeutics to treat this disease, remains an important target in research.

Two different definitions are used to describe the occurrence of cancer in a population. The term *incidence* describes the number of new cases per 100 000 people per year and the term *mortality* defines the number of deaths per 100 000 people per year. Incidence and mortality do not necessarily correlate.

Regarding incidence the most common cancers in women worldwide are breast, cervix and colorectal cancer. Breast cancer also has the highest mortality in women followed by lung, cervix and colorectal cancer. In men the most frequent cancer types are lung, prostate and colorectal cancer. Regarding mortality the most common cancers in men

worldwide are lung, stomach, liver and colorectal cancer. Thus, colorectal cancer is the third most frequent cancer type in both men and women, and the fourth most frequent cause of death worldwide (Fig. 1).

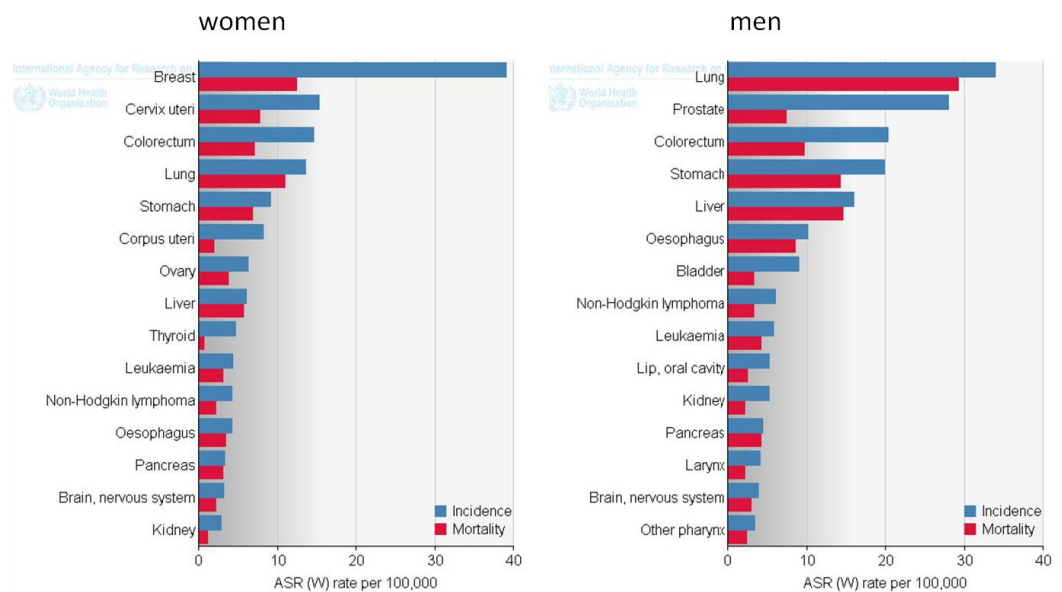


Fig. 1: Incidence and mortality of the most common cancer types in women and men worldwide
(Globocan 2011)

In 2010 in Austria 48.1% of the women died due to cardiovascular diseases. The second common cause of death in women is cancer with 22.9%. Cardiovascular diseases are also in men the most common cause of death in Austria with 37.4%, followed by cancer with 28.5% (Fig. 2).

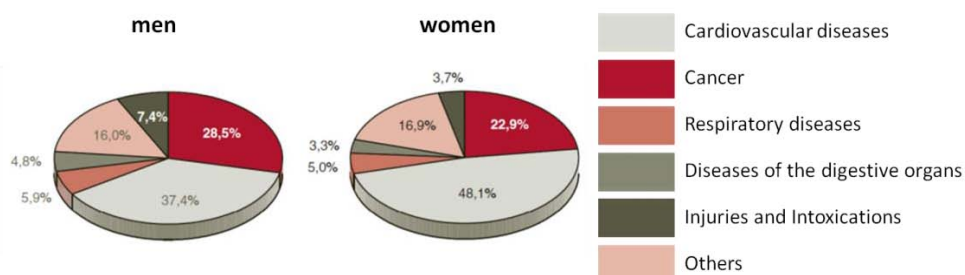


Fig. 2: Cause of deaths in men and women in Austria
(adapted from: Statistik Austria, 2010)

The distribution of cancer incidence and death in Austria is similar to the data worldwide. Regarding incidence and mortality, the most common cancers in women in Austria are

breast cancer, colorectal and lung cancer. In men prostate cancer, lung and colorectal cancer occur most frequently and exhibit the highest mortality as well (Fig. 3).

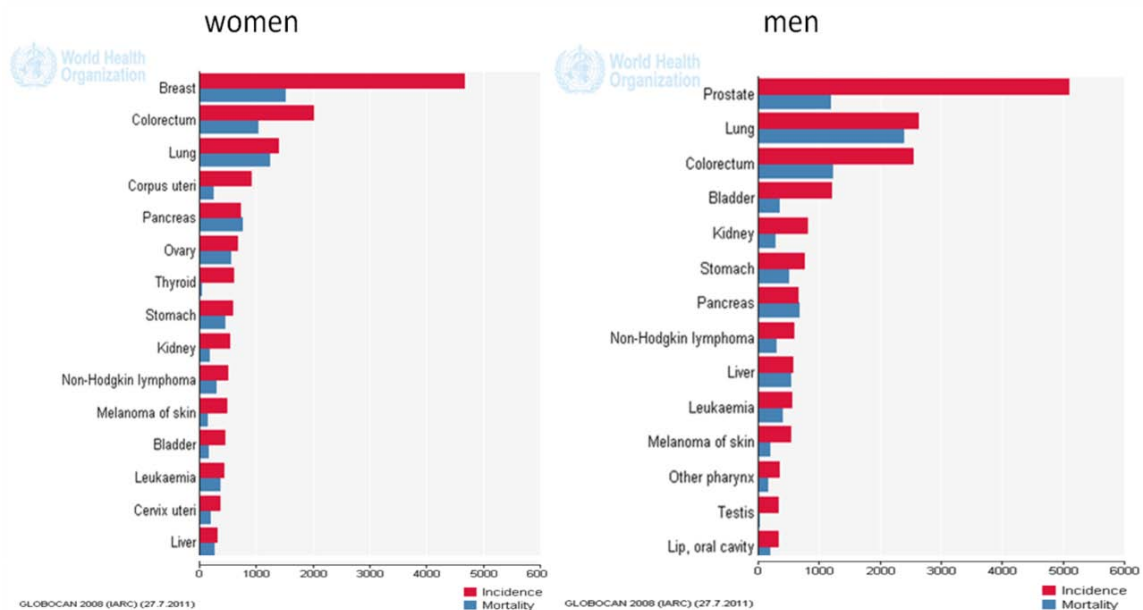


Fig. 3: Incidence and mortality of the most common cancer types in women and men in Austria
(Globocan 2011)

1.2 Epidemiology of colorectal cancer

Cancer originating in the colon or rectum is classified as colon cancer, rectal cancer or colorectal cancer.

Almost 60% of the cases of colorectal cancer occur in developed countries with the highest incidence in Western Europe, Australia and New Zealand. The lowest incidence for this cancer type is in Africa with the exception of South Africa. The incidence rates as well as the mortality rates are higher in men than in women Fig. 4).

The incidence of colorectal cancer increases in some countries historically at low risk like Spain and countries in Eastern Asia and Eastern Europe (Center *et al.*, 2009). The reasons for this trend are probably the changes in the dietary pattern, increased obesity and also an increased prevalence for smoking (Jemal *et al.*, 2011). In other countries like the United States or Australia the high incidence and mortality of colorectal cancer is stabilizing or declining (Center *et al.*, 2009) as a result of increased awareness, early detection due to colorectal cancer screening programs and improved treatment (Edwards *et al.*, 2010).

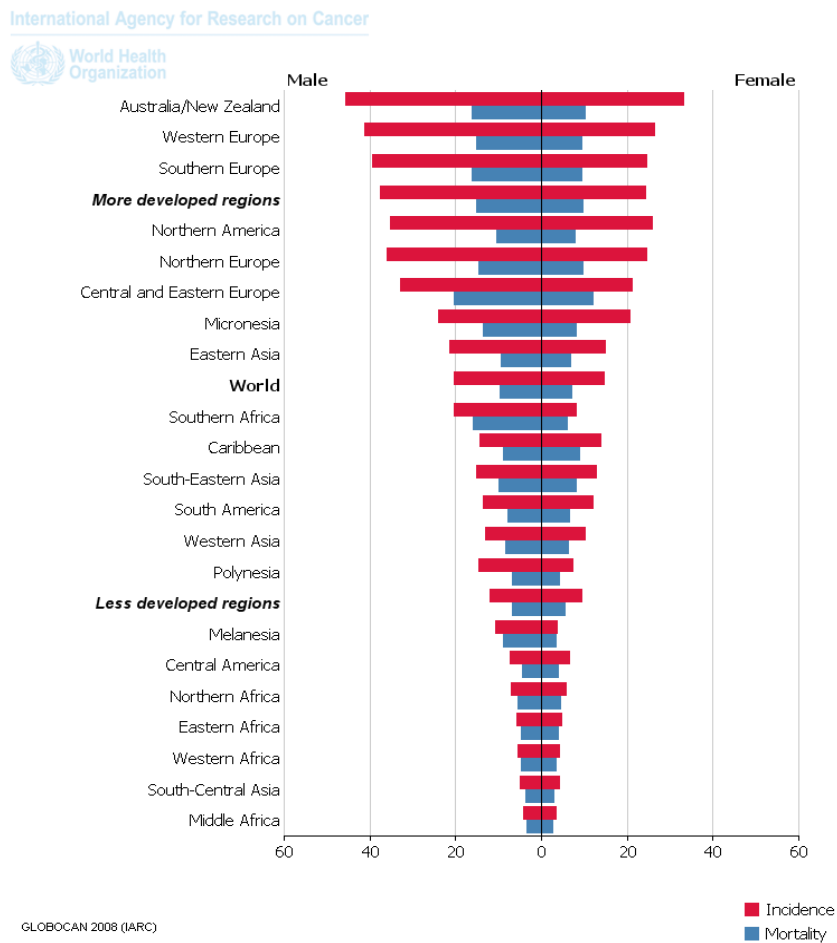


Fig. 4: Incidence and mortality of the colorectal cancer in women and men worldwide
(Globocan 2011)

The risk factors of colorectal cancer include obesity, physical inactivity, smoking and consumption of high amounts of red and processed meat as well as excessive consumption of alcohol (Ferrari *et al.*, 2007; Boyle *et al.*, 2008; Jemal *et al.*, 2011).

Each year approximately 5000 malignant tumors in the colon or rectum are diagnosed in Austria, representing 13% of all diagnosed cancers and about 2200 people die each year from colorectal cancer in Austria.

Incidence, as well as mortality, is higher in Austrian men than in Austrian women. In the last decade both, the incidence and the mortality of colorectal cancer, decreased (Fig. 5) (Statistik Austria, 2011). This is probably the result of preventive actions like screening and the removal of precancerous lesions.

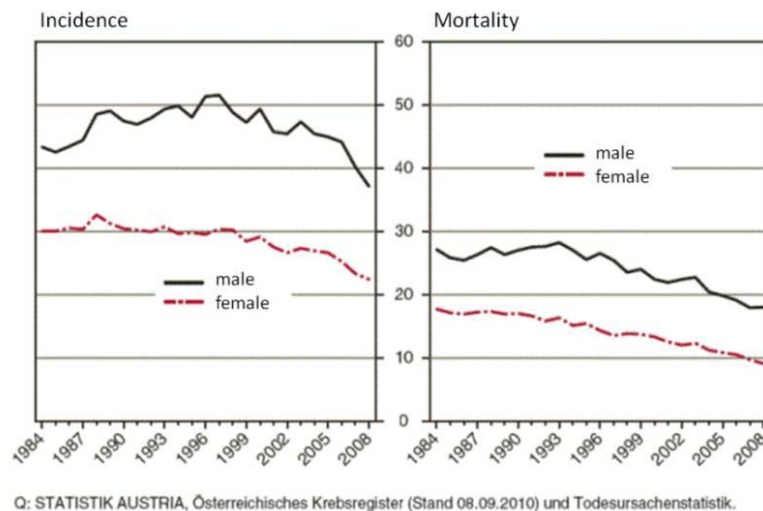


Fig. 5: Incidence and mortality of colorectal cancer in men and women in Austria
(adapted from: Statistik Austria, 2010)

1.3 Development of cancer – carcinogenesis

Normal cells are under the constant influence of several signals regulating the behaviour of the cell. Cancer is characterised by dysregulation of these intercellular signalling mechanisms (Schulte-Hermann 2004). The term carcinogenesis describes the multistage process of development from a normal cell to a malignant cancer cell. This complex successive transformation involves changes at genetic and cellular levels to acquire the malignant characteristics (Fig. 6) (Stratton *et al.*, 2009).

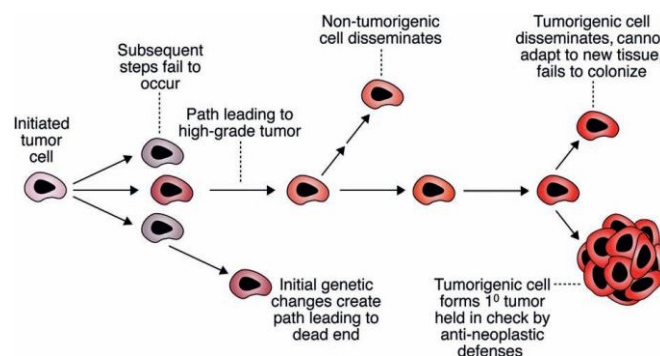


Fig. 6: Carcinogenesis
(Weinberg 2008)

Initiation – Promotion – Progression

Carcinogenesis is known to follow a specific order described in the three stage model of carcinogenesis as follows:

Initiation: Initiation is the first step of carcinogenesis. This rare and irreversible event occurs rapidly and only in proliferating cells. The outcome of initiation is a mostly genetic alteration that confers an advantage in proliferation compared to normal cells in the presence of tumor promoters and is passed on to the daughter cells. Initiation can occur spontaneously or due to replication mistakes or DNA lesions. The frequency for initiation is increased by DNA damaging exogenous agents such as chemicals like aflatoxin, polycyclic aromatic hydrocarbons, nitrosamine or arsenic, physical impacts like X-rays or UV-light and biological carcinogens such as human papilloma virus (HPV) or hepatitis B and C viruses. All these different agents can lead to damage in DNA, chromosomes or the genome (Reddy *et al.*, 2003). Usually these defects are repaired by efficient DNA repair systems. As initiation is not reversible, mutations will be transmitted to the daughter cells. Often genes regulating cell growth and differentiation are affected by mutations, but initiation alone does not lead to tumor development (Schulte-Hermann 2004).

Promotion: Promotion is the second step of carcinogenesis which needs to be maintained over a long period of time. It is considered to be a not gene-toxic and reversible process. When promotion stops, regression of neoplasia can be seen. Promoters can either activate growth signaling pathways or can lead to a decrease in apoptosis (Reddy *et al.*, 2003). Exogenous tumor promoters are over-nutrition, chronic inflammation or different environmental substances. Hormones such as estrogen and androgen, prostaglandins and growth factors like TGF- α are examples for endogenous tumor-promoting factors (Schulte-Hermann 2004).

As initiation is an irreversible process, the occurrence of promotion after a long period after initiation, supports initiated cell growth and leads to cancer. But as promotion is a reversible process it does not necessarily lead to cancer when a long period of time lies between individual promoting events. Promotion alone is not able to achieve malignant transformation of initiated cells and produces mainly benign tumors (Fig. 7) (Kufe *et al.*, 2003).

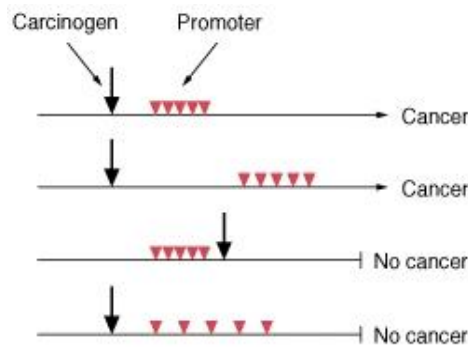


Fig. 7: The interaction of initiation and promotion

(Kufe *et al.*, 2003)

Progression: The transition from a benign to a malignant tumor and the third stage of carcinogenesis is called tumor progression (Fig. 8) (Reddy *et al.*, 2003). This stage is characterized by accumulation of further mutations, alterations in genes or in the repair mechanism of the cells. Genetic instability which can promote further mutations is essential for progression. The mutations affect different oncogenes and tumor suppressor genes. Oncogenes encode proteins that control cell proliferation and/or apoptosis (Croce 2008) and promote cell growth. Tumor suppressor genes reduce the probability of the appearance of a tumor (Schulte-Hermann 2004; Weinberg 2007).

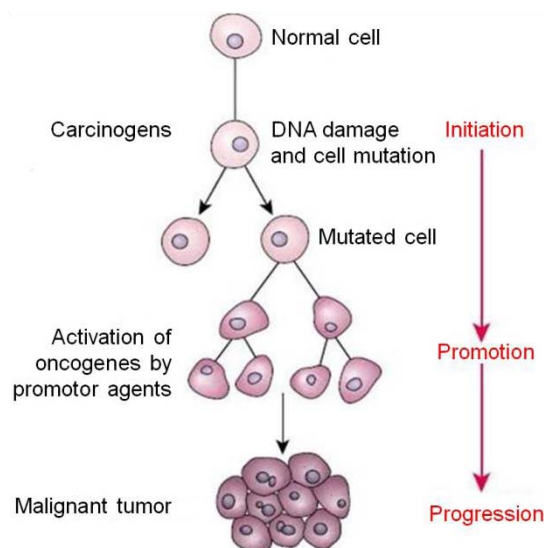


Fig. 8: The multistage concept of carcinogenesis

(modified from: <http://www.hakeem-sy.com>)

1.4 Hallmarks of cancer

The hallmarks of cancer described by Hanahan and Weinberg consist of six biological capabilities acquired during the multistep development of human tumors (Hanahan and Weinberg 2011). These capabilities, needed to transform a normal cell into a cancer cell, include sustaining proliferative signalling, insensitivity to antigrowth signals, the ability to resist apoptosis, limitless replicative potential, sustained angiogenesis and tissue invasion and metastasis (Hanahan and Weinberg 2000) (Fig. 9).

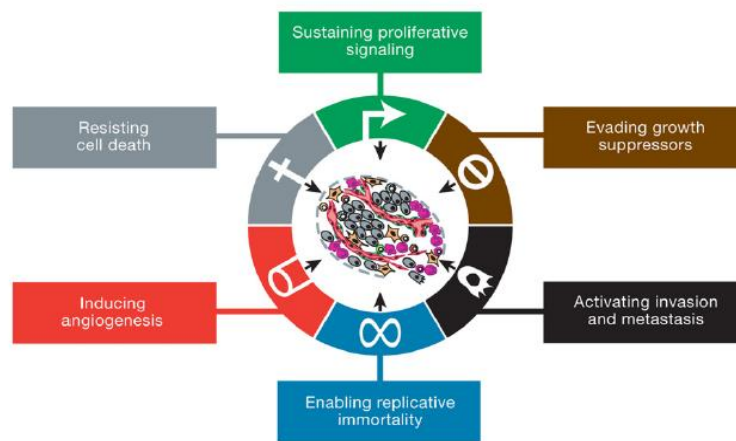


Fig. 9: The hallmarks of cancer

(Hanahan and Weinberg 2000)

1.4.1 Sustained proliferative signaling

In normal cells the production and release of growth promoting signals is controlled carefully, but cancer cells are able to deregulate these signals of growth factors typically involving intracellular tyrosine kinase receptor domains (Hanahan and Weinberg 2011). But cancer cells can also acquire this capability to sustain proliferation in some alternative ways and may produce growth factors themselves (Bhowmick *et al.* 2004) or send signals to stimulate normal cells which supply the cancer cells with growth factors (Cheng *et al.*, 2008; Hanahan and Weinberg 2011).

1.4.2 Evading growth suppressors

In addition, cancer cells have to lose sensitivity to signals negatively regulating cell proliferation depending on inactivation of tumor suppressor genes in cancer cells (Hanahan and Weinberg 2011). One typical tumor suppressor encodes the

retinoblastoma associated protein which blocks proliferation and its signaling pathway (Hanahan and Weinberg 2000). Cancer cells often have a defect in the retinoblastoma pathway resulting in continuous cell proliferation. A second typical tumor suppressor is TP53 which receives the inputs from signals within the cell and can stop further cell cycle progression or trigger apoptosis. This tumor suppressor can be defect in tumor cells as well (Hanahan and Weinberg 2011).

1.4.3 Resisting cell death

Cell death or apoptosis is defined as programmed cell death and intracellular apoptotic signals lead to specific cell morphology characteristics and death of cells. Tumor cells evolve different strategies to limit or circumvent apoptosis e.g. by loss of function of the tumor suppressor TP53, by increasing the levels of anti-apoptotic proteins like BCL 2 or BCL-XL or by decreasing the levels of the pro-apoptotic proteins BAX or BIM (Hanahan and Weinberg 2011).

1.4.4 Inducing angiogenesis

Angiogenesis is defined as the formation of new blood vessels and is important for nutrient and oxygen supply to the tumor. During tumor progression angiogenesis is an essential step as soon as tumors exceed a diameter approximately 2mm. Activation is achieved by different stimulators of angiogenesis like vascular endothelial growth factor-A (VEGF-A) or members of the fibroblast growth factor (FGF) family that are chronically upregulated in tumors (Baeriswyl and Christofori 2009; Hanahan and Weinberg 2000). The new blood vessels, produced within tumors, show abnormal characteristics like enlargement of vessels, aberrant blood flow, leakiness and excessive vessel branching (Nagy *et al.*, 2010; Baluk *et al.*, 2005). Angiogenesis also serves the tumor to metastasize, when single cancer cells enter the blood vessels and start a secondary tumor in another part of the body (Hanahan and Weinberg 2000).

1.4.5 Enabling replicative immortality

Cancer cells depend on an unlimited replicative potential in order to form big tumors (Hanahan and Weinberg 2000). Most established cancer cell lines have the ability to proliferate in culture without evidence of senescence or crisis (Hanahan and Weinberg 2011). There is evidence that the induction of telomerase, which prevents the

chromosomal ends from shortening during replication, is involved in the capability for unlimited proliferation (Blasco 2005; Hanahan and Weinberg 2011).

1.4.6 Activating invasion and metastasis

Carcinomas from epithelial tissues develop alterations in their attachment to other cells and to the extracellular matrix resulting in higher pathological grades of malignancy. The best described alteration is the loss of E-cadherin by carcinoma cells. E-cadherin is a key cell-to-cell adhesion molecule and plays an essential role in the maintenance of intercellular contacts within epithelia (Hanahan and Weinberg 2011). The decline of E-cadherin is known to potentiate invasion and metastasis (Berx and van Roy 2009). Development of metastasis causes 90% of human cancer deaths (Sporn 1996; Hanahan and Weinberg 2000).

1.4.7 Enabling characteristics and emerging hallmarks of cancer

The acquisition of these six hallmarks is made possible by chromosomal abnormalities leading to genetic instability and local chronic inflammation maintained by innate immune cells.

In the last decade more research evidence suggested two additional hallmarks of cancer. The first emerging hallmark is the capability to reprogram the cellular energy metabolism in order to support the proliferation most efficiently. The second emerging hallmark is the evasion of immune destruction by T- and B-lymphocytes, natural killer cells and macrophages (Fig. 10) (Hanahan and Weinberg 2011).

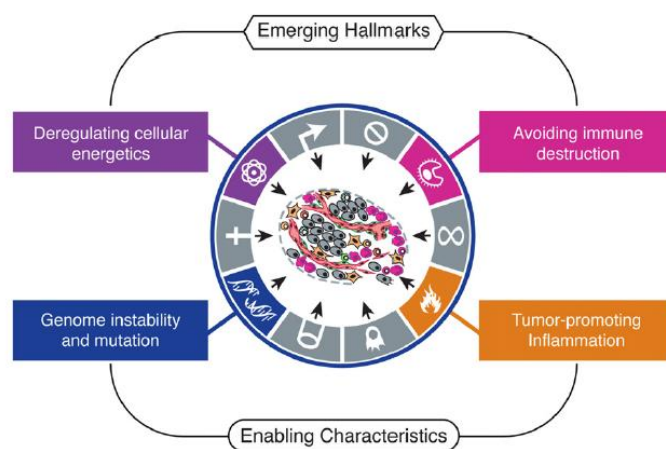


Fig. 10: The emerging hallmarks of cancer

(Hanahan and Weinberg 2011)

1.5 Carcinogenesis of colorectal cancer

1.5.1 Anatomy of the colon

The gastrointestinal tract consists of the upper and the lower part. The upper gastrointestinal tract consists of the mouth, the pharynx, the esophagus and the stomach. The lower gastrointestinal tract includes the small intestine, consisting of the duodenum, the jejunum and the ileum and the large intestine, consisting of the cecum, the colon, the rectum and the anal canal (Fig. 11). In mammals, the colon consists of the ascending colon, the transverse colon, the descending colon and the sigmoid colon. The ascending colon is the part of the colon from the cecum to the hepatic flexure where the transverse colon begins and leads into the descending colon at the splenic flexure. The part from the splenic flexure to the beginning of the sigmoid colon is called descending colon, where the stool is stored. The last part of the large intestine after the descending colon to the rectum is the sigmoid colon. The main function of the large intestine is storing waste, absorbing some fat-soluble vitamins, reclaiming water and maintaining the water balance. (<http://hopkinscoloncancercenter.org>).

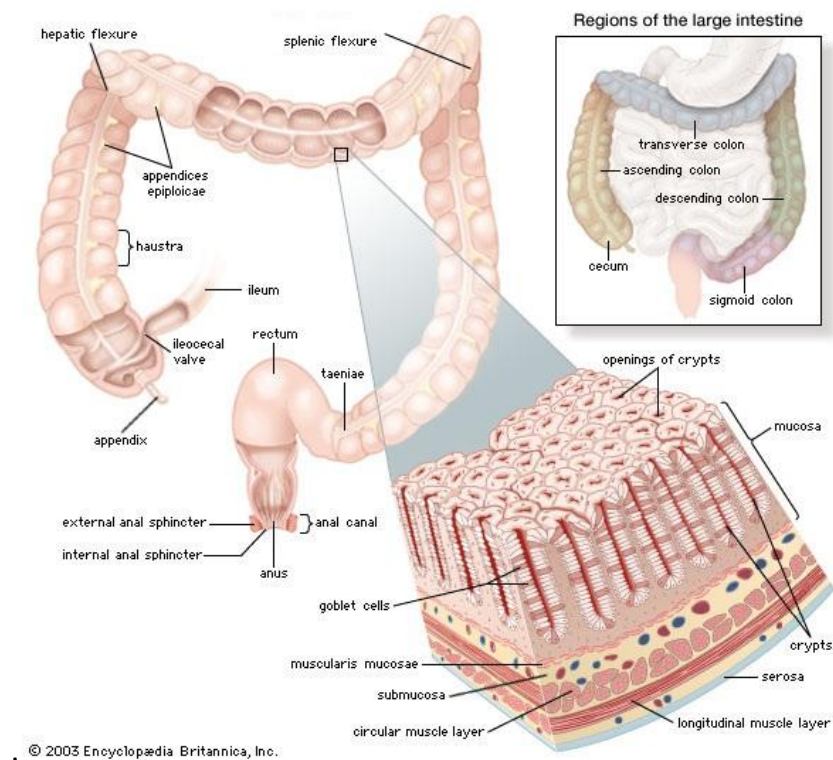


Fig. 11: Anatomy of the large intestine

(<http://www.britannica.com/EBchecked/topic/330544/large-intestine>)

1.5.2 Histopathology of the colon

The gastrointestinal tract has a general histology consisting of 5 different layers. The inner layer surrounding the lumen of the gastrointestinal tract is the mucosa, an epithelial layer responsible for digestion and absorption of the nutrients. The second layer is the muscularis mucosa and the third layer is the submucosa. The submucosa consists of large mesenchymal cells and is rich in vessels and immune cells. The fourth layer is called muscularis propria which consists of smooth muscle cells and moves the content of the colon. The outer fifth layer is the serosa (Thomson and Shaffer, 1994).

The epithelium of the colon is rapidly renewing itself every four to six days. Stem cells at the bottom of the crypts are dividing continuously by a coordinated process of cell proliferation and differentiation. The new cells migrate towards the luminal surface where they undergo apoptosis (Fig. 12). A loss of the proliferation control in the crypt is the cause for colorectal cancer.

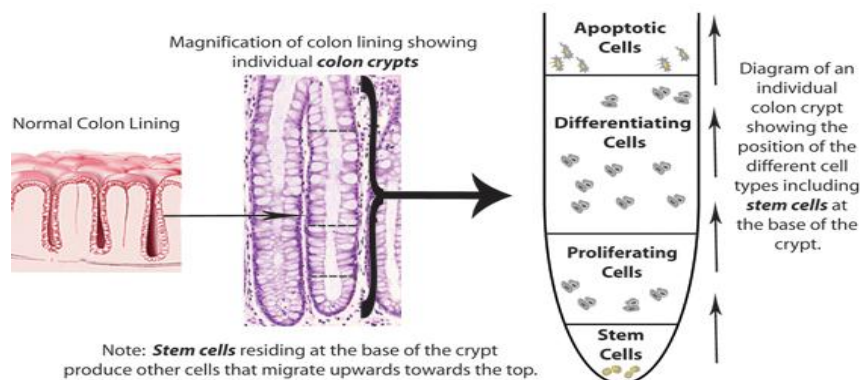


Fig. 12: Depiction of colorectal stem cells and crypts

(<http://hopkinscoloncancercenter.org>)

1.5.3 Development of colorectal cancer

Malignant transformations which lead to colorectal cancer occur mostly in the mucosa, where colorectal cancer usually starts as a benign polyp. Most of these hyperplastic polyps remain benign showing almost normal histopathology. However, these hyperplastic areas have an unusual high division rate leading to a thicker epithelia over time and to alterations in the morphology of the cells which is called dysplastic cells or adenoma. The higher the degree of dysplasia in an adenoma the higher is the risk of developing into a malignant carcinoma. 95% of colorectal cancers develop from

adenomas in this way. Polyps that grow into the colonic lumen on a stalk can be removed by colonoscopy to prevent progression to malign adenocarcinomas. They invade surrounding colon tissue and grow into the wall of the colon. In advanced stages the cancer cells metastasize and spread to other organs, mainly the liver (Fig. 13). (<http://hopkinscoloncancercenter.org>; Weinberg 2007).

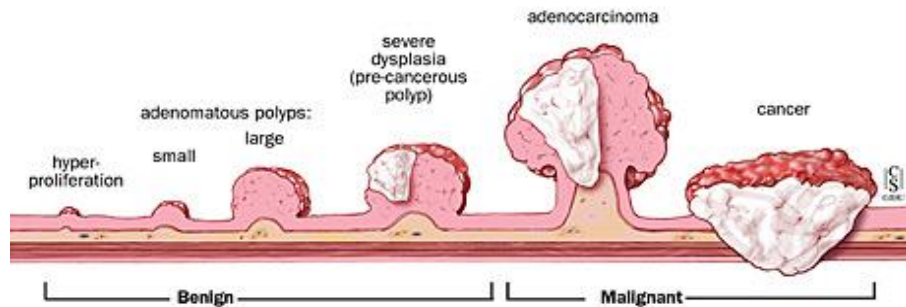


Fig. 13: Benign to malignant tumor progression

(<http://hopkinscoloncancercenter.org>)

About 10% of colorectal tumors occur in the transverse colon, 15% in the descending colon, 25% in the sigmoid colon, 30% in the ascending colon and about 20% in the rectum (<http://hopkinscoloncancercenter.org>).

1.5.3.1 Hereditary colorectal cancer

The tendency to develop colorectal cancers can be inherited (Kinzler and Vogelstein 1996). Although about 60% of colorectal cancers are sporadic, there are different inherited conditions with a significant high risk of colorectal cancer (Fig. 14) like FAP, HNPCC, MAP and Hamartomatous Polyposis Syndromes.

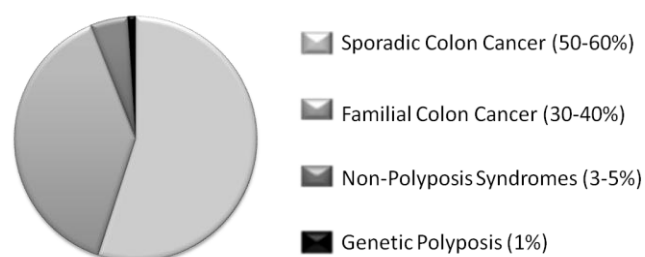


Fig. 14: Incidence of types of colorectal cancer

(modified from: <http://hopkinscoloncancercenter.org>)

1.5.3.1.1 Hereditary non polyposis colorectal cancer (HNPCC)

The Hereditary Non Polyposis Colorectal Cancer (HNPCC) is also known as the Lynch syndrome or the cancer family syndrome and is the most common form of inherited colorectal cancer responsible for about 5% of all colorectal carcinomas (Lynch *et al.*, 1996). Patients with HNPCC carry mutations in DNA mismatch repair genes (MMR) involved in growth regulation like TGF- β . In contrast to FAP patients, people with HNPCC do not develop many of polyps, but carcinogenesis progresses rapidly. These patients have an 80% risk to develop colorectal cancer in their life (Hisamuddin and Yang 2004, <http://hopkinscoloncancercenter.org>).

1.5.3.1.2 Familial adenomatous polyposis (FAP)

Familial Adenomatous Polyposis (FAP), also called familial polyposis or Gardner's syndrome, is a dominantly inherited disease that is characterized by the formation of hundreds of adenomatous polyps (Fig. 15) caused by a mutation on the APC gene (Grodin *et al.*, 1991; Stratte 2005) and is responsible for less than 1% of all colorectal cancers (see also chapter 1.5.5.1).

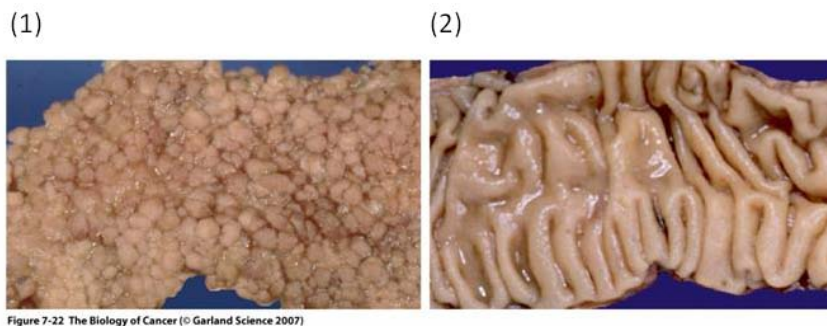


Figure 7-22 The Biology of Cancer (© Garland Science 2007)

Fig. 15: Comparison of the colon of a FAP patient (1) and a healthy colon (2)
(Weinberg 2007)

1.5.3.1.3 MYH associated polyposis (MAP)

The MYH Associated Polyposis (MAP) is a hereditary condition leading to the formation of multiple adenomatous polyps and an increased risk to develop colorectal cancer. The MYH gene is located on the short arm of the chromosome 1 and the MYH protein is essential for DNA damage repair (Jass 2005; Lipton and Tomlinson 2006).

1.5.3.1.4 Hamartomatous polyposis syndromes

The Hamartomatous Polyposis Syndromes are a heterogeneous group of inherited disorders forming hamartomatous polyps leading to an increased risk for colorectal cancer. These group include syndromes like Juvenile Polyposis syndrome, Peutz Jeghers syndrome, Cowdens syndrome (Schreibmann 2005) with mutations in e.g. the PTEN or SMAD4 gene responsible for less than 1% of all colorectal tumors (Hisamuddin and Yang 2004).

1.5.3.2 Inflammation and colorectal cancer

Inflammation is known to be an important tumor promotor. There is clear evidence about a connection between inflammatory diseases of the colon such as Morbus Crohn or ulcerative colitis and colorectal tumors. Colorectal cancers associated with inflammatory diseases seem to be based on an early mutation in p53 and fewer mutations in APC and K-Ras genes compared to sporadic tumors (Ilyas *et al.*, 1999).

1.5.3.2.1 Morbus Crohn

Morbus Crohn is a chronic inflammatory disease of the intestinal tract. It is assumed to be an autoimmune disease, but the cause of this condition is still not known. Levels of TNF- α , interleukin-2 and interferon- γ are elevated due to chronic inflammation and patients suffering from Morbus Crohn have an increased risk to develop cancer (Freeman 2008).

1.5.3.2.2 Ulcerative colitis

Ulcerative colitis is a chronic inflammatory disease of the large intestine that is characterized by ulcers in the colon. The cause of this disease is not known as well, but patients suffering from this condition have an increased cancer risk (NDDIC 2011).

1.5.3.3 Nutrition and colorectal cancer

The incidence of cancer in developed countries as well as in developing countries is still increasing as a result of aging population on the one hand and different life style factors on the other hand (Jemal *et al.*, 2011). As stated before, cancer can be caused by internal

factors such as immune conditions or inherited mutations, but only 5-10% of all cancers can be related to genetic defects, whereas all others are resulting from different lifestyle factors (Fig.16) (Anand *et al.*, 2008) such as smoking, excessive alcohol consumption, infections, physical inactivity, obesity or an unbalanced diet. It is reported that 20-25% of all cancer related deaths are due to smoking, 15-20% are due to infection and almost 35% are due to the diet (Anand *et al.*, 2008; Boyle and Levin 2008; Giovannucci and Wu 2006). Regarding colorectal cancer an unbalanced diet is reported to account for 80% of all cases (Reddy *et al.*, 2003).

The risk to develop colorectal cancer is closely related to an unbalanced diet and overnutrition. For obese men with an BMI higher than 30 a 2-fold and in obese women a 1,5-fold increased risk of colorectal cancer was reported and the risk is reduced in physically active persons (McTiernan *et al.*, 1998). There is also evidence, that the intake of red meat, processed meat or meat cooked at high temperatures, is related to a higher risk to develop colorectal cancer (Larsson and Wolk 2006). In meat prepared at high temperatures, heterocyclic amines and polycyclic aromatic hydrocarbons are produced and processed meat contains N-nitroso compounds, which are also known to be carcinogenic. The intake of red meat is associated with an increased risk of adenoma in the descending and sigmoid colon linked to two heterocyclic amines, 2-amino-3,8-dimethylimidazo[4,5]quinoxaline and 2-amino-1-methyl-6-phenyl imidazo[4,5]pyridine as well as benzo(a)pyrene (Shina *et al.*, 2005). Another risk factor is the consumption of high fat diets. Fatty acid hydroperoxides from unsaturated fatty acids are also assumed to be a risk factor of colorectal cancer (Jurek *et al.*, 2005).

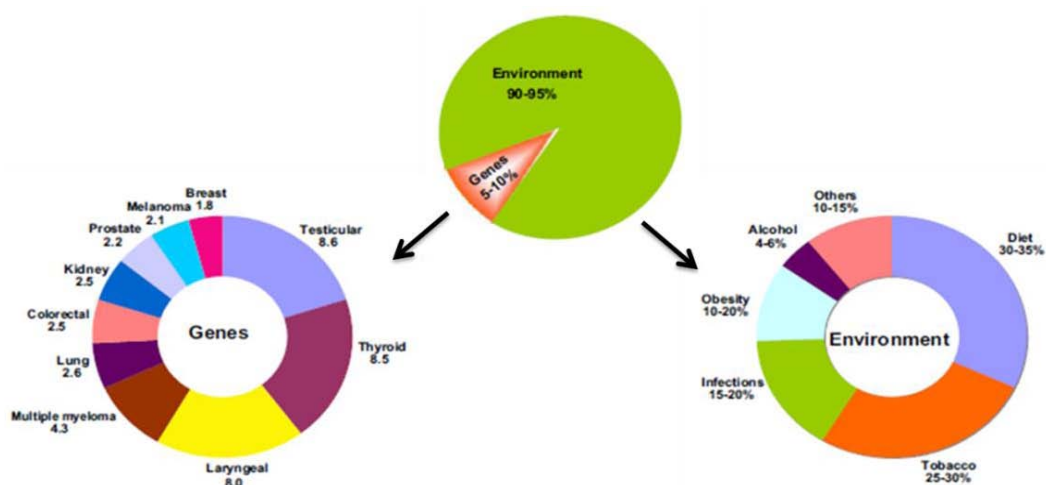


Fig. 16: The role of genes and environment in the development of cancer

(modified from: Anand *et al.*, 2008)

In order to reduce the cancer risk a stop of smoking, exercise, reduction of the intake of alcohol and red meat, combined with an increased intake of fruits, vegetables and whole grains and regular medicinal check-ups are highly recommended (Anand *et al.*, 2008).

1.5.4 Staging of Colorectal Cancer

Staging describes the extent of local growth and invasion of a cancer. Staging information is important to plan the treatment and serves as a prognostic factor. Tumors are classified according to evidence of invasion and tumor spread on which the aggressiveness of colorectal tumors are based. The size of the tumor is usually not of high importance for the outcome, but there is a close correlation between advanced stage and mortality.

There are different systems for cancer classification. The first one established by Dr. Cuthbert Dukes has been modified and is now called the Astler-Coller modification of the Dukes' classification (MAC) (Schölmerich 2005) (Fig. 17).

Carcinoma in situ	May be referred to a high grade dysplasia – an intramucosal carcinoma that does not penetrate the mucosae muscularis
Stage A	Tumors that invade through the mucosa muscularis into the submucosa but do not reach the muscularis propria
Stage B1	Tumors that invade into the muscularis propria
Stage B2	Tumors that completely penetrate the smooth muscle layer into the serosa
Stage C	Tumors that encompass any degree of invasion but are defined by regional lymph node involvement
Stage C1	Tumors that invade the muscularis propria with fewer than four positive nodes
Stage C2	Tumors that completely penetrate the smooth muscle layer into the serosa with four or more involved nodes
Stage D	Lesions with distant metastases

Fig. 17: Dukes' classification (Astler-Coller modification)

(<http://hopkinscoloncancercenter.org>)

Nowadays the TNM classification of malignant tumors (Fig. 18) developed by the American Joint Committee on Cancer (AJCC), is frequently used for staging. The TNM Staging System is based on the size of the tumor (T), the extent of spread to the lymph nodes (N), and the presence of metastasis (M) (AJCC 2011).

T-category describes the size of the primary tumor and invasion into nearby tissue	
TX	Primary tumor cannot be evaluated
T0	No evidence of primary tumor
Tis	Carcinoma in situ (early cancer that has not spread to nearby tissue)
T1-T4	Size and/or extent of the primary tumor
N-category describes regional lymph node involvement	
NX	Regional lymph nodes cannot be evaluated
N0	No regional lymph node involvement
N1-N3	Involvement of regional lymph nodes (number and extent of spread)
M-category describes presence of Metastasis	
M0	No distant metastasis
M1	Distant metastasis

Fig. 18: TNM classification of malignant tumors

(AJCC 2011)

After determination of the T, N and M stage, an overall stage of I, II, III and IV is assigned as well. Stage I cancers are defined as the least advanced and have the best prognosis. Higher stage cancers are more advanced and most stage IV tumors are inoperable (AJCC 2011).

TNM Classification				Dukes' Classification
Stages	T	N	M	
Stage 0	Tis	N0	M0	
Stage I	T1	N0	M0	A
	T2	N0	M0	B1
Stage II	T3	N0	M0	B2
	T4	N0	M0	B2
Stage III	T1, T2	N1 or N2	M0	C1
	T3, T4	N1 or N2	M0	C2
Stage IV	Any T	Any N	M1	D

Fig. 19: Comparison of the TNM classification with the Dukes' classification

(<http://hopkinscoloncancercenter.org>)

1.5.5 Genetic alterations in colorectal cancer

Vogelstein and Fearon described a series of mutations responsible for colorectal carcinogenesis. They defined a preferred sequence of accumulation for these mutations regarding the histological changes of tumor progression (Vogelstein *et al.*, 1988). They determined a loss of heterozygosity (LOH) in the long arm of chromosome 5 in many early

adenomas. The region on chromosome 5 affected by this loss of the normal function of one allele is carrying the APC (adenomatous polyposis coli) gene, a tumor suppressor gene. In larger adenomas a high rate of LOH on the long arm of chromosome 18 was proven and 50% of the carcinomas show additionally a loss of heterozygosity on the short arm of chromosome 17 which carries p53. A mutated K-ras oncogene was also detectable in about 50% of the adenomas (Fig. 20) (Vogelstein *et al.*, 1988). These findings established the acceptance that the genetic modifications during carcinogenesis involve the activation of one proto-oncogene and the inactivation of at least three tumor suppressor genes, of which APC is always the first to be altered (Vogelstein *et al.*, 1988; Weinberg 2007).

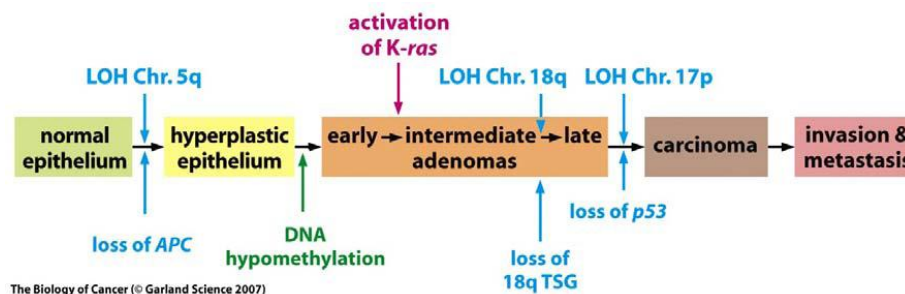


Fig. 20: Genetic alterations during the colorectal cancer progression

(modified from: Weinberg 2007)

The prominent mutated genes responsible for development of colorectal cancer are adenomatous polyposis coli (APC) gene, K-RAS, p53, “Deleted in Colorectal Cancer” (DCC) gene and genes involved in TGF- β response (Kinzler and Vogelstein 1996).

1.5.5.1 Adenomatous polyposis coli (APC) gene

The adenomatous polyposis coli (APC) gene, a tumor suppressor gene, is located on the long arm of chromosome 5 and plays an essential role in the early development of colorectal cancer. The APC protein helps to control proliferation and movements of cells and ensures that the chromosome number in cells is correct. β -catenin level is controlled by a complex containing the APC protein involved in the Wnt-pathway that induces rapid degradation of the protein. The most common and first mutation in colorectal cancer is the inactivation of APC which must be followed by other mutations to become malignant. In most colorectal cancers both alleles of the APC gene are inactivated (Nagase 1993).

APC is not expressed in the crypts of the colon but its level increases with the cells migrating upwards. Mutation of APC leads to an accumulation of β -catenin in the cells and the cells keep proliferating but do not differentiate while migrating upwards the crypt. When further migration becomes impossible due to the increased proliferation they develop an adenomatous polyp (Weinberg 2007).

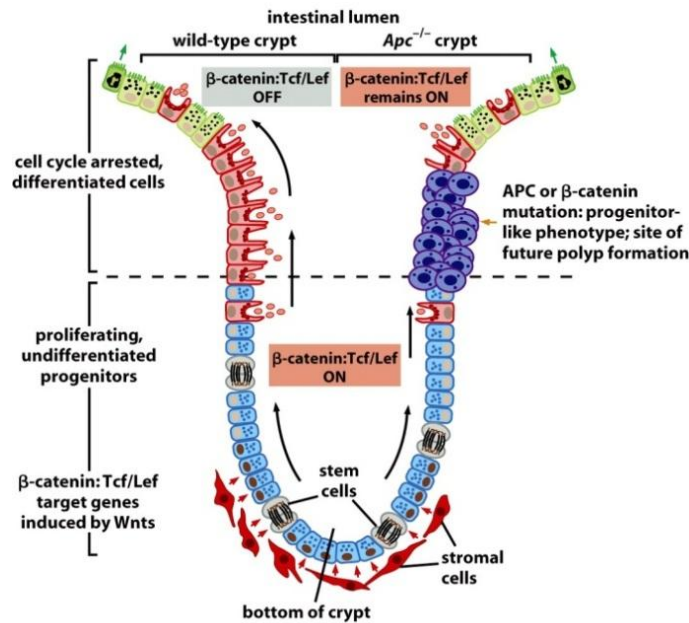


Figure 7-24a The Biology of Cancer (© Garland Science 2007)

Fig. 21: The biology of colonic crypts and APC/ β -catenin

(Weinberg 2007)

In people carrying an APC inactivating mutation, the risk to suffer from colorectal cancer at the age of 40 is almost 100% (Markowitz and Bertagnoli 2009). The loss of APC functions seems to be the initiating mutation common to most human colorectal carcinomas.

1.5.5.2 Kirsten – Ras (K-Ras) gene

Members of the Ras family are GTPases and serve as key effectors of growth factors (Ross *et al.*, 2001). Ras is involved in three important pathways: The Ras/Raf pathway controls cell proliferation, differentiation and apoptosis, the Ras/PI3kinase pathway modulates mainly apoptosis and the Ras/Ral pathway regulates membrane transport, cell migration, cell proliferation and apoptosis (Castagnola *et al.*, 2005; Alberts 2002; Camonis *et al.*, 2005).

Ras is activated when GTP is bound to the protein and inactive when GDP is bound (Fig. 22). Three different Ras genes (Kirsten-, Harvey- and Neuroblastoma-Ras) are known, but K-Ras is most frequently mutated in cancer. In approximately 10% of adenomas smaller than 1cm, about 50% of larger adenomas and even more of the colorectal carcinomas K-Ras mutation have been determined resulting in the hyperactivation of Ras (Bos *et al.*, 1987; Vogelstein *et al.*, 1988). This Ras mutation is not the initiating event in tumors, but its occurrence after APC mutation promotes carcinogenesis (Ross *et al.*, 2001; Fearon and Vogelstein 1990; Weitz 2004).

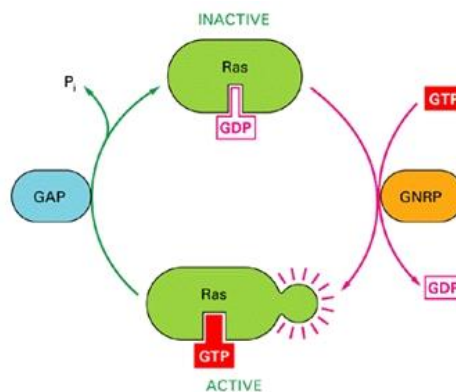


Fig. 22: The regulation of Ras activity

(Alberts 2002)

1.5.5.3 p53 gene

One of the most important tumor suppressor genes is p53 which is located on the short arm of chromosome 17 and obviously mutated and deleted in 70% of all sporadic colorectal cancers (Ilyas *et al.*, 1999). p53 plays an important role in inducing cell cycle arrest, apoptosis and in inhibiting angiogenesis. DNA damage sensors like ATM activate p53 leading to a temporary cell cycle arrest in G1-phase (Grady 2004). If DNA damage cannot be repaired, p53 activates the apoptotic machinery (Miyashita 1994).

Mutations of p53 are often accompanied by loss of heterozygosity. This mutation is rare in polyps, but frequent in carcinomas suggesting that it occurs later during carcinogenesis. Germ line mutations of p53 lead to the Li-Fraumeni syndrome which frequently leads to cancer in affected persons (Bartram 2004). Mutations on p53 leading to the loss its function occur mostly during the transition of a benign adenoma to an invasive malignant adenocarcinoma.

1.5.5.4 Deleted in colorectal cancer (DCC) gene

The Deleted in Colon Cancer (DCC) gene is located on the long arm of chromosome 18 and is one of the genes lost due to LOH during carcinogenesis. This has been shown in approximately 13% of the early adenomas and in around 70% of carcinomas (Vogelstein *et al.*, 1988). DCC cannot lead to tumor formation, but is one of many reasons to promote existing tumor growth and is involved in the progression of a benign adenoma to a malignant carcinoma (Miyaki *et al.*, 1990).

1.5.5.5 Transforming growth factor beta (TGF- β)

The Transforming Growth Factor Beta (TGF- β) signaling pathway consists of a sequence of tumor suppressor genes which possesses anti-proliferative activity and can induce apoptosis by triggering the SMAD or the DAXX pathway (Markowitz and Roberts 1996). In about 30% of colorectal tumors mutations of the TGF- β -receptor or the SMAD transcription factors lead to a loss of function as a tumor suppressor gene. Furthermore, TGF- β signaling is involved in tumor progression (White 1998).

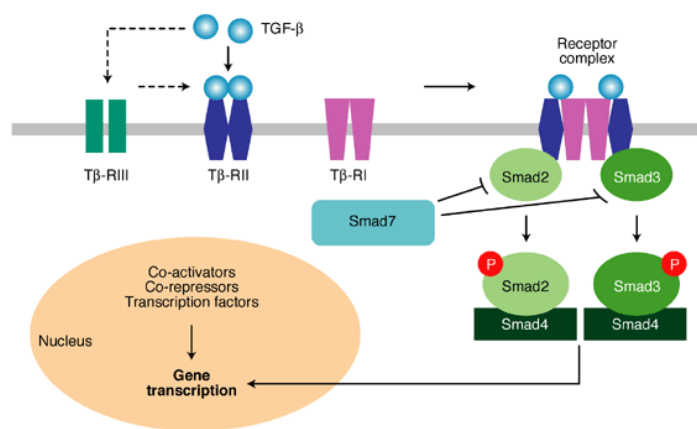


Fig. 23: The transforming growth factor β (TGF- β) signalling pathway

(http://journals.cambridge.org/fulltext_content/ERM/ERM5_05/S1462399403005684sup008.htm)

1.6 The cell cycle

The cell cycle is a complex process involving numerous regulatory proteins responsible for proliferation, the regulation of DNA damage repair and the replication of cells. (Schafer 1998; Alberts *et al.*, 2002).

It consists of four successive phases, the G₁-, S-, G₂- and M-phase (Fig.19). G₀-phase is a resting state of cells that temporarily or permanently leave the cell cycle. Cells are growing in G₁-phase which is the first gap from the end of the previous M-phase until the beginning of DNA synthesis. The replication of DNA resulting in two equal copies of each chromosome takes place in the S-phase. Then the cells enter the G₂-phase preparing for the entry into mitosis (Garrett 2001) (Fig. 24). During M-phase the chromosomes are distributed equally and the cytoplasm is divided to the daughter cells. Mitosis consists of six stages, the prophase, pro-metaphase, metaphase, anaphase, telophase and cytokinesis. In prophase the chromosomes condense and the cytoskeleton begins to reorganize. During pro-metaphase the condensed chromosomes connect to the microtubules. At metaphase the mitotic spindle is formed and during anaphase the sister chromatids of the chromosomes separate and migrate to the poles of the cell. During telophase the chromosomes at the two poles of the cell start to decondense and an envelope reforms around the new chromosomes (Garrett 2001).

The activation of each phase of the cell cycle is dependent on the correct progression and completion of the previous phase regulated by different proteins.

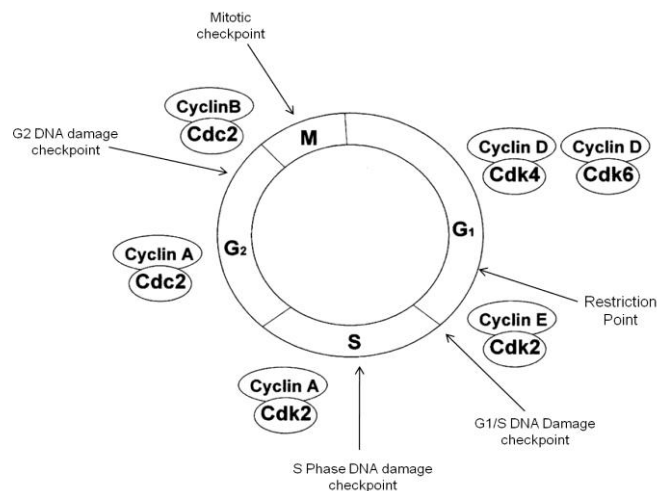


Fig. 24: The cell cycle and cell cycle regulation

(modified from: Garrett 2001)

1.6.1 Cell cycle regulation

There are two classes of regulatory proteins, the cyclins and the cyclin-dependent kinases (CDKs), necessary for the regulation of cell cycle progression (Nigg 1995). The CDKs are the key regulatory proteins and cause modifications in the phosphorylation of proteins

important for the regulation of cell cycle events and are controlled by the cyclins (Alberts *et al.*, 2002). Cyclins have no catalytic activity but are the activating regulatory domains of their partner cyclins. The protein levels of CDKs remain stable during cell cycle progression, but the protein levels of cyclins rise and fall during cell cycle as different cyclins are required at different time points of the cell cycle (Vermeulen *et al.*, 2003). Cyclin D and E are mainly expressed in G₁-phase, cyclin A in S-phase and cyclin B is required in M-phase. Cyclin E also plays an important role in G₁- to S-phase transition and cyclin A in G₂- to M-phase transition. Cyclin D binds to CDK4 and CDK6 and cyclin E activates CDK2. Cyclin A associates with CDK2 to initiate the DNA replication and with CDK1 regulating the entry into mitosis. Cyclin B forms complexes with CDK1 to further promote mitosis (Fig. 25) (Vermeulen *et al.*, 2003; Sanchez and Dynlacht 2005).

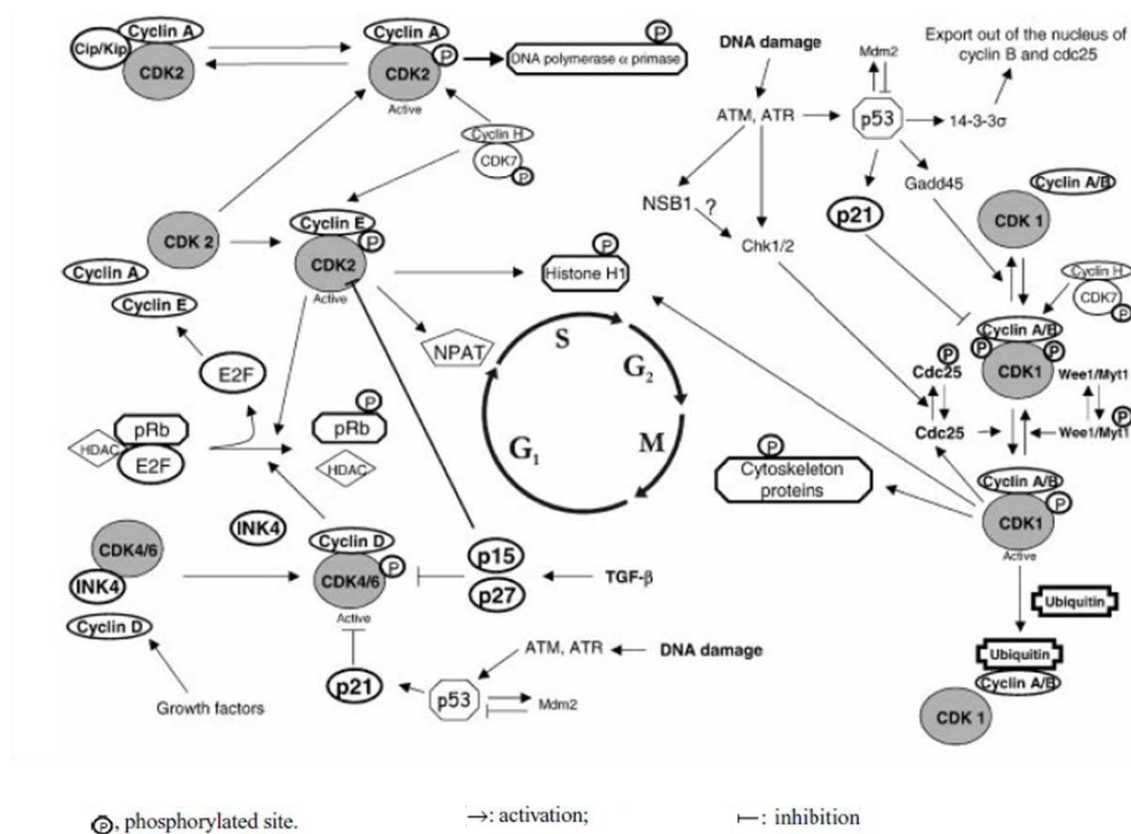


Fig. 25: Overview of some essential steps in cell cycle regulation

(Vermeulen *et al.*, 2003)

Restriction points and checkpoints are the quality control of cell cycle progression. The restriction point is the „point of no return“ in G₁-phase when the cell enters the cell cycle (Vermeulen *et al.*, 2003). At checkpoints the cell cycle is arrested in response to e.g. DNA damage until the damage is repaired. One DNA damage checkpoint is positioned before

entering the S-phase (G1-S-checkpoint) and is p53 dependent. DNA damage recognized by different protein kinases like ATM and ATR, leads to an increase in the levels of p53, which stimulates different repair mechanisms and results in CDK inhibition and cell cycle arrest (Ko and Prives 1996; Vermeulen *et al.*, 2003).

As mitosis is an irreversible process, the completion of DNA replication and the absence of genomic lesions are crucial criteria that must be met for the cell to enter mitosis (Tapia-Alveal *et al.*, 2009). Therefore the second important DNA damage checkpoint is positioned after DNA replication (G2-M-checkpoint). At this point of the cell cycle arrest can be p53 dependent or p53 independent. The entry into mitosis is prevented by the protein kinases Chk1 and Chk2 which phosphorylate Cdc25 and the CDK1-cyclin B complex will not be activated.

Chk1 and Chk2 are the checkpoint effector kinases necessary for the cell cycle arrest at the G2-M-checkpoint. They get phosphorylated and activated by ATM and ATR in response to diverse genotoxic insults including DNA crosslinks, stalled replication forks or radiation damage (Stracker *et al.*, 2009). Chk2 is expressed in all cell cycle phases (Lukas *et al.*, 2001) and is activated mainly by ATM. Chk1 is largely in S and G2-phase and mainly activated by ATR (Bartek and Lukas 2003).

1.6.2 Cell cycle and cancer

Common features of tumors are genetic mutations that allow them to proliferate outside their normal growth restraint. In cancer cells mutations affect predominantly proto-oncogenes and tumor suppressor genes (Vermeulen *et al.*, 2003). A number of these genes are important in cell cycle checkpoints and DNA-damage recognition (Garrett 2001). Important examples are mutations in genes affecting Cdks, cyclins and checkpoint proteins (McDonald and Deiry 2000). Especially mutations in checkpoint proteins are frequent in all types of cancer. The tumor suppressor gene p53 is able to induce cell cycle arrest or apoptosis and is known to be the most frequently mutated gene in human cancer (Vermeulen *et al.*, 2003).

The cell cycle is therefore an attractive target for the development of novel anti-cancer agents. An example of therapeutically targeting the cell cycle, are cyclin-dependent kinase (Cdk) inhibitors. Flavopiridol, a flavonoid isolated from the Indian plant *Dysoxylum binectariferum* Hook F., is reported to inhibit Cdk1 and Cdk2 (Raju *et al.*, 2003). Other

compounds such as roscovitine and butyrolactone inhibit CDK4. Staurosporine, a microbial alkaloid, is an inhibitor of CDK1 (Vermeulen *et al.*, 2003; Schwartz and Shah 2005).

1.7 Cell death

It is possible to discriminate up to 12 pathways of cell death occurring in mammals (Fig. 26), 10 of which are genetically programmed. The different types of cell death are: necrosis, apoptosis, anoikis, caspase-independent apoptosis, autophagy, Wallerian degeneration (WD), excitotoxicity, erythropoiesis, platelets, cornification, lens and mitotic catastrophe. Apoptosis, autophagy or cornification are best known among the genetically programmed forms of cell death, but necrosis or mitotic catastrophe which are not genetically programmed lead to cell death as well (Melino *et al.*, 2005).

Different types of "Cell Death"											
	NECROSIS	APOPTOSIS	ANOIKIS	CASPASE-INDEPENDENT APOPTOSIS	AUTOPHAGY	WD	EXCITO-TOXICITY	ERYTHRO-POIESIS	PLT	CORNI-FICATION	LENS
Genetic Program	None	yes	yes	yes	yes	yes	yes	yes	yes	yes	yes
Membrane	Lysed	intact PS exposure	intact PS exp.	intact PS exp.	intact PS exposure	intact	intact	intact	intact	intact	
Organelles	Lysed	intact	intact	intact	intact lipid-reassembly	intact	intact	intact	intact	crosslinked lipid-reassembly lost	
Mitos	Blown	intact	intact					lost		lost	lost
Nucleus		chr.condens. DNA fragm.	chr.cond. DNA frag	chr.cond DNA fragm.	chr.condens. DNA fragm.			lost	lost	lost	lost
Enzymes	None	caspases	caspases	calpains	lysosomal beclin1	VPR	calpains NCX	calpains		TG 1,3,5	TG
Receptors		Death Rec									
Regulators		Bcl family IAP					NO calcium	GATA2		AP1 calcium	

Fig. 26: Different types of cell death

(Melino *et al.*, 2005)

Necrosis occurs predominantly in pathological conditions and is the end point of very severe damage, resulting in a loss of membrane integrity, swelling and disruption of the cells. The cellular contents are released into the cells environment leading to a strong inflammatory response (Leist and Jaattela 2001). Necrosis can be secondary to apoptosis. (Melino *et al.*, 2005).

1.7.1 Apoptosis

Apoptosis is a programmed cell death which occurs in response to physiological signals during embryonic development, in maintenance of homeostasis in multicellular organisms or to eliminate dysfunctional cells (Norbury and Hickson 2001). Apoptosis is strictly regulated and can be recognized by morphological modifications such as cellular shrinking, cell deformation and loss of contact to neighbouring cells. The chromatin condenses, marginates at the nuclear membrane and the cell membrane starts to show protrusions (blebs). The process of entire cell condensation and fragmentation into apoptotic bodies is called budding. The apoptotic bodies are engulfed by macrophages and removed from the tissue without causing an inflammatory response (Fig. 27) (Kurosaka *et al.*, 2003; Häcker 2000; Saraste and Pulkki 2000; Elmore 2007).

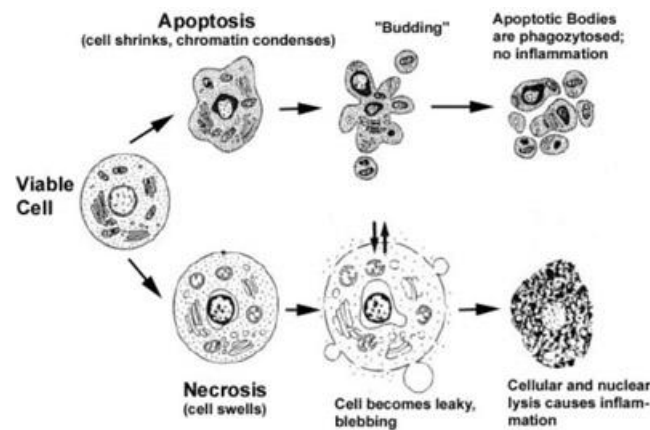


Fig. 27: Comparison of apoptosis and necrosis

(modified from: Van Cruchten *et al.*, 2002)

Dysfunction of the apoptotic machinery is involved in a variety of diseases, especially in cancer cells the balance is shifted towards uncontrolled cell proliferation.

Mechanisms of apoptosis: Apoptosis can be triggered through an intrinsic or an extrinsic pathway both leading to activation of caspases. The intrinsic pathway is initiated by death signals within the cell. Pro-apoptotic proteins like BAX and BAK are up-regulated, resulting in the release of cytochrome C from the mitochondria into the cytosol. Caspase 9, an initiator caspase, is activated and cleaves and activates caspase 3, an effector caspase, leading to apoptosis.

The extrinsic pathway is initiated by extracellular signals. A death-ligand binds to death-receptors like Fas and the initiator caspase 8 is activated leading to further activation of caspase 3 which is followed by apoptosis (Fig. 28) (Elmore 2007).

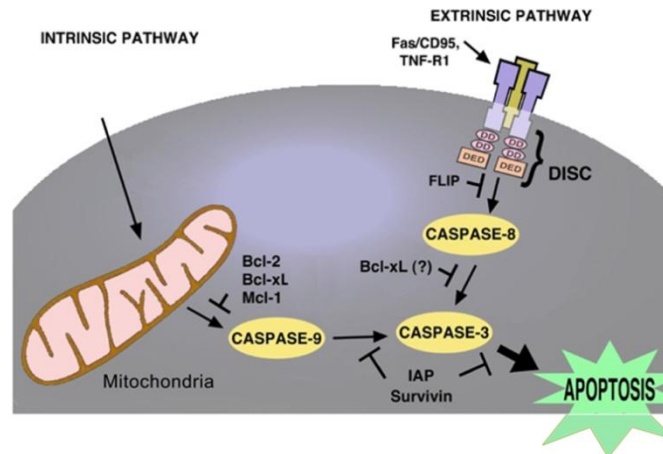


Fig. 28: The intrinsic and extrinsic pathway of apoptosis

(Pai *et al.*, 2006)

Caspases are cysteine proteases with an important role in the apoptotic machinery. They can be divided into two groups, the initiator and the effector caspases. Caspase 3, an effector kinase, is only activated in cells during apoptosis (Peng *et al.*, 2004). After proteolytic activation of caspase 3 from its proenzyme form, it cleaves various protein substrates during apoptosis such as poly(ADP-ribose) polymerase (PARP) (Shin *et al.*, 2000; Nicholson *et al.*, 1995; Kaufmann *et al.*, 1993). Caspase 6 and 7 also belong to the group of the effector caspases. Initiator caspases are caspase 8, 9 and 10. These caspases are auto-activated in a signal-dependent manner and are responsible for activation of the effector caspases.

Caspase 2 has features of both groups (Zhivotovsky and Orrenius, 2005), but unlike initiator caspases, caspase 2 does not directly activate effector caspases (Bouchier-Hayes 2010). The function of caspase 2 in apoptosis seems to be stimulus- and/or cell type specific (Bergeron *et al.*, 1998). There is evidence for potential roles of caspase-2 in non-apoptotic processes, including DNA repair and cell cycle regulation (Vakifahmetoglu-Norberg and Zhivotovsky 2010).

The BCL 2 family serves a central function in apoptosis and is divided into a pro- and an anti-apoptotic subfamily. Specifically, BAX and BAK are pro-apoptotic proteins and operate at both the mitochondria and endoplasmic reticulum to regulate the intrinsic

apoptotic pathway (Ruiz-Vela *et al.*, 2005; Oltvai *et al.*, 1993). BCL-XL and BCL 2, members of the anti-apoptotic sub-family and play an important role in inhibiting mitochondria-dependent cell death pathways (Kim 2005).

The apoptotic machinery is an important target in research for the development of new cancer therapeutics capable of killing continuously proliferating cells or restoring the normal growth rate of the cells.

1.7.2 Mitotic catastrophe

There still exists no broadly accepted definition of mitotic catastrophe (Niida *et al.*, 2005). The term mitotic catastrophe is used to describe cell death that occurs during or after incorrect mitosis characterized by formation of large cells that contain multiple or polyploid nuclei, but the mechanisms of regulation and the signals involved are barely characterized (Portugal *et al.*, 2010).

It has been discussed that mitotic catastrophe is totally different from apoptosis (Fig. 29) (Roninson *et al.*, 2001) because some manipulations preventing apoptosis, such as overexpression of BCL 2, enhance the frequency of catastrophic mitoses (Lock and Stribinskiene 1996; Ruth and Roninson 2000; Castedo *et al.*, 2004). But in fact there is no clear line between apoptosis and mitotic catastrophe. The latter can also be accompanied by the release of pro-apoptotic proteins and caspase activation (Portugal *et al.*, 2010). Most examples of mitotic catastrophe seem to be characterized by the activation of caspase 2. The treatment of human breast carcinoma cells with doxorubicin, one of the most effective anti-tumor drugs ever developed, induces polyploidy and cell death by mitotic catastrophe and activation of caspase 2 (Mansilla *et al.*, 2006). HCT116 colon carcinoma cells treated with doxorubicin undergo mitotic catastrophe as well (Chan *et al.*, 1999; Castedo *et al.*, 2004).

	Apoptosis	Mitotic catastrophe	Necrosis
Definition and characteristics	<ul style="list-style-type: none"> * Programmed cell death. * Cells shrink with blebbing of cell membranes. * Condensed chromatin and DNA fragmentation. 	<ul style="list-style-type: none"> * Cell death occurring during or after a faulty mitosis. * Giant cells with two or more nuclei and partially condensed chromatin. * Can lead to necrosis or apoptosis-like death (p53-independent). 	<ul style="list-style-type: none"> * Identifies, in a negative fashion, cell death lacking the features of apoptosis or autophagy. * Cells visible swell with breakdown of cell membrane. * Typical nuclei with vacuolization, and disintegrated cell organelles.
Associated genetic changes	<ul style="list-style-type: none"> * Stimulated by cyclin D1 activation and by Myc. * Can be inhibited by loss of wild-type p53. * Caspase activation. 	<ul style="list-style-type: none"> * Stimulated by deficiencies in proteins involved in G1 and G2 checkpoints and in mitotic spindle assembly: p53, p21, Cdk1, Chk1, Chk2, etc. * Can follow caspase-dependent or – independent routes. 	<ul style="list-style-type: none"> * In general, it is not considered genetically determined (this is open to debate).
Detection methods	<ul style="list-style-type: none"> * Sub-G1 peak in flow cytometry. * Annexin-V-staining. * Internucleosomal laddering, etc. 	<ul style="list-style-type: none"> * Cells with two or more nuclei detected by Microscopy or <i>Laser Scanning Cytometry</i>. * Accumulation in G2/M and polyploidy. 	<ul style="list-style-type: none"> * Early permeability to vital dyes. * Staining with propidium iodide. * Electron microscopy.

*Other antiproliferative responses, such as autophagy and induced senescence, have been reported [3, 4, 55, 61].

Fig. 29: Summary of several pathways of cell death

(Portugal *et al.*, 2010)

Several other anti-cancer drugs as well as ionizing radiation are known to induce mitotic catastrophe (Portugal *et al.*, 2010). For a long time apoptosis was considered to be the key mechanism of cell death in drug-treated cancer cells (Brown and Attardi 2005; Abend 2003). But mitotic catastrophe might be the main mechanism of tumor selectivity in the search for new anti-tumor agents since cell death by mitotic catastrophe showed a more intense and longer lasting effect *in vivo* (Portugal *et al.*, 2010; Roninson *et al.*, 2001). Another advantage of mitotic catastrophe in treatment could be that it is not regulated via p53, as this protein is frequently mutated in malignant tumor cells (Ianzini *et al.*, 2006 and 2007). Apoptosis is regulated by wild-type p53 and frequently inactivated due to a non-functional p53 protein (Levesque and Eastman 2007). Another advantage is, that in contrast to apoptosis, mitotic catastrophe is enhanced by some changes during the development of the tumor (Portugal *et al.*, 2010).

1.8 Traditional medicine

There is evidence in fossils that humans used plants as medicine at least from the Middle Paleolithic age (Solecki and Shanidar 1975). The best known and still used traditional medicines are Ayurveda, the traditional Indian medicine, and the traditional Chinese medicine (TCM). In the last decades there has been an increased interest in traditional medicine (Patwardhan *et al.*, 2005). Ethnomedicine or traditional medicine may be

defined as the use of plants by humans as herbal remedies, but literally it is a broad term used to define any non-Western medical practice (Farnsworth 1994; Bannerman *et al.*, 1983). For almost 65% of the world's population traditional medicine is their primary modality of health care (Farnsworth *et al.*, 1985).

Ethnopharmacology is a highly manifold approach to drug discovery involving the observation, description and experimental investigation of indigenous drugs and their biological activities. It is based on botany, chemistry, biochemistry and pharmacology (Rivier and Bruhn 1979; Fabricant and Farnsworth 2001).

Plants are used as sources of therapeutic agents to isolate bioactive principles for direct use as morphine, quinine or taxol on the one hand and on the other hand to find novel structures as lead compounds for semisynthesis like metformin, nabilone or taxotere. Another option is to use plant extracts as herbal remedies like echinacea or ginkgo biloba (Fabricant and Farnsworth 2001).

1.9 Natural products as sources of new drugs

Plants used in traditional medicine are a rich source for novel compounds for the development of new drugs (Kim and Park 2002). Numerous drugs have entered the international pharmacopoeia via the study of traditional medicine (Fig. 30) (Patwardhan 2009).

Drug	Medical use	Mechanism of action	Source
Aspirin	Analgesic, anti-inflammatory, antipyretic	Inhibition of COX	Plant
Atropine	Pupil dilator	Antagonist of ACh at muscarinic receptors at post-ganglionic parasympathetic neuroeffector sites	Plant
Caffeine	Stimulant	Adenosine receptor antagonist	Plant
Codeine	Analgesic, antitussive	Opioid receptor agonist	Plant
Digoxin	For atrial fibrillation and CHF	Inhibition of the Na ⁺ /K ⁺ ATPase membrane pump	Plant
Eugenol	Toothache	Reduces excitability of sensory nerves (increased K ⁺ efflux and reduced Ca ²⁺ influx)	Plant
Morphine	Analgesic	Opioid receptor agonist	Plant
Pilocarpine	Glaucoma	Muscarinic receptor agonist	Plant
Quinine	Malaria prophylaxis	Inhibition of protein synthesis in the malaria parasite	Plant
Taxol	Anticancer agent	Antimitotic agent (binds to and stabilizes microtubules)	Plant

Fig. 30: Drugs developed from natural sources

(selected compounds from: da Rocha *et al.*, 2001)

From 1984 to 1995 over 60% of the newly approved drugs were of natural origin. Drugs of natural origin have been classified into original natural products, products derived semisynthetically from natural products, synthetic products based on natural product models (Cragg *et al.*, 1997) and natural product mimics (Newmann and Cragg 2007). The figures of approval of new chemical entities (NCE) demonstrate that natural products are still involved in about 50% of all small molecules in the years 2000 to 2006 (Fig. 31) (Newmann and Cragg 2007).

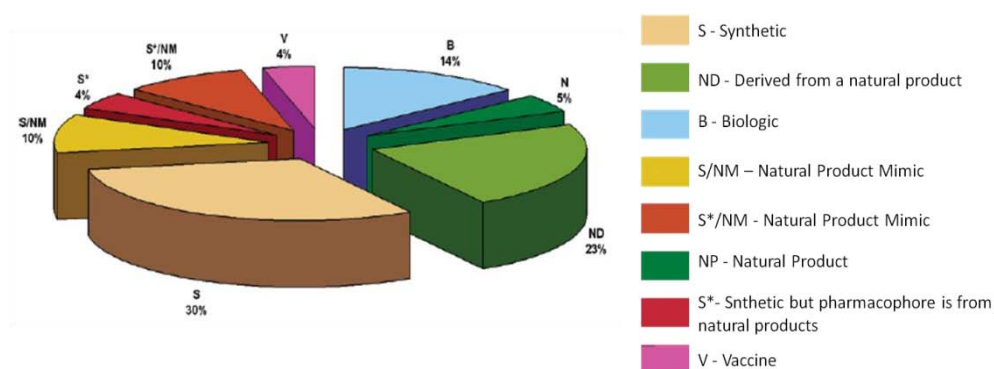


Fig. 31: All new chemical entities

(modified from: Newman and Cragg 2007)

1.9.1 Natural products as sources of new anti-cancer therapeutics

The chemical diversity of millions of species of plants, microorganisms and marine organisms is an attractive source of new therapeutic agents in cancer research (da Rocha *et al.*, 2001) In the field of cancer research around 50% of the drugs in current use are of natural origin (see Fig. 32) (Newmann and Cragg 2007).

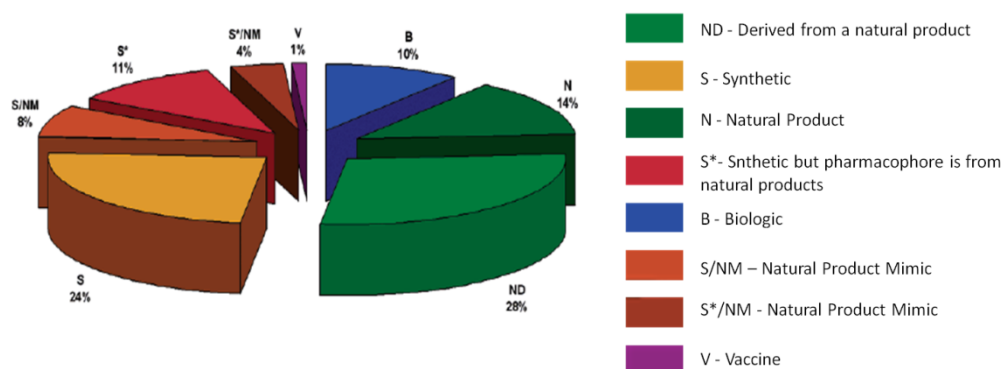


Fig. 32: All available anti-cancer drugs from 1940-2006

(modified from: Newman and Cragg 2007)

Especially plant species with the capacity to defend themselves against potential predators and inhibit other plants competing for space to grow with numerous chemical substances are a very rich source for new cytotoxic compounds (da Rocha *et al.*, 2001). The immense variety of secondary metabolites isolated from plants has been source of important pharmaceutical compounds (Hemalswarya and Doble 2006).

1.9.1.1 Alkaloids

From the ancient medicinal plant *Catharanthus roseus* G. Don. (Apocynaceae) the very potent cytotoxic compounds vinblastine and vincristine were isolated (da Rocha *et al.*, 2001). These substances and several structural relatives like vinorelbine and vindesine are used for a long time to treat childhood leukaemia, testicular cancer, Hodgkin's disease and several other cancers (Mann 2002; Cragg and Newman 2005).

Another class of clinically active anti-cancer agents derived from camptothecin isolated from *Camptotheca acuminata* Decne (Nyssaceae) (Rahier *et al.*, 2005). The effective derivatives are topotecan, which is used for the treatment of ovarian and small cell lung cancers, and irinotecan, which is used to treat colorectal cancers (Cragg and Newman 2005). Elliptinium, a derivative of the alkaloid ellipticine, was isolated from different species of the Apocynaceae family and is marketed in France for the treatment of breast cancer (Cragg and Newman 2005).

The most important anti-cancer drug isolated from the bark of *Taxus brevifolia* Nutt. is paclitaxel or Taxol (Fig. 33) which is used to treat refractory breast and ovarian cancers and non-small lung cancer and is, at present, the bestselling anticancer drug. From *Taxus baccata* L. a related chemical structure, 10-deacetylbaccatin, could be isolated which can be converted easily into taxol and another even more potent analogue, docetaxel or taxotere, which is used to treat non-small lung cancer and breast cancer (Mann 2002). Additionally, 23 taxanes are in preclinical development as potential anti-cancer drugs (Cragg and Newman 2005).

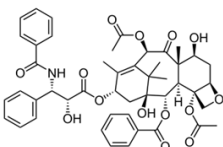
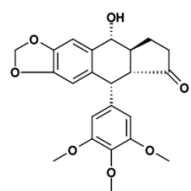
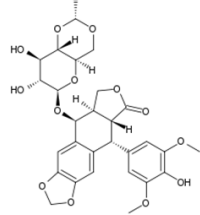
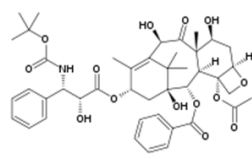
Compound	Cancer use	Status		
Vincristine	Leukemia, lymphoma, breast, lung, pediatric solid cancers and others	Phase III/IV	 Taxol	 Etoposide
Vinblastine	Breast, lymphoma, germ-cell and renal cancer	Phase III/IV		
Paclitaxel	Ovary, breast, lung, bladder, and head and neck cancer	Phase III/IV		
Docetaxel	Breast and lung cancer	Phase III	 Podophyllotoxin	 Docetaxel
Topotecan	Ovarian, lung and pediatric cancer	Phase II/III		
Irinotecan	Colorectal and lung cancer	Phase II/III		
Flavopiridol	Experimental	Phase I/II		
Acronyciline	Experimental	Phase II/III		
Bruceantin	Experimental	Preclinical/ phase I		
Thalicipin	Experimental	Preclinical/ phase I		

Fig. 33: Plant derived anti-cancer agents

(da Rocha *et al.*, 2001 and Cragg and Newman 2005)

1.9.1.2 Lignans

Native Americans already used extracts from the roots of *Podophyllum peltatum* L. (Podophyllaceae) to treat skin cancers. Later, the main constituent of this plant was identified as podophyllotoxin, which is the precursor of the podophyllins, a group of anticancer agents, which includes etoposide and teniposide (da Rocha *et al.*, 2001) (Fig. 33). Etoposide, the glycoside of the lignan podophyllotoxin, is in regular use for the effective treatment of testicular teratoma and small-cell lung cancer and teniposide is effective against acute lymphocytic leukaemia and neuroblastoma in children and against non-Hodgkin's lymphomas and brain tumours in adults (Mann 2002).

1.9.1.3 Flavonoids

In different studies the intake of certain polyphenols such as flavonoids and lignans in the diet was correlated with low incidence of colorectal cancer (Taraphdar *et al.*, 2001). Dietary flavonoids are known to be antiproliferative and may play an important role in cancer chemoprevention, especially for cancers of the gastrointestinal tract. Two potent dietary flavonoids, quercetin and genistein, induced apoptosis in colon cancer cells and genistein inhibits angiogenesis and cell-cycle progression (Taraphdar *et al.*, 2001; Hemalswarya and Doble 2006; Richter *et al.*, 1999; Kaindl *et al.*, 2008).

Tangerine peel, with its main flavonoid tangeretin, is used in Japan in Kampo medicines for treatment of cancer. Tangeretin blocks cell cycle progression and inhibits cancer cell growth through induction of apoptosis (Taraphdar *et al.*, 2001). Another flavonoid, baicalein, contained in the Japanese herbal medicine sho-saiko-to, inhibits the activity of topoisomerase II and induces apoptosis in different cell lines (Matsuzaki *et al.* 1996; Taraphdar *et al.*, 2001).

1.9.1.4 Xanthones

Some prenylated xanthones possess anti-cancer activity against MCF-7 and NCI-H460 cell lines (Castanheiro *et al.*, 2009) as well as against HeLa and MDA-MB-231 cancer cell lines (Lim *et al.*, 2011). α -Mangostin, the best studied prenylated xanthone isolated from *Garcinia mangostana* Linn., induces cell-cycle arrest in G1 and induce apoptosis through the activation of intrinsic pathway in human colon cancer DLD-1 cells (Matsumoto *et al.*, 2005; Akao *et al.*, 2008).

An ideal anti-cancer agent should have little or no toxicity related to cell necrosis, show high efficacy in multiple sites with a known mechanism of action, be capable of oral consumption, low in cost and have a high acceptance (Rajamanickam and Agarwal 2008).

2 AIMS OF THE THESIS

Cancer therapy is one of the most addressed issues in drug discovery and natural products and their structural relatives are an important source of novel anticancer agents, providing over 50% of the drugs in present clinical use (Newman and Cragg 2007). The chemical diversity of plants and the great variety of secondary metabolites are an attractive source of new pharmaceutical compounds (Hemalswarya and Doble 2006; da Rocha *et al.*, 2001). Numerous drugs have entered the international pharmacopoeia via the study of ethnopharmacology and traditional medicine (Patwardhan 2009).

As tropical plants used in traditional medicine are an interesting source for novel structures, *Metaxya rostrata* C. Presl, *Stachytarpheta jamaicensis* L. Vahl and *Maranta arundinacea* Pulm., which are used in traditional medicine against intestinal diseases in Costa Rica, were investigated.

Therefore the aim of this study was to

- 1) phytochemically investigate the tree fern *Metaxya rostrata*, as there is very little phytochemical data available.
- 2) isolate and elucidate the structures of the cytotoxic principles of the herbal remedies *Metaxya rostrata*, *Stachytarpheta jamaicensis* and *Maranta arundinacea* using a bioactivity-guided approach.
- 3) give an insight into the underlying mechanisms of action of the active compounds.

3 MATERIALS AND METHODS

3.1 Phytochemistry

3.1.1 Plant Material

Three different plants, used in Costa Rican traditional medicine, were collected. Rhizomes and/or leaves of *Stachytarpheta jamaicensis* L. Vahl, *Maranta arundinacea* Pulm. Ex. L. and *Metaxya rostrata* C. Presl were collected and sun dried in the surroundings of La Gamba (8° 41'N – 83° 13'W) near Golfito, south western Costa Rica, in autumn 2009 by Dr. Werner Huber. The plant material was authenticated in the Herbarium of the Museo Nacional in San Jose. Voucher specimens are deposited at the Herbarium of the Department of Pharmacognosy, University of Vienna, Austria (Fig. 34).¹



Fig. 34: Voucher specimen of the plant material

Metaxya rostrata is a tree fern, belonging to the family of the Metaxiaceae. It is widespread in the low land forests of Central- and Southamerica and used for the treatment of intestinal diseases by traditional healers in Costa Rica. *Maranta arundinacea* a herb, belonging to the family of the Marantaceae and *Stachytarpheta jamaicensis* a shrub, belonging to the family of the Verbenaceae, both used in traditional medicine as well.

¹ I am grateful to Dr. Werner Huber (Department of Structural and Functional Botany, University of Vienna) for collecting and identifying the plant material.



Fig. 35: Plant material

3.1.2 Extraction and Fractionation

In a previous study, the rhizomes of *Metaxya rostrata* were extracted by sonification with water. After vacuum liquid chromatography 15 fractions were obtained (Virtbauer 2007). Fraction 12 was not investigated in the previous work and due to the pattern of compounds and the moderate cytotoxic activity, this fraction was chosen for further separation.

For the bioactivity-guided approach, the rhizomes and rootlets of *Metaxya rostrata* were separated. The rhizomes, rootlets and leaves of the different plants were pulverized. All drug material was extracted in the same manner:

For pretesting, first extraction and fractionation steps the Accelerated Solvent Extraction (ASE) was used. For pretesting, 5 - 10g plant material were extracted 3 times at 40°C with CH₂Cl₂, EA, MeOH and water using ASE (Table 1). For the extraction of the active extracts after pretesting, 100g rootlets (for CH₂Cl₂- and EA-extract), 120g leaves (EA-extract) and 300g rhizomes (MeOH-Extract) were used. Portions of around 20g of the drug material were extracted 3 times at 40°C with the respective solvent using ASE (Table 2). For the re-extraction and re-fractionation of the most active fractions, 920g of rootlets were

pulverized and portions of 200g were extracted 4 times in the ultrasonic bath at 40°C for 1 hour with 800ml CH₂Cl₂, each.

	Leaves <i>Metaxya rostrata</i> 5,8g	Rootlets <i>Metaxya rostrata</i> 7,6g	Rhizomes <i>Metaxya rostrata</i> 7,5g	Roots Maranta arundinacea 9g	Roots Stachytarpheta jamaicensis 5,4g
CH ₂ Cl ₂	148	99	39	53	124
EA	33	33	19	8	20
MeOH	1006	480	636	339	117
Water	18	175	455	151	218

Table 1: Yields (in mg) of the extracts for pretesting

	Leaves <i>Metaxya rostrata</i> 120g	Rootlets <i>Metaxya rostrata</i> 100g	Rootlets <i>Metaxya rostrata</i> 920g	Rhizomes <i>Metaxya rostrata</i> 300g
CH ₂ Cl ₂	-	1.01	5.37	-
EA	0.82	1.22	-	-
MeOH	-	-	-	30.63

Table 2: Yields (in g) of selected extracts

3.1.3 Chromatographic Methods

3.1.3.1 Thin layer chromatography (TLC)

Stationary phases	
1	Silica gel 60 F ₂₅₄ -precoated plates, 20 x 20cm, Merck
2	Polyamide plates, 20 x 20cm, Merck

Table 3: Stationary phases in thin layer chromatography

Mobile phases		
1	ethylacetate : formic acid : MeOH : H ₂ O	70 : 8 : 8 : 11
2	acetonitrile : formic acid : acetic acid : H ₂ O	100 : 11 : 11 : 26
3	ethylacetate : acetic acid : MeOH : H ₂ O	100 : 11 : 11 : 26
4	cyclohexane : dichlormethane : formic acid : ethylformiate	35 : 30 : 5 : 30
5.1	dichlormethane : formic acid : ethylformiate	30 : 5 : 30
5.2	dichlormethane : formic acid : ethylformiate	60 : 5 : 30
6	n-pentane : ethylacetate	85 : 15
7.1	chloroform : MeOH : H ₂ O	70 : 22 : 3
7.2	chloroform : MeOH : H ₂ O	60 : 40 : 10

7.3	chloroform : MeOH : H ₂ O	85 : 8 : 0,5
8	ethylacetate : MeOH : H ₂ O	81 : 11 : 8
9	MeOH : H ₂ O : trifluor-acetic acid	1 : 1 : 0.6
10	toluene : ethylformiate : formic acid	10 : 4 : 1
12	ethylacetate : formic acid : acetic acid : H ₂ O	100 : 6 : 6 : 2
13	2-propanol : acetone : 1M lactic acid	40 : 40 : 20

Table 4: Mobile phases in thin layer chromatography

After development, the plates were dried and sprayed with one of the following detection reagents:

Detection			
1	Anisaldehyde-H ₂ SO ₄ reagent	85ml MeOH + 10ml conc. acetic acid + 5ml conc. sulphuric acid + 0,5ml anisaldehyde	After spraying the plate was heated at 110° for 5-10 min and analysed by daylight
2	Naturstoff(NS)–Polyethylenglycol (PEG)–reagent	1% methanolic solution of Naturstoffreagens A 5% ethanolic solution of PEG	After spraying with NS, the plate was dried, then sprayed with PEG and analysed under UV ₃₆₆
3	Anilin - diphenylamin – reagent	0,5ml of aniline + 0,5g of diphenylamine + 20ml Aceton + 4ml of 85% phosphoric acid	After spraying the plate was dried and analysed by daylight

Table 5: Detection reagents in thin layer chromatography

3.1.3.2 Column chromatography

The columns were packed with the respective stationary phase. The application of the sample depended on the stationary phase. For Sephadex columns the sample was dissolved in a very small amount of the mobile phase and applied on the column. For silica gel columns the sample was adsorbed on double amount of the stationary phase and placed on top of the column.

Stationary phases	
SP 1	Silica gel 60, particle size 0,063-0,200mm, Merck
SP 2	Sephadex LH-20, Pharmacia Biotech AB

Table 6: Stationary phases in column chromatography

Mobile phases for SP 1		used for:
MP 1/1	water-saturated EtOAc : MeOH (90+10)	CC-2, CC-5, CC-6
MP 1/2	water-saturated EtOAc : MeOH (80+20)	CC-7
MP 1/3	water-saturated EtOAc	CC-4

Mobile phases for SP 2		used for:
MP 2/1	80% MeOH	CC-1, CC-12
MP 2/2	50% MeOH	CC-3, CC-8
MP 2/3	EtOAc	CC-9, CC-10, CC-11, CC-13

Table 7: Mobile phases in column chromatography

3.1.3.3 HPLC

HPLC data were recorded on a Shimadzu instrument using LC solution software.

HPLC-Instrumentation:

<i>Degasser</i>	Shimadzu DGU 20A5 prominence Degasser
<i>Controller</i>	Shimadzu CBM 20A prominence Communication Bus Module
<i>Autosampler</i>	Shimadzu SIL 20AC HAT prominence Auto Sampler
<i>Pump</i>	Shimadzu LC 20AD prominence Liquid Chromatograph
<i>Detector</i>	1 Shimadzu SPD M20A prominence Diode Array Detector 2 Shimadzu ELSD-LT (Low Temperature Evaporative Light Scattering Detector)
<i>Column Oven</i>	Shimadzu CTO 20AC prominence Column Oven
<i>Software</i>	LC Solution

Method 1		Used for:
Column	LiChroCART, 250x4mm, RP-18e, 5µm	SPE-3/4
Eluent A	1% formic acid in water	SPE-3/3
Eluent B	acetonitrile	SPE-7/3
Flow Rate	1ml/min	SPE-8/4
Temperature	25°C	
Gradient program 1	time, min	% Eluent B
	Start	60 %
	0 - 25 min	60 %
	26 - 65 min	100 %
	66 - 70 min	100 %

Method 2		Used for:
Column	LiChroCART, 250x4mm, RP-18e, 5µm	SPE-5/2
Eluent A	1% formic acid in water	SPE-6/2
Eluent B	acetonitrile	
Flow Rate	1ml/min	
Temperature	25°C	
Gradient program 2	time, min	% Eluent B
	Start	40 %
	0 – 15 min	40 %
	16 – 25 min	60 %
	26 – 45 min	60 %
	46 – 55 min	100 %
	56 – 60 min	100 %

Method 3		Used for:
Column	LiChroCART, 250x10mm, RP-18e, 5µm	CC-9/5
Eluent A	1% formic acid in water	
Eluent B	acetonitrile	
Flow Rate	10ml/min	
Temperature	25°C	
Gradient program 3	time, min	% Eluent B
	Start	48 %
	0 - 35 min	51 %
	36 - 37 min	100 %
	38 - 48 min	100 %

Table 8: Methods for HPLC

3.1.4 Removal of chlorophyll

As chlorophyll is known to interfere unspecifically with different test systems, it was removed using liquid - liquid partition. 1g CH₂Cl₂-extract was dissolved in 150ml CH₂Cl₂ and 150ml MeOH water (1:1) were added. After evaporation of CH₂Cl₂, the chlorophyll precipitated in the MeOH - water mixture and was removed by filtration.

3.1.5 Solid phase extraction (SPE)

RP-cartridges (C-18, 20ml, Bond Elut, Varian) were conditioned with 2 reservoir volumes MeOH and 2 reservoir volumes water. The fractions were dissolved in CH₂Cl₂, applied on the cartridges and dried by air purge. The fractions were eluted with 4 reservoir volumes

of 20%, 40%, 60%, 70%, 80%, 90% and 100% MeOH, each. The fractions of identical polarity were pooled and evaporated.

3.1.6 Spectroscopic and spectrometric methods

3.1.6.1 Mass-spectrometry (MS)

ESI-MS data were recorded on a API 4000 triple quadrupole mass spectrometer (AB Sciex Instruments, Foster City, CA, USA) configured for both negative and positive ionization mode. Mass spectra were acquired over the range m/z 100-1000, scan time was 1s. Product ions (MS/MS) were scanned from m/z 40-400 within 1s of scan time. FIA was carried out using MeOH/aqueous ammoniumacetate 5mmol (80:20).²

3.1.6.2 Nuclear magnetic resonance (NMR)

NMR spectra were recorded on a Bruker Advance DRX 600 NMR spectrometer using a 5 mm switchable quadruple probe (QNP, ^1H , ^{13}C , ^{19}F , ^{31}P) with z axis gradients and automatic tuning and matching accessory. The resonance frequency for ^1H NMR was 600.13 MHz, for ^{13}C NMR 150.92 MHz. All measurements were performed for a solution in fully deuterated methanol at 298 K. Standard 1D and gradient-enhanced (ge) 2D experiments, like double quantum filtered (DQF) COSY, TOCSY, NOESY, HSQC, and HMBC, were used as supplied by the manufacturer. Chemical shifts are referenced internally to the residual, non-deuterated solvent signal for ^1H ($\delta = 3.31$ ppm) or to the carbon signal of the solvent for ^{13}C ($\delta = 49.00$ ppm) The analysis of the ^1H – ^1H coupling constants (given in Hertz) were supported by the program Spin-Works (provided by Kirk Marat, University of Manitoba, Canada).³

3.1.6.3 Infrared spectroscopy (IR)

Infrared spectra were measured on a Perkin Elmer FT-IR 2000 instrument in attenuated total reflection mode using a Golden Gate ATR unit.

² I am grateful to Dr. Martin Zehl and Mag. Oliver Donath (Department of Pharmacognosy, University of Vienna) for performing the MS experiments.

³ I am grateful to Dr. Hanspeter Kählig (Institute of Organic Chemistry, University of Vienna) for performing the NMR experiments.

3.1.6.4 UV / VIS Spectroscopy

UV-VIS spectra of KK1 were measured in a methanolic solution on a Beckman DU 640 Spectrophotometer using MeOH as blank.

3.1.7 Crystallography

Compound KK1 was crystallized from a solvent mixture of methanol and diethylether. Single crystal X-ray structure analysis was performed on a Bruker X8 APEXII CCD diffractometer with graphite-monochromated MoK α radiation, $\lambda = 0.71073 \text{ \AA}$.⁴

3.1.8 Histone deacetylase (HDAC) assay

A fluorimetric *in vitro* enzyme assay was used to evaluate the influence of KK1 on HDACs. The principle of the assay is the deacetylation of ϵ -acetylated lysine-based substrate coupled with 4-methyl-coumarine-7-amide by HDAC. The endopeptidase recognizes the deacetylated substance as a substrate and releases 7-amino 4-methylcoumarin, which is highly fluorescent and can be measured.⁵

3.1.9 Antibacterial assay

A standard *S. aureus* strain (ATCC 25923) and a clinical isolate (XU212), which possesses the TetK efflux pump and is also a MRSA strain, were obtained from E. Udo. Strain RN4220, which has the MRSA macrolide efflux pump, was provided by J. Cove. EMRSA-15 and EMRSA-16 were obtained from Paul Stapleton. Strain SA-1199B, which overexpresses the NorA MDR efflux pump, was the gift of Professor Glenn Kaatz. Norfloxacin was obtained from Sigma Chemical Co. Mueller-Hinton broth (MHB) was adjusted to contain 20 mg/L Ca²⁺ and 10 mg/L Mg²⁺.

Overnight cultures of each strain were made up in 0.9% saline to an inoculum density of 5×10^5 cfu by comparison with a MacFarland standard. Tetracycline and oxacillin were dissolved directly in MHB, whereas norfloxacin and erythromycin were dissolved in DMSO and then diluted in MHB to give a starting concentration of 512 $\mu\text{g/mL}$. Using Nunc 96-

⁴ I am grateful to Dr. Vladimir Arion (Institute of Inorganic Chemistry, University of Vienna) for performing the X-ray diffraction crystallography.

⁵ I am grateful to Dr. Stanimira Krasteva (Department of Pharmacognosy, University of Vienna) for performing the HDAC assay.

well microtiter plates, 125 μ L of MHB was dispensed into wells 1-11. Then, 125 μ L of the test compound or the appropriate antibiotic was dispensed into well 1 and serially diluted across the plate, leaving well 11 empty for the growth control. The final volume was dispensed into well 12, which being free of MHB or inoculum served as the sterile control. Finally, the bacterial inoculum (125 μ L) was added to wells 1-11, and the plate was incubated at 37°C for 18 h. A DMSO control (3.125%) was also included. All MICs were determined in duplicate. The MIC was determined as the lowest concentration at which no growth was observed. A methanolic solution (5 mg/mL) of 3-[4,5-dimethylthiazol-2-yl]-2,5-diphenyltetrazolium bromide (MTT) was used to detect bacterial growth by a colour change from yellow to blue.⁶

3.1.10 Antiviral assay

Verocells were seeded in 96-well plates and grown for 24 h before treatment with 1, 10 and 100 μ M of compound KK1 in serumfree MEM (SFM) with and without Herpes Simplex 1 virus (HSV-1 17 syn⁺) for 48 h and one control with cells in SFM and one control with cells plus HSV-1.⁷

3.1.11 Insecticidal assay

The test organism for the insecticidal assay was *Spodoptera littoralis*, a Noctuidae, which is an important pest in tropical areas and feeds on over 50 different plant families. For the assay the compound was incorporated in different concentrations into the food and 20 freshly slipt larvae were put directly on the food piece. After 4 and 7 days the larvae were weighed.⁸

⁶ I am grateful to Dr. Simon Gibbons and his working group (School of Pharmacy, University of London) for performing the antibacterial tests.

⁷ I am grateful to Dr. Andreas Hensel and his working group (Institut für pharmazeutische Biologie und Phytochemie, Westfälische Wilhelms-Universität Münster) for performing the antiviral tests.

⁸ I am grateful to Mag. Johann Schinnerl (Department of Systematic and Evolutionary Botany, University of Vienna) for the support in performing the insecticidal assay.

Food for <i>Spodoptera littoralis</i>	
white beans	150g
37 % formaldehyde (Merck, Nr.4003)	1 ml
ascorbic acid (Merck, Nr.500074)	3 g
Nipagin (Sigma, Nr.H-2128)	3 g
Gentamycin (Serva, Nr.22185)	0,18 g
yeast	30 g
Agar-Agar (Merck, Nr.1614)	10 g
water	775 ml



Table 9: Food for *Spodoptera littoralis*

3.1.12 Antifungal assay

The test organism for the fungal assay was *Cladosporium sphaerospermum*. The fractions were separated on a TLC plate. After the complete removal of the mobile phase, the plate was sprayed with fungal spores and a growth medium. After 2 days the growth inhibition of active compounds were seen.⁹

3.1.13 *In Silico* screening

Pharmacophore profiling against more than 2200 models representing over 280 pharmacological targets was performed using DiscoveryStudio 2.5 (www.accelrys.com). A structural similarity search in the MDL Drug Data Report (MDDR) database was conducted with sea.docking.org.¹⁰

3.1.14 Chemicals and Solvents

All solvents used for extraction, chromatography and other phytochemical work were from highest purity grade available and purchased from VWR (Vienna, Austria).

⁹ I am grateful to Mag. Johann Schinnerl (Department of Systematic and Evolutionary Botany, University of Vienna) for the support in performing the anti-fungal assay.

¹⁰ I am grateful to Dr. Daniela Schuster (Department of Pharmaceutical Chemistry, University of Innsbruck) for performing the *in silico* screening.

3.2 Cell Biology

3.2.1 Cell lines

All cell lines used (SW480, HT29, CaCo2, LT97 and F331) were obtained from ACCT.

3.2.1.1 SW480

SW480 is a human colorectal adenocarcinoma cell line, male, which was established by A. Leibovitz. SW480 cells have epithelial form and the chromosome number is hypertriploid. This cell line expresses elevated levels of p53 and is positive for expression of myc, ras, myb, sis and fos oncogenes (www.atcc.org). SW480 cells grow attached with MEM with 10% FCS and 4% Penstrep and have a doubling time of 24 hours.

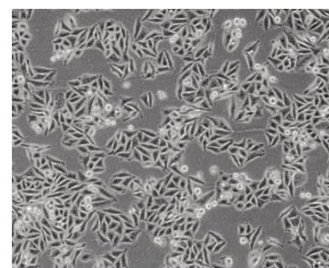


Fig. 36: SW480

3.2.1.2 HT29

HT29 is a human colorectal adenocarcinoma cell line, female, which was established by J. Fogh. HT29 cells have epithelial form and are hypertriploid. p53 is overproduced and the cells show positive expression of myc, ras, myb, sis and fos oncogenes (www.atcc.org). HT29 cells grow in monolayers and are cultivated in MEM with 10% FCS and 4% Penstrep and show a doubling time of 36 hours.

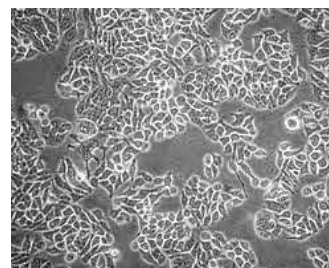


Fig. 37: HT29

3.2.1.3 Caco-2

Caco-2 is a human colorectal adenocarcinoma cell line, male, which was established by J. Fogh (www.atcc.org). CaCo-2 are cultivated with MEM plus 20% FCS and 4% Penstrep and show a doubling time of 60-72 hours.

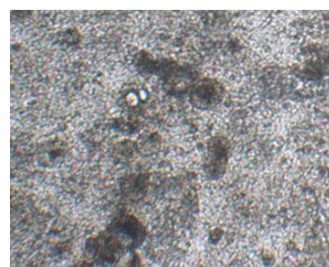


Fig. 38: CaCo-2

3.2.1.4 LT97

LT97 is a human colon adenoma cell line which was established in our laboratory by B. Marian and M. Richter. LT97 have lost both APC allele and show a Ki-ras mutation. This cell line is cultivated in HAM-F12 media plus 20% L-15 media, 2% FCS, $5 \cdot 10^{-9}$ M natriumselenit, $2 \cdot 10^{-10}$ M triiodotyronin, 10 µg/ml insulin, 2µg/ml transferrin, 1 µg/ml hydrocortisone, 30 ng/ml EGF. Under these conditions the cells show a doubling time 72-96 hours.

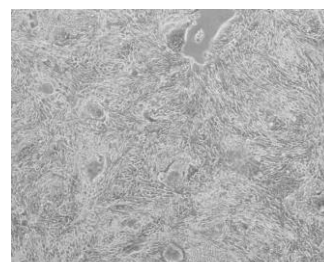


Fig. 39: LT97

3.2.1.5 F331

F331 cells are embryonic human colon associated fibroblasts, which are cultivated in DMEM media plus 4% Penstrep and 10% FCS. Under these conditions they show a doubling time 24 hours.

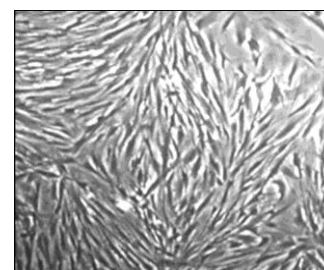


Fig. 40: F331

3.2.2 Passaging of cells

SW480, HT29, Caco2 and F331 cells are passaged when they reach a confluence of about 90%. Medium is removed and the cells are washed with 5-10ml of PBS/EDTA and incubated with 0,5ml Trypsin/PBS for 5-10min at 37°C. The detached cells are taken up in 10ml culture medium and passaged into new Petri dishes (PD).

LT97 cells are split when they reach a confluence of about 90%. Culture medium is aspirated and the cells are washed with PBS/EDTA and incubated at 37°. The detached cells are taken up in medium, washed and passaged.

SW480	HT29	Caco-2	LT97	F331
1:10	1:10	1:3	1:3	1:3

Table 10: Passaging of cells

10cm PD	6cm PD	12-well plate	24-well plate	96-well plate
1.3×10^6	5×10^5	5×10^4	2×10^4	3×10^3

Table 11: Density of cells in different culture dishes

3.2.3 Materials used for cell culture

Petridishes (10cm and 6cm)	Sarsted, Nümbrecht, Germany
6-well plates, 24-well plates and 96-well plates	Sarsted, Nümbrecht, Germany
Penicillin/Streptomycin (Penstrep)	PAA, Pasching, Austria
Fetal calf serum (FCS)	PAA, Pasching, Austria
Trypsin/PBS 10x (for use diluted 1:10 in PBS)	PAA, Pasching, Austria
Eagles Minimal Essential Medium (MEM)	Sigma-Aldrich, St. Louis, MO, US
Bovine Serum Albumin (BSA)	Sigma-Aldrich, St. Louis, MO, US
Phosphate buffered saline (PBS)	Sigma-Aldrich, St. Louis, MO, US
Tween	Sigma-Aldrich, St. Louis, MO, US
Triton X-100	Sigma-Aldrich, St. Louis, MO, US
DMSO	Sigma-Aldrich, St. Louis, MO, US
PBS/EDTA (10mM EDTA in PBS)	Merck, Darmstadt, Germany
Milk Powder	Fluka Biochemika, Buchs, Switzerland

3.2.4 Measurement of cell viability

3.2.4.1 MTT assay – EZ4U

The MTT assay is a colorimetric assay which measures the activity of the mitochondrial dehydrogenase of living cells. The water soluble light yellow 3-(4,5-dimethylthiazol-2-yl)-2,5-diphenyltetrazolium bromide (MTT) is taken up by living cells and reduced to an intensely coloured formazan by a mitochondrial dehydrogenase. As the amount of product is proportional to the number of viable cells in the culture, this reaction is suitable to assess the number of viable cells.

Cells were seeded at a density of 3×10^3 cells per well into 96-well plates and after treatment with active compounds, the supernatant was replaced by 100µl of freshly prepared EZ4U solution (EZ4U, Biomedica, Vienna, Austria). The cells were incubated at 37°C for 2 hours and the absorbance was measured at 492 nm in a microplate reader Synergy H1 (Szabo Scandic, Vienna, Austria).

3.2.4.2 Neutralred uptake

This colorimetric assay is based on the ability of viable cells to incorporate and bind neutral red in their lysosomes, where due to the acidic pH-value it changes its colour into pink red. Dead cells cannot store Neutralred and are therefore not stained.

Cells were seeded at a density of 3×10^3 cells per well into 96-well plates and 5×10^4 cells per well into 24-well plates. 50 µg/ml Neutralred (Merck, Darmstadt, Germany) were dissolved in serumfree MEM at 37°C for 1 hour and filtered. After treatment with active compounds, the supernatant was removed and 200µl for each 96-well and 500µl of the neutral red solution for each 24-well were added. After incubation of the plates at 37°C for 2 hours, the neutral red solution was removed and the cells were washed with 1xPBS. Thereafter Neutralred was extracted with 100µl of 70% Ethanol + 1% acetic acid in 96-wells and 250µl in 24-wells for 10 minutes at room temperature while shaking gently. The absorbance was measured at 562nm wavelength in a microplate reader Synergy H1 (Szabo Scandic, Vienna, Austria).

3.2.5 Fluorescence activated cell sorting (FACS)

Fluorescence activated cell sorting is a specialized type of flow cytometry which is used to divide a heterogeneous mixture of cells with regard to size, complexity and fluorescence emission.

3.2.5.1 Cell cycle distribution

Cells were seeded at a density of 5×10^5 cells per 6cm PD. The supernatant of treated cells was removed and the cells were washed with PBS/EDTA and Trypsin/EDTA was added. After incubation at 37°C for 5-10 minutes MEM with 10% FCS was added and the cells were transferred in a 15ml Falcon tube. After centrifugation at 1200 rpm for 5 minutes the cell pellet was resuspended in 1ml 1xPBS and transferred into a 1.5ml tube. 1ml of nuclear isolation buffer was added, mixed well and incubated for 5 minutes on ice. Nuclei were prepared and separated using a syringe. Then they were collected by centrifugation for 5 minutes at 4°C at 2000 rpm, resuspended in 0.5 ml propidium iodide staining solution and transferred into light protected FACS vials. Cell cycle was measured using a FACS Calibur (BD, Franklin Lakes, NJ, USA).

Nuclear isolation buffer:		RNase stock solution:	
10.5g	citric acid	10mg	RNase A
0.5ml	Tween 20	10ml	1xPBS
to 100ml	aqua bidest	incubate 15 min 100°C	
		Put on ice immediately; store at -20°C	

Propidium Iodide stock solution:		Staining solution:	
5mg	Propidium Iodide	0.05ml	RNAse stock solution
10ml	1xPBS	0.05ml	PI stock solution
		5ml	1xPBS

3.2.5.2 Quantification of apoptosis: JC-1-FACS

Cells were seeded at a density of 5×10^5 cells per 6cm PD. The supernatant of treated cells was removed and the cells were washed twice with PBS/EDTA and Trypsin/EDTA was added. After incubation at 37°C for 5-10 minutes MEM with 10% FCS was added, the cells were transferred in a 15ml Falcon tube and centrifuged at 1200 rpm for 5 minutes. Under light protection, the cell pellet was suspended in 1 ml JC-1 solution (10µg JC-1 per 1 ml 10% FCS MEM) and transferred into a 1.5 ml tube and incubated for 10 minutes at 37°C. After centrifugation at 4°C for 5 minutes at 1200 rpm the cell pellet was washed twice with cold 1xPBS, resuspended in 0.5 ml cold 1xPBS and transferred into FACS vials. Apoptosis was measured immediately on a FACS Calibur (BD, Franklin Lakes, NJ, USA).

3.2.6 Detection of apoptosis: Hoechst-Staining

Hoechst stain-33258 intercalates into DNA and is used to visualize the nuclei in the fluorescence microscope. This blue fluorescent dye is excited by ultraviolet light at 365nm. The fixed cells after neutral red assay were used for Hoechst - Staining. The cells were washed with 1xPBS and thereafter 500µl of staining solution (5µg Hoechst in 1ml SFM) was added and incubated for 10 minutes under light protection. The cells were washed with 10mM citratebuffer (pH3) and covered with Geltol. Under the fluorescence microscope the apoptotic cells were counted.

3.2.7 Lactatdehydrogenase (LDH)-assay

The LDH-assay (Roche Diagnostics GmbH, Basel, Switzerland) is an enzymatic assay for the quantification of viable cells. Necrotic cell lysis is assessed by LDH release into the supernatant as a marker of dead cells.

In the first step the released LDH reduces the NAD^+ to $\text{NADH} + \text{H}^+$ and lactate is oxidized to pyruvate. In a second enzymatic reaction a tetrazolium salt is reduced to deep red formazan as shown in Fig. 41.

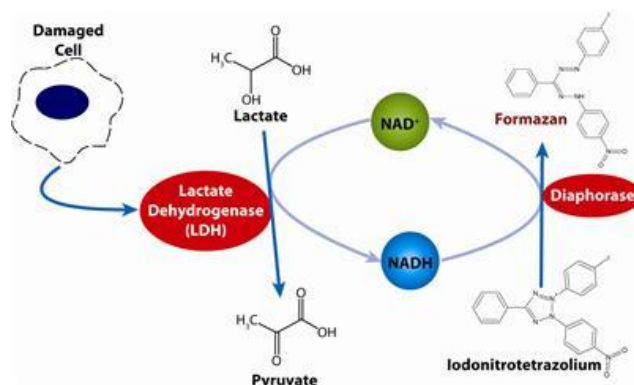


Fig. 41: Principle of the LDH-assay

(<http://www.gbiosciences.com>)

After the treatment of the cells with the active compound, 100 μl of the supernatant were mixed with 100 μl of the reagent (Diaphorase/ NAD^+ Mixture, iodonitrotetrazolium chloride, sodiumlactate) and incubated for 30 minutes at room temperature with light protection. The intensity was measured at 490nm. As a positive control cells treated with 1% Triton X 100 were used. The cytotoxicity is stated in % of this maximum value and calculated according to: $\text{Cytotoxicity (\%)} = [(measured\ data - neg.\ control) / (pos.\ control - neg.\ control)] \times 100$

3.2.8 FoxM1-staining

The forkhead transcription factor FoxM1 is an important regulator of gene expression during the G2 phase (Laoukili *et al.*, 2008). Loss of the transcriptional factor FoxM1 affects genes necessary for chromosome segregation, generates mitotic spindle defects and delays in mitosis and leads to mitotic catastrophe (Vakifahmetoglu *et al.*, 2008; Wonsey *et al.*, 2005). Fixed cells were incubated with PBS containing 0.25% Triton X-100 for 10 minutes. Thereafter the cells were washed 3 times with PBS and then incubated with 1% BSA in PBS-T for 30 minutes to block the unspecific binding. The cells were incubated then with the diluted antibody in 1% BSA in PBS-T for 1 hour. The solution was decanted and the cells were washed 3 times with PBS. Incubation with the secondary antibody (FICTS

anti-rabbit) in dark and again 3 washing steps with PBS in dark followed. After counter staining with Hoechst-stain and covering with Geltol the cells were analyzed with the fluorescence microscope.

3.3 Protein chemistry

3.3.1 Western blotting

Western blotting is an analytical technique used to identify and locate proteins based on their ability to bind to specific antibodies which can give information on protein expression.

Proteins are isolated and equal amounts of these protein lysates are applied to a polyacrylamid gel containing sodiumdodecylsulfate (SDS). SDS charges the proteins negativ so that the proteins can be separated via gel electrophoresis due to their size. Proteins are then transferred to a polyvinylidene fluoride membrane (PVDF), where they are detected using antibodies specific to the target protein. After incubation with an enzyme-coupled second antibody, detection is achieved by an enzymatic reaction producing chemoluminescence and exposure to a photosensitive film.

3.3.1.1 Protein isolation

The treated cells were scraped from the PD surface, centrifuged, washed twice with cold 1xPBS containing phosphatase inhibitors (1 μ l/ml Na₃VO₄ and 10 μ l/ml 1M NaF) and lysed with Hepes lysis buffer. The lysates were incubated for 30 minutes on ice and vortexed 3 times. Thereafter they are exposed to ultrasound for 10 minutes to break up DNA and centrifuged at 15000rpm for 5 minutes. The supernatant, which contains the proteins is transferred into tubes and stored at -20°C.

Hepes lysis buffer	
1M Hepes	1ml
1M NaCl	10ml
0,5M EDTA solution	40 μ l
1M NaF solution	200 μ l
1M NaVO ₄ solution	100 μ l
Igepal (NP40)	200 μ l
1M MgCl ₂ solution	30 μ l
Complete	2 tablettes
aqua bidest	8,03ml

3.3.1.2 Evaluation of protein concentration with Coomassie

For the protein standard curve aqua bidest, Hepes lysis buffer and BSA solution (1 μ g/ μ l) are pipetted into a 96-well plate according to the following scheme:

BSA concentration [μ g/ μ l]	0	1	2	3	4	5	6	7	8	9
Aqua bidest [μ l]	9	8	7	6	5	4	3	2	1	0
Hepes lysis buffer [μ l]	1	1	1	1	1	1	1	1	1	1
BSA [μ l]	0	1	2	3	4	5	6	7	8	9
Total volume [μ l]	10	10	10	10	10	10	10	10	10	10

Table 12: Pipette schemata for the evaluation of protein concentration

For protein samples 1 μ l protein lysate and 9 μ l aqua bidest were mixed in a 96-well. Thereafter 150 μ l of a 1:5 diluted Coomassie Protein Assay Dye Reagent Concentrate (BioRad, Berkeley, US) solution was added to each well of the standard curve and protein samples. Standard curve and protein samples were determined in duplicates. The absorption was measured at 590nm and the protein concentration of the samples was calculated according to the standard curve.

3.3.1.3 SDS-polyacrylamid gel electrophoresis (PAGE)

An SDS separating gel was poured into a sandwich made of glass plates, overlayed with ethanol and left for 1 hour to polymerise. Then the ethanol was removed, the separating gel was overlayed with an SDS collecting gel and a comb inserted during polymerisation to create slots. 30 μ g protein were mixed with 4x sample buffer, heated at 80°C for 5 minutes and then loaded onto the gel. 5 μ l protein ladder (PageRuler™ Prestained Protein Ladder, Fermentas, Burlington, Canada) were loaded into the reference slot. The chambers were filled with electrophoresis buffer and the run performed for 15 minutes with 60 Volt and then for 1 hour at 125 Volt. Gel electrophoresis apparatus was obtained from Bio-Rad.

SDS separating gel	7%	12%	15%	SDS collecting Gel	
40% Acrylamid	0.875ml	1.5 ml	1.875ml	40% Acrylamid	0.25ml
1.5M Tris pH 8.8	1.25ml	1.75 ml	1.25ml	1.5M Tris pH 6.8	0.313ml
Aqua bidest	2.8ml	2.15 ml	1.8ml	Aqua bidest	1.9ml
10% SDS	50 μ l	50 μ l	50 μ l	10% SDS	25 μ l
10% APS	25 μ l	25 μ l	25 μ l	10% APS	12.5 μ l
TEMED	2.5 μ l	2.5 μ l	2.5 μ l	TEMED	2.5 μ l

Electrophoresis buffer		4x Sample buffer	
Glycin	72g	SDS	0.2g
Tris	15g	Glycerol	1g
SDS	5g	2-mercaptoethanol	0.5ml
Aqua bidest	fill up to 500ml	Tris/HCl pH 6.8	fill up to 2.5ml
		Bromphenolblue	traces of

3.3.1.4 Western blot

Using a BioRad wet-blot system the proteins are blotted on a PVDF membrane (VWR).

The blotting sandwich is prepared according to the following order:

thick pad
3 filter papers
PVDF membrane (activated in methanol)
Gel
3 filter papers
thin pad

Table 13: Schemata for sandwich preparation

This blot was running at 25 Volt over night at 4°C in 1x blotting buffer. The cathode was placed on the side of the gel, so that the negatively loaded proteins moved towards the positively charged anode and were bound on the membrane. After blotting the membrane was washed with aqua bidest, dried with methanol and either treated with the first antibody or stored at 4°C.

10x Blotting buffer		1x Blotting buffer	
Glycin	72g	10x blotting buffer	10%
Tris	15g	Methanol	20%
SDS	1g	Aqua bidest	70%
Aqua bidest	to 500 ml		

3.3.1.5 Ponceau S staining

The Ponceau S staining was used to visualize all protein bands on the membrane. The membrane was incubated in Ponceau S (Sigma-Aldrich, St. Louis, MO, US) solution for 10 minutes, fotocopied for documentation and washed in aqua bidest.

3.3.1.6 Immunological detection of protein

The membrane was incubated with the primary antibody in 1-5% non-fat dry milk in PBS-T (1ml Tween in 1l 1xPBS) over night at 4°C. Thereafter the membrane was washed at least 3 times for 10 minutes with PBS-T before incubating with the secondary antibody (conjugated to horse radish peroxidase) in 1% non-fat dry milk in PBS-T for 1 hour at room temperature. For the phosphoproteins 1-5% BSA in TBS-T (1ml Tween in 1l 1xTBS) was used. After washing at least 3 times for 10 minutes each the membrane was covered with detection reagent (ECL Plus Western Blotting Detection System, AmershamTM, GE Healthcare) and visualized by exposing to an x-ray film. The protein bands were quantified after scanning in comparison to the expression of the housekeeping protein β -Actin.

Primary Antibody	Dilution	Source	buffer	MW	Provider
BCL-2	1:500	mouse	2% milk in PBS-T	26kDa	BD biosciences
BCL-XL (H5)	1:500	mouse	5% milk in PBS-T	30kDa	Santa Cruz
BAX (B-9)	1:500	rabbit	2% milk in PBS-T	23kDa	Santa Cruz
BAK (Ab-1)	1:1000	mouse	2% milk in PBS-T	30kDa	Calbiochem
Caspase 2 (mAB-415)	1:500	mouse	2% milk in PBS-T	47, 14kDa	Enzo Life Science
Caspase 3 (Asp-175)	1:2000	rabbit	2% milk in PBS-T	17, 19kDa	Cell Signaling
Cyclin A (H-432)	1:500	rabbit	2% milk in PBS-T	54kDa	Santa Cruz
Cyclin B	1:500	rabbit	2% milk in PBS-T	60kDa	Cell Signaling
Cyclin E (M-20)	1:500	rabbit	2% milk in PBS-T	53kDa	Santa Cruz
ATR (C-19)	1:500	goat	2% BSA in TBS-T	250kDa	Santa Cruz
ATM (Ab-1981)	1:500	rabbit	5% BSA in TBS-T	260kDa	abm inc.
CHK 1	1:500	rabbit	2% BSA in TBS-T	56kDa	Cell Signaling
Phospho CHK 1 (Ser317)	1:500	rabbit	2% BSA in TBS-T	56kDa	Cell Signaling
CDK 1	1:500	rabbit	2% BSA in TBS-T	34kDa	Cell Signaling
Phospho CDK 1 (Tyr15)	1:500	rabbit	2% BSA in TBS-T	34kDa	Cell Signaling
Survivin	1:1000	rabbit	3% BSA in TBS-T	16kDa	Novus Biologicals
PARP (C2-10)	1:1000	mouse	2% milk in PBS-T	116, 85kDa	R&D systems

Cdc25C (5H9)	1:1000	rabbit	3% BSA in TBS-T	60kDa	Cell signaling
FoxM1 (D12D5)	1:1000	rabbit	5% BSA in TBS-T	110kDa	Cell signaling
Phospho-Histone H3 Ser10	1:1000	rabbit	5% BSA in TBS-T	17kDa	Cell signaling
β-Actin (AC-15)	1:500	mouse	1% milk in PBS-T	42kDa	Sigma-Aldrich

Table 14: Primary antibodies

All antibodies were diluted in PBS-T or TBS-T and when recommended by the provider, BSA or milk powder was added.

Secondary Antibody	Dilution	buffer	Provider
Goat Anti-mouse HRP-conjugated (#1858413)	1:5000	3% milk in PBS-T or 3% BSA in TBS-T	Pierce, Thermo Scientific, Rockford, US
Goat Anti-rabbit IgG-h + I HRP (#A120-201P)	1:20000	3% milk in PBS-T or 3% BSA in TBS-T	Bethyl Laboratories Inc, Montgomery, US
Polyclonal rabbit Anti-goat Immunoglobulin/ HRP	1:2000	3% BSA in TBS-T	Dako Cytomation
Anti-rabbit IgG FITC, developed in goat (#114K6044)	1:2000	3% BSA in TBS-T	Sigma-Aldrich, St. Louis, MO, US

Table 15: Secondary antibodies

3.4 Statistics

Statistical analysis was performed using GraphPad PRISM™. Results were analyzed by student's t-test or Kruskal-Wallis test depending on the results of normality testing. Data are expressed as means of at least three independent experiments including standard deviation and significance. Significances are indicated as *, **, and *** for significant increase at $p \leq 0.05$, 0.01, and 0.001, respectively.

4 RESULTS

4.1 Phytochemical investigations of *Metaxya rostrata*

In a previous work 800g dried roots of *Metaxya rostrata* had been extracted by sonification with hot water according to the ethnomedicinal use. After lyophilization 80g water extract had been obtained and sequentially been extracted with ethylacetate and butanol. The residue of the water phase had additionally been extracted with methanol. The fractions had been subjected to vacuum liquid chromatography (VLC) on silica using EtOAc/MeOH/H₂O mixtures of increasing polarity as mobile phases (Fig. 42) to yield 15 fractions. Fraction 12 had shown reasonable cytotoxic activity (Virtbauer 2007).

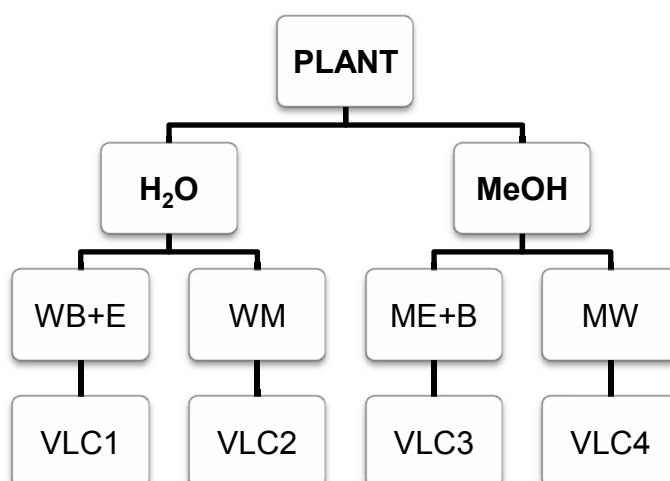


Fig. 42: Extraction and fractionation scheme of the rhizomes of *Metaxya rostrata*
(according to: Virtbauer 2007)

As a further fractionation of fraction 12 had not been performed yet, in this study 2,96g of fraction 12 were subjected to column chromatography on Sephadex LH-20 under elution with 80% MeOH to obtain 13 subfractions from a total of 288 fractions collected in CC-1 (Table 16). Every tenth fraction was analysed by TLC (stationary phase 1, mobile phase 1, see p. 41) and the fractions with similar compounds were combined (Fig. 43).

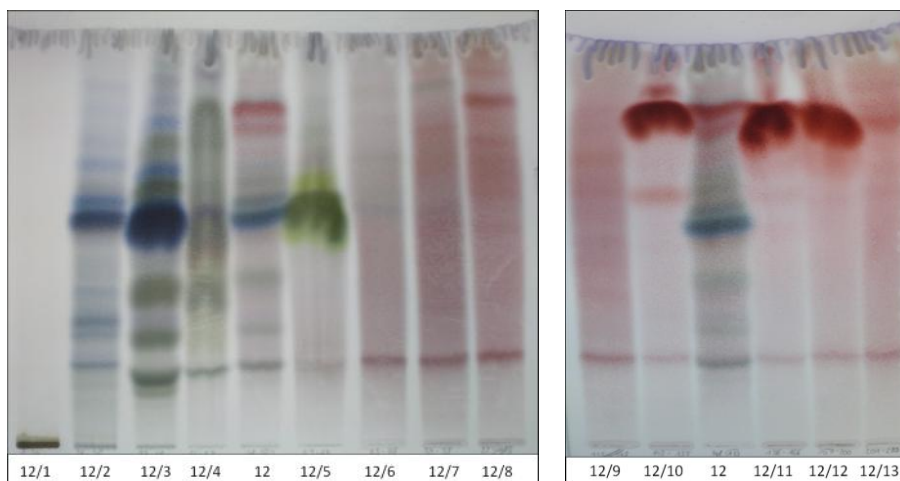


Fig. 43: TLC of the combined fractions of CC-1

Stationary phase 1, mobile phase 1, detection 1

CC-1 parameters	Mobile Phase	Fraction No.	Pooled fractions	mg	Further separation
<u>Stationary phase:</u> Sephadex LH-20 <u>Column diameter:</u> 3cm <u>Column height:</u> 65cm <u>Fraction separation:</u> 2960mg of fraction 12 <u>Fraction size:</u> 8 ml/30 min	80% MeOH	12/1	1-30	80	none
	"	12/2	31-36	83	none
	"	12/3	37-41	509	CC-2 (p.64)
	"	12/4	42-52	691	CC-5 (p.70)
	"	12/5	53-64	555	CC-6 (p.71)
	"	12/6	65-78	60	none
	"	12/7	79-98	75	none
	"	12/8	99-118	172	none
	"	12/9	119-148	178	none
	"	12/10	149-155	101	CC-8 (p.73)
	"	12/11	156-166	186	none
	"	12/12	167-200	199	none
	"	12/13	201-288	40	none

Table 16: Conditions for CC-1

Fractions 12/3, 12/4, 12/5 and 12/10 were chosen for further separation. Due to the smaller amounts of the other fractions no further experiments were performed.

4.1.1 Isolation and structure elucidation of compound KK1

Fr. 12/3 was chosen for further separation to isolate its main blue compound at R_f 0.56 with detection 1. 509mg of fr.12/3 were subjected to column chromatography on Silica Gel 60 (particle size 0.063-0.200mm, Merck) under elution with water-saturated EtOAc:MeOH (90+10) (Table 17). Total 215 fractions were obtained from CC-2 and controlled by TLC (stationary phase 1, mobile phase 1, see p. 41) before pooling (Fig. 44).

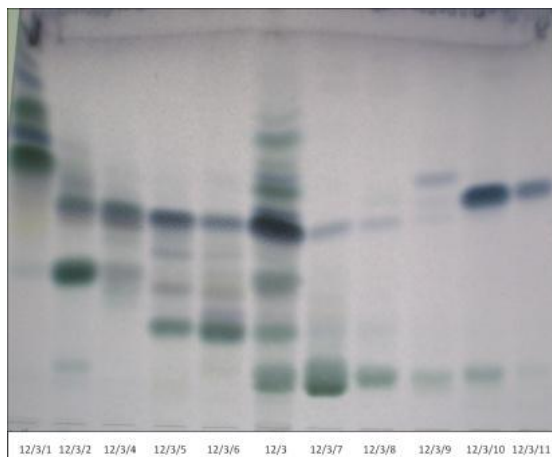


Fig. 44: TLC of the combined fractions of CC-2

Stationary phase 1, mobile phase 1, detection 1

In fractions 24 to 28 compound KK1 crystallized (Fig. 45). After removal of the supernatant, TLC comparison of fractions 24 to 28 (Fig.46) proved that compound KK1 was the main substance at R_f 0.56 of fr. 12/3 with the blue colour after detection 1. Thus, the fractions were combined and 58mg of pure compound KK1 was obtained.



Fig. 45: Crystallization of compound KK1

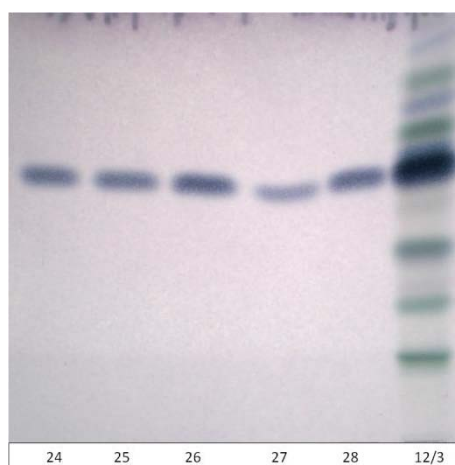


Fig. 46: TLC of compound KK1 in 5 fractions

Stationary phase 1, mobile phase 1, detection 1

As KK1 was a polar compound, a TLC comparison with different sugars was performed. Glucose, fructose, lactose, saccharose, mannose and rhamnose were used as authentic compounds. KK1 was less polar as the tested sugars and could not be identified. The use of aniline-diphenylamin-reagent, a reagent for the detection of compounds containing sugars, showed that compound KK1 contains a sugar moiety (Fig. 47).

Results

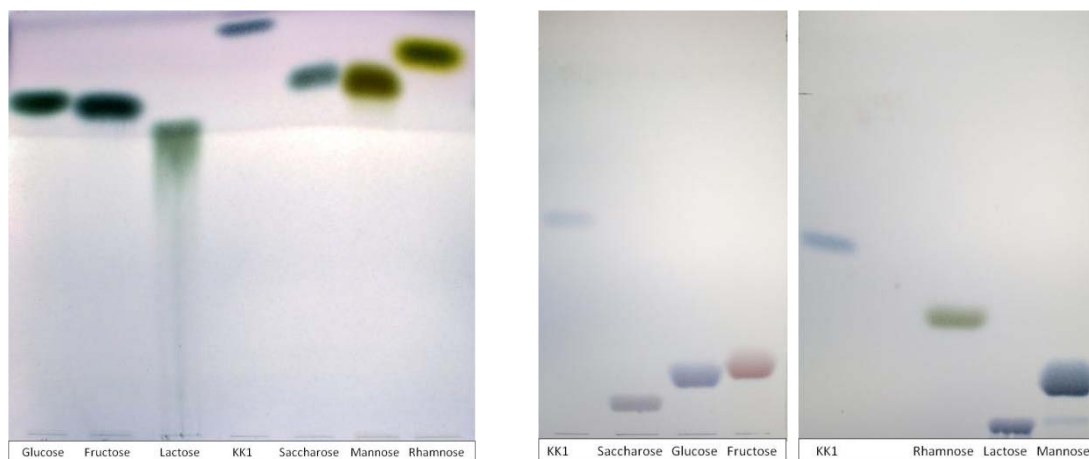


Fig. 47: TLC comparison of KK1 with different sugars

Stationary phase 1, mobile phase 13, detection 1

Stationary phase 1, mobile phase 1, detection 3

CC-2 parameters	Mobile Phase	Fraction No.	Pooled fractions	mg	Further separation
Stationary phase: Silica Gel 60 Column diameter: 2cm Column height: 85cm Fraction separation: 509mg of fraction 12/3 Fraction size: 5 ml/60 min	Water sat. EtOAc:MeOH	12/3/1	1-19	156	none
	90 : 10	12/3/2	20-23	30	CC-4 (p.69)
	"	12/3/3	24a-28a	58	KK1 crystalls
	"	12/3/4	24b-28b	19	mother liquor
	"	12/3/5	29-34	21	none
	"	12/3/6	35-50	20	none
	"	12/3/7	51-67	16	none
	"	12/3/8	68-88	39	none
	"	12/3/9	89-110	6	none
	"	12/3/10	111-140	26	CC-3 (p.68)
	"	12/3/11	141-160	33	none
	"	12/3/12	161-180	7	none
	"	12/3/13	181-215	29	none

Table 17: Conditions for CC-2

The characterization of compound KK1 was performed by mass spectrometry and detailed NMR-analysis. From the ESI-MS spectra, a molecular weight of 318 amu was deduced. Using Flow Injection Analysis the mass spectrum in the negative mode displayed a quasimolecular ion at m/z 317 $[M - H]^-$, and accordingly in the positive mode m/z 341 $[m + Na]^+$ was measured. Product ions were recorded by MS/MS in both the positive and negative mode at various collision energies. Fragmentation showed quasimolecular ions in the positive mode at m/z 336 $[M + NH_4]^+$, m/z 319 $[M + H]^+$, m/z 157 $[M\text{-dehydrohexose}]^+$ and m/z 139 $[aglycone - H_2O]^+$. Product ions of m/z 317 $[M-H]^-$ in the

negative mode were m/z 179 [hexose – H][–], m/z 161 [(hexose – H)H₂O][–], m/z 119 [^{0,2}A][–] and m/z 89 [^{0,3}A][–] (Kainz *et al.*, 2011).

NMR experiments, using extensive one and two dimensional techniques, revealed the sugar part as a β -glucopyranose. The aglycon showed mainly signals for CH₂ groups in the aliphatic region, one double bond CH signal and an additional CH signal at 4.2 ppm in the ¹H NMR. The key structure was identified as a methylenecyclopropane moiety, linked glycosidically with the glucose via an alcohol attached to the cyclopropane ring. This analysis was based on the characteristic ¹H and ¹³C NMR chemical shifts of the cyclopropane signals together with rather large ¹H-¹³C one bond coupling constants, namely 188.2 Hz for CH-9' and 163.9 and 161.0 Hz for the CH₂-8', respectively (Xu *et al.*, 1992). The measured C=C stretching frequency of 1775 cm^{–1} in the infrared spectrum of KK1 correlates with published data of similar methylenecyclopropane structures (Stang *et al.*, 1974; Kainz *et al.*, 2011) (see supplementary information).

Numerous HMBC correlations and NOESY crosspeaks established all connectivities, as well as the geometry of the double bond. Attached to the double bond is a 5 carbon aliphatic chain terminated by an alcohol function. Finally, a molecular weight of 318 resulting from mass spectrometry established compound KK1 as (2E)-2-(6-hydroxyhexylden)cyclopropyl- β -glucopyranoside (Fig. 48) (Kainz *et al.*, 2011).

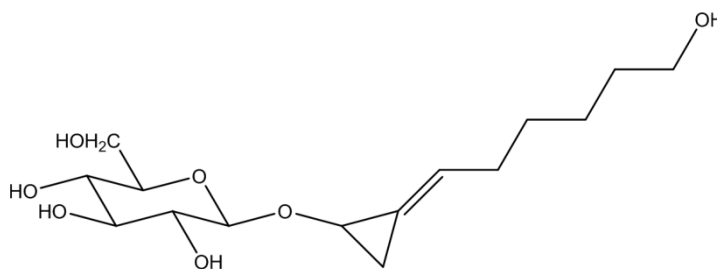


Fig. 48: Compound KK1 - (2E)-2-(6-hydroxyhexylden)cyclopropyl- β -glucopyranoside

Compound KK1 was crystallized from a solvent mixture of methanol and diethylether. Analysis of a derived single crystal by X-ray diffraction established the relative stereochemistry of the chiral centre in the methylenecyclopropylalcohol moiety relative to glucose (Fig. 49). The absolute configuration was deduced by comparing the optical rotatory power of compound KK1 with published data for β -alkylglucosides. The $[\alpha]_D$ for

β -D-glucosides is about -30 to -90 , only few examples for β -L-glucosides are available showing an $[\alpha]_D$ of $+30$ to $+60.6,7$. The measured $[\alpha]_D$ of -74.9 established compound KK1 as (1R,2E)-2-(6-hydroxyhexyliden)cyclopropyl- β -D-glucopyranoside (Kainz *et al.*, 2011).

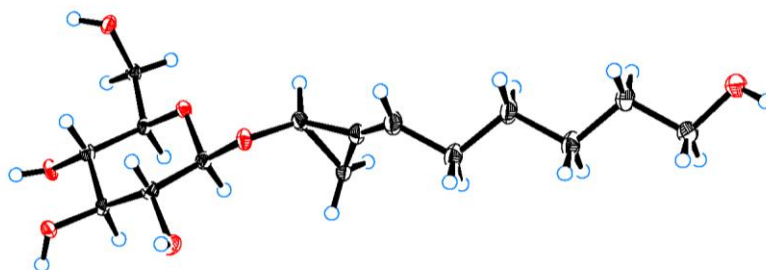


Fig. 49: ORTEP plot (ellipsoids 50% probability) of compound KK1

This compound, with the very uncommon structural feature of a methylenecyclopropane alcohol, has never been described before, neither isolated from natural sources nor totally synthesized.

4.1.2 Isolation and structure elucidation of compound KK5

As Fraction 12/3/10 showed one major compound in TLC, it was chosen to isolate the blue compound at R_f 0.58 (Fig. 44). The fraction was subjected to column chromatography on Sephadex LH-20 under elution with 50% MeOH (Table 18). 180 fractions were obtained from CC-3 and every tenth fraction was controlled by TLC before pooling the fractions. In the combined fraction 12/3/10/1 4,9mg of compound KK5 were obtained. A TLC comparison with KK1 revealed a very similar polarity (Fig. 51).

The characterization of compound KK5 was performed by NMR analysis and mass spectrometry. The MS showed the quasimolecular ion in the negative mode at m/z 331 $[M - H]^-$. In the positive mode m/z 333 $[M + H]^+$, m/z 350 $[M + NH_4]^+$ and m/z 355 $[M + Na]^+$ were determined in FIA resulting in a molecular weight of 332 amu. MS/MS in the negative mode indicated an increased fragmentation of m/z 331 $[M - H]^-$ related to the enhancement of collision energy. Relevant product ions were m/z 169 $[M - \text{dehydrohexose}]^-$, m/z 151 $[\text{aglycone} - H_2O]^-$, m/z 119 $[0,2A]^-$ and m/z 89 $[0,3A]^-$. Both

MS/MS measurements in the positive mode revealed corresponding results (Kainz *et al.*, 2011).

In the NMR experiments, using extensive one and two dimensional techniques, the spectroscopic data for compound KK5 were very similar to compound KK1. Again the sugar part was a β -glucopyranose with the glycosidic bond to the unusual methylenecyclopropan alcohol. Differences were seen in the side chain. The signals for the terminal $\text{CH}_2\text{-OH}$ group were missing, one CH_2 group was shifted to lower field, and a carbonyl signal at 182.90 ppm appeared in the ^{13}C NMR spectrum.

Therefore the terminal alcohol in the alkane side chain of KK1 had to be oxidized in KK5 giving the corresponding carboxylic acid, (6E)-6[2-(β -glucopyranosyloxy)cyclopropylidene]hexanoic acid (Fig. 50) (Kainz *et al.*, 2011).

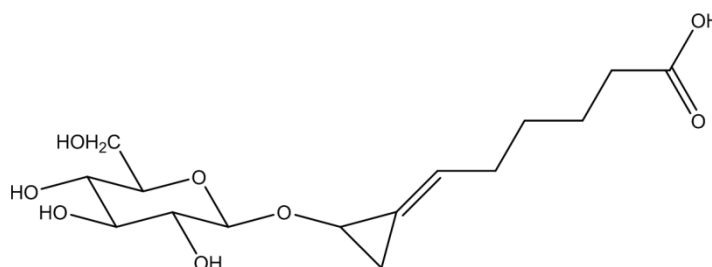


Fig. 50: Compound KK5 - (6E)-6[2-(β -glucopyranosyloxy)cyclopropylidene]hexanoic acid

(6E)-6[2-(β -glucopyranosyloxy)cyclopropylidene]hexanoic acid has also never been described before. The main structural feature of this new glycosidic compound is the extremely uncommon methylenecyclopropan alcohol in the aglycon as also seen in compound KK1.

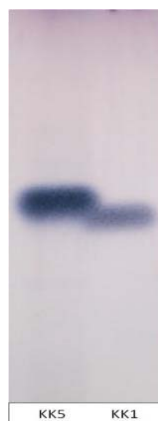


Fig. 51: TLC comparison of compound KK1 and KK5

Stationary phase 1, mobile phase 1, detection 1

CC-3 parameters	Mobile Phase	Fraction No.	Pooled fractions	mg	Further treatment
<u>Stationary phase:</u> Sephadex LH-20	50% MeOH	12/3/10/1	1-10	5	KK5
<u>Column diameter:</u> 1cm	"	12/3/10/2	11-20	1	none
<u>Column height:</u> 40cm	"	12/3/10/3	21-30	3	none
<u>Fraction separation:</u> 26mg of fraction 12/3/10	"	12/3/10/4	31-40	1	none
<u>Fraction size:</u> 5 ml/60 min	"	12/3/10/5	41-50	1.5	none
	"	12/3/10/6	51-60	2	none
	"	12/3/10/7	61-70	1	none
	"	12/3/10/8	71-90	4	none
	"	12/3/10/9	91-110	5	none
	"	12/3/10/10	111-130	1	none
	"	12/3/10/11	131-150	3	none
	"	12/3/10/12	151-180	2	none

Table 18: Conditions for CC-3

4.1.3 Isolation and structure elucidation of compound KK7

Fraction 12/3/2 was further purified by column chromatography on Silica Gel 60 using water-saturated EtOAc as a mobile phase (Table 19). Total 204 fractions were obtained from CC-4 and every tenth fraction was controlled with TLC before pooling (Fig. 52). In fraction 12/3/2/13 7mg of compound KK7 were obtained.

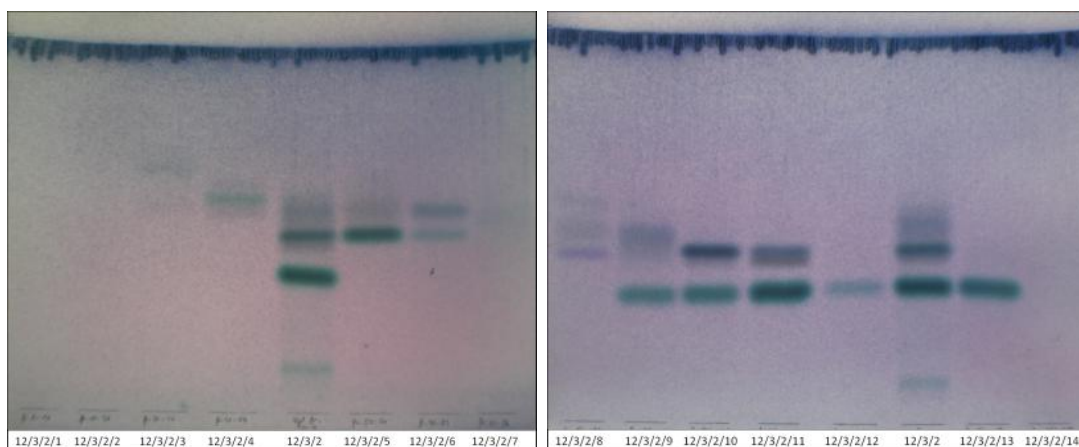


Fig. 52: TLC of the combined fractions of CC-4

Stationary phase 1, mobile phase 1, detection 1

CC-4 parameters	Mobile Phase	Fraction No.	Pooled fractions	mg	Further treatment
<u>Stationary phase:</u> Silica Gel 60 <u>Column diameter:</u> 0,5cm <u>Column height:</u> 50cm <u>Fraction separation:</u> 30mg of fraction 12/3/2 <u>Fraction size:</u> 5 ml/30 min	Water sat. EtOAc	12/3/2/1	1-10	0.5	none
	100%	12/3/2/2	11-30	2	none
	"	12/3/2/3	31-40	1	none
	"	12/3/2/4	41-50	1	none
	"	12/3/2/5	51-70	3	none
	"	12/3/2/6	71-83	1	none
	"	12/3/2/7	84-96	1.5	none
	"	12/3/2/8	97-103	2	none
	"	12/3/2/9	104-120	3	none
	"	12/3/2/10	121-133	5	none
	"	12/3/2/11	134-153	1	none
	"	12/3/2/12	154-159	1	none
	"	12/3/2/13	160-190	7	KK7
	"	12/3/2/14	191-204	2	none

Table 19: Conditions for CC-4

In NMR experiments compound KK7 was identified as a methyl glycoside. Two CH₂ groups and one quarternary carbon are indicative for a ketose. The detailed NMR analysis and the comparison of the ¹³C NMR data with the literature (Duker and Serianni, 1993) revealed compound KK7 as methyl- α -fructofuranoside (Fig. 53) (Kainz *et al.*, 2011)

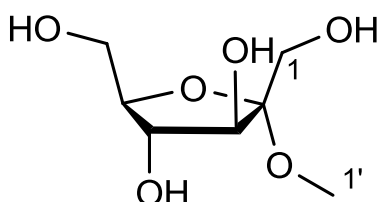


Fig. 53: Compound KK7 - methyl- α -fructofuranosid

4.1.4 Isolation and structure elucidation of compound KK6

Fraction 12/4 was subjected to column chromatography on Silica gel under elution with water-saturated EtOAc:MeOH (90+10). 300 fractions were collected from CC-5 (Table 20) and TLC comparison combined to 13 collective fractions (Fig. 54). In fraction 12/4/9 5mg of compound KK6 were obtained.

Results

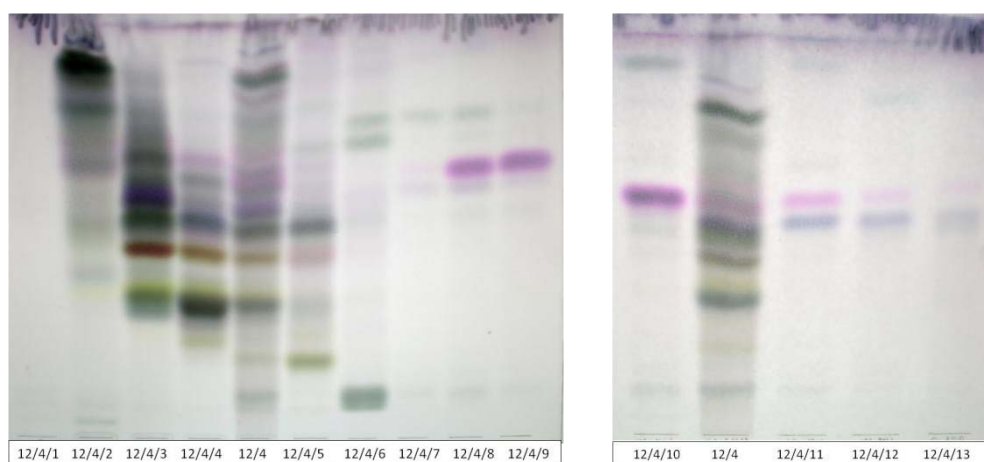


Fig. 54: TLC of combined fractions of CC-5

Stationary phase 1, mobile phase 1, detection 1

In the NMR experiments β -glucopyranose was determined. Compound KK6 was a phenolic acid and showed only two duplet signals. KK6 could be identified as *p-trans*-coumaric acid. HMBC cross peaks established the glycosidic linkage to the *p*-phenol group of the conjugated acid. Compound KK6 could be identified as 4-O- β -D-glucopyranosyl-*p-trans*-coumaric acid. The NMR spectroscopic data correspond to the published values Fig. 55) (Cui *et al.*, 1990).

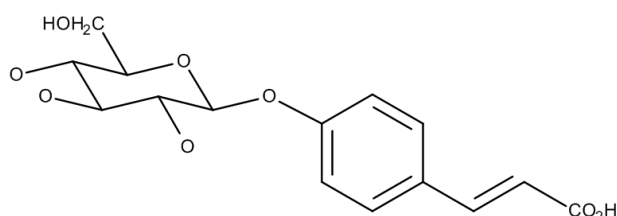


Fig. 55: Compound KK6 – 4-O- β -D-glucopyranosyl-*p-trans*-coumaric acid

CC-5 parameters	Mobile Phase	Fraction No.	Pooled fractions	mg	Further treatment
<u>Stationary phase:</u> Silica Gel 60 <u>Column diameter:</u> 2cm <u>Column height:</u> 70cm <u>Fraction separation:</u> 691mg	Water sat. EtOAc:MeOH	12/4/1	1-8	9	none
	90 : 10	12/4/2	9-14	292	none
	"	12/4/3	15-20	137	none
	"	12/4/4	21-40	72	none
	"	12/4/5	41-60	54	none
	"	12/4/6	61-80	24	none
	"	12/4/7	81-90	2	none
	"	12/4/8	91-106	6	none
	"	12/4/9	107-113	5	KK6

of fraction 12/4	"	12/4/10	114-140	13	none
<u>Fraction size:</u>	"	12/4/11	141-160	16	none
7 ml/60 min	"	12/4/12	161-232	12	none
	"	12/4/13	232-300	7	none

Table 20: Conditions for CC-5

4.1.5 Isolation and structure elucidation of compound KK3

Fraction 12/5 was subjected to column chromatography on Silica Gel 60 under elution with water-saturated EtOAc:MeOH (90+10) (Table 21). After TLC comparison of every tenth fraction, the fractions were combined to obtain 9 pooled fractions (Fig. 56).

CC-6 parameters	Mobile Phase	Fraction No.	Pooled fractions	mg	Further separation
<u>Stationary phase:</u>	Water sat. EtOAc:MeOH	12/5/1	1-28	12	none
Silica Gel 60	90 :10	12/5/2	29-32	26	none
<u>Column diameter:</u>	"	12/5/3	33-36	121	none
2cm	"	12/5/4	37-38	116	none
<u>Column height:</u>	"	12/5/5	39-40	69	none
80cm	"	12/5/6	41-53	70	none
<u>Fraction separation:</u>	"	12/5/7	54-62	9	none
555mg	"	12/5/8	63-109	25	none
of fraction 12/5	"	12/5/9	110-150	58	CC-7 (p.73)
<u>Fraction size:</u>	"				
7 ml/60 min					

Table 21: Conditions for CC-6

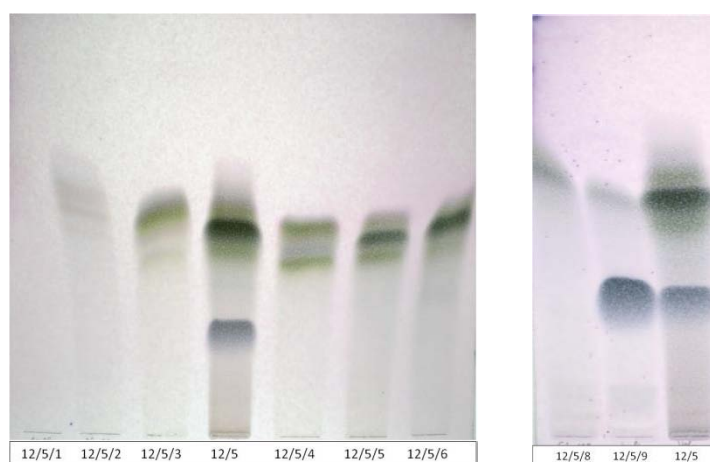


Fig. 56: TLC of the combined fractions of CC-6

Stationary phase 1, mobile phase 1, detection 1

Results

Subfraction 12/5/9 was further purified by column chromatography on Silica Gel 60 under elution with water-saturated EtOAc:MeOH (80+20) to isolate the greyish compound at R_f 0.32 (Table 22). The CC resulted in 6 pooled fractions (Fig. 57). In the combined fractions 12/5/9/2, 12/5/9/3 and 12/5/9/4 the compound crystallized (Fig. 58) yielding 7 mg of compound KK3. Due to the small amounts of other subfractions no further separation was performed.

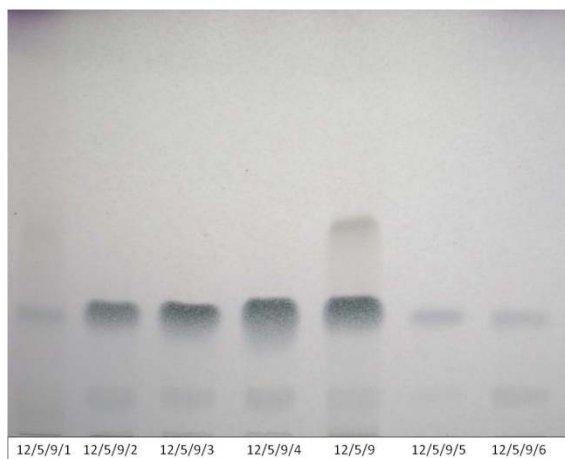


Fig. 57: TLC of combined fractions of CC-7

Stationary phase 1, mobile phase 1, detection 1



Fig. 58: Crystallisation of KK3

The characterization of compound KK3 was performed with one and two dimensional NMR techniques. In compound KK3 β -glucopyranose was determined. The ^1H NMR spin system for a trisubstituted benzene together with the *trans* double bond revealed compound KK3 as caffeic acid derivative. HMBC cross peaks established the glycosidic linkage to the p-phenol opposite group to identify 4-O- β -D-glucopyranosyl-caffeic acid (Fig. 59). The NMR spectroscopic data corresponded to published values (Cui *et al.*, 1990; Kainz *et al.*, 2011).

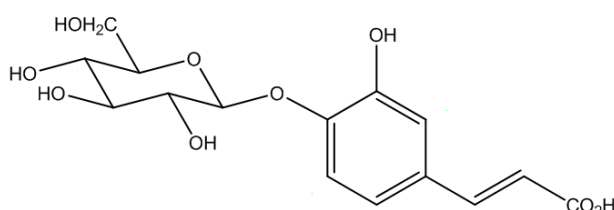


Fig. 59: Compound KK3 - 4-O- β -D-glucopyranosyl-caffeic acid

Results

CC-7 parameters	Mobile Phase	Fraction No.	Pooled fractions	mg	Further treatment
<u>Stationary phase:</u> Silica Gel 60 <u>Column diameter:</u> 1cm <u>Column height:</u> 95cm <u>Fraction separation:</u> 58mg of fraction 12/5/9 <u>Fraction size:</u> 5 ml/60 min	Water sat. EtOAc:MeOH	12/5/9/1	1-37	26	none
	80 : 20	12/5/9/2	38-60	20	KK3
	"	12/5/9/5	61-65	2	none
	"	12/5/9/6	66-95	7	none

Table 22: Conditions for CC-7

4.1.6 Isolation and identification of compound KK4

Fraction 12/10 was subjected to column chromatography on Sephadex LH-20 and elution with 50% MeOH to obtain 6 pooled fractions (Fig. 60). In fraction 12/10/3 compound KK4 could be identified by TLC comparison with two trimeric proanthocyanidines - cinnamtannin B-1 and aesculitannin B (JV-1) isolated before from *Metaxya rostrata* (Fig. 61) (Virtbauer 2007).

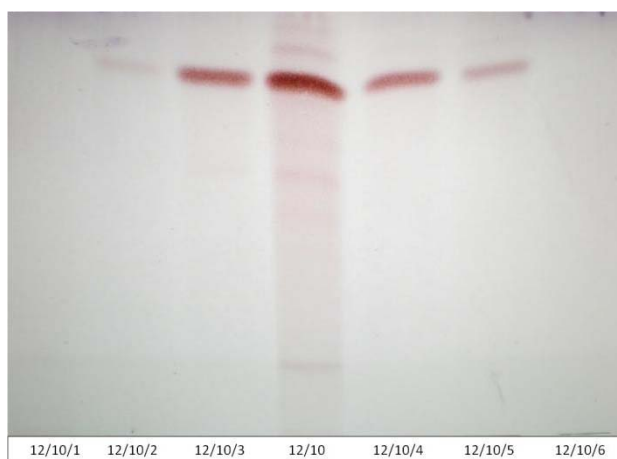


Fig. 60: TLC of the combined fractions of CC-7



Fig. 61: TLC comparison KK4 with JV-1

Stationary phase 1, mobile phase 1, detection 1

CC-8 parameters	Mobile Phase	Fraction No.	Pooled fractions	mg	Further treatment
<u>Stationary phase:</u> Sephadex LH-20 <u>Column diameter:</u> 1cm <u>Column height:</u>	Water sat. EtOAc:MeOH	12/10/1	1-19	11	none
	"	12/10/2	20-23	4	none
	"	12/10/3	24-26	22	KK4

40cm Fraction separation: 101mg of fraction 12/10 Fraction size: 8 ml/60 min	"	12/10/4	27-33	28	none
	"	12/10/5	34-40	6	none
	"	12/10/6	41-70	7	none

Table 23: Conditions for CC-8

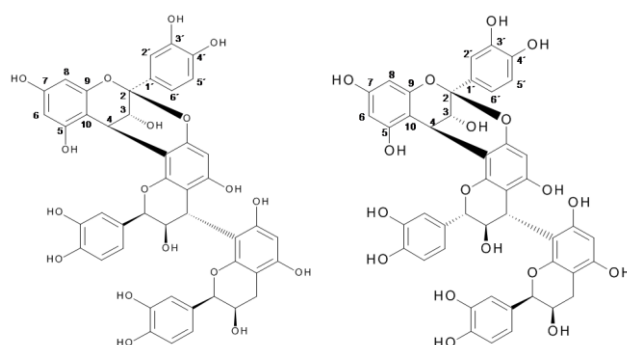


Fig. 62: Compound KK4 – mixture of cinnamtannin B-1 and aesculitannin B

4.1.7 Overview over the isolation of the pure compounds from *Metaxya rostrata*

The chromatographic separation of a fraction from a water extract from the rhizomes of *Metaxya rostrata* prepared in a previous study (Virtbauer 2007) was continued. In this thesis, fraction 12 was fractionated and several compounds were isolated (Fig. 81). Two new compounds (KK1 and KK5), with the very uncommon structural feature of a methylenecyclopropan alcohol in the aglycon, two phenolic acid glycosides (KK3 and KK6) and a methyl- α -fructofuranosid (KK7) were isolated for the first time from the tree fern *Metaxya rostrata*.

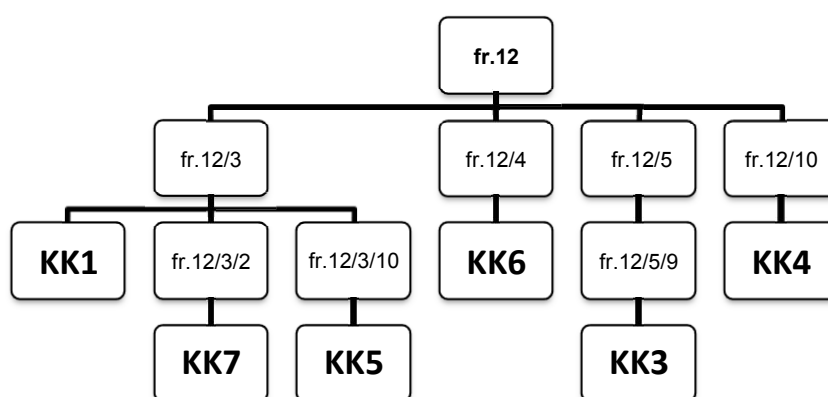


Fig. 63: Isolation scheme of the compounds from *Metaxya rostrata* isolated in this study

4.1.8 Biological Testing of compound KK1

Compound KK1 - (2E)-2-(6-hydroxyhexyliden)cyclopropyl- β -glucopyranoside – a new unusual natural compound, was tested for several biological activities.

As fraction 12, from which KK1 was isolated, showed moderate cytotoxic activity, the cytotoxicity of the compound was tested as well.

4.1.8.1 Bioviability assay of compound KK1 and KK1 aglycon

In order to determine the effect of compound KK1 on cancer cell viability, SW480 human colon carcinoma cells were exposed to increasing concentrations of KK1 for 48h. Using neutralred assay, no significant loss of cells could be seen up to a concentration of 500 μ M. The KK1 aglycon (see chapter 4.1.8.8.) showed a stronger effect on cell viability compared to compound KK1 (Fig. 64).

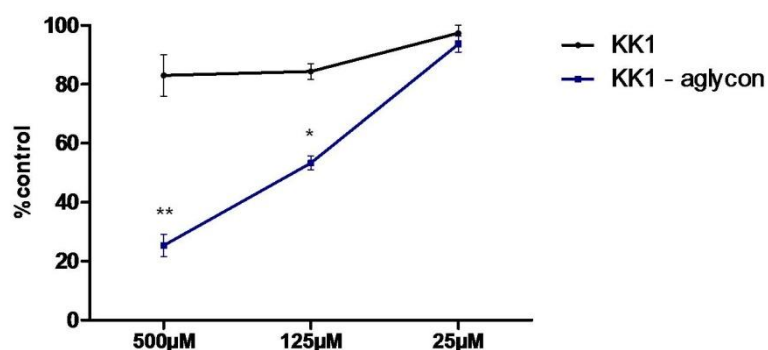


Fig. 64: Viability of SW480 treated with KK1

Viability of SW480 cells treated with KK1 and the aglycon of KK1 was assessed using neutralred assay. The cells were cultivated on 24-well plates and incubated for 48 hours with increasing concentrations (25, 125 and 500 μ M). Data represent mean \pm s.e.mean from three independent experiments performed in triplicate.

4.1.8.2 HDAC assay of compound KK1

Histone deacetylase inhibitors (HDACi) are in the focus of research as anti-cancer drugs. HDACi are reported to induce growth arrest and apoptosis of cancer cells. Therefore the HDAC inhibition of KK1 was measured using a fluorimetric assay. Even at a concentration of 250 μ M only a low inhibition of about 18% was measured (Fig. 65).

Results

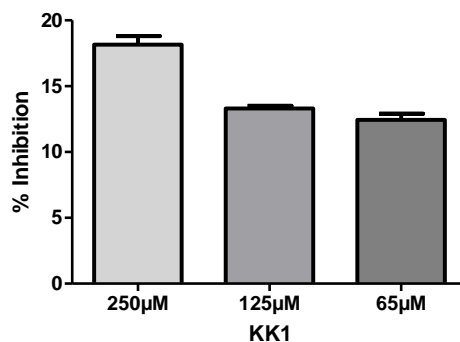


Fig. 65: HDAC inhibition by KK1

HDAC inhibition of compound KK1 in different concentrations was assessed using a fluorimetric assay. Data represent mean \pm s.e.mean from two independent experiments.

4.1.8.3 *In silico* screening of compound KK1

An *in silico* guided search for possible anti-viral activities of KK1 was realized because very few compounds with the extremely uncommon structural part of methylenecyclopropane had shown anti-viral activity against Epstein-Barr-, Human Herpes-, Hepatitis B-, Human Immunodeficiency- and Human Cytomegalo Virus in vitro (Rybak *et al.*, 2000, Qiu *et al.*, 1998, Uchida *et al.*, 1999). Pharmacophoric profiling against more than 2200 models representing over 280 pharmacological targets (Rollinger *et al.*, 2009) suggested α -glucosidase as potential target for KK1. A structural similarity search in the MDL Drug Data Report (MDDR) database (Keiser *et al.*, 2007) was conducted and confirmed this result making α -glucosidase a promising target for biological evaluation of compound KK1.

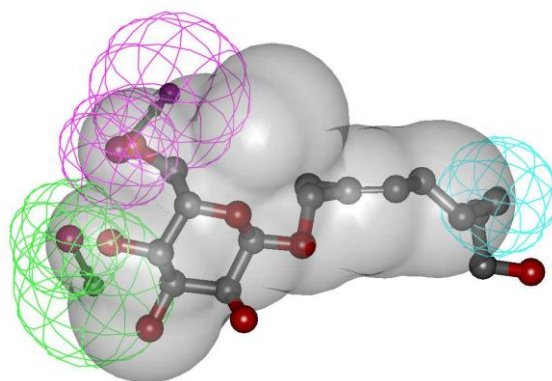


Fig. 66: Fitting of compound KK1 into the α -glucosidase inhibitor pharmacophore model

Chemical features are color-coded: hydrogen bond donor, hydrogen bond acceptor, hydrophobic, compound shape

4.1.8.4 Antiviral activity of compound KK1

The antiviral activity against Herpes simplex Virus 1 was determined. KK1 did not have an effect on the cell viability and did not show antiviral activity (Fig. 67).

As an in silico guided search suggested α -glucosidase as potential target for KK1, the anti-HIV activity should be evaluated as well, but could not be performed within this study.

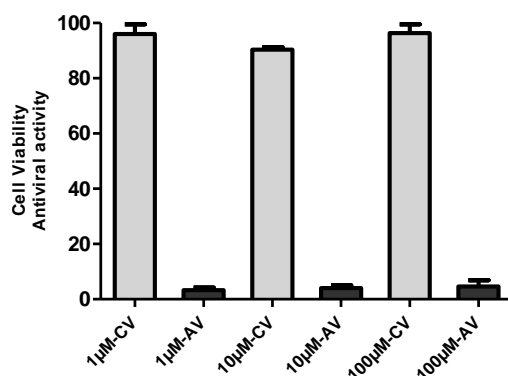


Fig. 67: Cell viability and antiviral activity of compound KK1

The grey bars show viability of vero cells treated with compound KK1. The cells were incubated with increasing concentrations (1, 10 and 100µM). The black bars show the activity (1, 10 and 100µM) on Herpes simplex virus 1. Data represent mean \pm s.e.mean from two independent experiments.

4.1.8.5 Insecticidal activity of compound KK1

As KK1 was isolated in large amounts from the rootlets of *Metaxya rostrata* an insecticidal activity of KK1 was assumed and evaluated. For the assay KK1 was incorporated in different concentrations to the food of the test organism *Spotoptera littoralis* (see page). 20 freshly slipt larvae were put directly on the food piece. After 4 and finally after 7 days the larvae were weighed (Fig. 68).

	$\mu\text{g/piece}$	solvent	Larvae alive	Larvae dead	Rel. weight	% dead	Larvae alive	Larvae dead	Rel. weight	% dead
			After 4 days				After 7 days			
KK1	1	MeOH	15	0	109,2%	0	15	0	99,8%	0
KK1	2,4	MeOH	15	0	120,9%	0	15	0	110,3%	0
Control 1	-	MeOH	15	0	100%	0	15	0	100%	0
Azadirachtin 1	1,8	MeOH	14	1	90,6%	6,7	14	1	94,3%	6,7
Azadirachtin 2	9	MeOH	14	1	86,6%	6,7	14	1	88,6%	6,7
Azadirachtin 3	45	MeOH	11	4	75,9%	26,7	5	10	68,3%	66,7

Table 24: Conditions and results of the insecticidal assay of compound KK1

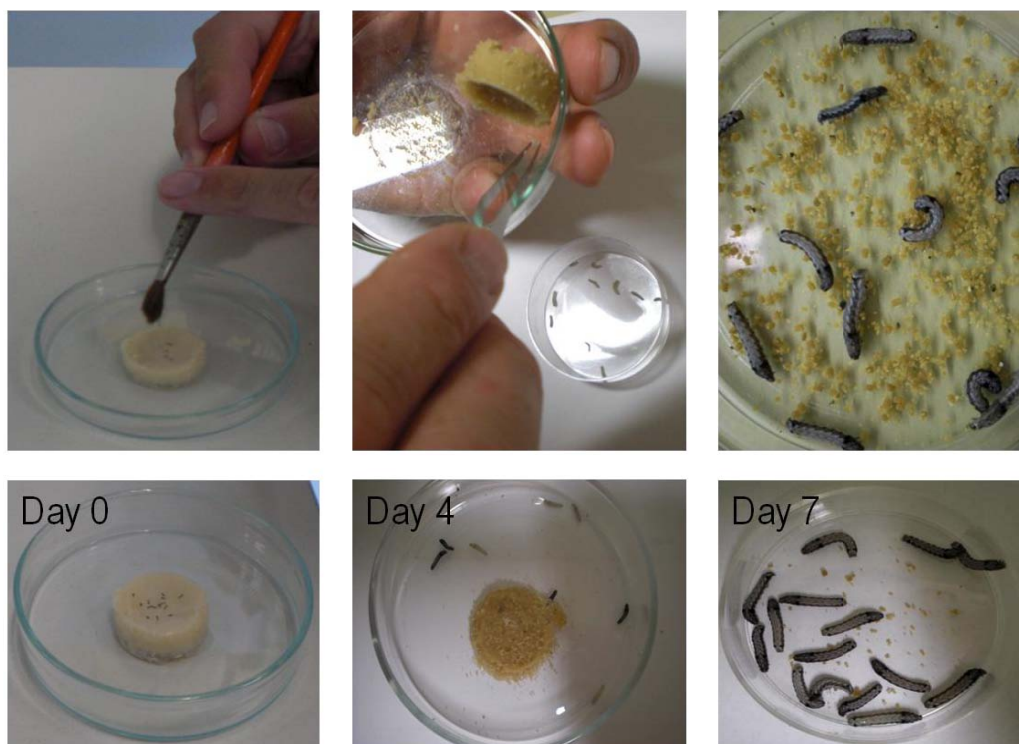


Fig. 68: Insecticidal activity of compound KK1

Larvae on the food piece at day 0, day 4 and day 7.

In the positive control (azadirachtin) group 6.7% of the larvae died at the lowest concentration of 1.8mg/piece. At the highest concentration of 45mg/piece 26.7% died after 4 days. After 7 days 66.7% of the larvae receiving the highest azadirachtin concentration were dead.

KK1 showed the same results as the negative control. No larvae died after 4 and 7 days (Table 24).

4.1.8.6 Antifungal Activity of compound KK1

Compounds KK1, KK3, KK4, KK5, KK6 and KK7, as well as fractions 12/3/5, fraction 12/10/4, fraction 12/4/4 and the MeOH-extract, the water extract and the MeOH-water phase were applied on a TLC plate. After complete removal of the solvents a suspension of the fungus *Cladosporium sphaerospermum* in growth medium was sprayed onto the plate (Fig. 70). After 3 days of incubation the inhibition zones without fungus were evaluated (Fig. 69).

Most pure compounds, fractions and extracts did not show any growth inhibition. Only compound KK5 seemed to inhibit the growth of the fungus.

Results

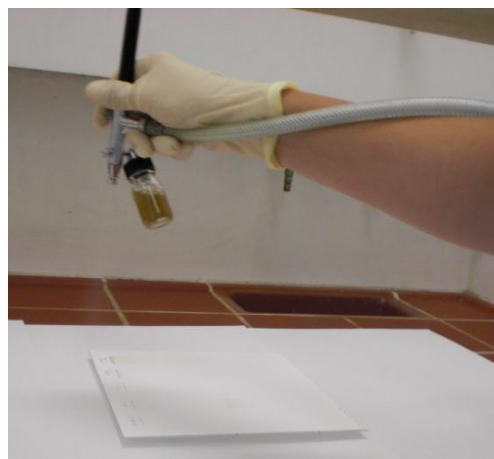
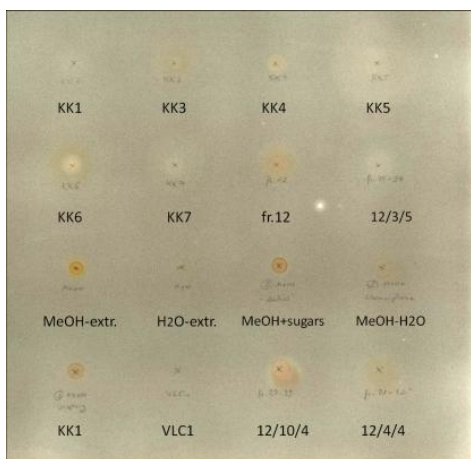


Fig. 69: Antifungal Activity of different compounds **Fig. 70:** Application of the fungus in growth medium

Fraction 12, fraction 12/3/5, VLC-1 (Virtbauer 2007), the MeOH-extract and the water extract (Virtbauer 2007) were applied on a TLC plate, developed in mobile phase 1 and dried well in order to remove the solvent. Then the plate was sprayed with the fungus *Cladosporium sphaerospermum* in growth medium (Fig.72).

The components of the extracts and fraction VLC-1 did not show any inhibition. In fraction 12 an inhibiting compound at R_f 0.68 was detected. The compounds coloured red after detection with anisaldehyde sulfuric acid reagent at R_f 0.6 – 0.75 are trimeric proanthocyanidines. In fraction 12/3/5 at R_f 0.55 an inhibiting zone was visible. As KK1 did not show any antifungal activity, the weak inhibition was probably caused by compound KK5 (Fig. 71).

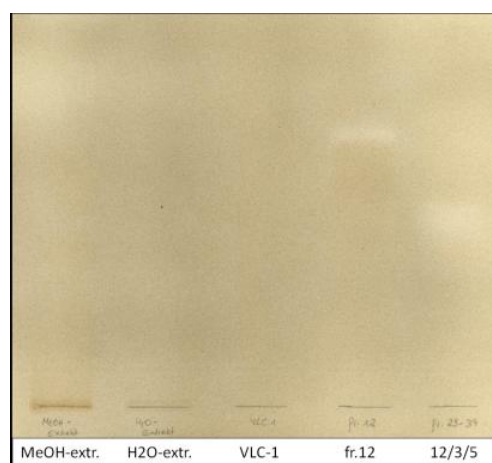
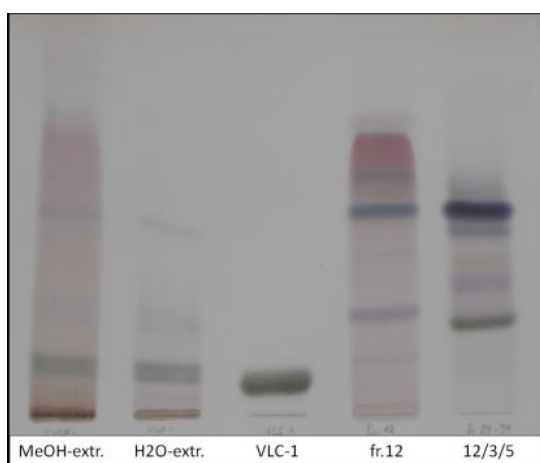


Fig. 71: TLC of different fractions tested for antifungal activity

Fig. 72: Antifungal activity of different fractions

Stationary phase 1, mobile phase 1, detection 1

Stationary phase 1, mobile phase 1, detection fungus

4.1.8.7 Antibacterial activity of compound KK1

As secondary metabolites often serve the plant as anti-microbial compounds, the antibacterial activity against six strains of *Staphylococcus aureus* was tested. KK1 did not show any activity up to a concentration of 128 μ M for any of the strains (Table 25).

	SA1199B	Xu212	ATCC	RN 4220	EMRSA 15	EMRSA 16
KK1	-	-	-	-	-	-
Norfloxacin	32	8	0,5	0,5	0,5	256

Table 25: MICs of KK1 and norfloxacin against six strains of *Staphylococcus aureus*

4.1.8.8 Hydrolysis of compound KK1

The unusual natural compound KK1 was evaluated for several biological activities, but did not exhibit an antibacterial, antiviral, antifungal or insecticidal activity and did not show effect on cell viability.

As glycosides are storage forms, the aglycon of KK1 might be the active principle. KK1 was hydrolysed and the aglycon of KK1 (Fig. 73) was obtained (Bleier 2011).¹¹ The effect of the aglycon of KK1 on cancer cell viability was evaluated (chapter) and exhibited a stronger effect on cell viability (Fig. 64).

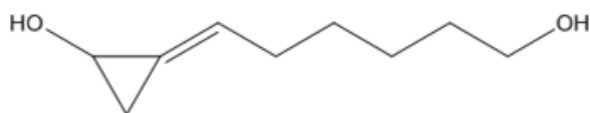


Fig. 73: Aglycon of KK1 - (2E)-2-(hydroxyhexyliden)cyclopropanol

¹¹ The hydrolysis of KK1 was performed by Johanna Bleier, a diploma student at the Department of Pharmacognosy, University of Vienna.

4.2 Bioactivity-guided fractionation and isolation of the active compounds from *Metaxya rostrata*

4.2.1 Extraction of plant material with solvents of different polarity

Metaxya rostrata C. Presl, *Stachytarpheta jamaicensis* L. Vahl and *Maranta arundinacea* Pulm. Ex. L. are used in traditional medicine in Costa Rica to treat intestinal diseases (Pekarek 2005) and were investigated in this work. To extract the secondary metabolites of these plants as exhaustive as possible within this study, the leaves, rootlets and rhizomes of *Metaxya rostrata*, as well as the roots of *Stachytarpheta jamaicensis* and *Maranta arundinaceae*, were ground and extracted with solvents of different polarity (CH_2Cl_2 , EA and MeOH). The water extract, which is used in traditional medicine, had already been fractionated in a previous work (Virtbauer 2007).

For the pretesting between 5 g and 9 g of the plant material were extracted with the respective solvent at 40° using Accelerated Solvent Extraction (ASE) (Table 26). The obtained extracts were investigated by TLC using different reagents for detection.

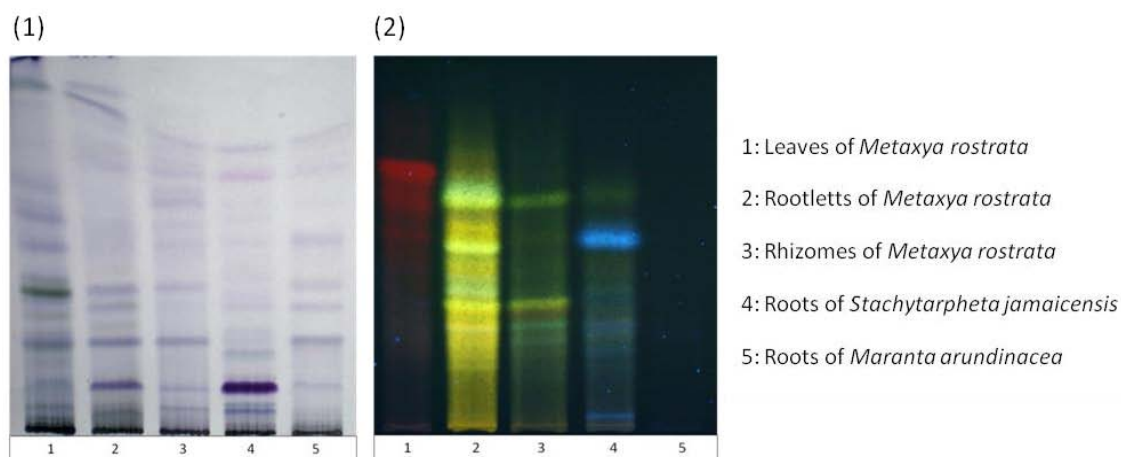


Fig. 74: TLC of the CH_2Cl_2 -extracts

- (1) Stationary phase 1, mobile phase 10, detection 1
- (2) Stationary phase 1, mobile phase 4, detection 2

Results

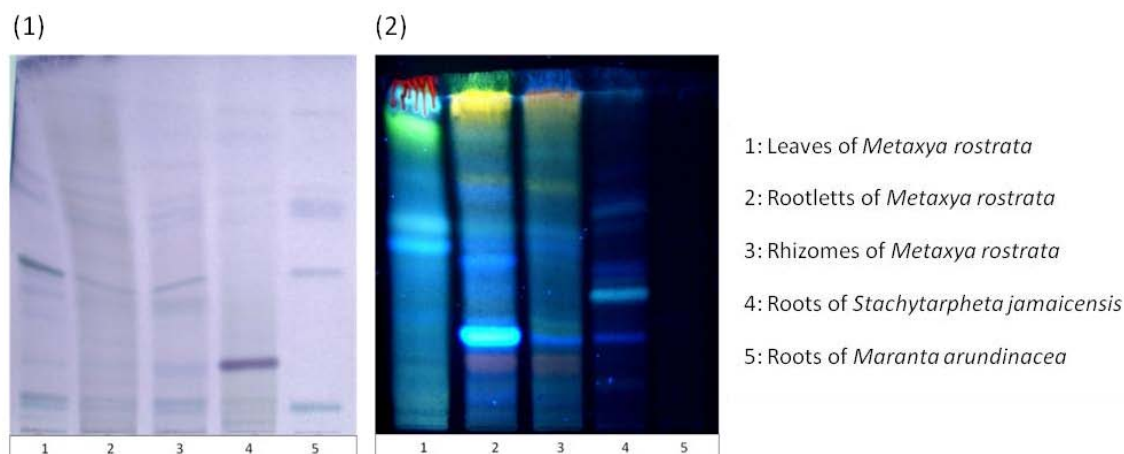


Fig. 75: TLC of the EA-extracts

(1) Stationary phase 1, mobile phase 8, detection 1

(2) Stationary phase 1, mobile phase 1, detection 2

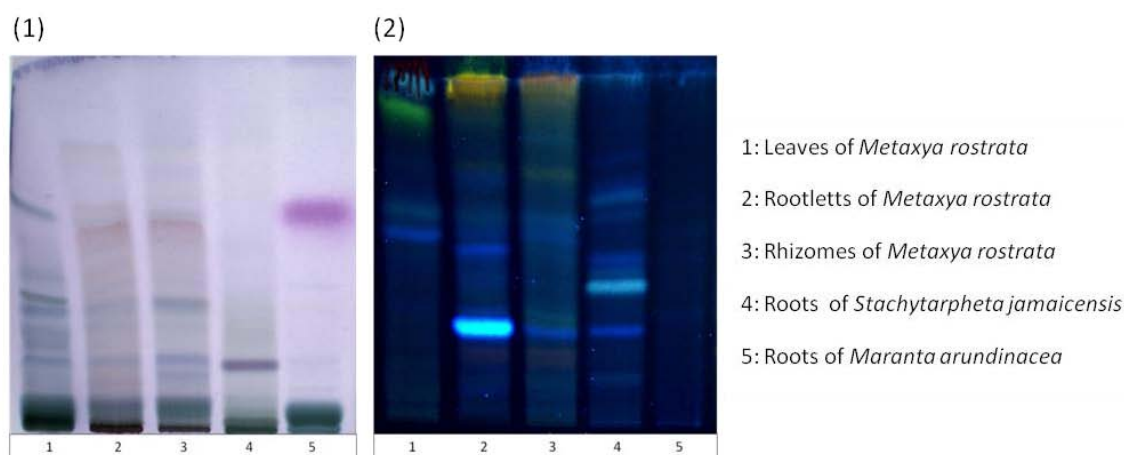


Fig. 76: TLC of the MeOH-extracts

(1) Stationary phase 1, mobile phase 8, detection 1

(2) Stationary phase 1, mobile phase 1, detection 2

In the TCL of the CH_2Cl_2 -extract of the rootlets of *Metaxya rostrata* (2) a very complex pattern of phenolic compounds was detected and in the EA-extract and MeOH-extract of the rootlets of *Metaxya rostrata* a major blue fluorescent phenolcarboxylic acid at R_f 0.27 was detected with detection 2. With detection 2 no phenolic compounds in the extracts of *Maranta arundinacea* (5) were seen, but one major pink compound and very polar compounds in the methanolic extract with detection 1. In the extracts of the rhizomes of *Metaxya rostrata* (3) and the roots of *Stachytarpheta jamaicensis* (4) phenolic components were detected. In the CH_2Cl_2 -extract of the leaves of *Metaxya rostrata* (1) large amounts of chlorophyll were seen with detection 2.

	1	2	3	4	5
	Leaves <i>Metaxya rostrata</i>	Rootlets <i>Metaxya rostrata</i>	Rhizomes <i>Metaxya rostrata</i>	Roots <i>Stachytarpheta jamaicensis</i>	Roots <i>Maranta arundinaceae</i>
<i>MeCl₂</i>	148	99	39	124	52
<i>EA</i>	33	32	19	20	7
<i>MeOH</i>	1005	480	636	117	339

Table 26: Yield (mg) of extracts from ASE

4.2.2 Pretesting of the extracts

In order to determine the effect on cancer cell viability, SW480 colon carcinoma cells, were exposed to increasing concentrations (0.6, 6 and 60µg/ml) of extracts and the percentage of viable cells was determined by neutralred assay.

The CH₂Cl₂-extract of the leaves (1) and the rhizomes of *Metaxya rostrata* (3) and the roots of *Maranta arundinacea* (5) led to a significant cell loss at a concentration of 60µg/ml. The extract from the roots of *Stachytarpheta jamaicensis* (4) and the rootlets of *Metaxya rostrata* (2) showed a significant loss of cells compared to control already at a concentration of 6µg/ml (Fig. 77).

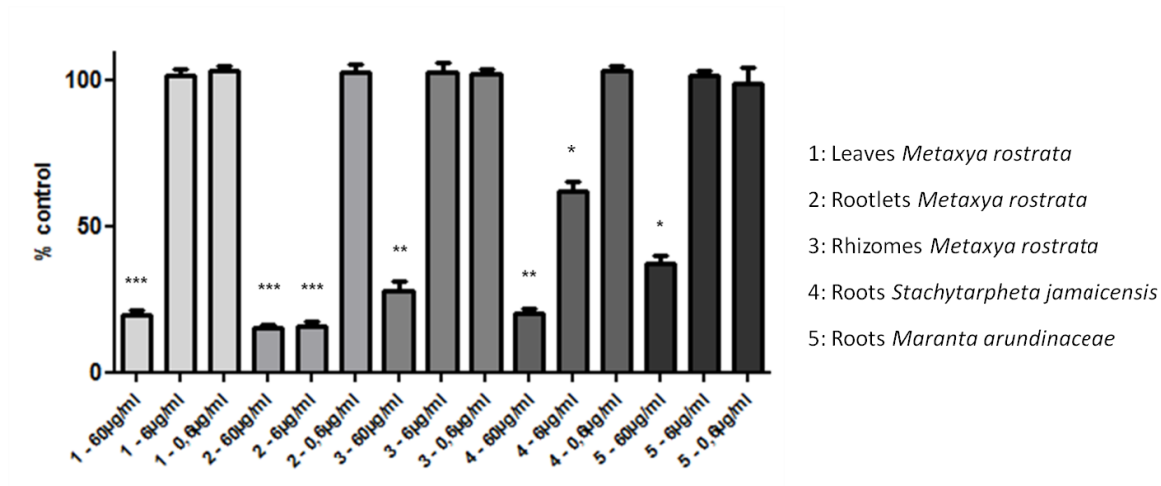


Fig. 77: Viability of SW480 cells treated with the CH₂Cl₂-extracts

Viability of SW480 cells treated with the CH₂Cl₂-extracts of the different plant material (1, 2, 3, 4 and 5) was assessed using neutralred assay. The cells were cultivated on 24-well plates and incubated for 72 hours with increasing concentrations (0.6, 6 and 60µg/ml). Data represent mean ± s.e.mean from three independent experiments performed in triplicate (*P<0.05, **P<0.01, ***P<0.001 as compared to control cells).

After treatment of the cells with the EA-extracts from the rhizomes of *Metaxya rostrata* (3) and the roots of *Stachytarpheta jamaicensis* (4) significant cell loss at a concentration of 60µg/ml was observed. Incubation with the extracts from the leaves (1) and the rootlets of *Metaxya rostrata* (2) led to significant loss of cells as compared to the control at concentrations of 60µg/ml and 6µg/ml and the EA-extract from the roots of *Maranta arundinacea* (5) was active from 0.6µg/ml upwards (Fig. 78).

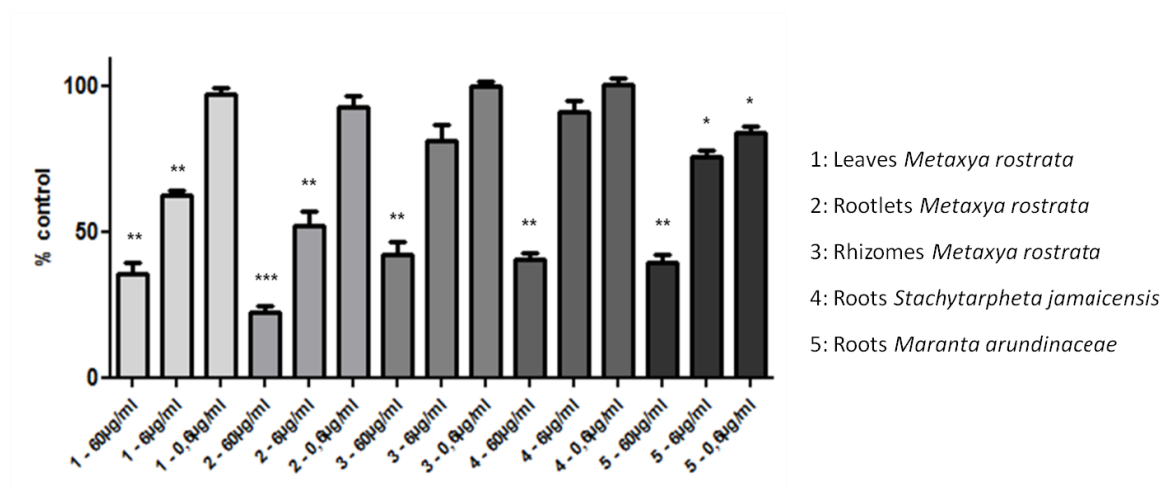


Fig. 78: Viability of SW480 cells treated with the EA-extracts

Viability of SW480 cells treated with the EA-extracts of the different plant material (1, 2, 3, 4 and 5) was assessed with neutralred assay. The cells were cultivated on 24-well plates and incubated for 72 hours with increasing concentrations (0.6, 6 and 60µg/ml). Data represent mean \pm s.e.mean from three independent experiments performed in triplicate (* P <0.05, ** P <0.01, *** P <0.001 as compared to control cells).

The MeOH-extracts of the roots of *Stachytarpheta jamaicensis* and the roots of *Maranta arundinacea* were inactive. The extracts from the leaves, the rootlets and the rhizomes of *Metaxya rostrata* showed a significant loss of cells compared to the control at a concentration of 60µg/ml (Fig. 79), with the extract from the rootlets being the most active.

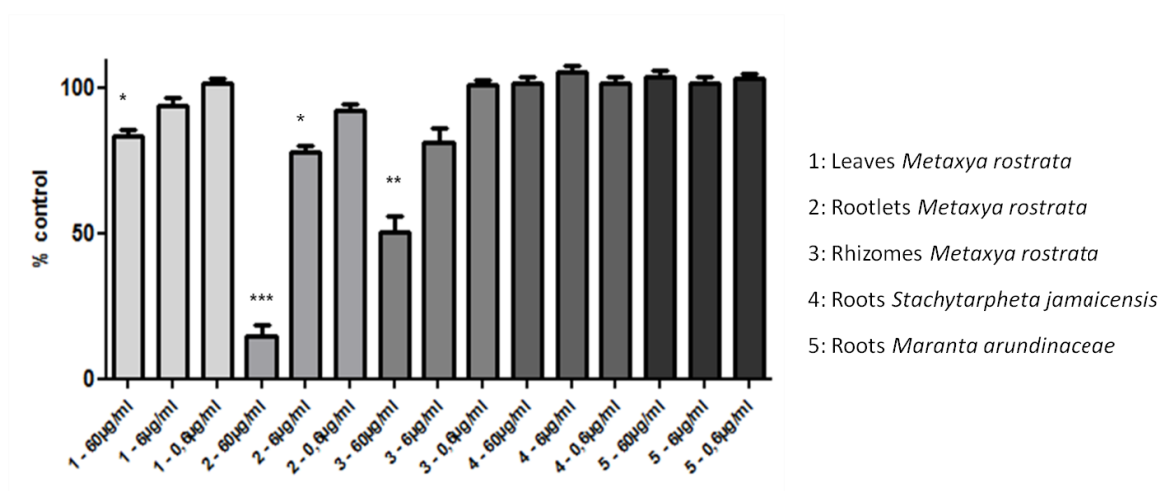


Fig. 79: Viability of SW480 cells treated with the MeOH-extracts

Viability of SW480 cells treated with the MeOH-extracts of the different plant material (1, 2, 3, 4 and 5) was assessed with neutralred assay. The cells were cultivated on 24-well plates and incubated for 72 hours with increasing concentrations (0.6, 6 and 60 µg/ml). Data represent mean \pm s.e.mean from three independent experiments performed in triplicate (* $P < 0.05$, ** $P < 0.01$, *** $P < 0.001$ as compared to control cells).

4.2.2.1 Time-dependence of effects for selected fractions

Due to the compounds pattern and the highest activity of the CH_2Cl_2 -extract of the rootlets of *Metaxya rostrata* (2 CH_2Cl_2), the roots of *Stachytarpheta jamaicensis* (4 CH_2Cl_2), the EA-extract of the leaves (1 EA), the rootlets of *Metaxya rostrata* (2 EA) and of the roots of *Maranta arundinaceae* (5 EA), as well as the MeOH-extracts of the rootlets (2 MeOH) and the rhizomes of *Metaxya rostrata* (3 MeOH) were selected for further investigation.

The effect of cell viability was measured with Neutralred assay. To assess necrosis the LDH-assay was performed. The cells were cultivated on 24-well plates and were exposed to the extracts for 24, 48 and 72 hours.

After 24 hours all studied extracts reduced the cell number significantly. 2 CH_2Cl_2 reduced cell viability to 20% and in the LDH assay proved that the cell loss was not due to necrosis. The cell loss after treatment with 4 CH_2Cl_2 and 2 MeOH was due to necrosis (see Fig. 80).

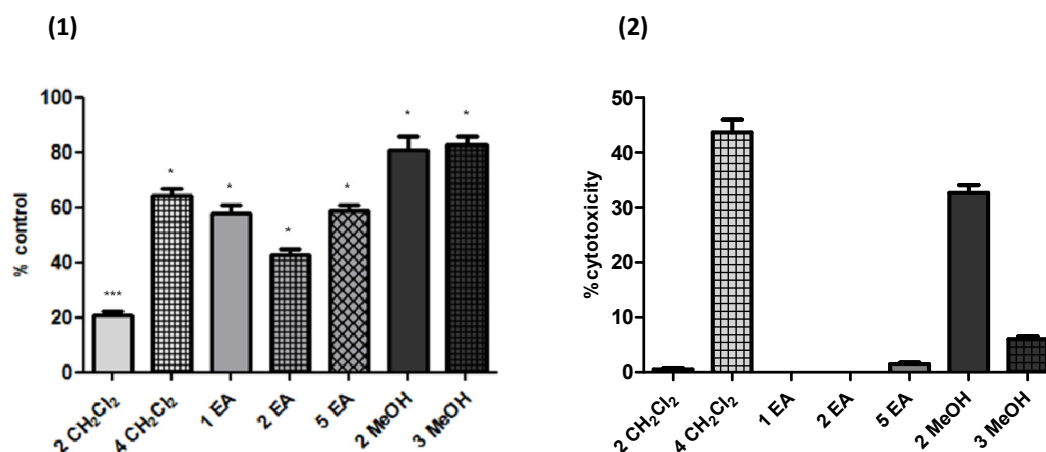


Fig. 80: Viability of SW480 cells (1) and LDH assay (2) after 24h

(1) Viability of SW480 cells treated with the most interesting extracts (2 and 4 CH₂Cl₂, 1, 2 and 5 EA and 2 and 3 MeOH) was assessed with neutralred assay. (2) Cytotoxicity of the most interesting extracts on SW480 cells was evaluated with the LDH assay. The cells were cultivated on 24-well plates and incubated for 24 hours with a concentration of 30µg/ml. Data represent mean \pm s.e.mean from three independent experiments performed in triplicate (*P<0.05, ***P<0.001 as compared to control cells).

After 48 hours the 5 EA, 2 MeOH and 3 MeOH showed low or no significant cell loss. The cell loss of 2 MeOH and of 4 CH₂Cl₂ was due to necrosis. 2 CH₂Cl₂ reduced cell viability to 30% and in the LDH assay it was shown that the cell loss was not due to necrosis. 1 EA and 2 EA showed significant cell loss which was not due to necrosis (Fig. 81).

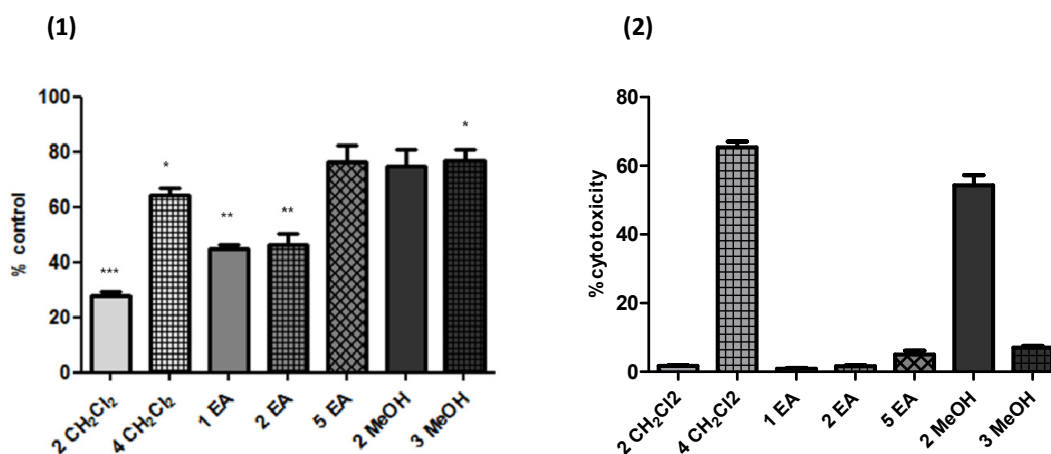


Fig. 81 Viability of SW480 cells (1) and LDH assay (2) after 48h

(1) Viability of SW480 cells treated with the most interesting extracts (2 and 4 CH₂Cl₂, 1, 2 and 5 EA and 2 and 3 MeOH) was assessed with neutralred assay. (2) Cytotoxicity of the most interesting extracts on SW480 cells was evaluated with the LDH assay. The cells were cultivated on 24-well plates and incubated for 48 hours with a concentration of 30µg/ml. Data represent mean \pm s.e.mean from three independent experiments performed in triplicate (*P<0.05, **P<0.01, ***P<0.001 as compared to control cells).

After 72 hours all extracts reduced the cell viability significantly. But the cell loss in 2 MeOH and 4 CH₂Cl₂ was due to necrosis. 1 EA and 2 EA showed significant cell loss which is not due to necrosis. 2 CH₂Cl₂ reduced cell viability to 20% with a little higher LDH level as after 48h.

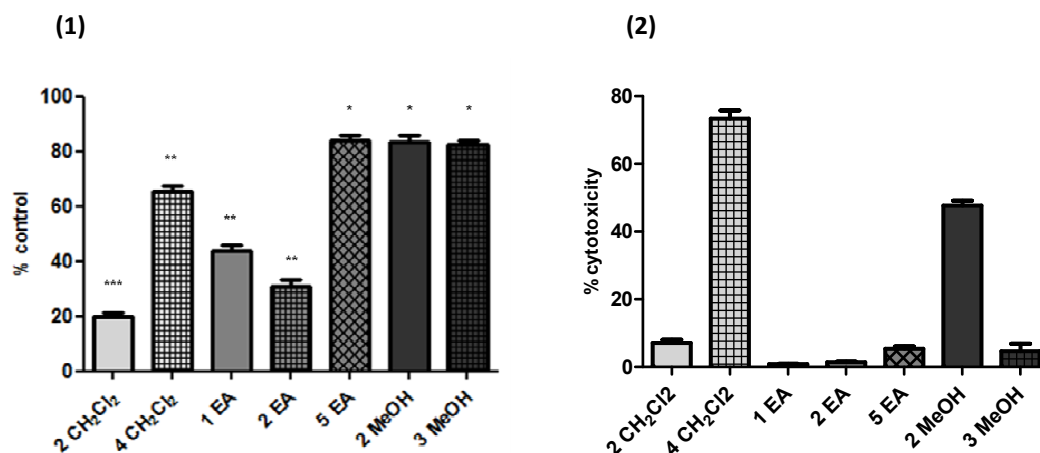


Fig. 82: Viability of SW480 cells (1) and LDH assay (2) after 72h

(1) Viability of SW480 cells treated with the most interesting extracts (2 and 4 CH₂Cl₂, 1, 2 and 5 EA and 2 and 3 MeOH) was assessed with neutralred assay. (2) Cytotoxicity of the most interesting extracts on SW480 cells was evaluated with the LDH assay. The cells were cultivated on 24-well plates and incubated for 72 hours with a concentration of 30 µg/ml. Data represent mean ± s.e.mean from three independent experiments performed in triplicate (*P<0.05, **P<0.01, ***P<0.001 as compared to control cells).

The results of the neutralred- and the LDH-assays in these experiments showed the highest activity for the CH₂Cl₂-extract of the rootlets of *Metaxya rostrata* (2 CH₂Cl₂), the EA-extract of the leaves (1 EA), the EA-extract of the rootlets of *Metaxya rostrata* (2 EA) and the MeOH-extracts of the rhizomes of *Metaxya rostrata* (3 MeOH). Cell loss was not caused by necrosis. Thus, these extracts were chosen for the isolation of the active principles.

4.2.3 Extraction, fractionation and testing of the CH₂Cl₂-extract from the rootlets of *Metaxya rostrata*

From 97g plant material after extraction with dichloromethane at 40° using Accelerated Solvent Extraction (ASE) 1g CH₂Cl₂-extract was obtained. This extract was subjected to column chromatography on Sephadex LH-20 under elution with EtOAc (Table 27) to obtain 9 pooled subfractions CC-9/1 to CC-9/9 (Fig. 83).

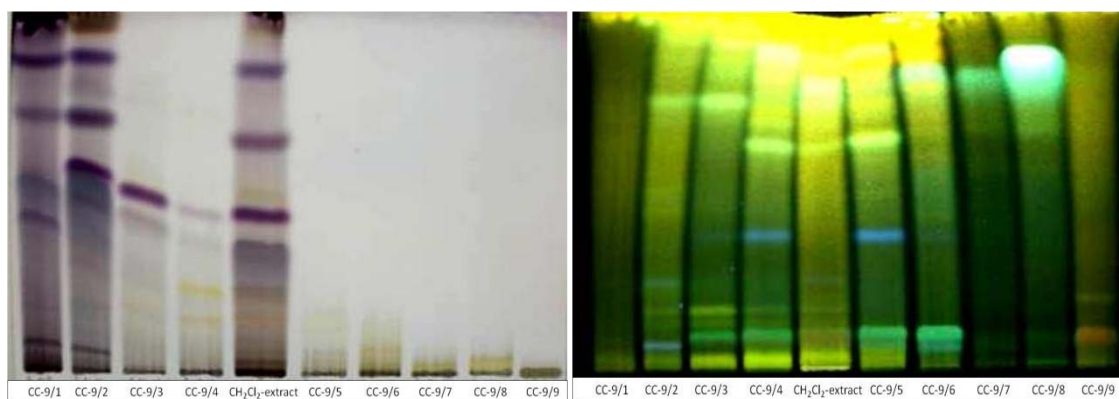


Fig. 83: TLC of the combined fractions of CC-9

Stationary phase 1, mobile phase 1, detection 1 and 2

The TLC of the pooled fractions of CC-9 showed terpenoid compounds in fractions CC-9/1 to fraction CC-9/3 and very polar compounds in fractions CC-9/5 to CC-9/9 with detection 1. With detection 2 a complex pattern of phenolic compounds was detected.

CC-9 parameters	Mobile Phase	Fraction No.	Pooled fractions	mg	Further treatment
<u>Stationary phase:</u> Sephadex LH-20 <u>Column diameter:</u> 2cm <u>Column height:</u> 85cm <u>Fraction separation:</u> 1g of CH ₂ Cl ₂ Extract <u>Fraction size:</u> 12 ml/60 min	EtOAc	CC-9/1	1-7	308	testing
	"	CC-9/2	8-11	304	testing
	"	CC-9/3	12-18	99	testing
	"	CC-9/4	19-33	61	testing
	"	CC-9/5	34-62	43	testing
	"	CC-9/6	63-90	18	testing
	"	CC-9/7	91-120	9	testing
	"	CC-9/8	121-145	18	testing
	"	CC-9/9	146-200	35	testing

Table 27: Conditions for CC-9

All fractions were tested for their cytotoxic potential. The neutralred assay revealed a dose-dependent reduction of cell viability. At a concentration of 6µg/ml, fractions CC-9/3,

CC-9/4, CC-9/5 reduced cell viability significantly to 10% and fraction CC-9/6 and CC-9/8 down to 20% of the control (Fig. 84).

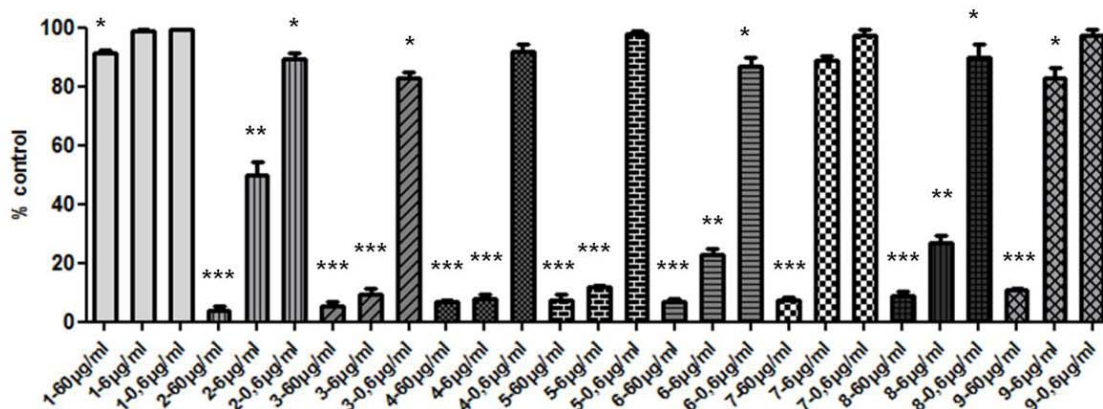


Fig. 84: Viability of SW480 cells treated with the fractions of CC-9

Viability of SW480 cells treated with the fractions of CC-9 (fraction CC-9/1 to fraction 9) was assessed with neutralred assay. The cells were cultivated on 24-well plates and incubated for 48 hours with increasing concentrations (0.6, 6 and 60 µg/ml). Data represent mean \pm s.e.mean from three independent experiments performed in triplicate (* P <0.05, ** P <0.01, *** P <0.001 as compared to control cells).

4.2.4 Extraction, fractionation and testing of the EA extract from the rootlets of *Metaxya rostrata*

After extraction with dichloromethane the plant material (see p.88) was extracted with ethylacetate at 40° using Accelerated Solvent Extraction (ASE) to yield 1.2g of EA-extract fractionated by column chromatography CC-10 on Sephadex LH-20 under elution with EtOAc and EtOAc-MeOH (Table 28) to obtain 20 pooled subfractions (Fig. 85 and 86).

(1)

(2)

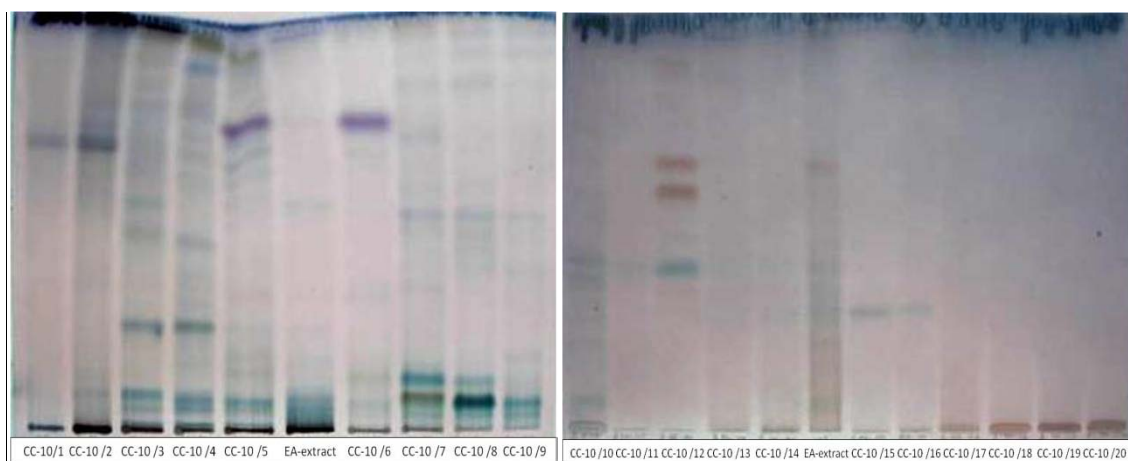


Fig. 85: TLC -1 of the combined fractions of CC-10

(1) Stationary phase 1, mobile phase 5.1, detection 1. (2) Stationary phase 1, mobile phase 1, detection 1.

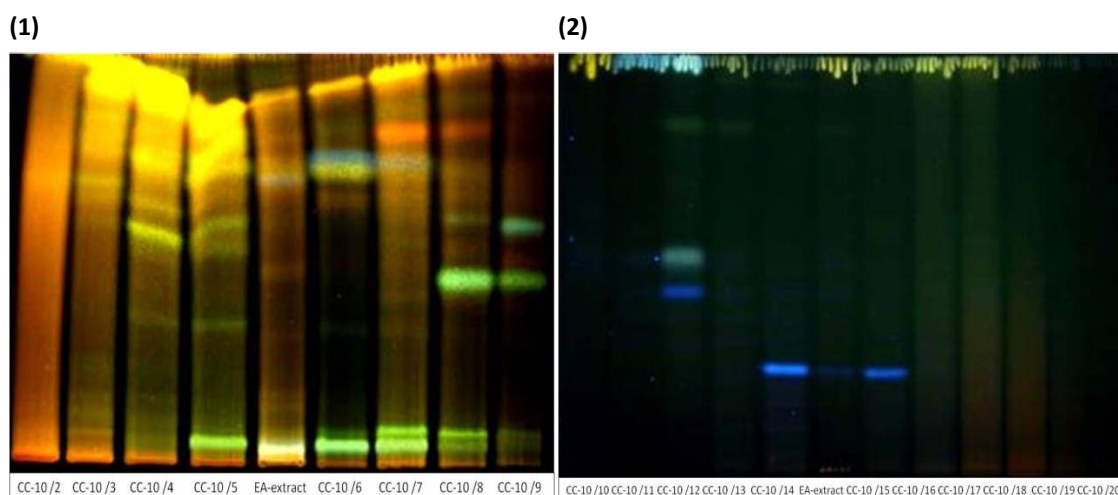


Fig. 86: TLC-2 of the combined fractions of CC-10

(1) Stationary phase 1, mobile phase 5.1, detection 2. (2) Stationary phase 1, mobile phase 1, detection 2.

The TLC of the pooled fractions of CC-10 showed a complex pattern of phenolic compounds in fractions CC-10/2 to 9. In fractions CC-10/14 and CC-10/15 a major blue fluorescent compound at R_f 0.24 can be detected with detection 2. Proanthocyanidines coloured red with detection 1 were seen in fraction CC-10/12 at R_f 0.57 and 0.66 and the blue compound at R_f 0.39 in the same fraction was identified as KK1.

CC-10 parameters	Mobile Phase	Fraction No.	Pooled fractions	mg	Further treatment
Stationary phase: Sephadex LH-20	EtOAc	CC-10/1	1-6	27	testing
	"	CC-10/2	7-11	96	testing
	"	CC-10/3	12-20	67	testing
	"	CC-10/4	21-30	31	testing
	"	CC-10/5	31-40	21	testing
	"	CC-10/6	41-50	14	testing
	"	CC-10/7	51-70	21	testing
	"	CC-10/8	71-90	19	testing
	"	CC-10/9	91-120	16	testing
Column diameter: 2cm	EA:MeOH(70:30)	CC-10/10	121-170	327	testing
	"	CC-10/11	171-221	45	testing
	"	CC-10/12	222-250	32	testing
	"	CC-10/13	251-280	16	testing
	"	CC-10/14	281-300	21	testing
	"	CC-10/15	301-324	10	testing
	"	CC-10/16	325-333	14	testing
	"	CC-10/17	334-360	57	testing
	"	CC-10/18	361-400	61	testing
Column height: 90cm	"	CC-10/19	401-430	33	testing
	"	CC-10/20	431-470	38	testing
Fraction separation: 1200mg of EA Extract	"	CC-10/1	1-6	27	testing
	"	CC-10/2	7-11	96	testing
	"	CC-10/3	12-20	67	testing
	"	CC-10/4	21-30	31	testing
	"	CC-10/5	31-40	21	testing
	"	CC-10/6	41-50	14	testing
	"	CC-10/7	51-70	21	testing
	"	CC-10/8	71-90	19	testing
	"	CC-10/9	91-120	16	testing
Fraction size: 12 ml/60 min	"	CC-10/10	121-170	327	testing
	"	CC-10/11	171-221	45	testing
	"	CC-10/12	222-250	32	testing
	"	CC-10/13	251-280	16	testing
	"	CC-10/14	281-300	21	testing
	"	CC-10/15	301-324	10	testing
	"	CC-10/16	325-333	14	testing
	"	CC-10/17	334-360	57	testing
	"	CC-10/18	361-400	61	testing

Table 28: Conditions for CC-10

The cytotoxic activity of fractions CC-10/1 to CC-10/17 was determined in the neutralred assay which revealed a significant dose-dependent reduction of cell viability in fraction CC-10/2, CC-10/3, CC-10/4, CC-10/5 and CC-10/6. These fractions showed significant cell loss down to a concentration of 6 μ g/ml or 0.6 μ g/ml. The other fractions exhibited lower or no activity (Fig. 87 and Fig. 88).

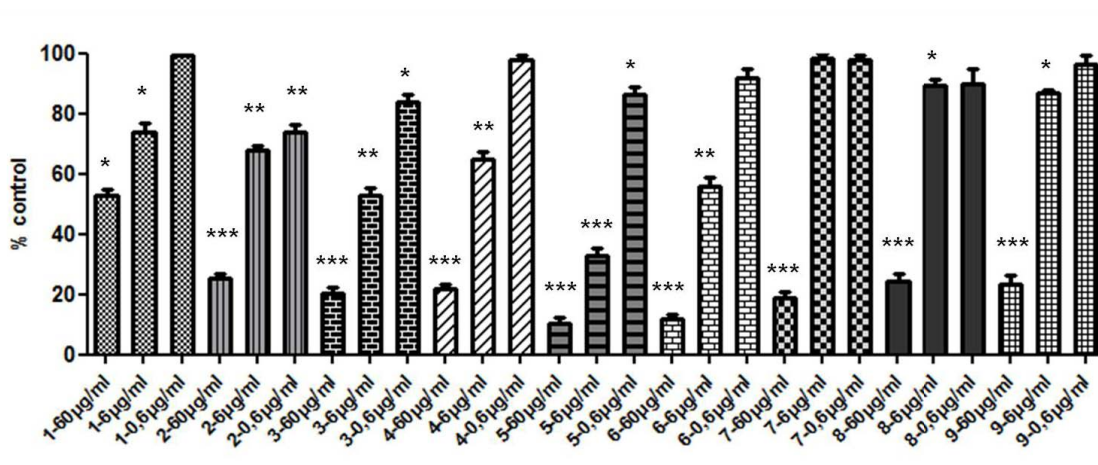


Fig. 87: Viability of SW480 cells treated with the fractions of CC-10

Viability of SW480 cells treated with the fractions of CC-10 (fraction CC-10/1 to fraction 9) was assessed with neutralred assay. The cells were cultivated on 24-well plates and incubated for 48 hours with increasing concentrations (0.6, 6 and 60 μ g/ml). Data represent mean \pm s.e.mean from three independent experiments performed in triplicate (* P <0.05, ** P <0.01, *** P <0.001 as compared to control cells).

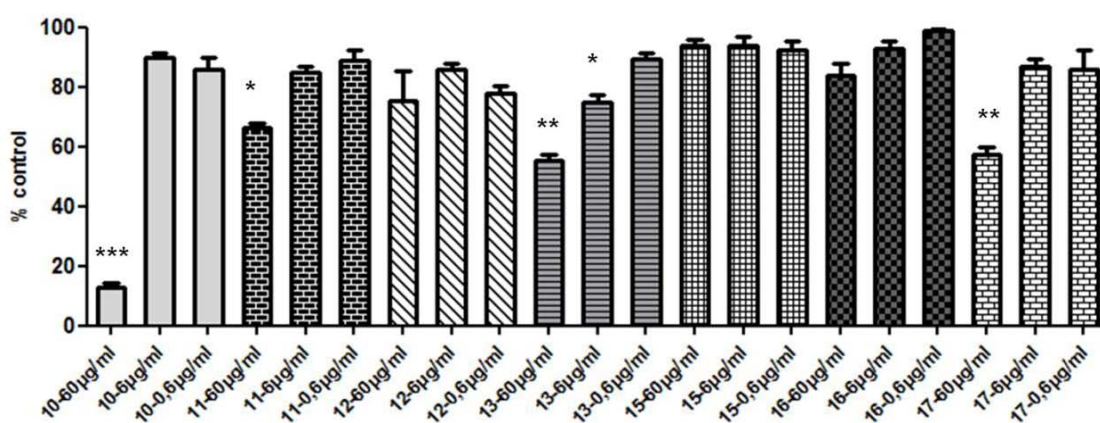


Fig. 88: Viability of SW480 cells treated with the fractions of CC-10

Viability of SW480 cells treated with the fractions of CC-10 (fraction CC-10/10 to fraction 17) was assessed with neutralred assay. The cells were cultivated on 24-well plates and incubated for 48 hours with increasing concentrations (0.6, 6 and 60 μ g/ml). Data represent mean \pm s.e.mean from three independent experiments performed in triplicate (* P <0.05, ** P <0.01, *** P <0.001 as compared to control cells).

To additionally confirm the previous results, the experiment was repeated with the most active fractions. Fractions CC-10/3, CC-10/4, CC-10/5, CC-10/6 reduced cell viability significantly at a concentration of 60µg/ml to about 20%. At a concentration of 6µg/ml the cell viability in these fractions is reduced to 40% in CC-10/5 or about 65% in CC-10/3, CC-10/4 and CC-10/6 (see Fig. 89).

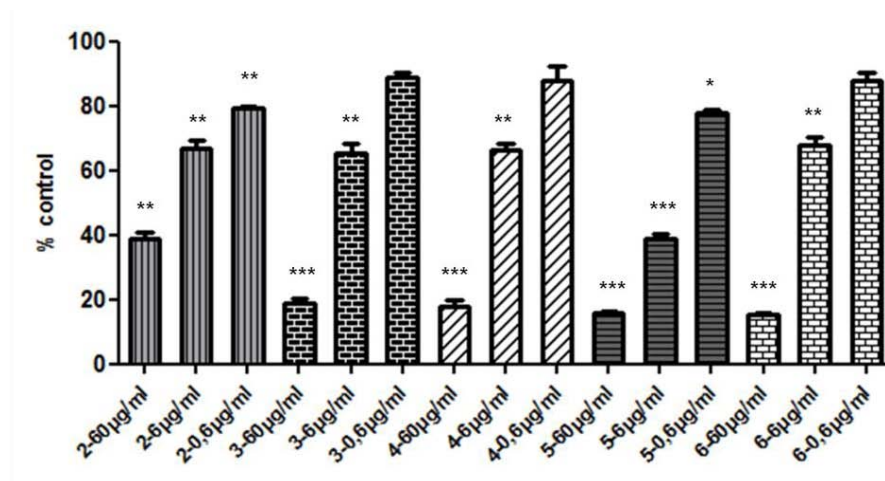


Fig. 89: Viability of SW480 cells treated with the selected fractions of CC-10

Viability of SW480 cells treated with the most active fractions of CC-10 (fractions CC-10/2, 3, 4, 5 and 6) was assessed with neutralred assay. The cells were cultivated on 24-well plates and incubated for 48 hours with increasing concentrations (0.6, 6 and 60µg/ml). Data represent mean \pm s.e.mean from three independent experiments performed in triplicate (* P <0.05, ** P <0.01, *** P <0.001 as compared to control cells).

4.2.5 Extraction, fractionation and testing of the EA extract from the leaves of *Metaxya rostrata*

120g leaves, after extraction with dichloromethane and drying, were extracted by ASE with ethylacetate at 40° to obtain 820mg of EA-extract. Before fractionation by column chromatography, chlorophyll was removed using liquid/liquid partition (see p.44). TLC analysis was used to confirm the removal of a large amount of chlorophyll. The intensive red colored zones with an R_f values of 0.9 and above and the enriched polar compounds showed that the procedure had been effective (Fig. 90).

Results

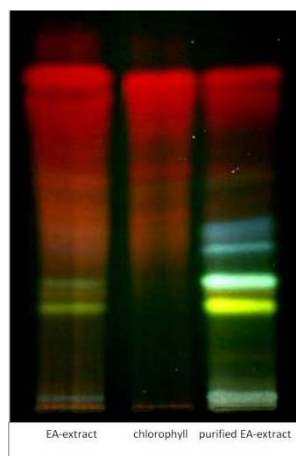
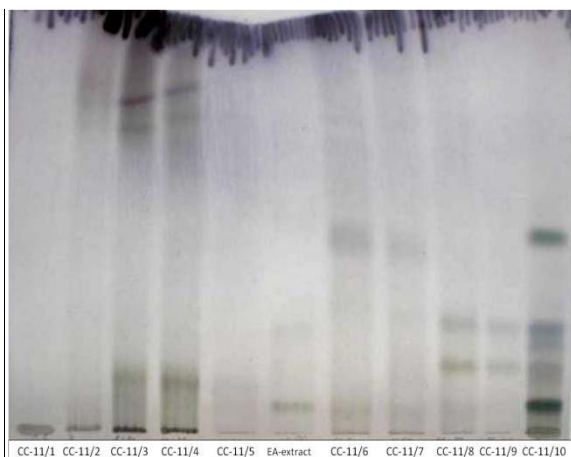


Fig. 90: TLC of the fractions after removal of chlorophyll

Stationary phase 1, mobile phase 14, detection 2

The purified EA-extract was further subjected to column chromatography on Sephadex under elution with EtOAc. Column chromatography CC-11 yielded 10 pooled fractions (Table 29) which were tested for their activity on cell proliferation. The blue fluorescent compound in CC-11/9 at R_f 0.76 was identified as caffeic acid by TLC comparison with the authentic reference (Fig. 91).

(1)



(2)

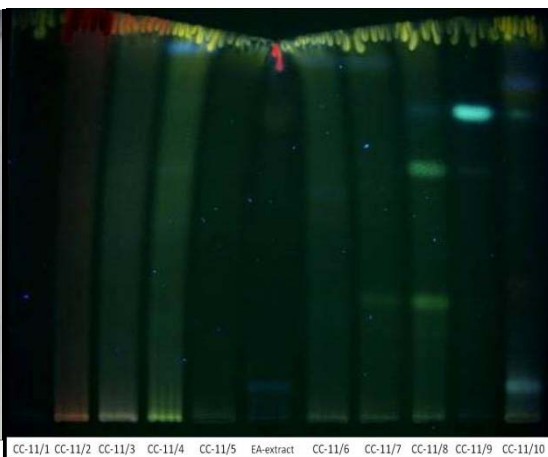


Fig. 91: TLC of the combined fractions of CC-11

(1) Stationary phase 1, mobile phase 5.2, detection 1

(2) Stationary phase 1, mobile phase 5.1, detection 2

CC-11 parameters	Mobile Phase	Fraction No.	Pooled fractions	mg	Further treatment
Stationary phase: Sephadex LH-20 Column diameter: 2cm Column height: 85cm Fraction separation: 240mg of purified EA Extract Fraction size: 6 ml/60 min	EtOAc	CC-11/1	1-6	3	testing
	"	CC-11/2	7	13	testing
	"	CC-11/3	8-14	33	testing
	"	CC-11/4	15-28	7	testing
	"	CC-11/5	29-40	7	testing
	"	CC-11/6	41-60	10	testing
	"	CC-11/7	61-80	10	testing
	"	CC-11/8	81-92	7	testing
	"	CC-11/9	93-115	12	testing
	"	CC-11/10	116-200	79	testing

Table 29: Conditions for CC-11

In order to evaluate the effect of the fractions of the EA-extract on cancer cell viability, the SW480 cells were exposed to increasing concentrations (0.6, 6 and 60 µg/ml) of these fractions.

The neutralred assay revealed a significant dose-dependent reduction of cell viability in fraction CC-11/3, CC-11/7, CC-11/8 and CC-11/9. These fractions showed significant cell loss at a concentration of 6 µg/ml. For other fractions lower or no activity was revealed (Fig. 92).

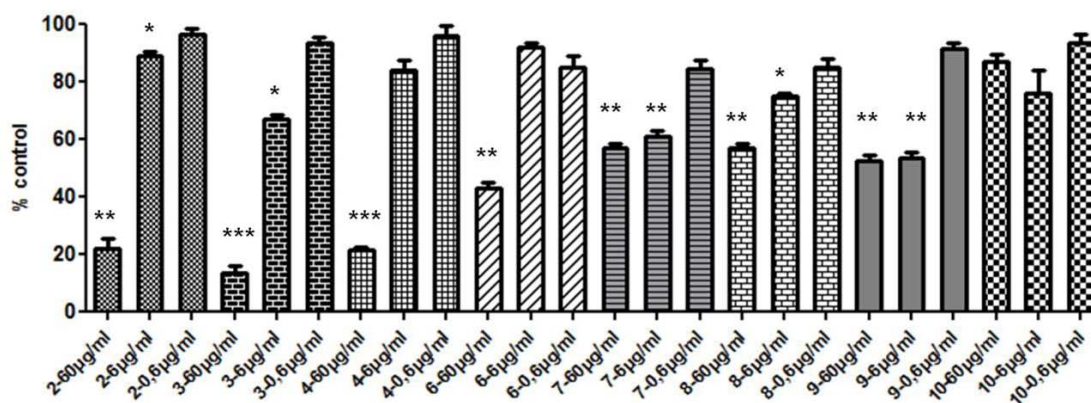


Fig. 92: Viability of SW480 cells treated with the selected fractions of CC-11

Viability of SW480 cells treated with the fractions of CC-11 (fractions CC-11/2 to 10) was assessed with neutralred assay. The cells were cultivated on 24-well plates and incubated for 48 hours with increasing concentrations (0.6, 6 and 60 µg/ml). Data represent mean \pm s.e.mean from three independent experiments performed in triplicate (*P < 0.05, **P < 0.01, ***P < 0.001 as compared to control cells).

4.2.6 Extraction, fractionation and testing of the MeOH extract from the rhizomes of *Metaxya rostrata*

300g of the plant material were extracted with methanol at 40° using Accelerated Solvent Extraction (ASE) to obtain 30,6g of MeOH-extract. Due to the content of tannins in this extract and to avoid interferences of these compounds with the assay, a detannification step was performed following the scheme depicted in Fig. 93.

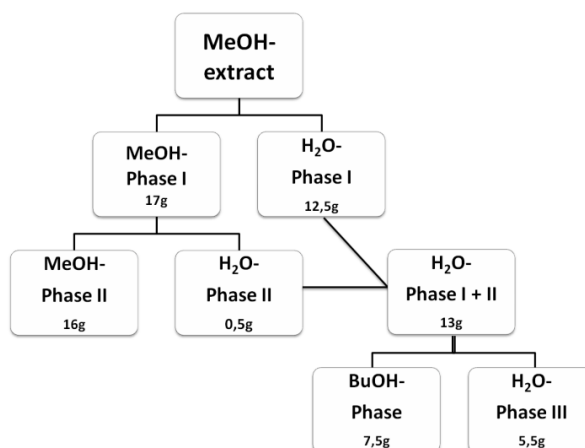


Fig. 93: Scheme of detannification of the MeOH-extract of the rhizomes of *Metaxya rostrata*

The methanol extract was dissolved in water by sonification for 15min. After centrifugation the supernatant was collected (H₂O-Phase I). The tannins remained in the residue, which was again sonicated with water (H₂O-Phase II). The two water phases were combined and partitioned with butanol (BuOH-Phase) (Fig. 94) which was then subjected to column chromatography on Sephadex LH-20.

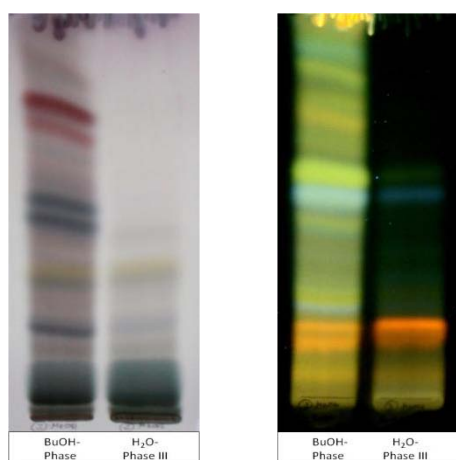


Fig. 94: TLCs of detannification of the MeOH-extract of the rhizomes from *Metaxya rostrata*

Stationary phase 1, mobile phase 1, detection 1 and 2

Results

After detection with anisaldehyde-sulfuric acid reagent a red compound in the BuOH-phase with R_f 0.81 was identified as a mixture of cinnamintannin B and aesculitannin B1 by TLC-comparison with the reference compound. A blue compound at R_f 0.54 was identified as compound KK5 and another blue compound at R_f 0.48 as compound KK1.

The purified MeOH-extract was further subjected to column chromatography on Sephadex LH-20 under elution with 80% MeOH (Table 30). Column chromatography CC-12 yielded 13 fractions (Fig. 95 and Fig. 96), which were tested for their activity on cell proliferation.

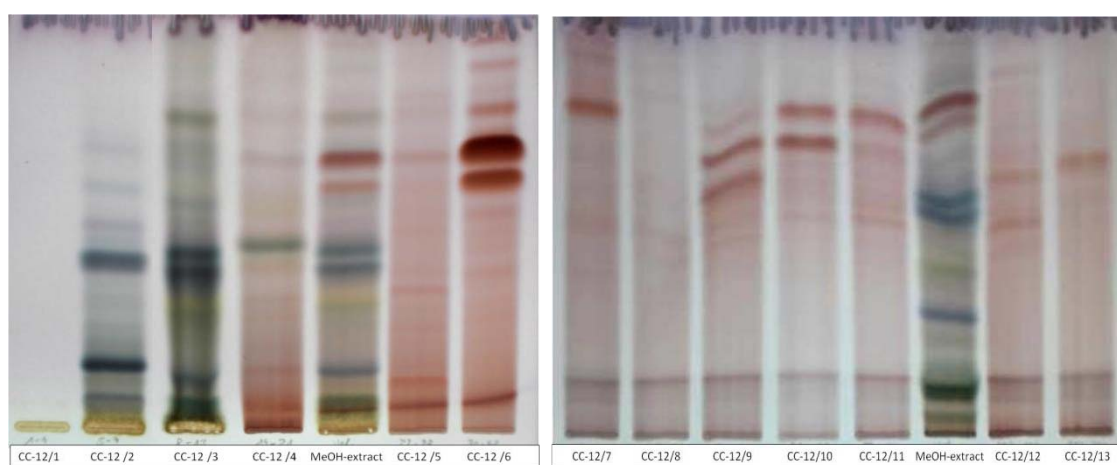


Fig. 95: TLC of the combined fractions of CC-12

Stationary phase 1, mobile phase 1, detection 1

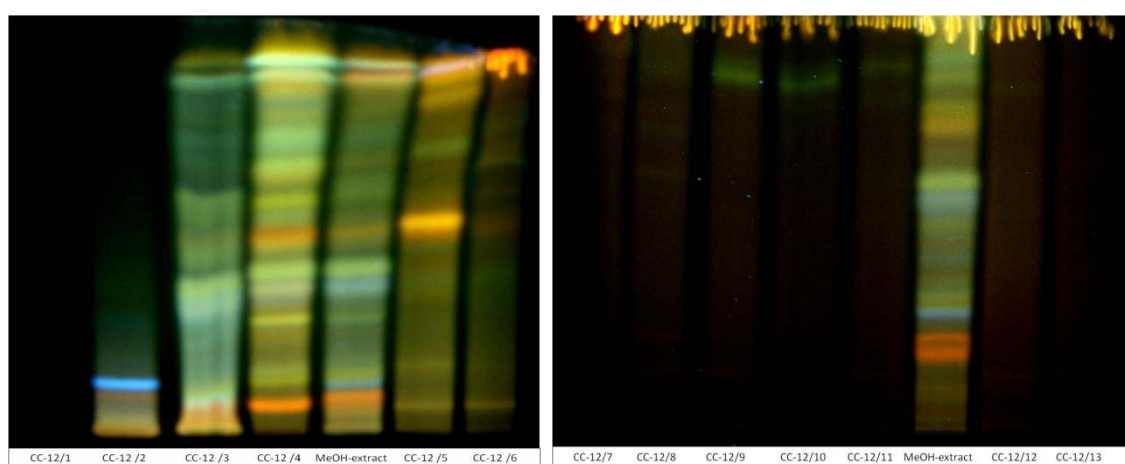


Fig. 96: TLC of the combined fractions of CC-12

Stationary phase 1, mobile phase 1, detection 2

CC-12 parameters	Mobile Phase	Fraction No.	Pooled fractions	mg	Further treatment
<u>Stationary phase:</u> Sephadex LH-20 <u>Column diameter:</u> 2cm <u>Column height:</u> 85cm <u>Fraction separation:</u> 7500mg of MeOH Extract <u>Fraction size:</u> 10 ml/60 min	80% MeOH	CC-12/1	1-4	16	testing
	"	CC-12/2	5-7	934	testing
	"	CC-12/3	8-13	1366	testing
	"	CC-12/4	14-21	677	testing
	"	CC-12/5	22-29	334	testing
	"	CC-12/6	30-42	629	testing
	"	CC-12/7	43-55	130	testing
	"	CC-12/8	56-70	103	testing
	"	CC-12/9	71-81	62	testing
	"	CC-12/10	82-93	63	testing
	"	CC-12/11	94-102	31	testing
	"	CC-12/12	103-120	45	testing
	"	CC-12/13	121-140	34	testing

Table 30: Conditions for CC-12

In the bioassay, fractions CC-12/3 to CC-12/10 reduced cell viability significantly only at a concentration of 60µg/ml. At concentrations of 6µg/ml or lower the fractions had no effect on the cell viability (Fig. 97).

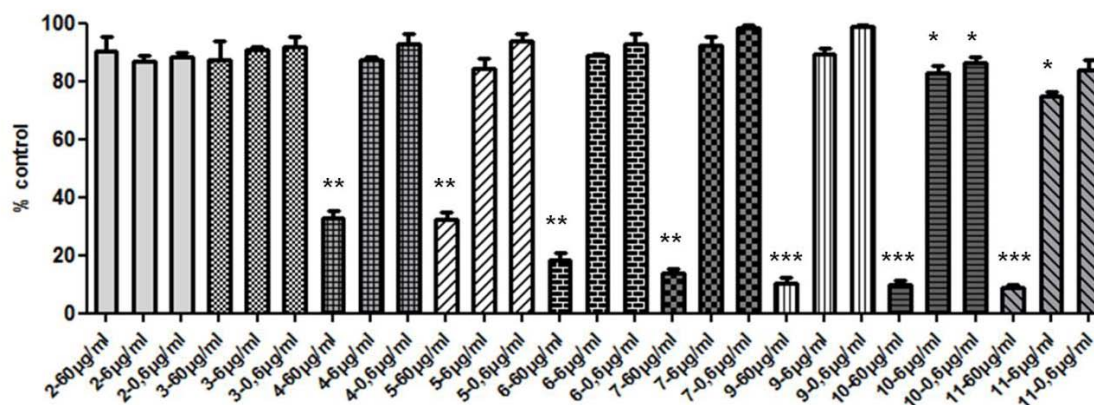


Fig. 97: Viability of SW480 cells treated with the fractions of CC-12

Viability of SW480 cells treated with the fractions of CC-12 (fractions CC-12/2 to 11) was assessed with neutralred assay. The cells were cultivated on 24-well plates and incubated for 48 hours with increasing concentrations (0.6, 6 and 60µg/ml). Data represent mean \pm s.e.mean from three independent experiments performed in triplicate (* P <0.05, ** P <0.01, *** P <0.001 as compared to control cells).

4.2.7 Bioassay of the most active CH₂Cl₂-fractions of CC-9

In order to confirm the earlier results on cancer cell viability, SW480 cells were again exposed to increasing concentrations (1.875, 3.75, 7.5, 15, 30 and 60 µg/ml) of the most active fractions obtained from the CH₂Cl₂-extract of the rootlets of *Metaxya rostrata*. After neutralred assay and LDH assay, the pooled fractions CC-9/3, CC-9/4, CC-9/5, CC-9/6 and CC-9/8, which caused no or little necrosis, were selected. Fraction CC-9/3 reduced cell viability significantly to about 20% down to a concentration of 3.75 µg/ml and more. Fraction CC-9/5 was almost as effective as CC-9/3. Fraction CC-9/4 and CC-9/6 showed similar activity reducing the cell viability significantly at concentrations from 7.5 µg/ml upwards. Only Fraction CC-9/3 was able to reduce the cell viability in a significant manner at a concentration of 1.875 µg/ml (Fig. 98).

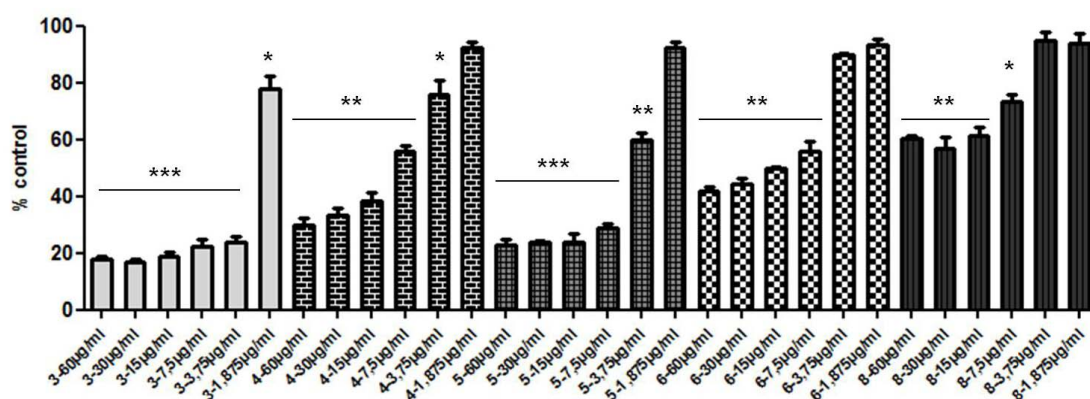


Fig. 98: Bioreactivity assay of the selected fractions of the CH₂Cl₂-extract of the rootlets of *Metaxya rostrata*

Viability of SW480 cells treated with the most active fractions of CC-12 (fractions CC-12/3, 4, 5, 6 and 8) was assessed with neutralred assay. The cells were cultivated on 24-well plates and incubated for 48 hours with increasing concentrations (1.875, 3.75, 7.5, 15, 30 and 60 µg/ml). Data represent mean ± s.e.mean from three independent experiments performed in triplicate (*P<0.05, **P<0.01, ***P<0.001 as compared to control cells).

4.2.8 Isolation and structure elucidation of the active compounds of the most active CH₂Cl₂-fractions of the rootlets of *Metaxya rostrata*

Due to their high activity, fractions CC-9/3, CC-9/4, CC-9/5 and CC-9/6 of the CH₂Cl₂-extract of the rootlets (Fig. 99) were selected for further fractionation and isolation of the active compounds. The small amount of the fractions made re-extraction and re-fractionation necessary for the isolation of the active principles.

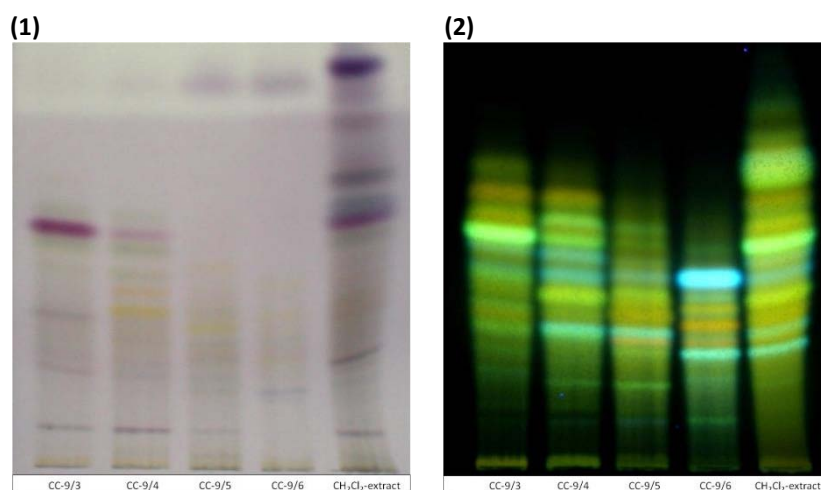


Fig. 99: TLC of the most active fractions of the CH_2Cl_2 -extract of the rootlets from *Metaxya rostrata*

- (1) Stationary phase 1, mobile phase 1, detection 1
- (2) Stationary phase 1, mobile phase 1, detection 2

The TLC of the most active fractions showed a complex pattern of phenolic compounds with detection 2. In fraction CC-9/3 a major compound coloured purple at R_f 0.72 with detection 1 and a major green fluorescent compound with detection 2 were detected. With detection 2 a major blue fluorescent compound in CC-9/6 can be seen.

4.2.8.1 Reextraction and refractionation of the CH_2Cl_2 -extract of the rootlets from *Metaxya rostrata*

The active fractions, which were further fractionated, were CC-9/3 (90mg), CC-9/4 (60mg), CC-9/5 (40mg) and CC-9/6 (15mg). Due to the small amount of these fractions, new plant material was extracted and fractionated in the same way to obtain more of the active fractions. 920g dried rootlets of *Metaxya rostrata* were pulverized and extracted by sonification with CH_2Cl_2 yielding 5,3g CH_2Cl_2 -extract. This CH_2Cl_2 -extract was compared by TLC to the first CH_2Cl_2 -extract. Detection with different spraying reagents revealed the qualitative composition and showed good correlations (Fig. 100).

Results

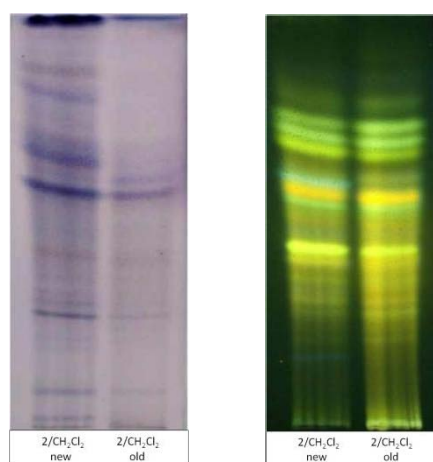


Fig. 100: TLC comparison of the two CH_2Cl_2 -extracts of the rootlets

- (1) Stationary phase 1, mobile phase 10, detection 1.
- (2) Stationary phase 1, mobile phase 10, detection 2.

Thus, the “new” extract was fractionated in the same manner as the first CH_2Cl_2 -extract and subjected to column chromatography on Sephadex LH-20 under elution with EtOAc (Table 31) to obtain a total of 290 fractions which were combined after TLC comparison to 16 subfractions CC-13/1 to CC-13/16 (Fig. 101 and Fig. 102).

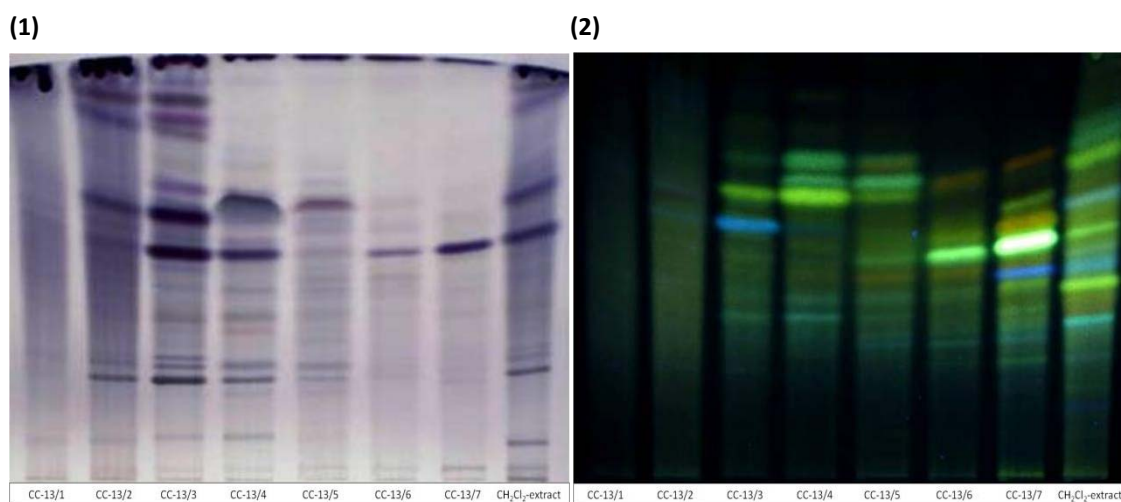


Fig. 101: TLC of the combined fractions 1-7 of CC-13

- (1) Stationary phase 1, mobile phase 1, detection 1
- (2) Stationary phase 1, mobile phase 1, detection 2

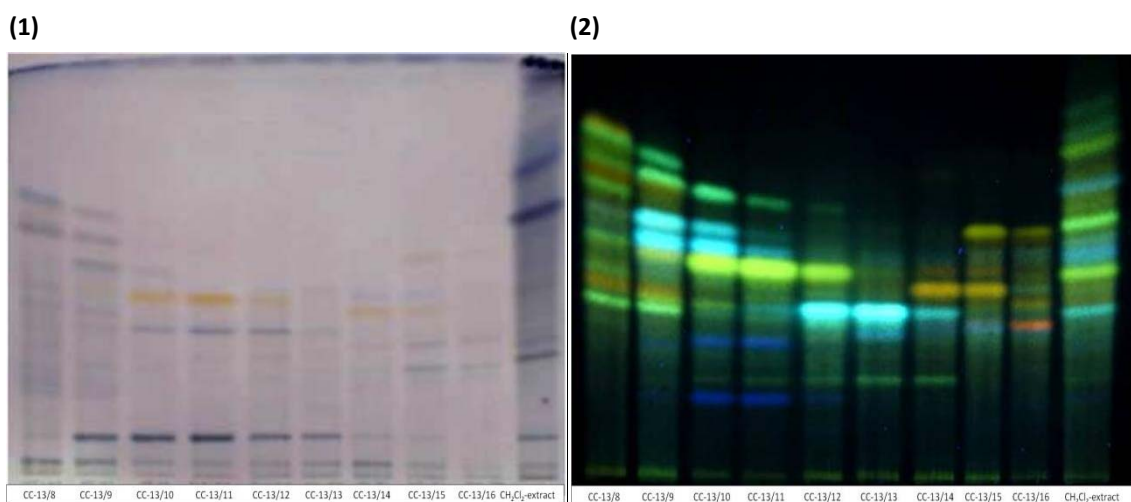


Fig. 102: TLC of the combined fractions 8 to 16 of CC-13

(1) Stationary phase 1, mobile phase 1, detection 1

(2) Stationary phase 1, mobile phase 1, detection 2

CC-13 parameters	Mobile Phase	Fraction No.	Pooled fractions	mg	Further treatment
Stationary phase: Sephadex LH-20 Column diameter: 4cm Column height: 75cm Fraction separation: 5370mg of new CH ₂ Cl ₂ Extract Fraction size: 8 ml/60 min	EtOAc	CC-13/1	1-42	540	testing
	"	CC-13/2	43-54	1620	testing
	"	CC-13/3	55-65	1390	testing
	"	CC-13/4	66-71	518	testing
	"	CC-13/5	72-77	171	testing
	"	CC-13/6	78-82	52	testing
	"	CC-13/7	83-101	192	testing
	"	CC-13/8	102-116	77	testing
	"	CC-13/9	117-127	51	testing
	"	CC-13/10	128-136	45	testing
	"	CC-13/11	137-140	25	testing
	"	CC-13/12	141-150	30	testing
	"	CC-13/13	151-180	25	testing
	"	CC-13/14	181-202	30	testing
	"	CC-13/15	203-224	30	testing
	"	CC-13/16	225-290	15	testing

Table 31: Conditions for CC-13

4.2.8.2 Bioassay of the fractions from CC-13

In order to evaluate the effect of the fractions of CC-13 on SW480 viability, the cells were exposed to increasing concentrations (0.6, 6 and 60µg/ml).

Fractions CC-13/2, CC-13/3, CC-13/4, CC-13/11 and CC-13/16 reduced cell viability significantly only at a concentration of 60µg/ml. At a concentration of 6µg/ml or lower

these fractions had no effect on the cell viability. Fractions CC-13/5, CC-13/6, CC-13/7, CC-13/8, CC-13/14 and CC-13/15 showed higher activity, reducing the cell viability in a significant manner at concentrations of 6 $\mu\text{g/ml}$ (see Fig. 103 and Fig. 104).

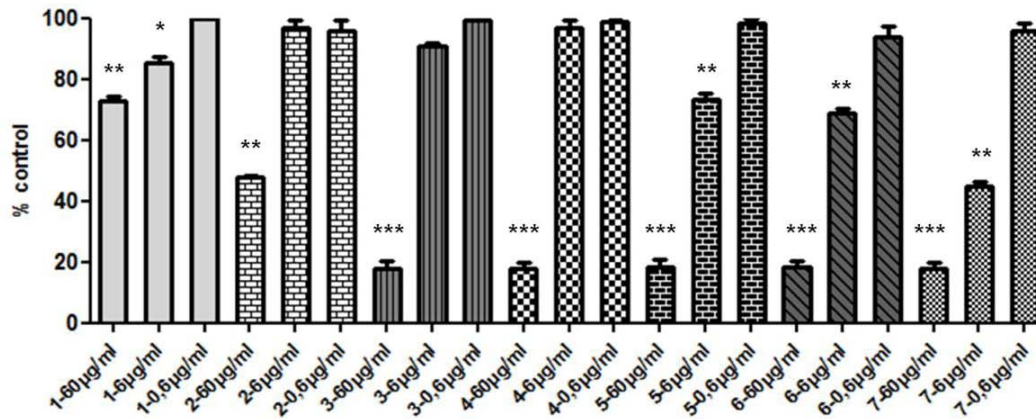


Fig. 103: Viability of SW480 cells after treatment with fractions 1-7 of CC-13

Viability of SW480 cells treated with the fractions of CC-13 (fractions CC-13/1 to 7) was assessed with neutralred assay. The cells were cultivated on 24-well plates and incubated for 48 hours with increasing concentrations (0.6, 6 and 60 $\mu\text{g/ml}$). Data represent mean \pm s.e.mean from three independent experiments performed in triplicate (* $P < 0.05$, ** $P < 0.01$, *** $P < 0.001$ as compared to control cells).

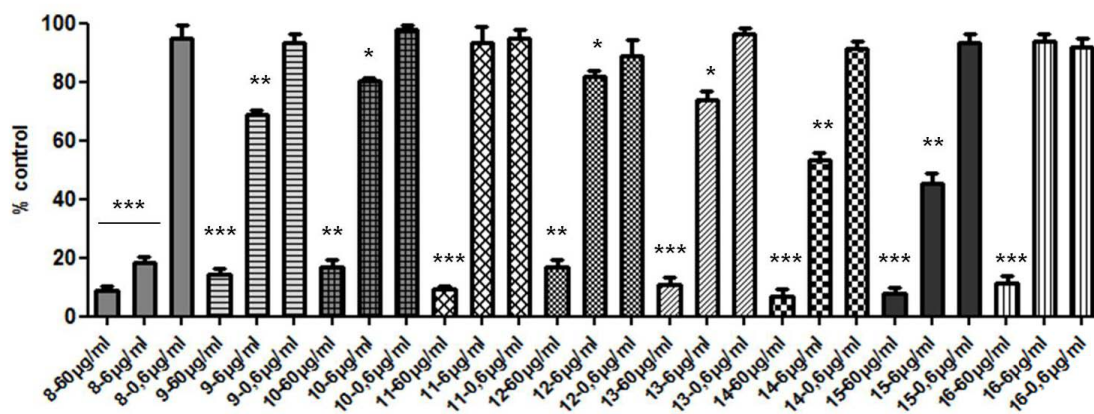


Fig. 104: Viability of SW480 cells after treatment with fractions 8-16 of CC-13

Viability of SW480 cells treated with the fractions of CC-13 (fractions CC-13/8 to 16) was assessed with neutralred assay. The cells were cultivated on 24-well plates and incubated for 48 hours with increasing concentrations (0.6, 6 and 60 $\mu\text{g/ml}$). Data represent mean \pm s.e.mean from three independent experiments performed in triplicate (* $P < 0.05$, ** $P < 0.01$, *** $P < 0.001$ as compared to control cells).

4.2.8.3 Bioassay of selected fractions of CC-13

Based on the results of the first screening, the pattern and the amount of the fractions, fractions CC-13/5, CC-13/6, CC-13/7, CC-13/8, CC-13/14 and CC-13/15 were selected for the isolation of the active compounds of the rootlets of *Metaxya rostrata*.

In order to confirm the earlier results on cancer cell viability a second set of experiments was performed. Results from the earlier experiments were confirmed making these fractions the most interesting ones for the isolation of the active principles (Fig. 105).

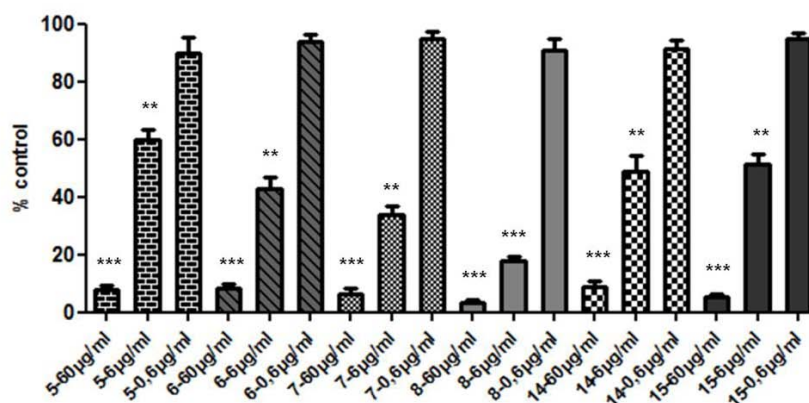


Fig. 105: Viability of SW480 cells after treatment with the selected fractions of CC-13

Viability of SW480 cells treated with the most active fractions of CC-13 (fractions CC-13/5, 6, 7, 8, 14 and 15) was assessed with neutral red assay. The cells were cultivated on 24-well plates and incubated for 48 hours with increasing concentrations (0.6, 6 and 60 µg/ml). Data represent mean \pm s.e.mean from three independent experiments performed in triplicate (* P <0.05, ** P <0.01, *** P <0.001 as compared to control cells).

A TLC comparison of the active fractions from the CC-9 and those from CC-13 showed similar composition (Fig. 106). Nevertheless, due to some differing compounds the fractions were not combined and further fractionated separately.

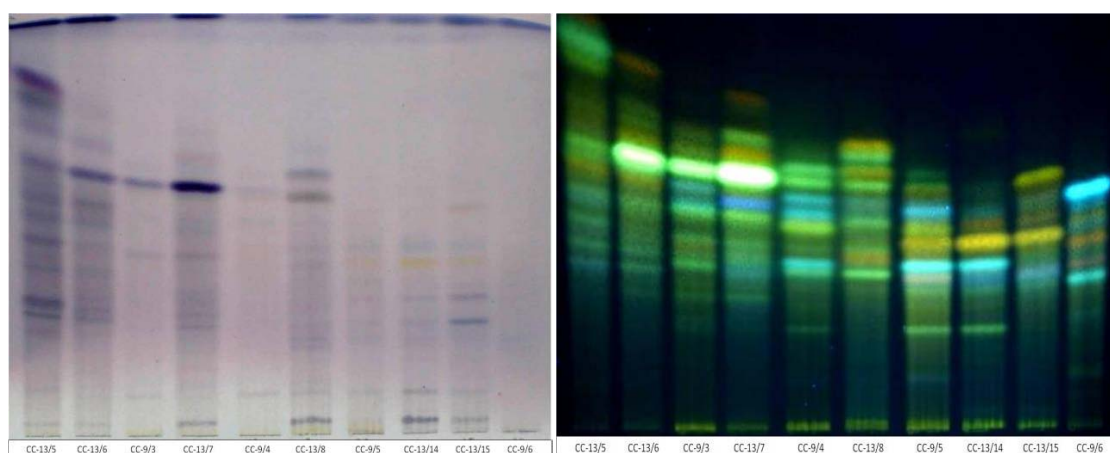


Fig. 106: TLC comparison of CC-9 and CC-13

Stationary phase 1, mobile phase 1, detection 1 and 2

Comparative TLC analysis of the active fractions with different methylated flavonoids¹² was performed based on the fluorescence and polarity of the compounds. But none of the major compounds in the fractions was identical to a standard and could be identified.

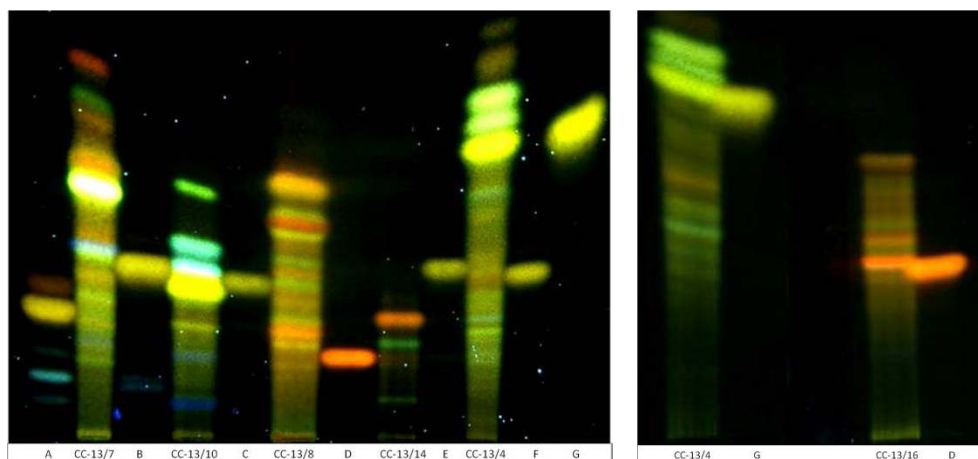


Fig. 107: TLC comparison of the active fractions of CC-13 with methylated flavonoids

Stationary phase 1, mobile phase 10, detection 2 (A=Quercetin-3-3'-4'-trimethylether, B=Kaempferol-3-4'-dimethylether, C=Kaempferol-3-7'-dimethylether, D=Quercetin-3-7'-dimethylether, E=Quercetin-3-7-3'-trimethylether, F=Quercetin-3-7-4'-trimethylether, G=Kaempferol-3-7-4'-trimethylether)

4.2.9 Fractionation of the most active fractions from CC-9 and CC-13 by solid phase extraction (SPE)

Selected based on their activity, the fractions CC-13/5, CC-13/6, CC-13/7, CC-13/8, CC-13/14, CC-13/15 and the fractions CC-9/3 and CC-9/4 were further fractionated using solid phase extraction.

Fraction	CC-13/5	CC-13/6	CC-13/7	CC-13/8	CC-13/14	CC-13/15	CC-9/3	CC-9/4
Yield (mg)	170	50	190	75	30	30	90	60

Table 32: Yield (mg) of the most active fractions of CC-9 and CC-13

4.2.9.1 Fractionation of fraction CC-13/5 by solid phase extraction (SPE-1)

The active fraction CC-13/5 of the CH₂Cl₂-extract of the rootlets of *Metaxya rostrata* was submitted to fractionation by SPE-1. The fraction was applied on the cartridges (C-18,

¹² The authentic substances were kindly provided by Prof. E. Wollenweber (Institut für Botanik, TU Darmstadt, Deutschland).

20ml, Bond Elut, Varian) and elution was performed sequentially with 4 reservoir volumes each of 60%, 70%, 80%, 90% and 100% MeOH. The fractions of identical polarity were pooled (Fig. 108).

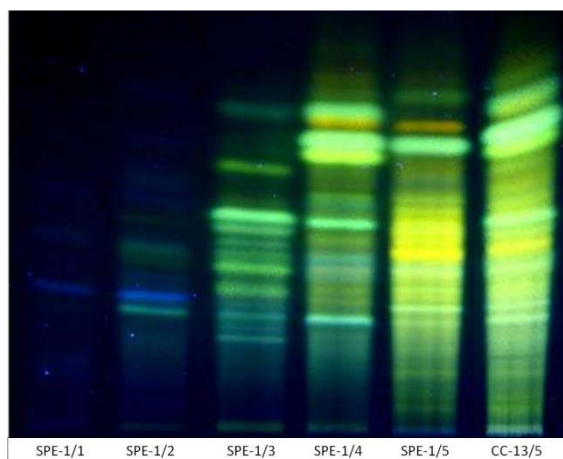


Fig. 108: TLC of the fractions of SPE-1

Stationary phase 1, mobile phase 10, detection 2

Fraction	SPE-1/1	SPE-1/2	SPE-1/3	SPE-1/4	SPE-1/5
Eluent	60%	70%	80%	90%	100%
Yield (mg)	5,3	7,4	22,3	49,9	35,3

Table 33: Yield (mg) of the fractions of SPE-1

In order to evaluate the effect of the SPE-1 fractions of fraction CC-13/5 on cancer cell viability, the cells were exposed to increasing concentrations (0.6, 6 and 60µg/ml) for 48h. The SPE-1/1 and SPE-1/2 fractions had no effect on cell viability below a concentration of 60µg/ml. Fractions SPE-1/3 and SPE-1/5 reduced cell number in a significant manner at a concentration of 6µg/ml. Fraction SPE-1/4 was the most active, reducing cell viability significantly already at a concentration of 0.6µg/ml (Fig. 109).

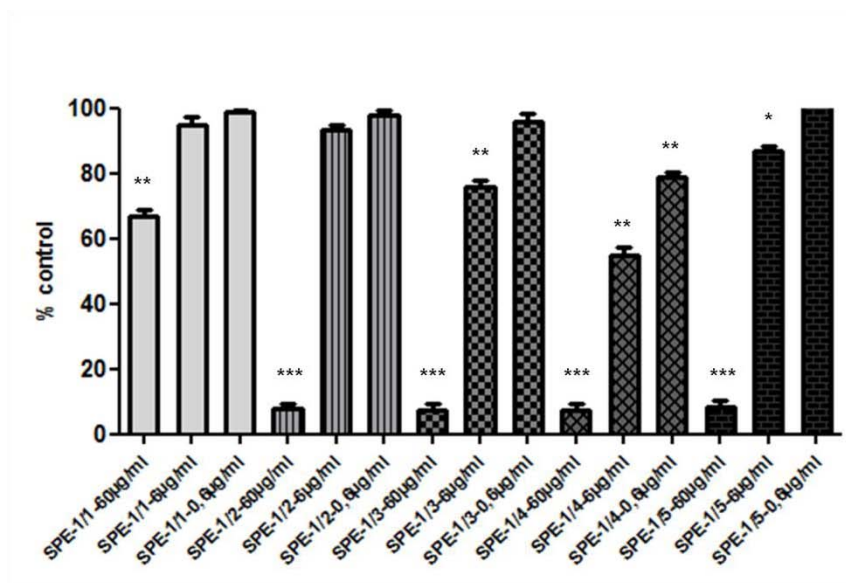


Fig. 109: Viability of SW480 cells treated with the fractions of SPE-1

Viability of SW480 cells treated with the SPE-1 fractions (SPE-1/1 to 5) of fraction CC-13/5 was assessed with neutralred assay. The cells were cultivated on 24-well plates and incubated for 48 hours with increasing concentrations (60, 6 and 0.6µg/ml). Data represent mean \pm s.e.mean from three independent experiments performed in triplicate (* P <0.05, ** P <0.01, *** P <0.001 as compared to control cells).

4.2.9.2 Fractionation of fraction CC-13/6 by solid phase extraction (SPE-2)

The active fraction CC-13/6 of the new CH_2Cl_2 -extract of the rootlets of *Metaxya rostrata* was further fractionated by SPE-2. The fraction was applied on the cartridges and eluted with 4 reservoir volumes each of 40%, 60%, 80% and 100% MeOH. The fractions of identical polarity were pooled and evaporated (Fig. 110).

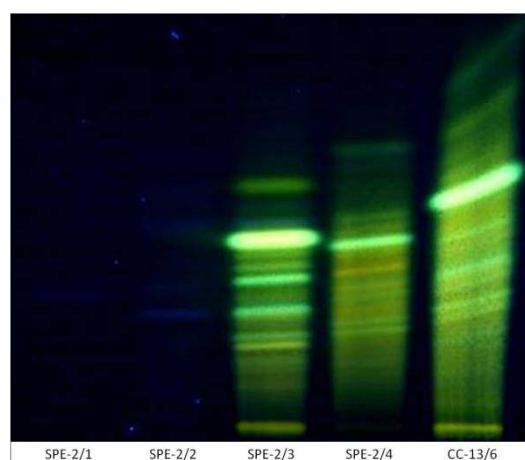


Fig. 110: TLC of the fractions of SPE-2

Stationary phase 1, mobile phase 10, detection 2

Fraction	SPE-2/1	SPE-2/2	SPE-2/3	SPE-2/4
Eluent	40%	60%	80%	100%
Yield (mg)	0.8	1.5	10.1	16.8

Table 34: Yield (mg) of the fractions of SPE-2

The fractions SPE-2/1 and SPE-2/2 eluted with 40% and 60% MeOH contained very low amounts, were not tested for their effect on cancer cell viability. Both, the SPE-2/3 and SPE-2/4 fractions reduced the SW480 cell viability significantly from a concentration of 0.6µg/ml upwards (Fig. 111).

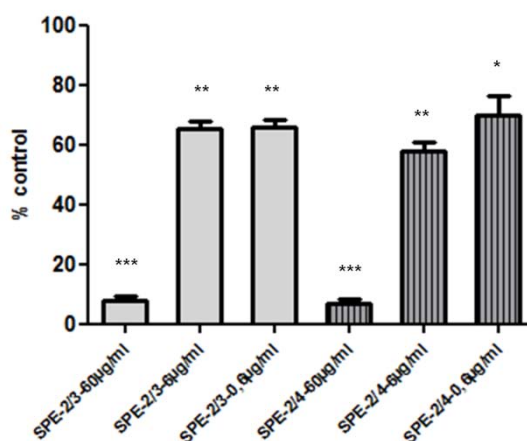


Fig. 111: Viability of SW480 cells treated with the fractions of SPE-2

Viability of SW480 cells treated with the SPE-2 fractions (SPE-2/3 and 4) of fraction CC-13/6 was assessed with neutralred assay. The cells were cultivated on 24-well plates and incubated for 48 hours with increasing concentrations (60, 6 and 0.6µg/ml). Data represent mean \pm s.e.mean from three independent experiments performed in triplicate (*P<0.05, **P<0.01, ***P<0.001 as compared to control cells).

4.2.9.3 Fractionation of fraction CC-13/7 by solid phase extraction (SPE-3)

Fraction CC-13/7 of the new CH₂Cl₂-extract of the rootlets of *Metaxya rostrata* was applied on the cartridges and eluted with 4 reservoir volumes each of 60%, 70%, 80%, 90% and 100% MeOH. The fractions of identical polarity were pooled and evaporated (Fig. 112).

Results

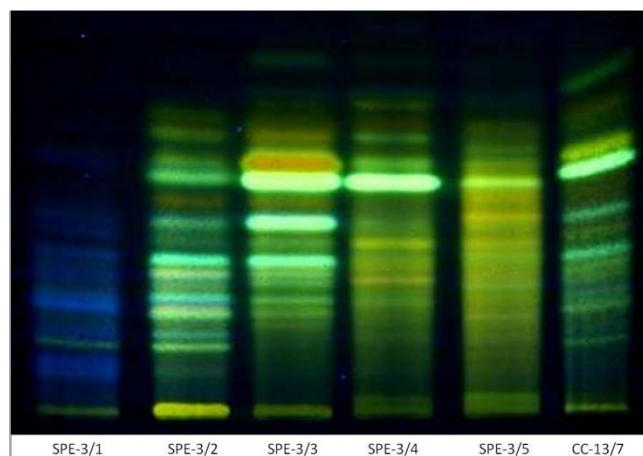


Fig. 112: TLC of the fractions of SPE-3
Stationary phase 1, mobile phase 10, detection 2

Fraction	SPE-3/1	SPE-3/2	SPE-3/3	SPE-3/4	SPE-3/5
Eluent	60%	70%	80%	90%	100%
Yield (mg)	18.4	21.4	35,5	57	28,3

Table 35: Yield (mg) of the fractions of SPE-3

In the biological assay, fraction fraction SPE-3/1 only reduced cell viability significantly at a concentration of 60 μ g/ml. Fractions SPE-3/2 and SPE-3/5 decreased the cell number in a significant manner down from a concentration of 6 μ g/ml upwards. Fractions SPE-3/3 and SPE-3/4 were able to reduce the cell viability significantly already at a concentration of 0.6 μ g/ml (Fig. 113). Thus, the latter were chosen for further investigation.

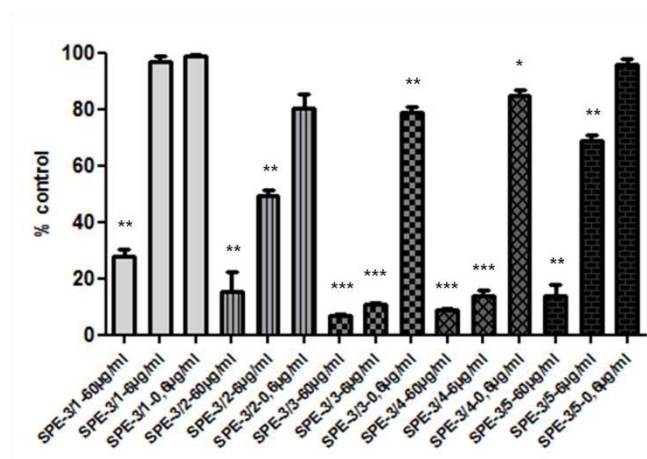


Fig. 113: Viability of SW480 cells treated with the fractions of SPE-3

Viability of SW480 cells treated with the SPE-3 fractions (SPE-3/1 to 5) of fraction CC-13/7 was assessed with neutralred assay. The cells were cultivated on 24-well plates and incubated for 48 hours with increasing

concentrations (60, 6 and 0.6 µg/ml). Data represent mean \pm s.e.mean from three independent experiments performed in triplicate (* $P < 0.05$, ** $P < 0.01$, *** $P < 0.001$ as compared to control cells).

4.2.9.4 Fractionation of fraction CC-13/8 by solid phase extraction (SPE-4)

Fraction CC-13/8, an active fraction of the new CH_2Cl_2 -extract of the rootlets of *Metaxya rostrata*, was further fractionated by SPE in the same manner as described before and eluted with 4 reservoir volumes each of 60%, 70%, 80%, 90% and 100% MeOH. The fractions of identical polarity were pooled and evaporated (Fig. 114).

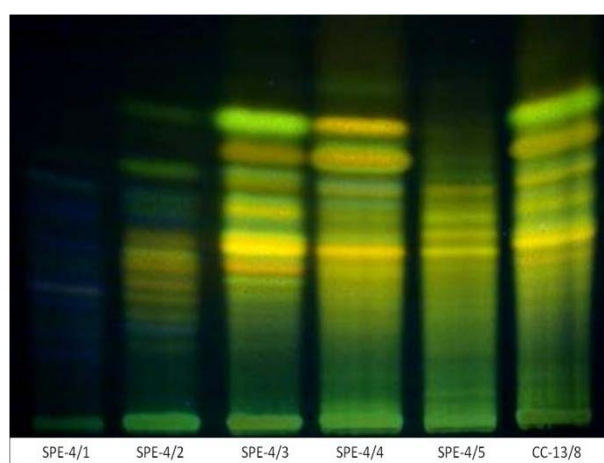


Fig. 114: TLC of the fractions of SPE-4

Stationary phase 1, mobile phase 10, detection 2

Fraction	SPE-4/1	SPE-4/2	SPE-4/3	SPE-4/4	SPE-4/5
Eluent	60%	70%	80%	90%	100%
Yield (mg)	5.5	4.8	14.8	13.4	7.9

Table 36: Yield (mg) of the fractions of SPE-4

After treatment of SW480 cells with fraction SPE-4/3 no effect on the cell viability was observed. A low activity with significant reduction of cell viability only at the highest concentration was determined for fractions SPE-4/2 and SPE-4/5. Fraction SPE-4/3 was able to decrease the cell number significantly at a concentration of 6 µg/ml and fraction SPE-4/4, the most active one reduced the cell viability significantly from a concentration of 0.6 µg/ml upwards (Fig. 115).

Results

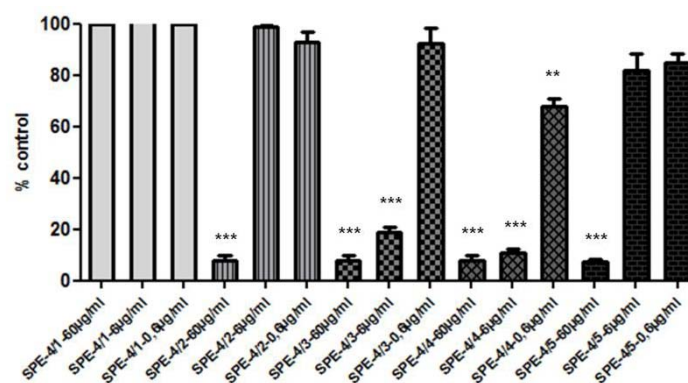


Fig. 115: Viability of SW480 cells treated with the fractions of SPE-4

Viability of SW480 cells treated with the SPE-4 fractions (SPE-4/1 to 5) of fraction CC-13/8 was assessed with neutralred assay. The cells were cultivated on 24-well plates and incubated for 48 hours with increasing concentrations (60, 6 and 0.6µg/ml). Data represent mean \pm s.e.mean from three independent experiments performed in triplicate (* P <0.05, ** P <0.01, *** P <0.001 as compared to control cells).

4.2.9.5 Fractionation of fraction CC-13/14 by solid phase extraction (SPE-5)

For SPE-5, fraction CC-13/14 of the new CH_2Cl_2 -extract of the rootlets of *Metaxya rostrata* was applied on the cartridges and eluted and pooled under the same conditions as described before (Fig.116).

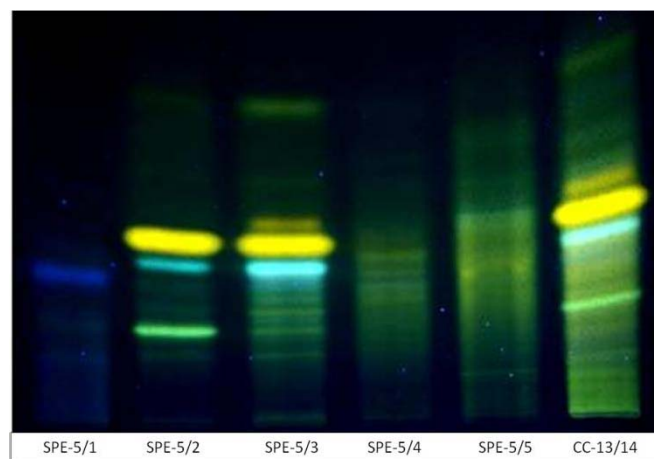


Fig. 116: TLC of the fractions of SPE-5

Stationary phase 1, mobile phase 10, detection 2

Fraction	SPE-5/1	SPE-5/2	SPE-5/3	SPE-5/4	SPE-5/5
Eluent	60%	70%	80%	90%	100%
Yield (mg)	4	8.2	5.5	3.8	6.4

Table 37: Yield (mg) of the fractions of SPE-5

In the cell assay, fraction SPE-5/1 showed little activity only. Treatment with fractions SPE-5/4 and SPE-5/5 resulted in a significant reduction of cell viability at a concentration of 6 µg/ml. Fractions SPE-5/2 and SPE-5/3 were the most active ones decreasing cell viability significantly from a concentration of 0.6 µg/ml upwards (Fig. 117) and SPE-5/2 was further investigated because of only 3 main compound in TLC after detection 2.

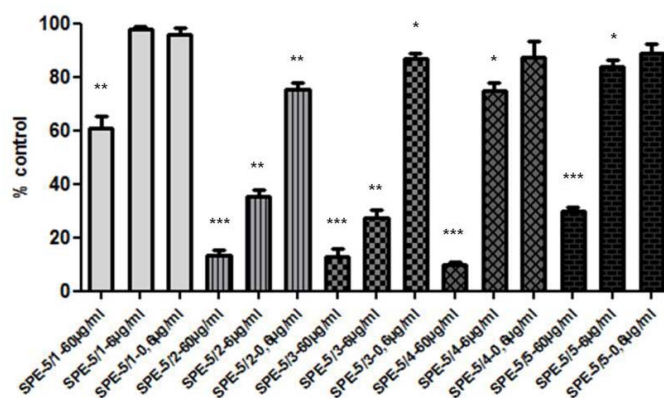


Fig. 117: Viability of SW480 cells treated with the fractions of SPE-5

Viability of SW480 cells treated with the SPE-5 fractions (SPE-5/1 to 5) of fraction CC-13/14 was assessed with neutralred assay. The cells were cultivated on 24-well plates and incubated for 48 hours with increasing concentrations (60, 6 and 0.6 µg/ml). Data represent mean \pm s.e.mean from three independent experiments performed in triplicate (* P <0.05, ** P <0.01, *** P <0.001 as compared to control cells).

4.2.9.6 Fractionation of fraction CC-13/15 by solid phase extraction (SPE-6)

The active fraction CC-13/15, an active fraction of the new CH₂Cl₂-extract of the rootlets of *Metaxya rostrata*, was further fractionated by SPE-6. The fraction was applied on the cartridges eluted with 4 reservoir volumes each of 60%, 70%, 80%, 90% and 100% MeOH. The fractions of identical polarity were pooled and evaporated (Fig.118).

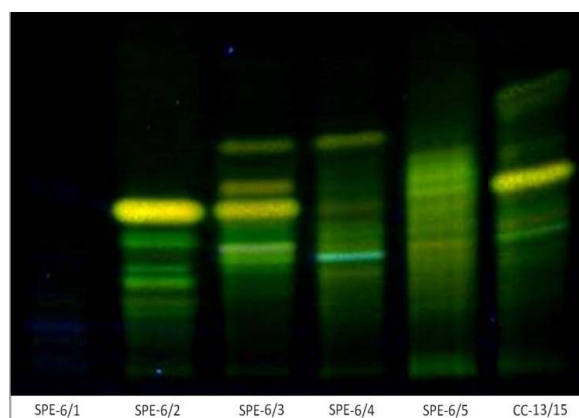


Fig. 118: TLC of the fractions of SPE-6

Stationary phase 1, mobile phase 10, detection 2

Fraction	SPE-6/1	SPE-6/2	SPE-6/3	SPE-6/4	SPE-6/5
Eluent	60%	70%	80%	90%	100%
Yield (mg)	3	5.9	4.1	3.9	4.6

Table 38: Yield (mg) of the fractions of SPE-6

In the bioviability assay, fraction SPE-6/5 reduced the cell number significantly only at a concentration of 60µg/ml. Fraction SPE-6/1 reduces cell viability at a concentration of 6µg/ml in a significant manner. Fractions SPE-6/2, SPE-6/3 and SPE-6/4 exhibited the highest activities reducing cell viability significantly already at a concentration of 0.6µg/ml (Fig. 119). Fractions SPE-6/2 was selected for further investigation due to its high activity and its major orange compound at Rf 0.45.

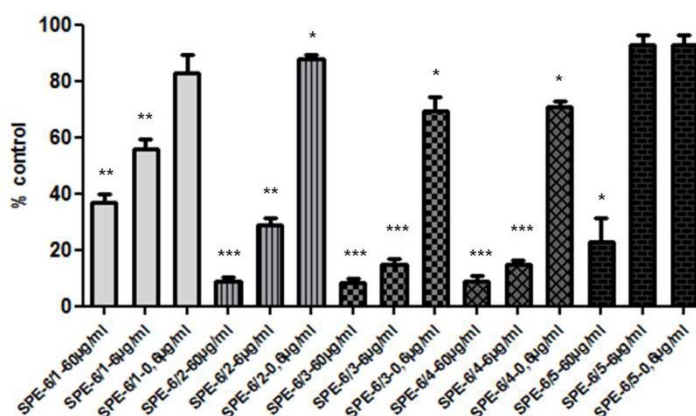


Fig. 119: Viability of SW480 cells treated with the fractions of SPE-6

Viability of SW480 cells treated with the SPE-6 fractions (SPE-6/1 to 5) of fraction CC-13/15 was assessed with neutralred assay. The cells were cultivated on 24-well plates and incubated for 48 hours with increasing concentrations (60, 6 and 0.6µg/ml). Data represent mean \pm s.e.mean from three independent experiments performed in triplicate (* P <0.05, ** P <0.01, *** P <0.001 as compared to control cells).

4.2.9.7 Fractionation of fraction CC-9/3 by solid phase extraction (SPE-7)

The active fraction CC-9/3 of the old CH₂Cl₂-extract of the rootlets of *Metaxya rostrata* was fractionated with SPE-7. The fraction was applied on the cartridges, eluted and pooled under the same conditions as described before (Fig. 120).

Results

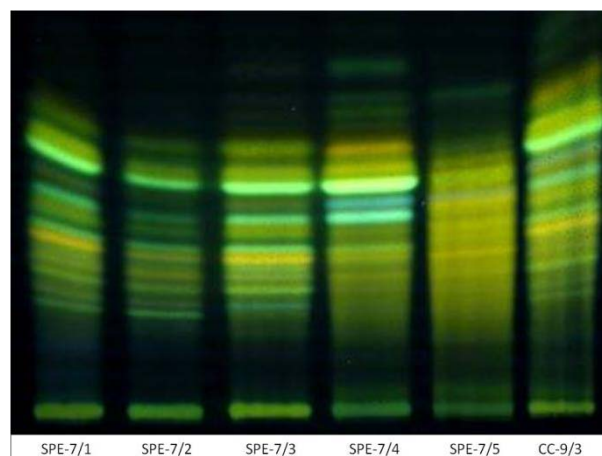


Fig. 120: TLC of the fractions of SPE-7

Stationary phase 1, mobile phase 10, detection 2

Fraction	SPE-7/1	SPE-7/2	SPE-7/3	SPE-7/4	SPE-7/5
Eluent	60%	70%	80%	90%	100%
Yield (mg)	15.3	7.5	26.7	13.8	14.7

Table 39: Yield (mg) of the fractions of SPE-7

After treatment of SW480 cells with fractions SPE-7/1, SPE-7/2, SPE-7/3 and SPE-7/5 the cell number was reduced significantly down to a concentration of 6g/ml. Fraction SPE-7/4 was the most active one reducing the cell viability in a significant manner at a concentration of 0.6µg/ml (Fig. 121). Due to a similar compound pattern of SPE-7/4 and SPE-7/3 and higher amounts of the latter, it was selected for further investigation.

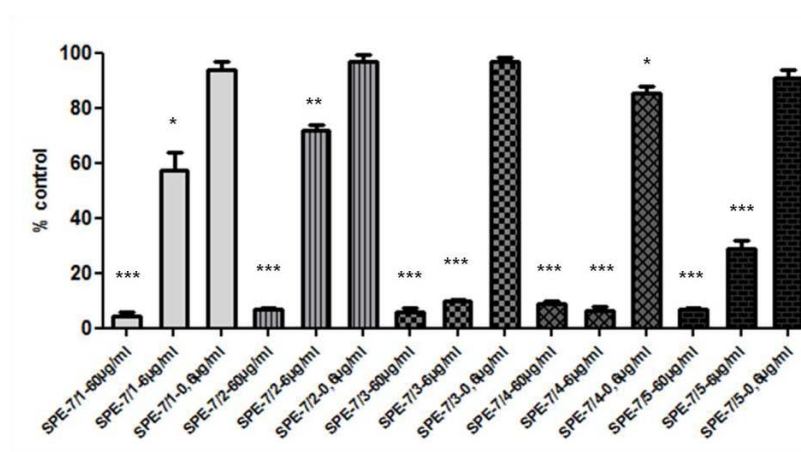


Fig. 121: Viability of SW480 cells treated with fractions of SPE-7

Viability of SW480 cells treated with the SPE-7 fractions (SPE-7/1 to 5) of fraction CC-9/3 was assessed with neutralred assay. The cells were cultivated on 24-well plates and incubated for 48 hours with increasing

concentrations (60, 6 and 0.6µg/ml). Data represent mean \pm s.e.mean from three independent experiments performed in triplicate (*P<0.05, **P<0.01, ***P<0.001 as compared to control cells).

4.2.9.8 Fractionation of fraction CC-9/4 by solid phase extraction (SPE-8)

Fraction CC-9/4, a fraction of the first CH₂Cl₂-extract of the rootlets of *Metaxya rostrata*, was further fractionated by SPE-8 under elution with 4 reservoir volumes of 40%, 60%, 80% and 100% MeOH. The fractions of identical polarity were pooled (Fig. 122).

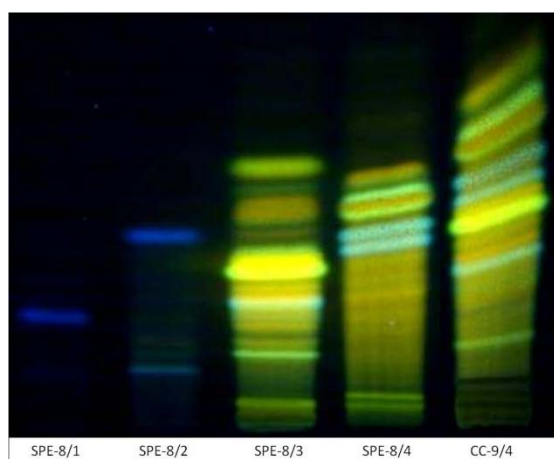


Fig. 122: TLC of the fractions of SPE-8

Stationary phase 1, mobile phase 10, detection 2

Fraction	SPE-8/1	SPE-8/2	SPE-8/3	SPE-8/4
Eluent	40%	60%	80%	100%
Yield (mg)	1.2	2.7	6.7	23.2

Table 40: Yield (mg) of the fractions of SPE-8

As fractions SPE-8/1 and SPE-8/2 eluted with 40% and 60% MeOH contained very little amounts, they were not tested for their effect on cancer cell viability. Fraction SPE-8/4 reduced cell viability significantly at a concentration of 6µg/ml. Fraction SPE-8/3 showed even higher activity reducing the cell number in a significant manner from a concentration of 0.6µg/ml upwards. Because of the bigger amounts and also high activity, of fraction SPE-8/4 was selected and further investigated.

Results

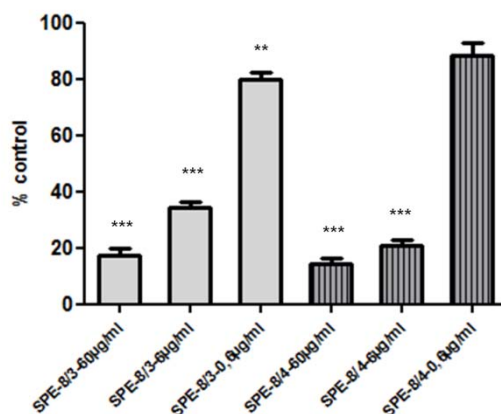


Fig. 123: Viability of SW480 cells treated with the fractions of SPE-8

Viability of SW480 cells treated with the SPE-8 fractions (SPE-8/3 and 4) of fraction CC-9/4 was assessed with neutralred assay. The cells were cultivated on 24-well plates and incubated for 48 hours with increasing concentrations (60, 6 and 0.6µg/ml). Data represent mean \pm s.e.mean from three independent experiments performed in triplicate (* P <0.05, ** P <0.01, *** P <0.001 as compared to control cells).

4.2.9.9 TLC comparison of the active SPE fractions with methylated flavonoids

The detection with Naturstoffreagent A after TLC-separation of the selected fractions with high activity showed numerous phenolic compounds with yellow, orange and green fluorescence and low polarity. Thus, the occurrence of methylated flavonoids in the fractions was assumed and a TLC comparison of these fractions with different authentic compounds was performed. Although some compounds showed similar fluorescence and polarity, none of the major compounds could be identified (Fig. 124).

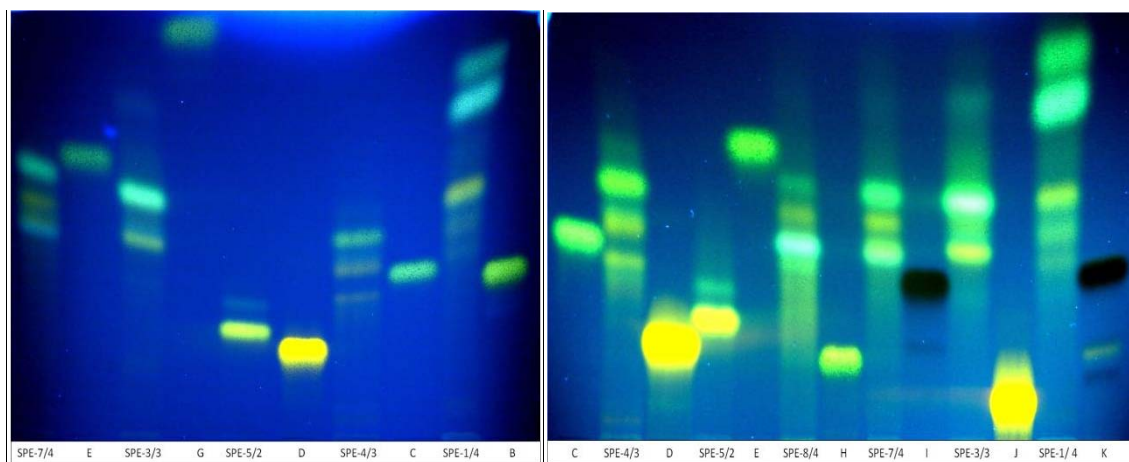


Fig. 124: TLC comparison of the active SPE fractions with methylated flavonoids

Stationary phase 2, mobile phase 10, detection 2 (B=Kämpferol-3-4'-dimethylether, C=Kämpferol-3-7'-dimethylether, D=Quercetin-3-7'-dimethylether, E=Quercetin-3-7-3'-trimethylether, G=Kämpferol-3-7-4'-

trimethylether, **H**= Quercetin-3-3'-dimethylether, **I**=Quercetagetin-3-6-4'-trimethylether, **J**=Quercetagetin-3-6-dimethylether, **K**=6-OH-Kämpferol-3-6-7-trimethylether).

4.2.10 Investigation of the selected SPE-fractions by high performance liquid chromatography (HPLC)

In order to identify and to isolate the active compounds in the most active SPE-fractions HPLC was performed.

4.2.10.1 Investigation of SPE-3/4 by HPLC

Due to its high activity, the fraction SPE-3/4 was studied in detail and subjected to a HPLC (Method 1, Gradient Programm 1, see p. 43). Besides UV detection at 290nm, Evaporative Light Scattering Detection (ELSD) was used to detect compounds without chromophors. Under UV detection fraction SPE-3/4 showed several minor compounds with uncharacteristic UV spectra, although in TLC (Fig.112) one prominent substance had been detected.

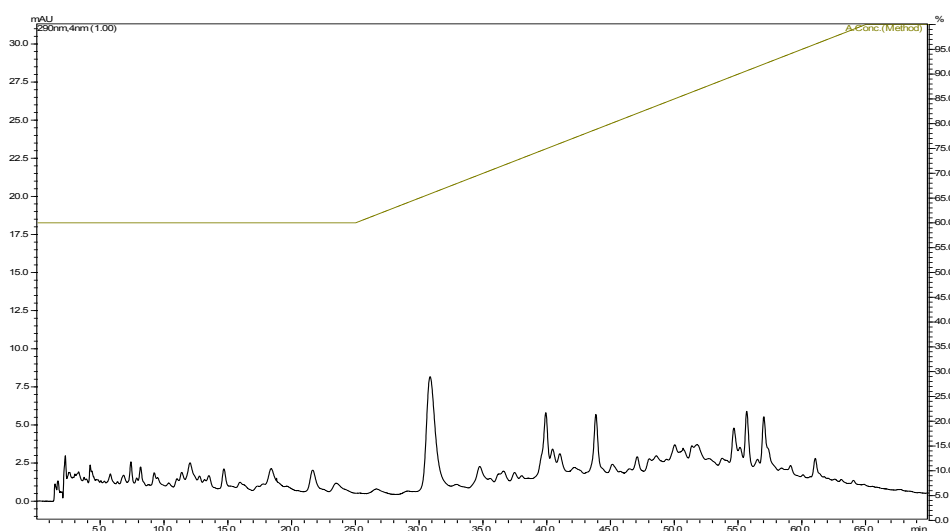


Fig. 125: HPLC analysis (1) of fraction SPE-3/4

Method 1, gradient programm 1, detection at 290nm

Thus, fraction SPE-3/4 was also analysed by ELSD-detection and showed one main peak at Rt 43,5min with a purity of 98% (Fig. 126).

Results

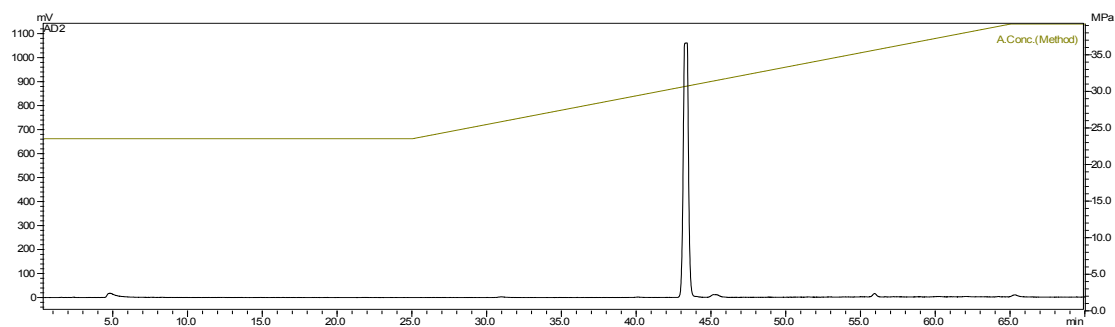


Fig. 126: HPLC analysis (2) of fraction SPE-3/4

Method 1, gradient programm 1, detection with ELSD

Additional experiments by LC-MS pointed to ursolic or betulinic acid. Final identification by TLC and rechromatography in HPLC with the reference compound, confirmed the major peak as betulinic acid (Fig. 127).



Fig. 127: TLC comparison of SPE-3/4 with ursolic and betulinic acid

As Betulinic acid is known for cytotoxic effects (Zuco *et al.*, 2001; Ciurlea *et al.*, 2010; Fulda *et al.*, 1997) and was the major compound in fraction SPE-3/4, betulinic acid was unambiguously identified as the active principle in this fraction.

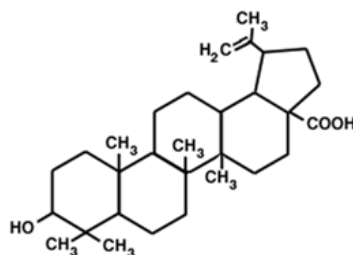


Fig. 128: Betulinic acid

4.2.10.2 Investigation of SPE-3/3 by HPLC

In fraction SPE-3/3 two major phenolic compounds were detected at R_f 0.58 and 0.47 by TLC (Fig. 112). Therefore and due to the high activity fraction SPE-3/3 was further investigation by RP-HPLC (Method 1, Gradient Programm 1, see p. 43) should reveal further informations on the structure. Both Evaporative Light Scattering Detection (ELSD) and UV detection at 290nm were used for this purpose.

The chromatogram with UV-detection showed four major compounds at R_t 11.5min, 18min, 19min and 26.5min (Fig. 129).

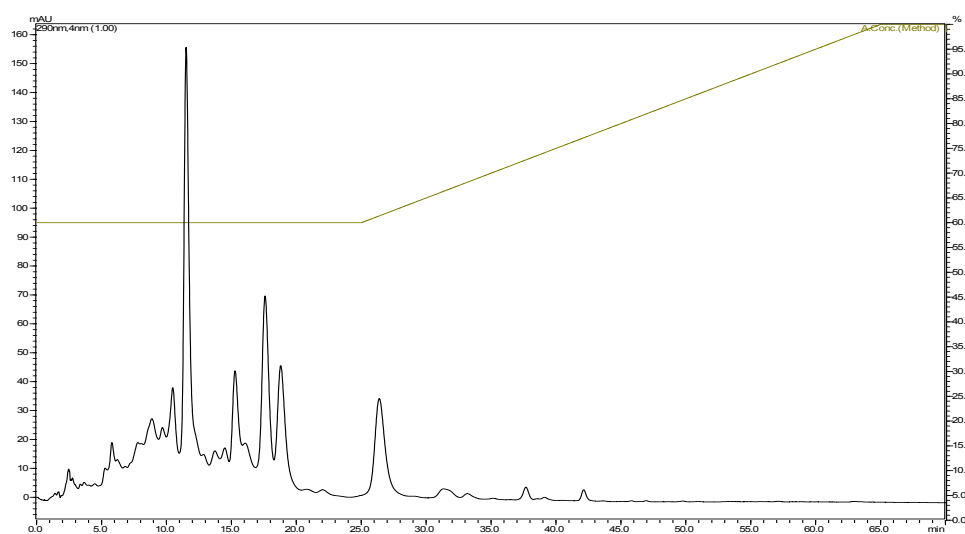


Fig. 129: HPLC analysis (1) of fraction SPE-3/3

Method 1, gradient programm 1, detection at 290nm

Under use of ELSD detection besides these peaks a further compound at R_t 43.5min without chromophor was detected. The retention time of the latter correlated to the one of betulinic acid (Fig. 130).

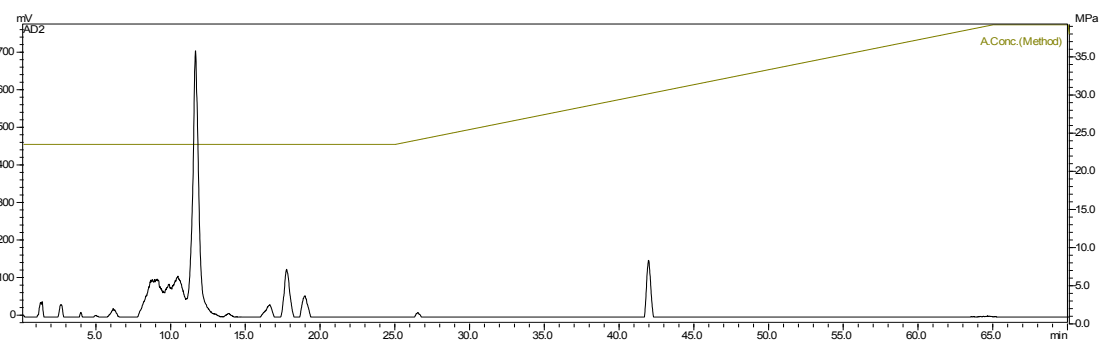


Fig. 130: HPLC analysis (2) of fraction SPE-3/3

Method 1, gradient programm 1, detection with ELSD

The identity of betulinic acid was confirmed by rechromatography with the authentic reference. The peak at Rt 11.5min was studied by MS analysis and identified as tetrahydroxy-C-prenylxanthone (MW 238). As in the bioassay fraction SPE-3/3 showed similar activity to fraction SPE-3/4, the activity was assigned to betulinic acid. However, xanthenes are also known to effect cell viability, so that a synergistic effect of both main compounds is possible.

4.2.10.3 Investigation of SPE-7/3 by HPLC

Fraction SPE-7/3 has shown several orange and green fluorescent phenolic substances in TLC (Fig. 120). HPLC analysis with UV-detection resulted in a major compound at Rt 31min and several minor compounds at Rt 24min, 25min, 27min, 37.5min (Method 1, Gradient Programm 1, see page 43).

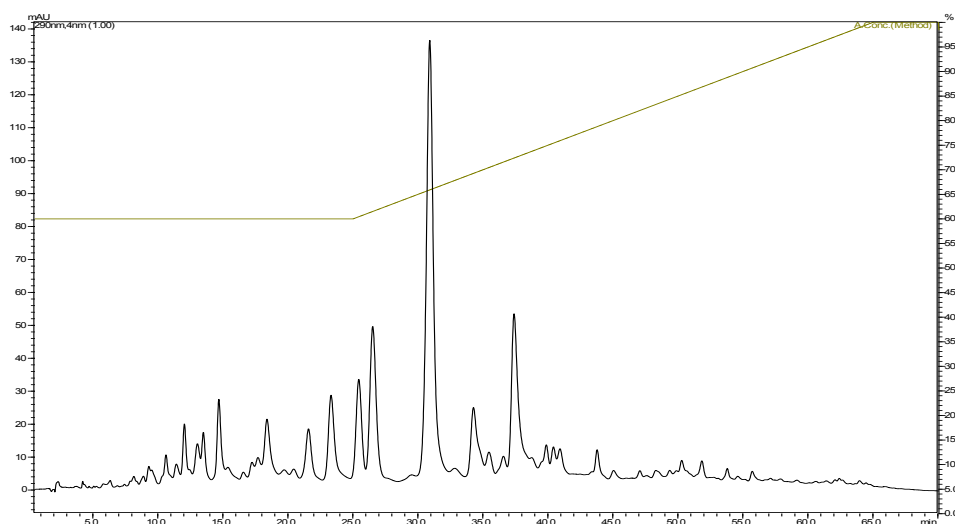


Fig. 131: HPLC analysis (1) of fraction SPE-7/3

Method 1, gradient programm 1, detection at 290nm

In the chromatogram with ELSD-detection again one major peak at Rt 43.5min was observed and identified by comparison with the authentic reference as betulinic acid with a purity of 98%. Thus, betulinic acid comprised as the active principle in this fraction as well.

Results

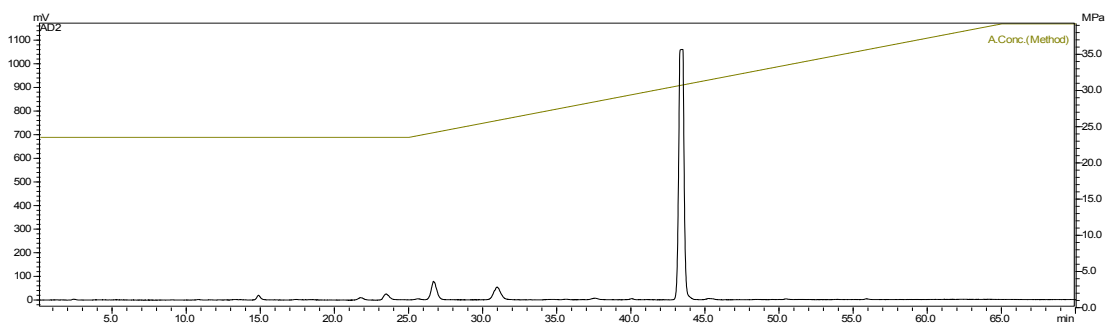


Fig. 132: HPLC analysis (2) of fraction SPE-7/3

Method 1, gradient program 1, detection with ELSD

4.2.10.4 Investigation of SPE-8/4 by HPLC

Fraction SPE-8/4 revealed a complex phenolic pattern in TLC after detection 2 (Fig. 122). By UV-detection after RP-HPLC separation (Method 1, Gradient Programm 1, see page) 5 major components at Rt 25min, 27min, 31min, 38min and 40.5min were observed (Fig. 133).

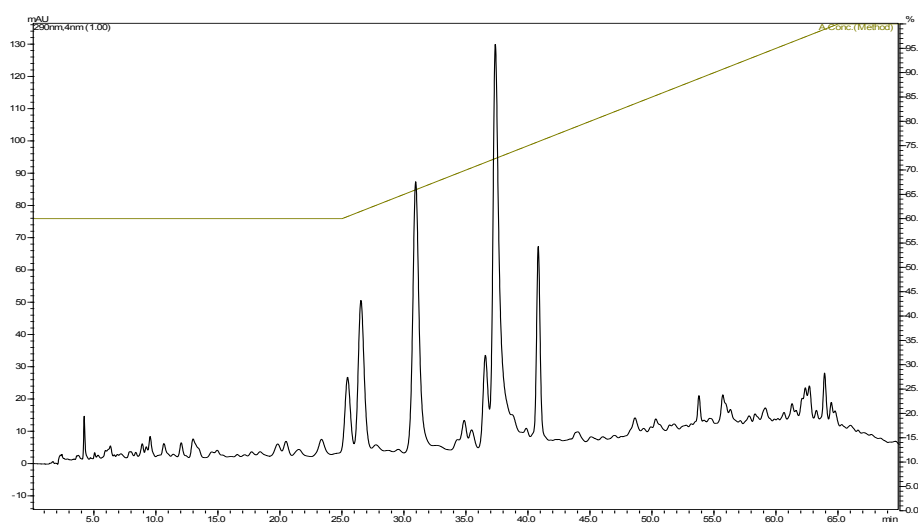


Fig. 133: HPLC analysis (1) of fraction SPE-8/4

Method 1, gradient program 1, detection at 290nm

The chromatogram after ELSD-detection showed the major compounds at Rt 27min and at 43.5min (Fig. 134).

Results

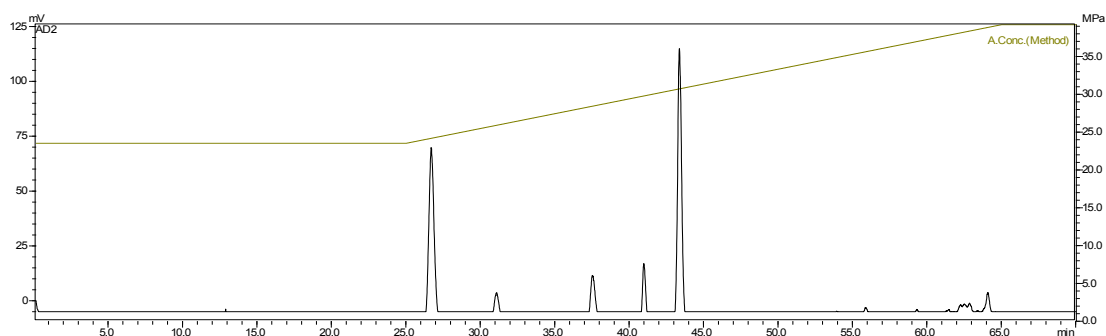


Fig. 134: HPLC analysis (2) of fraction SPE-8/4

Method 1, gradient programm 1, detection with ELSD

The main peak at Rt 43,5min was identified with the authentic reference as betulinic acid. The structure of the second main peak at Rt 27min was studied by MS analysis and identified as tetrahydroxy-di-C-prenylxanthone (MW 396). The substitution pattern could not be elucidated. Isolation of the substance was not possible due to the composition and the small amount of the fraction. The activity of SPE-8/4 could be a synergistic effect between betulinic acid and the xanthon.

4.2.10.5 Investigation of SPE-5/2 by HPLC

Fraction SPE-5/2 showed one major orange fluorescent compound with Rf 0.45 with small amounts of two further fluorescent substances at Rf 0.23 and 0.38 in TLC (Fig. 116). In RP-HPLC (Method 1, Gradient Programm 1, see page 43) the main compound was detected at Rt 24.5min in both detection modes (Fig. 135).

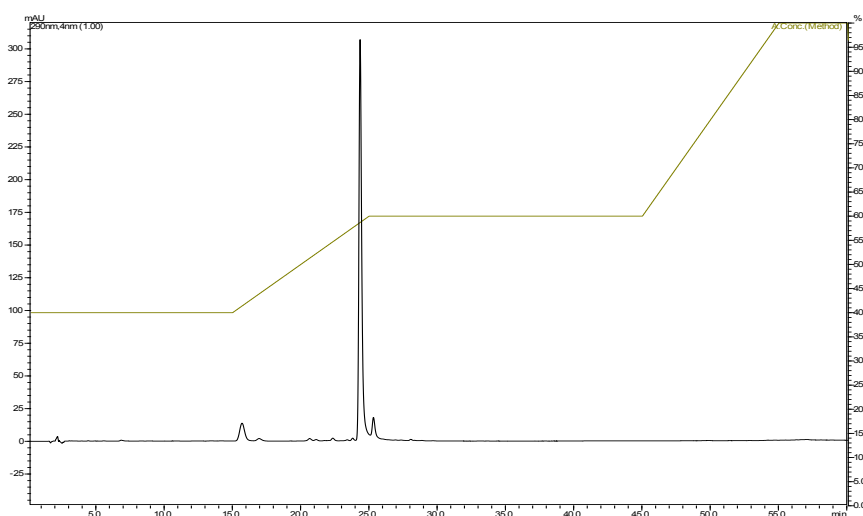


Fig. 135: HPLC analysis (1) of fraction SPE-5/2

Method 1, gradient programm 1, detection at 290nm

Results

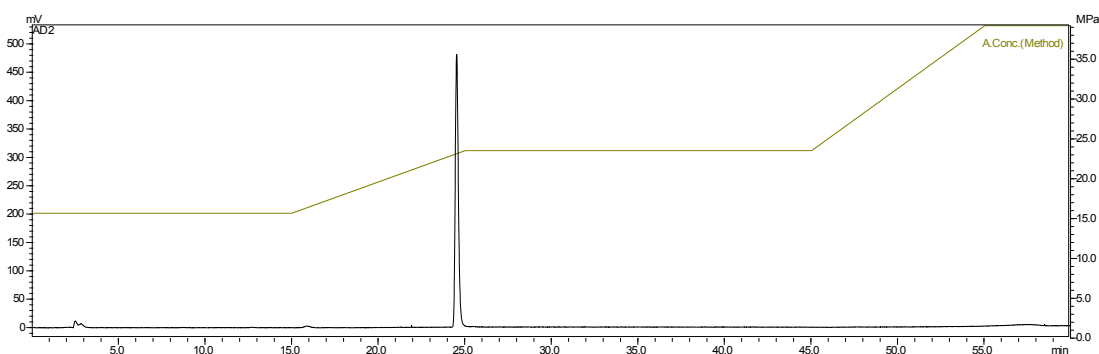


Fig. 136: HPLC analysis (2) of fraction SPE-5/2

Method 1, gradient programm 1, detection with ELSD

Due to only traces of accompanying substances in this fraction, structure elucidation by MS and NMR experiments was possible without further purification (Fig. 136). The compound at Rt 24.5min was identified as 2-deprenyl-rheediaxanthone B (MW 328). As 2-deprenyl-rheediaxanthone B is the major compound with a purity of 99% in fraction SPE-5/2, it is certain that the high activity in the bioassay is due to that rare natural compound (Fig. 137) (see supplementary information). Thus, for the biological tests 8mg of 2-deprenyl-rheediaxanthone B were available.

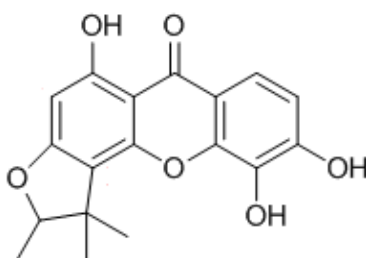


Fig. 137: 2-deprenyl-rheediaxanthone B

4.2.10.6 Investigation of SPE-6/2 by HPLC

The same orange fluorescent compound with detection 2 at Rf 0.45, seen in fraction SPE-5/2, was detected in fraction SPE-6/2 in TLC (Fig. 118). In RP-HPLC (Method 1, Gradient Programm 1, see p. 43) with UV-detection the compound at Rt 24.5 appeared to be pure (Fig. 138), but in ELSD-detection a second component was observed at Rt 16min (Fig. 139).

Results

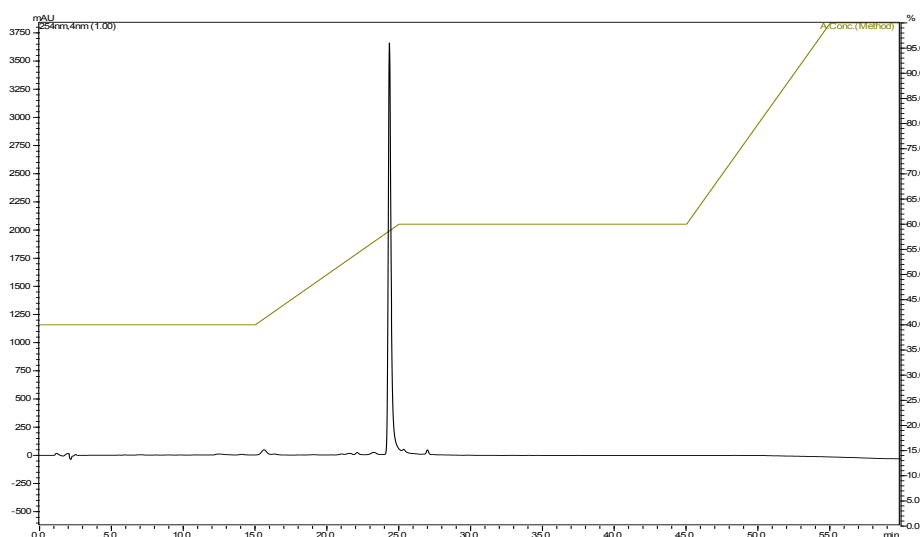


Fig. 138: HPLC analysis (1) of fraction SPE-6/2

Method 1, gradient programm 1, detection at 290nm

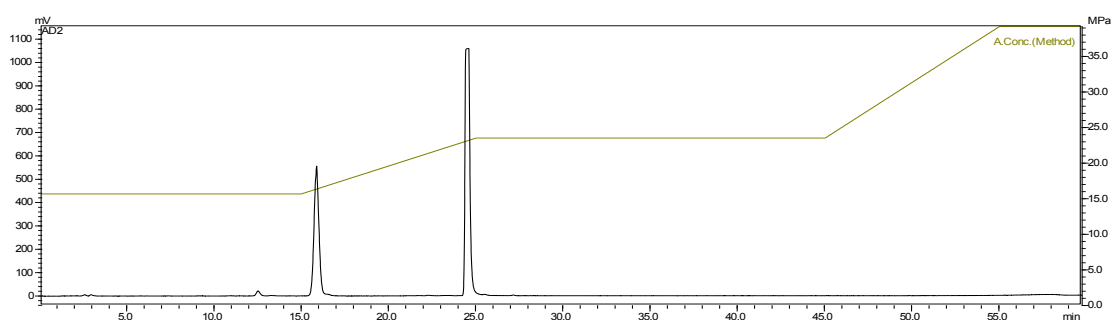


Fig. 139: HPLC analysis (2) of fraction SPE-6/2

Method 1, gradient programm 1, detection with ELSD

MS analysis revealed the peak at Rt 16min as tetrahydroxy-C-prenylxanthone and the peak at Rt 24.5min was confirmed as 2-deprenyl-rheediaxanthone B.

Both compounds had been already identified in other active fractions. In fraction SPE-5/2 2-deprenyl-rheediaxanthone B was identified as the active principle. Tetrahydroxy-C-prenylxanthone was also detected in fraction SPE-3/3 together with betulinic acid. The activity of fraction SPE-6/2 is assumed to be a synergistic effect of 2-deprenyl-rheediaxanthone B and the second xanthone.

4.2.11 Isolation of 2-deprenyl-rheediaxanthone B by semipreparative HPLC

Betulinic acid and 2-deprenyl-rheediaxanthone B were identified as the active principles in the most active fractions of the CH_2Cl_2 -extract of the rootlets of *Metaxya rostrata*. In order to isolate a higher amount of this compound for the biological assays, fraction CC-9/5, which also contained 2-deprenyl-rheediaxanthone B (Fig. 140) served for the isolation of this compound with semipreparative HPLC.

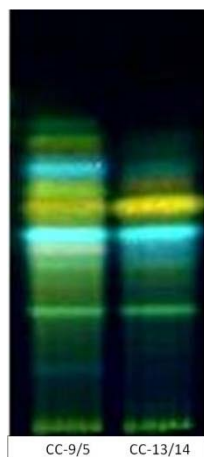


Fig. 140: TLC comparison of fraction CC-9/5 and CC-13/14

Stationary phase 1, mobile phase 10, detection 2

A HPLC method had to be developed for a separation of the peaks suitable for semipreparative HPLC. In several experiments the gradient was optimized for baseline separation resulting in method 3 (Method 3, Gradient Programm 3, see p. 44).

After optimization of the separation in the analytical scale, 43mg of fraction CC-9/5 were separated by semipreparative HPLC. 5 fractions were collected. Fraction 4 contained 2-deprenyl-rheediaxanthone B (Fig. 141).

Results

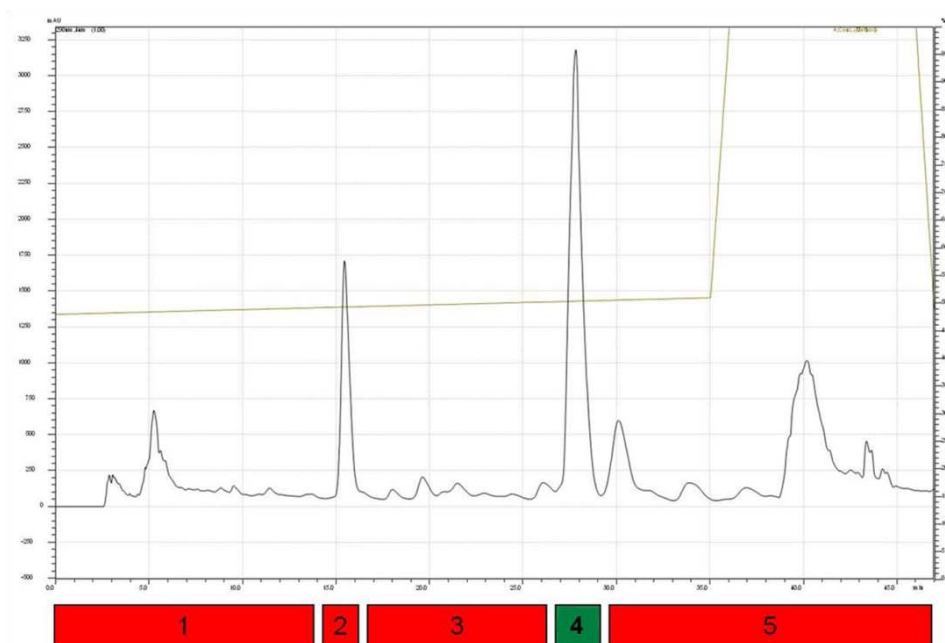


Fig. 141: Semipreparative HPLC of fraction CC-9/5

Method 3, gradient programm 3, detection at 290nm

After combining all fractions 4 (3mg), this combined fraction was evaporated and again analysed with HPLC to check the purity.

Only one major compound at 40min could be detected with UV detection (Fig. 142).

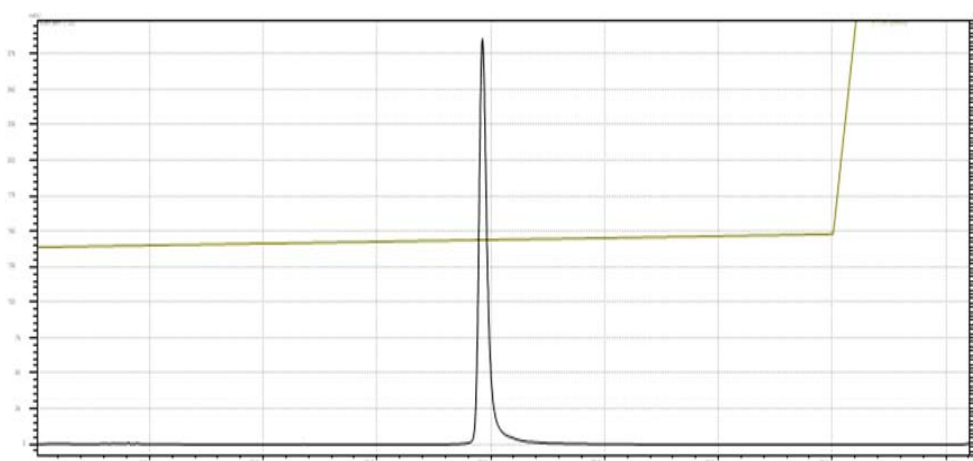


Fig. 142: HPLC analysis of fraction 4

Method 3, gradient programm 3, detection at 290nm

With the ELSD a purity of more than 99% was determined for this compound at Rt 40min (Fig. 143).

Results

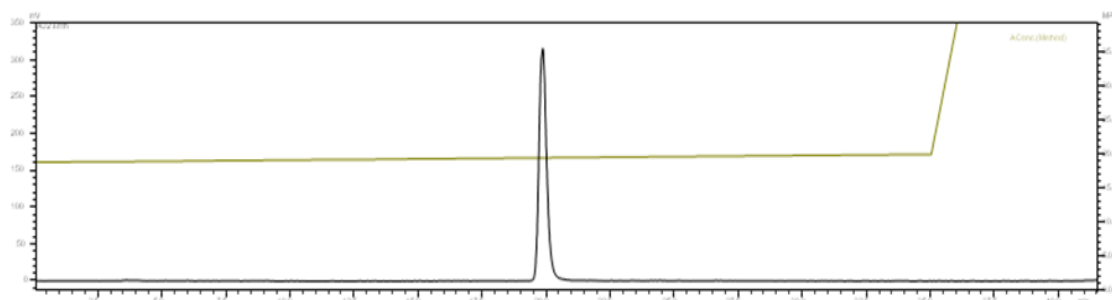


Fig. 143: HPLC analysis of fraction 4

Method 3, gradient programm 3, detection with ELSD

By MS analysis this compound was verified as 2-deprenyl-rheediaxanthone B. Thus, by semipreparative HPLC 3mg of 2-deprenyl-rheediaxanthone B were isolated additionally.

4.2.12 Biological effects of 2-deprenyl-rheediaxanthone B

Betulinic acid and 2-deprenyl-rheediaxanthone B were identified as the active compounds in the most active fractions of the CH_2Cl_2 extract of the rootlets of *Metaxya rostrata*. As the cytotoxic activity of betulinic acid is very well investigated, this compound was not studied further. For 2-deprenyl-rheediaxanthone B there have been no studies on cytotoxicity performed yet. Consequently, this compound was evaluated for its biological effects.

4.2.12.1 Effect of 2-deprenyl-rheediaxanthone B on cell viability

In order to evaluate the effect of 2-deprenyl-rheediaxanthone B (XB) on cell viability, SW480 cells were exposed to increasing concentrations (3, 6 and $9\mu\text{M}$) for 24, 48 and 72 h. The percentage of viable cells was determined by the Neutralred assay. To determine the impact on necrosis, a LDH-assay was performed.

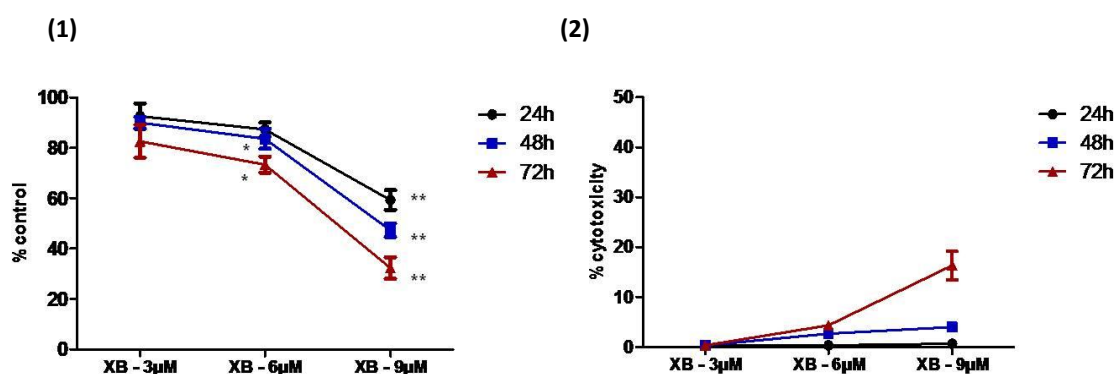


Fig. 144: Viability of SW480 (1) and LDH assay (2) of 2-deprenyl-rheediaxanthone B after 24, 48 and 72h

Viability of SW480 cells treated with 2-deprenyl-rheediaxanthone B (XB) was assessed with neutralred assay (1). Cytotoxicity of XB on SW480 cells was evaluated with the LDH assay (2). The cells were cultivated on 24-well plates and incubated for 24, 48 and 72 hours with increasing concentrations (3, 6 and $9\mu\text{M}$). Data represent mean \pm s.e.mean from three independent experiments performed in triplicate (* $P < 0.05$, ** $P < 0.01$ as compared to control cells).

After 24 hours no effect on cell viability at 3 and $6\mu\text{M}$ could be seen, but $9\mu\text{M}$ XB reduced cell viability significantly to about 60%. No cytotoxicity due to necrosis was detected under these conditions (Fig. 144). After 48 hours no effect on the cell number was seen at a concentration of $3\mu\text{M}$, but XB reduced cell viability in a significant manner at a concentration of $6\mu\text{M}$. In the LDH assay only very low cytotoxicity after 48h was seen. The

cell loss seemed not to be due to necrosis. After 72 hours 2-Deprenyl-rheediaxanthone B reduced cell viability significantly at a concentration of 6 μ M. At a concentration of 3 μ M no effect was observed. In the LDH assay slight cytotoxicity at a concentration of 9 μ M was determined. Thus, 48 hours incubation was chosen for further investigations.

4.2.12.2 Effect of 2-deprenyl-rheediaxanthone B on the cell viability of different cell types

To determine the activity of 2-deprenyl-rheediaxanthone B (XB) in another colon cancer cell line, experiments were performed with MTT assay using CaCo-2 cells, the non-malignant LT97 adenoma cell line and the normal colonic fibroblasts F331. SW480 was included to confirm the previous results in another viability assay and as a standard for assessment of cell line dependent relative activity.

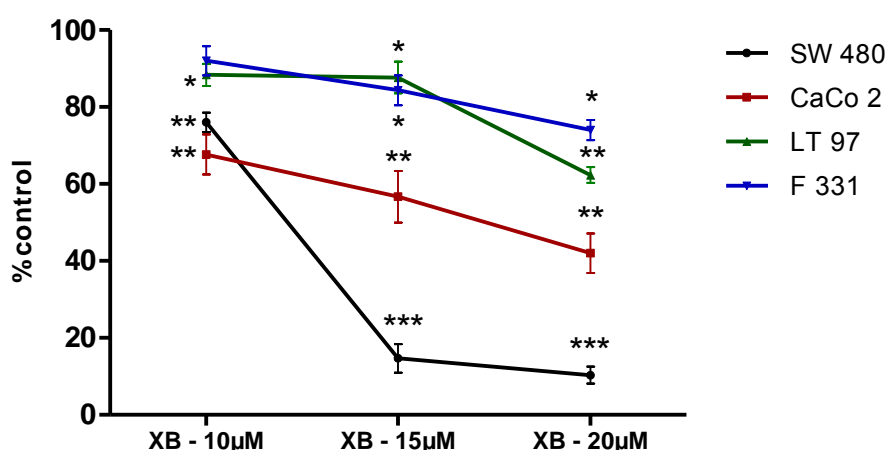


Fig. 145: Viability of SW480, CaCo-2, LT97 and F331 after treatment with 2-deprenyl-rheediaxanthone B

Viability of SW480, CaCo-2, LT97 and F331 cells treated with 2-deprenyl-rheediaxanthone B (XB) was evaluated with MTT assay. The cells were cultivated on 24-well plates and incubated for 48 hours with increasing concentrations (10, 15 and 20 μ M). Data represent mean \pm s.e.mean from three independent experiments performed in triplicate (*P<0.05, **P<0.01, *** P<0.001 as compared to control cells).

In CaCo-2 cells XB reduced cell viability at concentrations of 10, 15 and 20 μ M in a significant manner (Fig. 145). XB also reduced cell viability of LT97 at the same concentrations. At a concentration of 10 and 15 μ M the cell viability was reduced to about 85% and at a concentration of 20 μ M to about 60%.

The effect of the compound on human colon associated fibroblasts, F331, was evaluated as well. XB did not have an effect at 10 μ M, but reduced the cell number significantly to 75% at a concentration of 20 μ M. Compared to the effect of 2-deprenyl-rheediaxanthone B on the colon carcinoma cell lines, SW480 and CaCo-2, the effect on the adenoma cell line LT 97 and the fibroblasts is much weaker (Fig. 145).

4.2.12.3 Effect of 2-deprenyl-rheediaxanthone B on the cell cycle

In order to investigate the mechanism of the cytotoxicity induced by 2-deprenyl-rheediaxanthone B (XB) in SW480 cells, the first step was to assess the effect on cell cycle distribution. Flow cytometric analysis of PI-stained nuclei was employed after incubation with increasing concentrations (10, 15 and 20 μ M) for 48 and 72 h.

The results showed a concentration-dependent decrease of the proportion of cells in the G0-G1 phase. The percentage of cells in S phase increased slightly and the proportion of cells in G2-M phase increased dose-dependently and significantly after incubation with 2-deprenyl-rheediaxanthone B for 48h and 72h (Fig. 146).

The data suggest that 2-deprenyl-rheediaxanthone B induced a G2-M phase cell cycle arrest in SW480 cells.

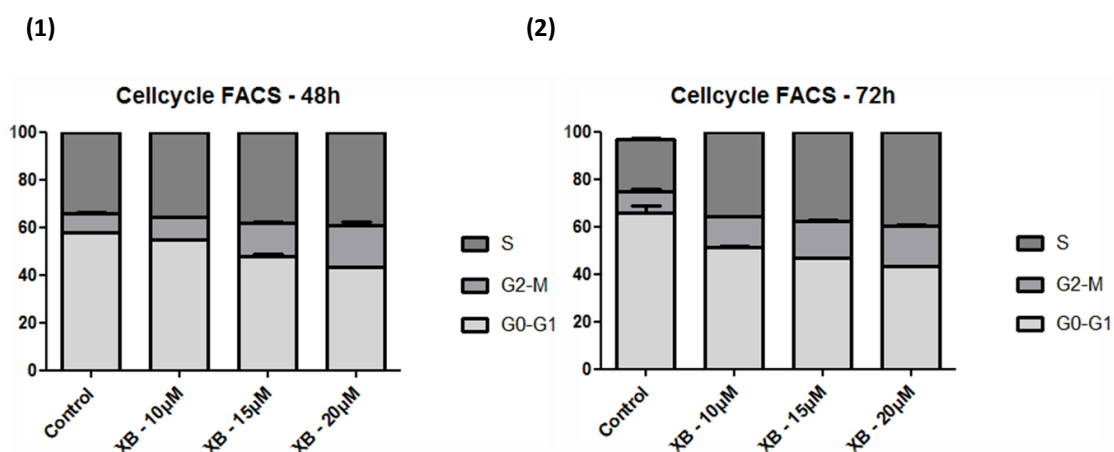


Fig. 146: Effect of XB on cell cycle distribution of SW480 after 48h (1) and 72h (2)

Cell cycle distribution of SW480 cells treated with 2-deprenyl-rheediaxanthone B (XB) after 48h (1) and 72h (2). Cells were cultivated on 6 Pd plates and incubated with increasing concentrations (10, 15 and 20 μ M) of XB. Cells were harvested, stained with PI and the percentage of cells in G0-G1, S and G2-M phase was quantified by flow cytometry. Data represent mean \pm s.e.mean from three independent experiments.

4.2.12.4 Expression of specific cell cycle signaling proteins

In order to confirm the cell cycle blockade shown by FACS analysis, specific cell cycle regulatory proteins were determined by western blot from cell lysates obtained after exposure to 2-deprenyl-rheediaxanthone B (XB).

The results showed a large increase in the level of cyclin A and a slight increase in the level of the cyclin B1 protein. The protein level of cyclin E was decreased compared to the control (Fig. 147). These changes confirmed the G2-M phase cell cycle arrest seen with FACS analysis.

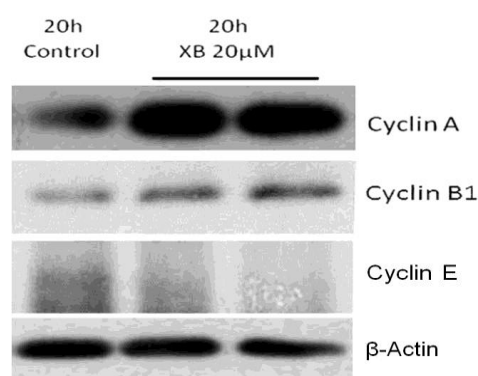


Fig. 147: Influence of XB on cell cycle signaling proteins

Cells were cultured for 24 h before incubation with 20μM 2-deprenyl-rheediaxanthone B for 20h. Cell lysates were then subjected to Western blot analysis for the indicated proteins. One representative blot is shown.

4.2.12.5 Microscopic analysis of 2-deprenyl- rheediaxanthone B treated SW480 cells

The SW480 cells were analysed by light microscopy for possible morphological changes associated with the 2-deprenyl-rheediaxanthone B treatment.

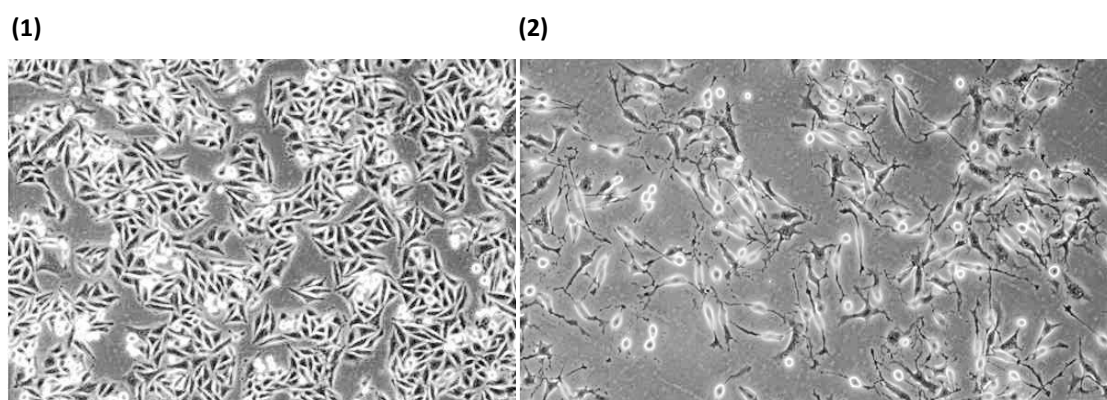


Fig. 148: Light microscopy analysis of control (1) and XB treated cells (2)

Results

SW480 cells were seeded in 24-well plates and grown for 24 h before treatment with 20 μ M 2-deprenyl-rheediaxanthone B, incubation for 48 h and examination by light microscopy.

Incubation of the cells with 20 μ M of XB (2) for 48h revealed morphological modifications such as cell shape alterations and cell detachment compared to the control (1).

Nuclear morphology was visualized by fluorescence microscopy after staining with Hoechst-33258, which intercalates into the DNA.

Treatment with 2-deprenyl-rheediaxanthone B (XB) for 48h caused morphological modifications such as pycnotic and fragmented nuclei (2). The most prominent change was an increase in the size of the nuclei compared to the control (1). In the control cultures most nuclei had almost the same size. Also one apoptotic body could be seen (1). After treatment with 20 μ M of XB a high number of giant polyploid nuclei as well as apoptotic bodies could be detected (2).

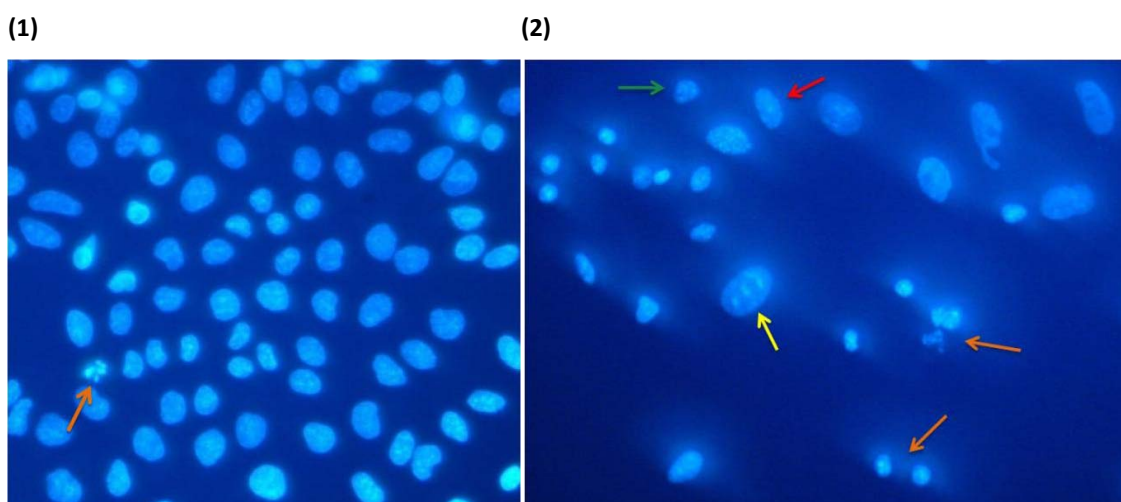


Fig. 149: Fluorescence microscopy analysis of control (1) and XB treated cells (2)

SW480 cells were seeded in 24-well plates and grown for 24 h before treatment with 20 μ M 2-deprenyl-rheediaxanthone B. After incubation for 48 h, the cells were stained with Hoechst-33258 and examined by fluorescence microscopy. The picture is color-coded: Normal Nucleus G1, Normal Nucleus G2, Apoptotic body, Giant nucleus.

4.2.12.6 Effect of 2-deprenyl-rheediaxanthone B on apoptosis

In order to investigate the effect on apoptosis, a JC-1 FACS analysis was conducted after incubation of SW480 cells with increasing concentrations (10, 15 and 20 μ M) of 2-deprenyl-rheediaxanthone B (XB) for 48 and 72 h. JC-1 is a mitochondrial tracer

concentrated in intact mitochondria. A loss of mitochondrial membran polarisation during apoptosis causes a shift in fluorescence and can be measured by FACS analysis.

The results showed a dose- and time-dependent increase in dying cells compared to the control (Fig. 150). After 48h about 18% dead cells were detected in the samples incubated with 10 μ M of the compound. At a concentration of 15 and 20 μ M about 50% of cells with depolarized mitochondria were seen. At 72h 10 and 15 μ M were sufficient to achieve this effect, and almost all cells were dead at a concentration of 20 μ M.

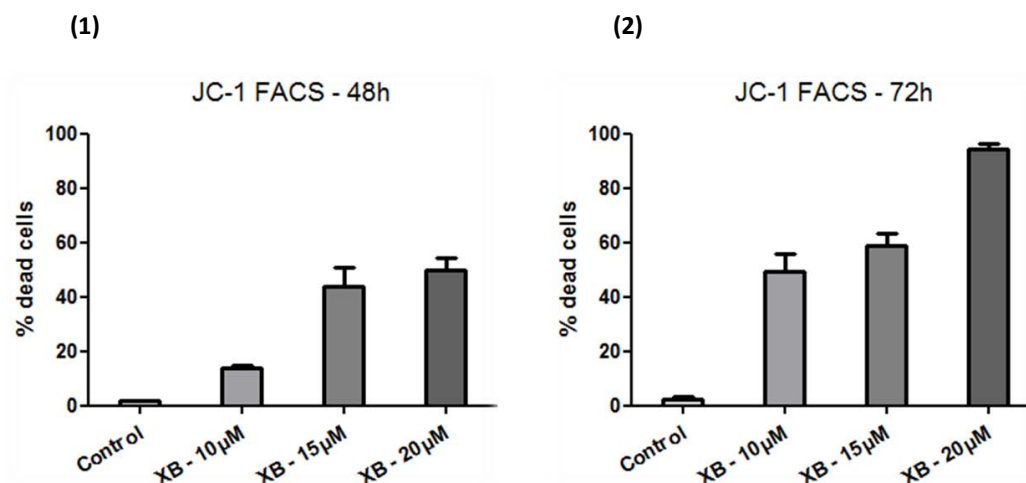


Fig. 150: JC-1 FACS analysis after treatment with XB after 48h (1) and 72h (2)

Results of JC-1 FACS analysis of SW480 cells treated with 2-deprenyl-rheediaxanthone B (XB) after 48h (1) and 72h (2). The cells were cultivated on 6 Pd plates and incubated with increasing concentrations (10, 15 and 20 μ M) of XB. Cells were harvested, stained with JC-1 and the percentage of dead cells was quantified by flow cytometry. Data represent mean \pm s.e.mean from two independent experiments.

4.2.12.7 Effect of 2-deprenyl-rheediaxanthone B on apoptosis related proteins

Treatment with 2-deprenyl-rheediaxanthone B led to concentration- and time-dependent loss of SW480 cells as detected with JC-1 FACS analysis, suggesting cell death due to apoptosis. In order to confirm this result, BAX, BAK and survivin were measured as specific pro- and anti-apoptotic effector molecules.

Cell lysates were obtained after incubation of SW480 cells with 20 μ M 2-deprenyl-rheediaxanthone B for 20h and analysed by western blotting. The results showed a slight increase in the levels of the pro-apoptotic proteins BAX and BAK as well as a slight decrease of survivin as compared to the control (Fig. 151). These changes in the levels of the apoptosis markers indicated the mitochondrial way of apoptosis.

Results

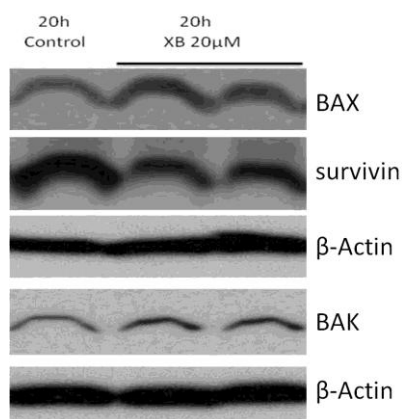


Fig. 151: Influence of XB on apoptosis signaling proteins I

Cells were cultured for 24 h before incubation with 20 μ M 2-deprenyl-rheediaxanthone B for 20h. Cell lysates were then subjected to Western blot analysis for the indicated proteins. One representative blot is shown.

Detection of the anti-apoptotic proteins BCL-XL and BCL 2, as well as the pro-apoptotic protein caspase 3 demonstrated an upregulation of BCL-XL and BCL 2, while caspase 3 almost not affected compared to the control (Fig. 152).

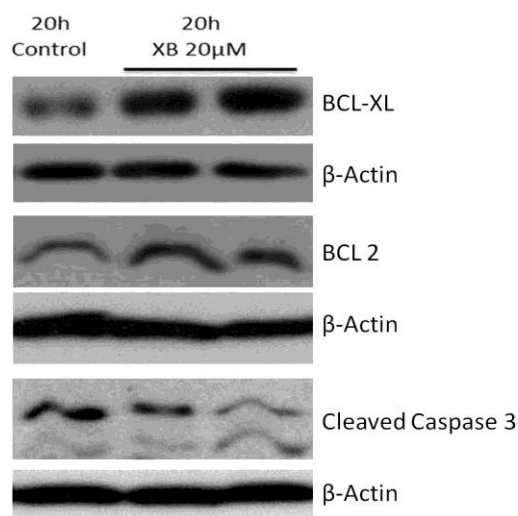


Fig. 152: Influence of XB on apoptosis signaling proteins II

Cells were cultured for 24 h before incubation with 20 μ M 2-deprenyl-rheediaxanthone B for 20h. Cell lysates were then subjected to Western blot analysis for the indicated proteins. One representative blot is shown.

2-deprenyl-rheediaxanthone B did not induce cleavage of poly(ADP-ribose) polymerase (PARP), which is catalyzed by caspase-3. PARP protein at 116 kDa was detected, but no cleavage with the cleavage product at 85 kDa (Fig. 153).

Results

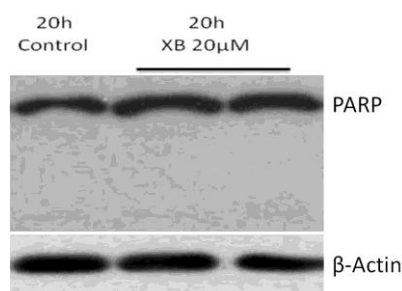


Fig. 153: Influence of XB on PARP

Cells were cultured for 24 h before incubation with 20µM 2-deprenyl-rheediaxanthone B for 20h. Cell lysates were then subjected to Western blot analysis for the indicated protein. One representative blot is shown. PARP protein at 116 kDa. No cleavage product at 85 kDa.

By contrast, an increase was observed in the levels of both caspase 2 and activated caspase 2 (Fig. 154).

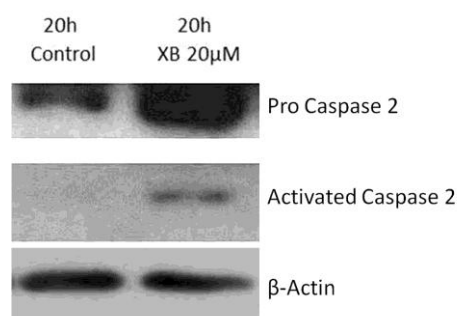


Fig. 154: Influence of XB on Caspase 2

Cells were cultured for 24 h before incubation with 20µM 2-deprenyl-rheediaxanthone B for 20h. Cell lysates were analysed by Western blot analysis for the indicated protein. One representative blot is shown.

The effect of 2-deprenyl-rheediaxanthone B on apoptotic cell death, investigated by the influence on pro- and anti-apoptotic markers, was evaluated. The results indicated that the cell loss, which was proven by JC-1 FACS analysis, MTT- and Neutralred-assays, is probably not due to apoptosis.

In order to analyse the induction of damage response after treatment with 2-deprenyl-rheediaxanthone B, the levels of the DNA damage marker Chk1 (total) and phosphorylated Chk1 (phospho-Chk1) were analysed by Western Blot analysis. The results showed an increase in total Chk1 as well as activation by phosphorylation of Chk1 and a

slight increase in total Cdc 2 and phosphorylated Cdc 2. The levels of Cdc25C were decreased clearly compared to the control (Fig. 155).

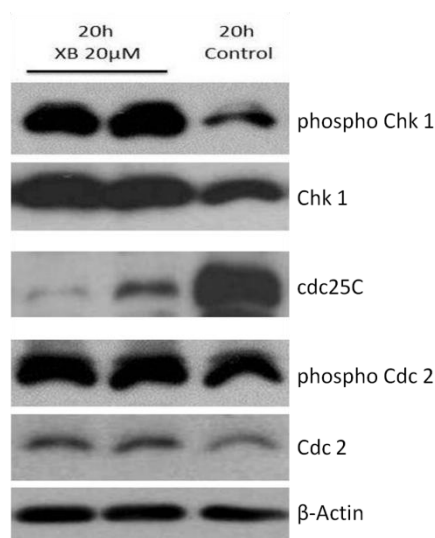


Fig. 155: Influence of XB on DNA-damage markers

SW480 cells were cultured for 24 h before incubation with 20μM 2-deprenyl-rheediaxanthone B for 20h. Cell lysates were analysed by Western blot for the indicated proteins. One representative blot is shown.

As the forkhead transcription factor FoxM1 is an important regulator of gene expression during the G2 phase and essential for correct mitotic progression, it was also evaluated. After incubation of SW480 cells with 20μM XB for 20h, FoxM1 was blocked completely compared to the control (Fig.156).

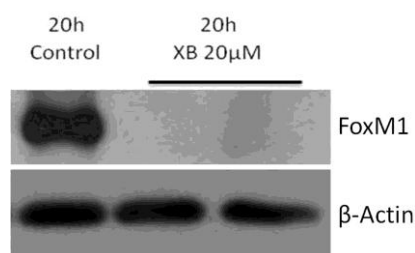


Fig. 156: Influence of XB on FoxM1

SW480 cells were cultured for 24 h before incubation with 20μM 2-deprenyl-rheediaxanthone B for 20h. Cell lysates were analysed by Western blot for the indicated protein. One representative blot is shown.

With FoxM1-staining the same effect as with Westernblot analysis could be seen. The staining of the giant nuclei after treatment with 2-deprenyl-rheediaxanthone B was weak or even absent.

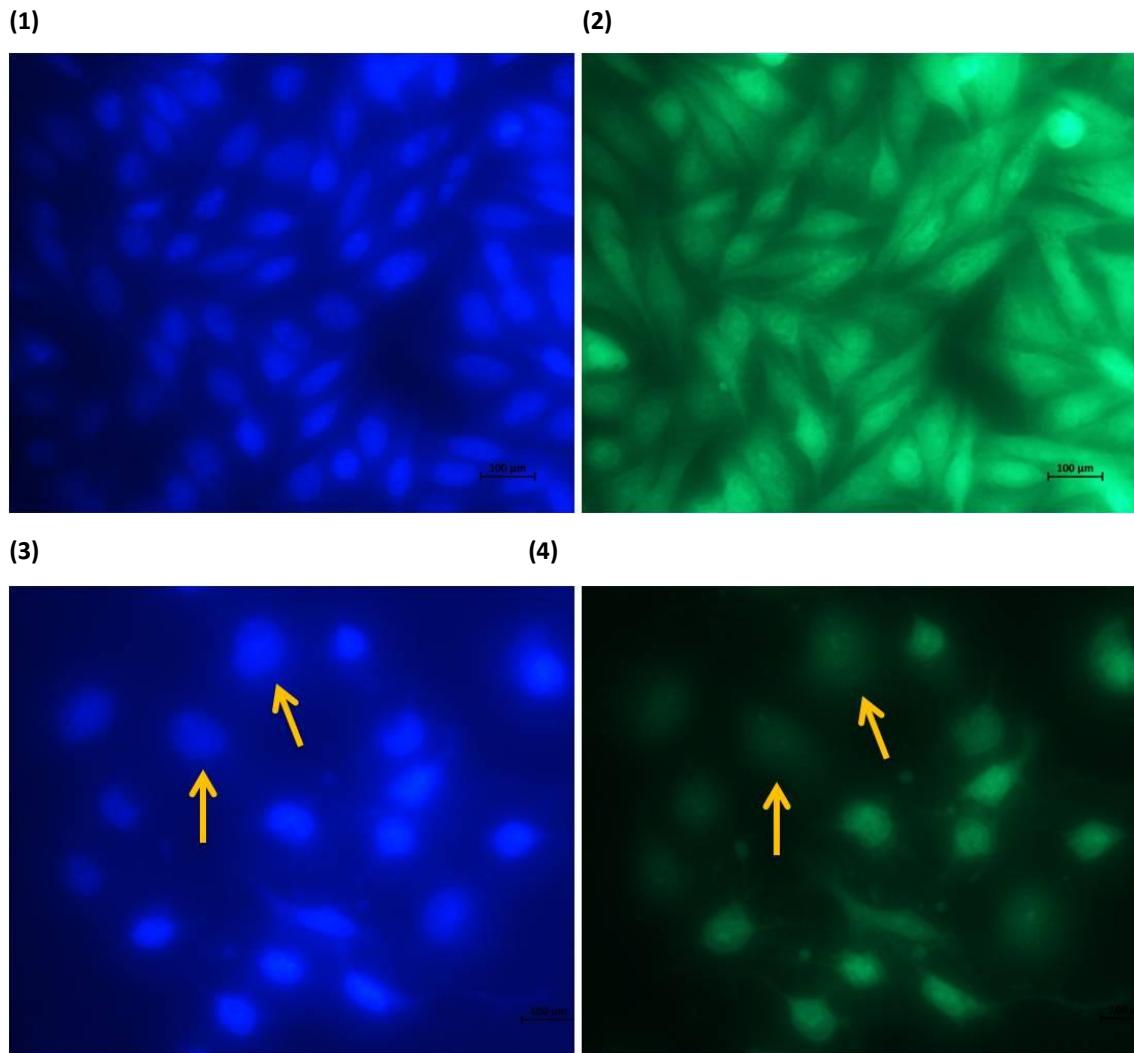


Fig. 157: Fluorescence microscopy analysis of control (1) and XB treated cells (3) with Höchst staining and analysis of control (2) and XB treated cells (4) with FoxM1 staining

SW480 cells were seeded in 24-well plates and grown for 24 h before treatment with 20µM 2-deprenyl-rheediaxanthone B. After incubation for 24 h, the cells were stained with Hoechst-33258 and FoxM1 and examined by fluorescence microscopy. The picture is color-coded: Giant nucleus.

As Chk1 is activated in response to different genomic lesions by ATR, the influence of 2-Deprenyl-rheediaxanthone B (XB) on this protein was also evaluated. After incubation of SW480 cells with 20µM XB for 20h, the results showed a slight increase of ATR protein. ATM seems not to be influenced (Fig.158).

Results

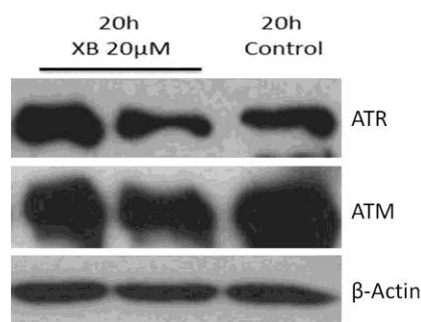


Fig. 158: Influence of XB on ATR and ATM

SW480 cells were cultured for 24 h before incubation with 20μM 2-deprenyl-rheediaxanthone B for 20h. Cell lysates were analysed by Western blot for the indicated proteins. One representative blot is shown.

Phosphorylation at Ser¹⁰ of Histone H3 is tightly correlated with chromosome condensation during mitosis. After treatment of the cells with 2-deprenyl-rheediaxanthone B for 20h, phospho Histone H3 (Ser¹⁰) was blocked completely.

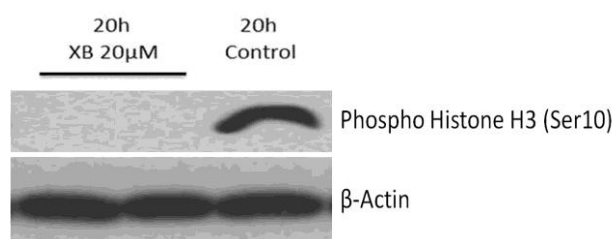


Fig. 159: Influence of XB on phospho Histone H3 (Ser¹⁰)

SW480 cells were cultured for 24 h before incubation with 20μM 2-deprenyl-rheediaxanthone B for 20h. Cell lysates were analysed by Western blot for the indicated proteins. One representative blot is shown.

5 DISCUSSION

Cancer therapy is one of the most addressed issues in drug discovery and natural products are an important source of anticancer agents, providing over 50% of the drugs in present clinical use (Newman and Cragg 2007). Tropical plants used in ethnic medicine are a rich source for such new cytotoxic compounds (Kim and Park 2002).

The present study describes the phytochemical investigation of the tree fern *Metaxya rostrata* used as traditional remedy as well as the bioactivity-guided fractionation and isolation of the active principles of this plant.

5.1 Phytochemical investigations of *Metaxya rostrata*

Metaxya rostrata, a tree fern belonging to the family of the *Metaxyaceae*, is used in traditional medicine in Costa Rica against intestinal diseases such as ulcers and tumors (Pekarek 2005). Until now only two proanthocyanidines (cinnamtannin B-1 and aesculitannin B), sugars and common sterols had been isolated from the plant (Virtbauer 2007). Therefore a profound chemical investigation, isolation and structure elucidation of the constituents of *Metaxya rostrata* was an important objective of this study.

In a previous study dried powdered roots of *Metaxya rostrata* had been extracted with water according to the ethnomedicinal use. Cinnamtannin B and aesculitannin B1 had been identified as cytotoxic principles (Virtbauer 2007). Another fraction of this water extract - fraction 12 - had shown reasonable cytotoxic activity as well (Virtbauer 2007) and thus was further fractionated by column chromatography by the use of different stationary and mobile phases. Several substances were isolated from this fraction:

The main compound of fraction 12 at R_f 0.56, coloured blue after detection 1, crystallized from several fractions and 58mg of compound KK1 were obtained (see chapter 4.1.1.).

After MS- and extensive one and two dimensional NMR-analysis the structure of KK1 was established as (2E)-2-(6-hydroxyhexylden)cyclopropyl- β -glucopyranoside. This compound has never been described before, neither isolated from natural sources nor totally

synthesized. The main structural feature of this new glycosidic compound is the extremely uncommon methylenecyclopropane alcohol in the aglycon (Kainz *et al.*, 2011).

In addition, 4.9mg of the novel compound KK5 were obtained by further CC separation of the combined fraction 12/3/10. Mass spectrometry and NMR experiments identified KK5 as a close relative to KK1. KK5 was unambiguously elucidated as (6E)-6[2-(β -glucopyranosyloxy)cyclopropylidene] hexanoic acid (Kainz *et al.*, 2011). Also this compound has never been isolated before.

The fraction also contained several known compounds that were identified by NMR and TLC experiments. Compound KK6 was identified as 4-O- β -D-glucopyranosyl-p-trans-coumaric-acid. This compound has been isolated before from the ferns *Drynaria fortunei* J. Sm. (Shang *et al.*, 2010), *Matteuccia struthiopteris* L. Todaro (Yang *et al.*, 2004) and *Davallia mariesii* Moore (Cui *et al.*, 1990). Furthermore, 4-O- β -D-glucopyranosyl-p-trans-coumaric-acid was proven in *Meconopsis quintuplinervia* Regel (Shang *et al.*, 2006), *Carthamus tinctorius* L. (Zhou *et al.*, 2008), *Ranunculus ternatus* Thunb. (Tian *et al.*, 2006), *Pinus sibirica* Du Tour (Khamidullina *et al.*, 2004), *Crataegus oxyacantha* L. (Sakai *et al.*, 2007), *Onobrychis viciifolia* Scop. (Lu *et al.*, 2000), *Clitoria ternatea* L. (Terahara *et al.*, 1990), *Scutellaria baicalensis* Georgi (Liu *et al.*, 2009) and in *Camptosorus sibiricus* Rupr. (Li *et al.*, 2006). 4-O- β -D-glucopyranosyl-p-trans-coumaric-acid was also found in flaxseed (Johnsson *et al.*, 2002), in bee-collected rape pollen (Guo *et al.*, 2009) and in white clover flowers (Foo *et al.*, 2000). 4-O- β -D-glucopyranosyl-p-trans-coumaric-acid and derivatives are reported to possess selective herbicidal activity against *Sesbania exaltata* Cory and other similar plant species (Ueda *et al.*, 2003).

The NMR characterization of compound KK3 identified it as 4-O- β -D-glucopyranosyl-caffeic-acid (Kainz *et al.*, 2011) that has been isolated before from ferns such as *Davillia mariesii* Moore. (Cui *et al.*, 1990), *Matteuccia struthiopteris* L. Todaro (Yang *et al.*, 2004), *Drynaria propinqua* (Wall) J. Smith (Li *et al.*, 2009; Liu *et al.*, 1992), *Cyathea phalerata* Mart. (Pizzolatti *et al.*, 2007) and *dregei* Kunze (Bringmann *et al.*, 1999). Additionally 4-O- β -D-glucopyranosyl-caffeic-acid has been proven in *Ilex rotunda* Thunb. (Hui *et al.*, 2009), *Olinia usambarensis* Gilg. (Nyandat *et al.*, 1993), *Camptosorus sibiricus* Rupr. (Li *et al.*, 2006), *Clematis trichotoma* Nakai (Ham *et al.*, 1999), in the *Colchicaceae* family in *Gloriosa rothschildiana* Carsonii (Mimaki *et al.*, 1991) and in Kiwi fruits (Fiorentino *et al.*, 2009).

Compound KK7 was identified as methyl- α -fructofuranoside (Kainz *et al.*, 2011). This substance has been isolated before from different plant species such as *Morinda citrifolia* L. (Su *et al.*, 2005), *Aralia cordata* Thunb. (Hyun *et al.*, 2010), *Turnera diffusa* Willd ex Schult. (Zhao *et al.*, 2007), *Castanea mollissima* Blume (Long *et al.*, 2009), *Saussurea lappa* C.B Clarke (Yin *et al.*, 2006), *Porana spectabilis* Kurz (Zhu *et al.*, 2001) and *Eurya tigang* K. Schum. & Lauterb. (Khan *et al.*, 1992) and others.

Besides two new unusual compounds, some known compounds were isolated and identified. The phenolic acid glycosides, 4-O- β -D-glucopyranosyl-caffeic-acid and 4-O- β -D-glucopyranosyl-p-trans-coumaric-acid, were proven in several plant families before, but seem to be enriched in ferns. Methyl- α -fructofuranoside was isolated before as well, but this simple sugar seems not to be very widespread in plant kingdom.

Biological activities were studied for the novel compound (2E)-2-(6-hydroxyhexyliden)-cyclopropyl- β -glucopyranoside (KK1). As this compound was isolated from fraction 12, which showed moderate cytotoxic activity (Virtbauer 2007), KK1 was tested for its cytotoxicity on colon carcinoma cells, but it did not show any effect on cancer cell viability up to a concentration of 500 μ M.

As secondary metabolites often serve the plant as anti-microbial substances, the anti-fungal activity against *Cladosporium sphaerospermum* (see chapter 4.1.8.6.), the anti-bacterial effect against six strains of *Staphylococcus aureus* (see chapter 4.1.8.7.) and the insecticidal activity against *Spodoptera littoralis* (see chapter 4.1.8.5.) of KK1 was evaluated. KK1 did not show any effect in these assays.

An in silico guided search for possible anti-viral activities of compound KK1 was undertaken because compounds with the extremely uncommon structural part of methylenecyclopropane have shown anti-viral activity against Epstein-Barr-, Human Herpes-, Hepatitis B-, Human Immunodeficiency- and Human Cytomegalo Virus in vitro (Rybak *et al.*, 2000, Qiu *et al.*, 1998, Uchida *et al.*, 1999). Pharmacophoric profiling (Rollinger *et al.*, 2009) and a structural similarity search in the MDL Drug Data Report (MDDR) database (Keiser *et al.*, 2007) suggested α -glucosidase as potential target for KK1. The antiviral activity against Herpes simplex Virus 1 was determined (see chapter 4.1.8.4.), but KK1 remained without any effect.

As compound KK1 did not show any activity in the evaluated assays, its aglycon was tested for biological activities. KK1 was hydrolysed and the effect on cancer cell viability of the KK1-aglycon was evaluated showing stronger activity than compound KK1 (see chapter 4.1.8.1.). The other experiments on anti-fungal, anti-viral and insecticidal activity need to be repeated with the aglycon of KK1 as well.

To sum up the phytochemical investigation of a fraction from the water extract of *Metaxya rostrata*, two unusual new compounds - (2E)-2-(6-hydroxyhexyliden)-cyclopropyl- β -glucopyranoside (KK1) and (6E)-6[2-(β -glucopyranosyloxy)cyclopropylidene]hexanoic acid (KK5) -, with the very uncommon structural feature of a methylenecyclopropane alcohol in the aglycon, two phenolic acid glycosides - 4-O- β -D-glucopyranosyl-caffeic-acid (KK3) and 4-O- β -D-glucopyranosyl-p-trans-coumaric-acid (KK6) - and a methyl- α -fructofuranosid (KK7) were isolated for the first time from the tree fern *Metaxya rostrata*.

5.2 Bioactivity-guided fractionation and isolation of the active compounds of *Metaxya rostrata*

The second objective of this study was a bioactivity-guided fractionation and isolation of the active principles of *Metaxya rostrata*. The water extract, which is used in traditional medicine, had already been analysed in a previous work (Virtbauer 2007). To extract the secondary metabolites of this plant as exhaustive as possible within this study, the dried and powdered leaves, rootlets and rhizomes of *Metaxya rostrata* were extracted with solvents of different polarity (CH_2Cl_2 , EA and MeOH).

After every step of fractionation the obtained fractions were evaluated for their effect on cancer cell viability on SW480, a colon cancer cell line. The most active extracts and fractions were chosen for further separation. The CH_2Cl_2 -extract and the EA-extract of the rootlets, the EA-extract of the leaves and the MeOH-extracts of the rhizomes of *Metaxya rostrata* reduced the cell viability significantly and cell loss was not due to necrosis (see chapter 4.2.2.1.).

Thus, these four extracts were fractionated by column chromatography on Sephadex LH-20. As chlorophyll and tannins are known to interact unspecifically with different proteins (Chernomorsky *et al.*, 1999; Lee *et al.*, 1990; Silvia *et al.*, 1998) and in order to exclude false positive results, chlorophyll was removed from the EA-extract of the leaves using liquid-liquid partition before further fractionation. From the methanol extract of the rhizomes tannins were removed before column chromatography (Wall *et al.*, 1996).

The obtained fractions after with column chromatography on Sephadex LH-20 were evaluated for their effect on cancer cell viability. Fractions of the CH₂Cl₂-extract CC-9/3, CC-9/4, CC-9/5, CC-9/6 and CC-9/8 showed a significant dose-dependent reduction of cell viability at a concentration of 0,6µg/ml (see chapter 4.2.3.). The fractions of the EA-extract of the rootlets CC-10/2, CC-10/3, CC-10/4 and CC-10/5 reduced the cell number in a significant manner at the same concentration (see chapter 4.2.4.). The fractions of the EA-extract of the leaves CC-11/3, CC-11/7, CC-11/8 and CC-11/9 revealed a reduction of cell viability at a concentration of 6µg/ml (see chapter 4.2.5.). Fractions CC-12/3 to CC-12/10 of the MeOH-extract of the rhizomes reduced cell viability significantly only at a concentration of 60µg/ml (see chapter 4.2.6.). All the other fractions showed lower or no effect on cell viability.

Due to the high activity and the pattern of compounds, the pooled fractions CC-9/3 and CC-9/4 of the CH₂Cl₂-extract of the rootlets of *Metaxya rostrata* were selected for further fractionation and isolation of the active compounds. Due to the small amount of these fractions, new plant material was extracted and fractionated in the same way to obtain a bigger amount of the active fractions (see chapter 4.2.8.1.).

Fractions CC-13/5, CC-13/6, CC-13/7, CC-13/8, CC-13/14 and CC-13/15 reduced the cell viability in a significant manner at a concentration of 6µg/ml (see chapter 4.2.8.1.). A TLC comparison of the active fractions from the first CH₂Cl₂-extract and the active fractions from the new CH₂Cl₂-extract showed some similarity, but due to some compounds occurring in one of the extracts only, the fractions were further fractionated separately using solid phase extraction (SPE).

The obtained fractions after SPE separation were again evaluated for their activity on cell viability. SPE-fractions SPE-3/3, SPE-3/4, SPE-5/2, SPE-6/2 of the new CH₂Cl₂-extract and

the SPE-fractions SPE-7/3 and SPE-8/4 of the first CH₂Cl₂-extract showed the highest activity and were chosen for the identification of the active principles by HPLC and spectroscopic methods.

In fractions SPE-3/4 of the new CH₂Cl₂-extract and SPE-7/3 of the first CH₂Cl₂-extract, the main compound eluting at Rt 42,5min was identified as betulinic acid by comparison the authentic reference. Betulinic acid was the major compound in these fractions with a purity of more than 98% and thus identified as the active principle. Betulinic acid, a pentacyclic triterpenoid widely distributed in plant kingdom, is a very well studied natural compound with a wide range of biological effects. *Betula alba* L., which contains high amounts of betulinic acid was already used by native americans to treat stomach and intestinal problems (Fulda 2008). Betulinic acid is known to be cytotoxic against melanoma, neuroectodermal and malignant brain tumor cell lines (Zuco *et al.*, 2001; Ciurlea *et al.*, 2010; Fulda *et al.*, 1997). Its cytotoxic effect on other types of cancer including glioblastoma, leukemia, colon, breast or cervix carcinoma was reported (Ehrhardt *et al.*, 2004; Ren *et al.*, 2010; Jung *et al.*, 2007; Fulda 2008). The anti-cancer activity of betulinic acid is associated to its ability to induce apoptosis by triggering the mitochondrial pathway of apoptosis (Fulda 2008; Mullauer *et al.*, 2009).

In fractions SPE-3/3 of the new CH₂Cl₂-extract and SPE-8/4 of the first CH₂Cl₂-extract betulinic acid was identified as one of the major compounds as well. In fraction SPE-3/3 of the new CH₂Cl₂-extract a second main compound with a retention time at 11,5min was identified by MS as a tetrahydroxy-C-prenylxanthone. In fraction SPE-8/4 the second major compound at Rt 27min elucidated by MS analysis as a tetrahydroxy-di-C-prenylxanthone. Due to the small amount of these fractions the two xanthone derivatives could not be isolated. Some prenylated xanthones exhibited inhibitory effects against *Mycobacterium tuberculosis* (Suksamrarn *et al.*, 2003), had potent immunomodulatory activities (Ngoupayo *et al.*, 2009), antiplasmodial activity (Mahabussarakam *et al.*, 2006; Molinar-Toribio *et al.*, 2006; Azebaze *et al.*, 2006) and antioxidant scavenging activity against DPPH radicals (Chen *et al.*, 2010). Furthermore, prenylated xanthones possess activity against MCF-7, NCI-H460 cell lines (Castanheiro *et al.*, 2009), HeLa and MDA-MB-231 cancer cell lines (Lim *et al.*, 2011). α -Mangostin, the best studied prenylated xanthone from *Garcinia mangostana*, induced cell-cycle arrest in G1 and apoptosis

through the activation of intrinsic pathway in human colon cancer DLD-1 cells (Matsumoto *et al.*, 2005; Akao *et al.*, 2008).

The activity of the fractions – SPE-3/3 of the new CH₂Cl₂-extract and SPE-8/4 of the first CH₂Cl₂-extract - could therefore be due to betulinic acid or to a synergistic effect of betulinic acid with the prenylated xanthenes.

In fraction SPE-5/2 of the new CH₂Cl₂-extract the major compound at Rt 24,5min was isolated and identified as 2-deprenyl-rheediaxanthone B using MS and NMR analysis. As 2-deprenyl-rheediaxanthone B was the major compound with a purity of more than 98% in this fraction, it is certain that the high activity in the bioassay is due to that compound. 2-Deprenyl-rheediaxanthone B is a very rare natural compound and has been isolated before only from two species of the family of the *Guttiferae*, from the roots of *Rheedia benthamiana* Pl. Triana (Monache *et al.*, 1981) and the roots of *Hypericum roeperanum* Schimp. ex A. Rich. (Rath *et al.*, 1996). Hostettmann and his group showed an anti-fungal activity against *Candida albicans* for this compound (Hostettmann *et al.*, 1996), but no further biological activity of 2-deprenyl-rheediaxanthone B had been studied before making it an interesting compound for further investigations.

The two main compounds at Rt 15,5min and 24,5min in fraction SPE-6/2 of the new CH₂Cl₂-extract were identified by MS analysis as tetrahydroxy-C-prenylxanthone and as 2-deprenyl-rheediaxanthone B. Both compounds were already identified in other active fractions. In fraction SPE-5/2 2-deprenyl-rheediaxanthone B was identified as the active principle. Tetrahydroxy-C-prenylxanthone was identified in fraction SPE-3/3 together with betulinic acid. The activity of fraction SPE-6/2 is probably due to 2-deprenyl-rheediaxanthone B or to a synergistic effect with the other xanthone derivative.

The bioactivity-guided approach led to the isolation of betulinic acid and 2-deprenyl-rheediaxanthone B. These compounds were elucidated as active principles in the cytotoxic fractions of the CH₂Cl₂-extract of the rootlets of *Metaxya rostrata*. As there is no data about the cytotoxicity of 2-deprenyl-rheediaxanthone B, this compound was chosen for detailed investigations to evaluate its biological effects and the underlying mechanisms.

5.3 Effect of 2-deprenyl-rheediaxanthone B on cell growth

2-deprenyl-rheediaxanthone B showed a significant dose and time-dependent reduction of cell viability of SW480 cells at a concentration of 6 μ M. In the LDH assay no cytotoxicity due to necrosis was detected after 24 and 48 hours. After 72 hours some probably secondary necrotic effects were seen.

2-deprenyl-rheediaxanthone B reduced the cell viability strongly in SW480 cell line. The effect on other cell lines was also studied. The compound significantly decreased the cell viability of CaCo-2, another colon carcinoma cell line, at a concentration of 10 μ M to about 70% and also reduced the cell viability of LT97, a human colon adenoma cell line, to about 85% at a concentration of 10 μ M and of human colon associated fibroblasts F331 to 75% at a concentration of 20 μ M. Compared to the effect of 2-deprenyl-rheediaxanthone B on cell viability of the colon carcinoma cell lines, SW480 and CaCo-2, the effect on the adenoma cell line LT97 and the fibroblasts was much weaker (see chapter 4.2.12.2.), making this compound very promising.

5.4 Effect of 2-deprenyl-rheediaxanthone B on cell cycle

Analysis of the cell cycle distribution after treatment with 2-deprenyl-rheediaxanthone B showed a concentration-dependent decrease of the proportion of cells in the G0-G1 phase and a concentration dependent accumulation of SW480 cells in the G2-M phase after 48 and 72h, suggesting a G2-M phase arrest (see chapter 4.2.12.3.). Analysis of the protein levels of specific cell cycle regulatory proteins like cyclin A, cyclin E and cyclin B1 by Western Blot analysis after exposure to 2-deprenyl-rheediaxanthone B confirmed that a cell cycle block had been induced. The cyclins are key regulators of the cell cycle as they activate members of the cyclin-dependent kinase (Cdk) family and effect cell cycle progression (Coverley *et al.*, 2002). Cyclin A functions in S phase and mitosis, starts to accumulate during S phase, is abruptly destroyed before metaphase and reaches high levels in G2-phase (Pagano *et al.*, 1992; Yam *et al.*, 2002). Cyclin E is needed for G1/S transition, cyclin B1 is the regulatory subunit of M-phase promoting factor and its correct regulation is essential for the initiation of mitosis (Pagano *et al.*, 1992; Sanchez & Dynlacht, 2005; Yuan *et al.*, 2004).

The 20 hours time point was chosen for Western Blot analysis because high cell loss was observed after 48 hours. Thus, 20 hours seemed a good time point for the observation of the responsible proteins. Due to the little amount of 2-deprenyl-rheediaxanthone B isolated, no other time points could be evaluated.

After incubation of SW480 cells with 2-deprenyl-rheediaxanthone B for 20h, the results showed a large increase in the level of cyclin A and a slight increase in the level of cyclin B1 protein. The protein level of cyclin E was decreased compared to the control. These changes in the regulatory protein expression confirmed the G2-M phase cell cycle arrest also seen in FACS analysis.

5.5 Effect of 2-deprenyl-rheediaxanthone B on apoptosis

JC-1 FACS analysis was conducted to investigate the effect of 2-deprenyl-rheediaxanthone B on apoptosis. The loss of mitochondrial membrane potential is a hallmark for apoptosis and mitochondrial permeability transition is an important step in the induction of apoptosis. When the electrochemical gradient across the mitochondrial membrane collapses it causes a shift in fluorescence. In non-apoptotic healthy cells, JC-1 accumulates as aggregates in the mitochondria which stain red. Whereas in apoptotic cells, JC-1 exists in monomeric form and the cytosol is stained green (Smiley *et al.*, 1991; Cossarizza *et al.*, 1993).

Treatment with 2-deprenyl-rheediaxanthone B led to a concentration- and time-dependent loss of SW480 cells detected by JC-1 FACS analysis.

Specific apoptosis markers were analyzed with Western Blot analysis after exposure to 2-deprenyl-rheediaxanthone B. BAX and BAK are pro-apoptotic proteins and operate at both the mitochondria and endoplasmic reticulum to regulate the intrinsic apoptotic pathway (Ruiz-Vela *et al.*, 2005; Oltvai *et al.*, 1993). After incubation of SW480 cells with 2-deprenyl-rheediaxanthone B for 20h, the results showed a slight increase in the levels of these pro-apoptotic proteins.

Survivin is an apoptosis inhibitor and a cell cycle regulator. It is required for suppression of apoptosis and for normal cell division in the G2/M phase of the cell cycle (Zaffaroni *et*

al., 2005; Shin *et al.*, 2001). Survivin protein level was decreased by XB compared to the control.

BCL-XL and BCL 2 are anti-apoptotic proteins of the BCL 2 family which play an important role in inhibiting mitochondria dependent cell death pathways (Kim 2005) and have anti-proliferative effects (Janumyan *et al.*, 2003). After treatment with 2-deprenyl-rheediaxanthone B for 20h, the protein levels of both BCL-XL and BCL 2 were upregulated.

Caspase 3, is proteolytically activated in cells during apoptosis (Peng *et al.*, 2004), but after treatment with 2-deprenyl-rheediaxanthone B for 20h, no increase of the active caspase 3 cleavage products was seen compared to the control. After activation of caspases from their proenzyme forms, they cleave different protein substrates during apoptosis such as PARP (Shin *et al.*, 2000; Nicholson *et al.*, 1995; Kaufmann *et al.*, 1993). After incubation of the SW480 cells with 2-deprenyl-rheediaxanthone B for 20h, the PARP protein at 116 kDa could be detected, but no cleavage product at 85 kDa could be seen. In summary, these observations indicate that the mode of XB-induced cell death in SW480 cells distinctly differs from classical apoptosis. The same conclusion is also supported by the morphological appearance of both cells and nuclei.

After treatment with 2-deprenyl-rheediaxanthone B, morphological modifications of the cells such as cell shape alterations and cell detachment compared to the control were detected by light microscopy. After Hoechst staining and analysis with fluorescence microscopy morphological modifications such as changes in the size of the nuclei was observed. A large fraction of giant polyploid nuclei as well as apoptotic bodies could be detected (see chapter 4.2.12.5.).

Upregulation of the anti-apoptotic proteins BCL-XL and BCL 2 further support the conclusion that the main mechanism of cell loss is not apoptosis. In contrast to caspase 3 another caspase, caspase 2, was highly activated after treatment with 2-deprenyl-rheediaxanthone B.

It has been difficult to formally characterize caspase 2 as an initiator or an executor caspase because it has features of both groups (Zhivotovsky and Orrenius, 2005). Unlike other initiator caspases, caspase 2 does not activate executor caspases directly (Bouchier-Hayes 2010). Its role in apoptosis seems to be stimulus- and/or cell type specific

(Bergeron *et al.*, 1998), but there is evidence for potential roles of caspase-2 in other processes like DNA repair and cell cycle regulation (Vakifahmetoglu-Norberg and Zhivotovsky 2010). After incubation of SW480 cells with 2-deprenyl-rheediaxanthone B for 20h, the results showed an increase in the levels of the caspase 2 and activated caspase 2 compared to the control.

There is evidence that in some cases, caspase 2 may be responsible for direct permeabilization of the mitochondria, which would explain our JC-1 FACS results. In other cases it may act in conjunction with BAX/BAK to amplify cytochrom C release (Zhivotovsky and Orrenius 2005). Different stimuli like DNA-damage inducers such as doxorubicin or cytoskeletal disruptors like paclitaxel, ER stress inducers like tunicamycin or others like resveratrol have been reported to activate caspase 2 (Bouchier-Hayes 2010). Exposure of doxorubicin, one of the most effective anti-tumor drugs, to human breast carcinoma cells induced polyploidy and cell death by mitotic catastrophe and activation of caspase 2 (Mansilla *et al.*, 2006). HCT116 colon carcinoma cells treated with doxorubicin undergo mitotic catastrophe as well (Chan *et al.*, 1999; Castedo *et al.*, 2004). Polyploidy and caspase 2 activation was also seen after treatment of SW480 cells with 2-deprenyl-rheediaxanthone B in this study suggesting that mitotic catastrophe could be the reason of cell loss.

It has been discussed that mitotic catastrophe is totally different from apoptosis (Roninson *et al.*, 2001) because some manipulations preventing apoptosis, such as overexpression of BCL 2 in etoposide-treated HeLa cells (Lock and Stribinskiene 1996; Ruth and Roninson 2000), reduce apoptosis, while they enhance the frequency of catastrophic mitoses (Castedo *et al.*, 2004). BCL 2 is reported to have the ability to enhance cell death in the interaction of BCL-XL with other factors. Kim discussed that BCL 2 and BCL-XL may switch their anti-apoptotic function to a pro cell death function in some situations (Kim 2005). In case of metaphase associated death, caspase 2 activation can be detected even when apoptosis is suppressed and it can not be inhibited by BCL 2 (Castedo *et al.*, 2004; Peart *et al.*, 2003). Both, the protein levels of BCL-XL and BCL 2 were increased after treatment with 2-deprenyl-rheediaxanthone B which leads to the conclusion that SW480 cells treated with this compound die due to mitotic catastrophe.

There is also evidence that depletion of survivin led to a defect in mitosis, without any direct induction of apoptosis. Inhibition of survivin was reported in glioma cells to be followed by spontaneous apoptosis, mitotic catastrophe and cell cycle arrest and the downregulation of survivin led to mitotic catastrophe in esophageal cancer cells as well (Zhen *et al.*, 2007; Ngan *et al.*, 2008; Vakifahmetoglu *et al.*, 2008). That indicates that the role of survivin as a protection from apoptosis is rather secondary to its role during mitosis (Castedo *et al.*, 2004; Carvalho *et al.*, 2003; Lens *et al.*, 2003). In this study, downregulation of survivin after the treatment with 2-deprenyl-rheediaxanthone B was also seen. Castedo discussed that survivin may play an important role in the coupling of abnormal mitotic progression to the onset of mitotic catastrophe (Castedo *et al.*, 2004).

5.6 Effect of 2-deprenyl-rheediaxanthone B on checkpoint kinases

After treatment of SW480 cells with 2-deprenyl-rheediaxanthone B, the levels of the DNA damage marker Chk1 and phosphorylated Chk1 were analyzed by Western Blot analysis. Chk1 is an essential component in the G2 damage checkpoint as it is activated in response to a variety of lesions and ensuring that Cdc2 remains in an inactive state until DNA repair is completed (Tapia-Alveal *et al.*, 2009; Stracker *et al.*, 2009). Cdc2, a subunit of the M-phase promoting factor, induces entry into mitosis and is a key player in cell cycle regulation (Draetta *et al.*, 1988). In late G2 phase Chk1 phosphorylates the protein phosphatase Cdc25C, which controls cell cycle transitions by dephosphorylating cyclin-dependent kinases. In response to DNA damage, Chk1 phosphorylates and inhibits Cdc25C, thus preventing activation of the Cdc2/Cyclin B complex and mitotic entry (Sanchez *et al.*, 1997; Graves *et al.*, 2000; Abraham 2001). It is believed that mitotic catastrophe occurred when the G2 damage checkpoint is inhibited (Niida *et al.*, 2005). However, there is now evidence that supports the multiplicity in the role of Chk1 in mitotic catastrophe. Huang and group reported that the mitotic exit damage checkpoint is Chk1 dependent and DNA damage not just delays mitotic exit but blocks it leading to mitotic catastrophe. Yamane and group showed that DNA damage induced mitotic catastrophe was mediated by Chk1 dependent mitotic exit. Thus, it seemed that checkpoint activation would result in an early event that was the mitotic exit followed by mitotic catastrophe (Huang *et al.*, 2005; Yamane *et al.*, 2007). Zhang and group reported

that exposure of human lung cancer cell line to 8-chloro-adenosine induced cell arrest in the G2/M phase accompanied by accumulation of polyploid cells and loss of phosphorylated Cdc25C that allows progression into mitosis. These results indicate a G2 checkpoint failure (Zhang et al., 2004). G2 checkpoint failure promotes mitotic catastrophe (Roninson et al., 2001).

After incubation of SW480 cells with 2-deprenyl-rheediaxanthone B for 20h, the results showed a large increase in the activation of phosphorylated Chk1 and total Chk1 indicating a cell cycle arrest which was also proven by FACS analysis. It is reported that overexpression of Chk1 alone caused a G2 cell cycle arrest (Walworth et al., 1993). A slight increase in total Cdc 2 and phosphorylated Cdc2 could be detected and in correlation with the upregulation of Chk1, Cdc25C is blocked after treatment with 2-deprenyl-rheediaxanthone B.

As Chk1 is activated in response to different genomic lesions by ATR (Tapia-Alveal *et al.*, 2009; Bartek and Lukas, 2003), this protein was also evaluated in our study. After incubation of SW480 cells with 2-deprenyl-rheediaxanthone B for 20h, the results showed a slight increase in the activation of ATR. ATM seems not to be influenced in accordance with literature linking Chk1 with ATR. The reason for seeing just a slight increase of ATR could be that at the time point when the upregulation of Chk1 was detected, ATR protein levels are already declining again. As ATR is a classical mediator of damage response, the results could indicate DNA damage after treatment with 2-deprenyl-rheediaxanthone B, which needs to be further investigated.

The forkhead transcription factor FoxM1 is an important regulator of gene expression during the G2 phase (Laoukili *et al.*, 2008) and is essential for correct mitotic progression (Laoukili *et al.*, 2005). Loss of the transcriptional factor FoxM1 affects genes that are essential for chromosome segregation, generates mitotic spindle defects, delays in mitosis and leads to mitotic catastrophe (Vakifahmetoglu *et al.*, 2008; Wonsey *et al.*, 2005). A more precise marker of mitotic cells is phosphorylation at Ser¹⁰ of Histone H3 which is tightly correlated with chromosome condensation in mitosis (Wei *et al.*, 1999; Portugal *et al.*, 2010). The incubation of SW480 cells with 2-deprenyl-rheediaxanthone B for 20h resulted in an almost complete loss of the FoxM1 protein compared to the control demonstrating the mechanistic basis for the delay of cells in late G2/M phase.

Phosphorylation at Ser¹⁰ of Histone H3 was also almost completely absent from giant nuclei, which indicates a defect in chromosome condensation and places the exact point of cell cycle arrest in late G2. Together these observations support the conclusion that SW480 cells treated with 2-deprenyl-rheediaxanthone B die due to mitotic catastrophe.

6 CONCLUSION

In the phytochemical investigation of the presented study, two unusual novel compounds - (2E)-2-(6-hydroxyhexyliden)cyclopropyl- β -glucopyranoside (KK1) and (6E)-6[2-(β -glucopyranosyloxy)cyclopropylidene] hexanoic acid (KK5) - with the very uncommon structural feature of a methylenecyclopropane alcohol in the aglycon, two phenolic acid glycosides - 4-O- β -D-glucopyranosyl-caffeic-acid (KK3) and 4-O- β -D-glucopyranosyl-p-trans-coumaric-acid (KK6) - and a methyl- α -fructofuranosid (KK7) were isolated for the first time from the tree fern *Metaxya rostrata*.

The present work also demonstrates for the first time the cytotoxicity of the rare natural compound 2-deprenyl-rheediaxanthone B, isolated from the rootlets of the traditional herbal remedy *Metaxya rostrata* and gives insight into the underlying mechanism of action. The present study shows that 2-deprenyl-rheediaxanthone B significantly reduces cell viability in the SW480 cell line, but does not affect normal fibroblasts as much, thus making this compound very promising.

After treatment with 2-deprenyl-rheediaxanthone B a G2-M phase arrest and a large number of giant polyploid nuclei as well as apoptotic bodies were detected. 2-deprenyl-rheediaxanthone B treatment did not affect caspase 3 and did not lead to PARP cleavage. An upregulation of the protein levels of caspase 2, BCL 2, BCL-XL, BAX, BAK, ATR, Chk1 was observed. Survivin was downregulated and FoxM1, phospho Histone H3 and Cdc25C were blocked completely compared to the control.

The results indicate that the cell loss after treatment of SW480 cells with 2-deprenyl-rheediaxanthone B is due to mitotic catastrophe.

7 SUMMARY

Natural products deriving from plants used in traditional medicine are an important source for anti-cancer agents or new lead-compounds. The structural relatives of natural compounds provide over 50% of drugs in current clinical use. Therefore the aim of this study was to identify the active principles in the tree fern *Metaxya rostrata*, which is used as a herbal remedy against intestinal diseases in Costa Rica.

Metaxya rostrata was investigated phytochemically and fractionated in a bioactivity-guided approach. The phytochemical investigation of a fraction from a water extract led to the isolation of two unusual new compounds - (2E)-2-(6-hydroxyhexyliden)cyclopropyl- β -glucopyranoside and (6E)-6[2-(β -glucopyranosyloxy)cyclopropylidene] hexanoic acid - with the very uncommon structural feature of a methylenecyclopropane alcohol in the aglycon. In addition, two phenolic acid glycosides - 4-O- β -D-glucopyranosyl-caffeic-acid and 4-O- β -D-glucopyranosyl-p-trans-coumaric-acid - and a methyl- α -fructofuranosid were isolated for the first time from *Metaxya rostrata*.

The bioactivity-guided approach led to the isolation of the cytotoxic principles betulinic acid and 2-deprenyl-rheediaxanthone B (XB), which is a very rare natural compound. The present study shows cytotoxic activity of XB for the first time and provides insight into the underlying mechanism. XB reduced the cell viability in the SW480 colon carcinoma cell line, but affected adenoma cells and normal fibroblasts much less, suggesting a very promising compound. Treated cells were arrested in G2-M phase causing appearance of giant polyploid nuclei as well as apoptotic bodies. Treatment with 2-deprenyl-rheediaxanthone B did not affect caspase 3 and did not lead to PARP cleavage indicating that cell loss is not due to apoptosis even though BAX and BAK were up-regulated and survivin was decreased. An upregulation of the protein levels of caspase 2, BCL 2, BCL-XL, ATR, Chk1 compared to the control was detected and FoxM1, phospho Histone H3 and Cdc25C were blocked completely.

These results indicate that 2-deprenyl-rheediaxanthone B induced reduction of cell viability due to mitotic catastrophe. The present work anticipates future studies to further elucidate the potential of 2-deprenyl-rheediaxanthone B and other xanthenes for the development of novel anti-cancer drugs.

8 ZUSAMMENFASSUNG

Naturstoffe aus ethnomedizinisch verwendeten Arzneipflanzen sind eine wichtige Quelle für neue Medikamente in der Krebstherapie, sodass pflanzliche Leitsubstanzen und von ihnen abgeleitete chemische Verbindungen über 50% aller klinisch verwendeten Chemotherapeutika ausmachen. Aus diesem Grund wurde der Baumfarn *Metaxya rostrata*, der in der traditionellen Medizin in Costa Rica bei Erkrankungen des Magen-Darm-Trakts Anwendung findet, untersucht.

Metaxya rostrata wurde phytochemisch untersucht und in einem zweiten Ansatz auch bioactivity-geleitet fraktioniert. Die phytochemische Untersuchung führte zur Isolierung zweier außergewöhnlicher neuer Substanzen - (2E)-2-(6-hydroxyhexyliden)cyclopropyl- β -gluco pyranosid and (6E)-6[2-(β -glucopyranosyloxy)cyclopropyliden] hexan säure – mit dem ungewöhnlichen Strukturmerkmal eines Methylencyclopropanalkohols im Aglycon. Außerdem wurden zwei Phenolcarbonsäureglycoside - 4-O- β -D-glucopyranosyl-Kaffeensäure and 4-O- β -D-glucopyranosyl-p-trans-Cumarsäure - sowie Methyl- α -fructofuranosid zum ersten Mal aus *Metaxya rostrata* isoliert.

Die bioactivity-geleitete Fraktionierung führte zur Isolierung der zwei zytotoxischen Verbindungen Betulinsäure und 2-Deprenyl-rheediaxanthone B (XB), eines sehr seltenen Naturstoffes. Die Arbeit weist zum ersten Mal Zytotoxizität von 2-Deprenyl-rheediaxanthone B nach und gibt Einblick in den zellulären Wirkmechanismus dieser Substanz. Die Überlebensfähigkeit von SW480 Kolonkarzinomzellen wurde durch Behandlung mit XB signifikant reduziert, während Adenomzellen und normale Fibroblasten deutlich weniger betroffen waren. Diese selektive Wirkung macht XB zu einer vielversprechenden Verbindung. Behandelte Zellen sind in der G2/M Phase arretiert, wodurch sich große polyploide Zellkerne sowie apoptotische Kerne anhäufen. Obwohl die pro-apoptotischen Protein BAX und BAK hochreguliert werden und Survivin reduziert wird, spricht eine fehlende Aktivierung von Caspase 3 und die Abwesenheit von PARP Spaltprodukten gegen das Vorliegen von Apoptose in mit XB behandelten Kulturen. Hochregulation von Caspase 2, BCL 2, BCL-XL, ATR, Chk1 im Vergleich zu Kontrollzellen, sowie ein kompletter Verlust von FoxM1 und Cdc25C wurden beobachtet. Diese

Ergebnisse beweisen, dass mitotische Katastrophe für die Induktion des Zelltodes nach Behandlung mit 2-Deprenyl-rheediaxanthone B verantwortlich ist. Weitere Studien an dieser wirksamen Verbindung und an der Substanzklasse der Xanthone könnten das Potential dieser Verbindungen für die Entwicklung neuer Krebstherapeutika evaluieren.

9 BIBLIOGRAPHY

Abend M. (2003) Reasons to reconsider the significance of apoptosis for cancer therapy. *Int J Radiat Biol* 79, 927-941.

Abraham R.T. (2001) Cell cycle checkpoint signaling through the ATM and ATR kinases. *Genes & Development* 15, 2177-2196.

Alberts B., Johnson A., Lewis J., Raff M., Roberts K., Walter P. (2002) *Molecular Biology of the Cell*, 4th ed. New York, Garland Science, Taylor & Francis Group, 907-950 and 983-1010.

Akao Y., Nakagawa Y., Nozawa Y. (2008) Anti-Cancer Effects of Xanthenes from Pericarps of Mangosteen. *Int. J. Mol. Sci.* 9(3), 355-370.

Altieri D.C. (2003). Validating survivin as a cancer therapeutic target. *Nat. Rev. Canc* 3, 46–54.

American Joint Committee on Cancer: <http://www.cancerstaging.org/mission/whatis.html> 28.7.2011 (9.00h)

American Cancer Society: <http://www.cancer.org> 25.7.2011 (10.55h)

Anand P., Kunnumakara A.B., Sundaram C., Harikumar K.B., Tharakan S.T., Lai O.S., Sung B., Aggarwal B.B. (2008) Cancer is a Preventable Disease that Requires Major Lifestyle Changes. *Pharmaceutical Research* 25(9), 2097-2116.

ATCC: <http://www.atcc.org> 14.4.2011 (11.20h)

Azebaze A.G.B., Meyer M., Valentin A., Nguemfo E.L., Fomum Z.T., Nkengfack A.E. (2006) Prenylated xanthone derivatives with antiplasmodial activity from *Allanblackia monticola* STANER L.C. *Chemical & Pharmaceutical Bulletin* 54(1), 111-113.

Baluk P., Hashizume H., McDonald D.M. (2005) Cellular abnormalities of blood vessels as targets in cancer. *Curr. Opin. Genet. Dev.* 15, 102-111.

Bartek J. and Lukas J. (2003) Chk1 and Chk2 kinases in checkpoint control and cancer. *Cancer Cell* 3, 421-429.

Bartram C.R. (2004) Genetische Grundlagen der Kanzerogenese. In: Hiddemann W.H.H., Bartram C. *Die Onkologie*. Heidelberg: Springer Verlag.

Baeriswyl V. and Christofori G. (2009) The angiogenic switch in carcinogenesis. *Semin. Cancer Biol.* 19, 329-337.

Bannerman R.H.O., Burton J., Chen W.C. (1983) *Traditional Medicine and Health Care Coverage: A Reader for Health Administrators and Practitioners*. Geneva: World Health Organization.

Basanez G., Nechushtan A., Drozhinin O., Chanturiya A., Choe E., Tutt S., Wood K.A., Hsu Y. T., Zimmerberg J., Youle R. J. (1999) Bax, but not Bcl-XL decreases the lifetime of planar phospholipid bilayer membranes at subnanomolar concentrations. *Proc. Natl. Acad. Sci.* 96, 5492-5497.

Bergeron L., Perez G.I., Macdonald G., Shi L., Sun Y., Jurisicova A., Varmuza S., Latham K.E., Flaws J.A., Salter J.C., Hara H., Moskowitz M.A., Li E., Greenberg A., Tilly J.L., Yuan J. (1998) Defects in regulation of apoptosis in caspase 2 deficient mice. *Genes Dev.* 12, 1304-1314.

- Berx G. and van Roy F. (2009) Involvement of members of the cadherin superfamily in cancer. *Cold Spring Harb. Perspect. Biol.* 1, 1-27.
- Bhowmick N.A., Neilson E.G., Moses H.L. (2004) Stromal fibroblasts in cancer initiation and progression. *Nature* 432, 332-337.
- Blasco M.A. (2005) Telomeres and human disease: ageing, cancer and beyond. *Nat. Rev. Genet.* 6, 611-622.
- Bleier J. (2011) Phytochemische Untersuchung des Baumfarns *Metaxya rostrata*. Diplomarbeit an der Universität Wien.
- Boonmee A., Reynolds C.D., Sangvanich P. (2007) α -Glucosidase inhibitor proteins from *Sesbania grandiflora* flowers. *Planta Medica* 73, 1197-1201.
- Borges de Melo E., Da Silveira Gomes A., Carvalho I. (2006) α - and β -Glucosidase inhibitors: chemical structure and biological activity. *Tetrahedron* 62, 10277-10302.
- Bouchier-Hayes L. (2010) The role of caspase 2 in stress induced apoptosis. *J. Cell. Mol. Med.* 14, 1212-1224.
- Boyle P. and Levin B. (2008) World Cancer Report 2008. Lyon, France: World Health Organization. International Agency for Cancer medicine.
- Bringmann G., Gunther C., Jumbam D. N. (1999) Isolation of 4-O- α -D-glucopyranosylcaffeic acid and gallic acid from *Cyathea dregei* KUNZE. *Pharmaceutical and Pharmacological Letters* 9(2), 41-43.
- Brown J.M. and Attardi L.D. (2005) The role of apoptosis in cancer development and treatment response. *Nat. Rev. Cancer* 5, 231-237.
- Bunz F., Dutriaux A., Lengauer C., Waldmann T., Zhou S., Brown J.P., Sedivy J.M., Kinzler K.W., Vogelstein B. (1998) Requirement for p53 and p21 to sustain G2 arrest after DNA damage. *Science* 282, 1497-1501.
- Camonis J.H. and White M.A. (2005) Ral GTPases: corrupting the exocyst in cancer cells. *Trend Cell Biology* 15, 327-323.
- Castagnola P. and Giaretti W. (2005) Mutant KRAS, Chromosomal instability and prognosis in colorectal cancer. *Biochim Biophys Acta* 1756, 115-125.
- Castanheiro R.A.P., Silva A.M.S., Campos N.A.N., Nascimento M.S.J., Pinto M.M.M. (2009) Antitumor activity of some prenylated xanthenes. *Pharmaceuticals* 2, 33-43.
- Castedo M., Perfettini J.L., Roumier T., Andreau K., Medema R., Kroemer G. (2004) Cell death by mitotic catastrophe: a molecular definition. *Oncogene* 23, 2825-2837.
- Castedo M. and Kroemer G. (2004) Mitotic catastrophe: a special case of apoptosis. *J. Soc. Biol.* 198, 97-103.
- Center M.M., Jemal A., Ward E. (2009) International trends in colorectal cancer incidence rates. *Cancer Epidemiol Biomarkers Prev.* 18, 1688-1694.
- Center M.M., Jemal A., Smith R.A., Ward E. (2009) Worldwide variations in colorectal cancer. *CA Cancer J. Clin.* 59, 366-378.
- Chao A.C., Hsu Y.L., Liu C.K., Kuo P.L. (2011) α -Mangostin, a dietary xanthone, induces autophagic cell death by activating the AMP-activated protein kinase pathway in glioblastoma cells. *Agricultural and Food Chemistry* 59(5), 2086-2096.

- Chen Y., Fan H., Yang G.Z., Jiang Y., Zhong F.F., He H.W. (2011) Two unusual xanthenes from the bark of *Garcinia xanthochymus*. *Helvetica Chimica Acta* 94, 662-668.
- Chen Y., Fan H., Yang G.Z., Jiang Y., Zhong F.F., He H.W. (2010) Prenylated xanthenes from the bark of *Garcinia xanthochymus* and their 1,1-diphenyl-2-picrylhydrazyl (DPPH) radical scavenging activities. *Molecules* 15, 7438-7449.
- Cheng N., Chytil A., Shyr Y., Joly A., Moses H.L. (2008) Transforming growth factor-beta signaling-deficient fibroblasts enhance hepatocyte growth factor signaling in mammary carcinoma cells to promote scattering and invasion. *Mol. Cancer Res.* 6, 1521-1533.
- Chernomorsky S., Segelman A., Poretz R.D. (1990) Effect of dietary chlorophyll derivatives on mutagenesis and tumor cell growth. *Teratogenesis, Carcinogenesis, and Mutagenesis* 19(5), 313-322.
- Ciurlea S.A., Dehelean C.A., Ionescu D., Berko S., Csanyi E., Hadaruga D.I., Ganta S., Amiji M.M. (2010) A comparative study regarding melanoma activity of Betulinic acid on topical ointment vs. Systemic nanoemulsion delivery systems. *Journal of Agroalimentary processes and technologies* 16(4), 420-426.
- Clevers H. (2006) Wnt/beta-catenin signaling in development and disease. *Cell* 127(3), 469-480.
- Cossarizza A., Baccarani-Contri M., Kalashnikova G., and Franceschi C. (1993) A new method for the cytofluorimetric analysis of mitochondrial membrane potential using the J-aggregate forming lipophilic cation 5,5',6,6'-tetrachloro-1,1',3,3' tetraethylbenzimidazolyl carbocyanine iodide (JC-1). *Biochem. Biophys. Res. Commun.* 197(1), 40-45.
- Coverley D., Laman H., Laskey R.A. (2002) Distinct roles for cyclins E and A during DNA replication complex assembly and activation. *Nat. Cell Biol.* 4, 523-528.
- Cragg G.M., Grothaus P.G., Newman D.J. (2009) Impact of natural products on developing new anti-cancer agents. *Chem. Rev.* 109, 3012-3043.
- Cragg G.M., Newman D.J., Snader K.M. (1997) Natural products in drug discovery and development. *J. Nat. Prod.* 60, 52-60.
- Cragg G.M. and Newman D.J. (2005) Plants as source of anti-cancer agents. *Journal of Ethnopharmacology* 100, 72-79.
- Creasy W.A. (1969) Antitumoral activity of the fern *Cibotium schiedeii*. *Nature* 222, 1282.
- Croce C.M. (2008) Molecular Origins of Cancer - Oncogenes and Cancer. *N. Engl. J. Med* 358, 502-511.
- Cui C.B., Tezuka Y., Kikuchi T., Nakano H., Tamaoki T., Park J.H. (1990) Constituents of a fern, *Davallia mariesii* Moore. I. Isolation and structures of davallialactone and a new flavanone glucuronide. *Chemical & Pharmaceutical Bulletin* 38(12), 3218-3225.
- Da Rocha A.B., Lopes R.M., Schwartzmann G. (2001) Natural products in anticancer therapy. *Current Opinion in Pharmacology* 1, 364-369.
- Desagher S., Osen-Sand A., Nichols A., Eskes R., Montessuit S., Lauper S., Maundrell K., Antonsson B., and Martinou J.C. (1999) Bid-induced conformational change of Bax is responsible for mitochondrial cytochrome c release during apoptosis. *J. Cell Biol.* 144 (5), 891-901.
- Ding M., Feng Y., Vandre D.D. (1997) Partial characterization of the MPM-2 phosphoepitope. *Experimental Cell Research* 231, 3-13.

- Ding L., Liu B., Qi L.L., Zhou Q.Y., Hou Q., Li J., Zhang G. (2009) Anti-proliferation, cell cycle arrest and apoptosis induced by a natural xanthone from *Gentianopsis paludosa* Ma, in human promyelocytic leukemia cell line HL-60 cells. *Toxicology in Vitro* 23, 408-417.
- Edwards B.K., Ward E., Kohler B.A. (2010) Annual report to the nation on the status of cancer, 1975-2006, featuring colorectal cancer trends and impact of interventions (risk factors, screening, and treatment) to reduce future rates. *Cancer* 116, 544-573.
- Ehrhardt H., Fulda S., Fuhrer M., Debatin K.M., Jeremias I. (2004) Betulinic acid induced apoptosis in leukemia cells. *Leukemia* 18, 1406-1412.
- El-Khatib M., Geara F., Haddadin M.J., Gali-Muhtasib H. (2010) Cell death by the quinoxaline dioxide DCQ in human colon cancer cells is enhanced under hypoxia and is independent of p53 and p21. *Radiation Oncology* 5, 107.
- Elmore S. (2007) Apoptosis: a review of programmed cell death. *Toxicologic Pathology* 35, 495 – 516.
- Fabricant D.S. and Farnsworth N.R. (2001) The Value of Plants Used in Traditional Medicine for Drug Discovery. *Environmental Health Perspectives* 109, 69-75.
- Farnsworth N.R., Akerele O., Bingel A.S., Soejarto D.D., Guo Z. (1985) Medicinal plants in therapy. *Bull WHO* 63, 965–981.
- Farnsworth N.R. (1990) The role of ethnopharmacology in drug development. *Ciba Found Symp* 154, 2–11.
- Farnsworth N.R. (1994) Ethnopharmacology and drug development. *Ciba Found Symp* 185, 42–51.
- Ferrari P., Jenab M., Norat T. (2007) Lifetime and baseline alcohol intake and risk of colon and rectal cancers in the European prospective investigation into cancer and nutrition (EPIC). *Int J Cancer* 121, 2065-2072.
- Fiorentino A., D'Abrosca B., Pacifico S., Mastellone C., Scognamiglio M., Monaco P. (2009) Identification and Assessment of Antioxidant Capacity of Phytochemicals from Kiwi Fruits. *Journal of Agricultural and Food Chemistry* 57(10), 4148-4155.
- Foo L., Lu Y., Molan A.L., Woodfield D.R., McNabb W.C. (2000) The phenols and prodelphinidins of white clover flowers. *Phytochemistry* 54(5), 539-548.
- Freeman H.J. (2008) Colorectal cancer risk in Crohn's disease. *Gastroenterol* 14(12), 1810-1811.
- Fulda S., Friesen C., Los M., Scaffidi C., Mier W., Benedict M., Nunez G., Krammer P.H., Peter M.E., Debatin K.M. (1997) Betulinic acid triggers CD95 and p53-independent apoptosis via activation of caspases in neuroectodermal tumors. *Cancer Research* 52, 4956-4964.
- Fulda S. (2008) Betulinic acid for cancer treatment and prevention. *Int. J. Mol. Sci.* 9, 1096-1107.
- Garcia M., Jemal A., Ward E.M., Center M.M., Hao Y., Siegel R.L., Thun M.J. (2007) Global Cancer Facts & Figures 2007. Atlanta, GA, American Cancer Society.
- Garrett M.D. (2001) Cell cycle control and cancer. *Current Science* 81, 515-522.
- Giovannucci E. and Wu K. (2006) Cancers of the colon and rectum. In: Schottenfeld D., Fraumeni J.F. *Cancer Epidemiology and Prevention*. New York, *Oxford University Press*, 809-829.
- Globocan: <http://globocan.iarc.fr/> 25.7.2011 (13.05h)

27. Grady W.M. (2004) Genomic instability and colon cancer. *Cancer Metast Rev*, 23(1-2), 11-27.
- Graves P.R., Yu L., Schwarz J.K., Gales J., Sausville E.A., O'Connor P.M., Piwnica-Worms H. (2000) The Chk1 Protein Kinase and the Cdc25C Regulatory Pathways Are Targets of the Anticancer Agent UCN-01. *The Journal of Biological Chemistry* 275, 5600-5606.
- Groden J., Thliveris A., Samowitz W., Carlson M., Gelbert L., Albertsen H. (1991) Identification and characterization of the familial adenomatous polyposis coli gene. *Cell* 66(3), 589-600.
- Guo J., Zhang P., Zhang Z. (2009) Studies on chemical constituents from bee-collected rape pollen. *Zhongguo Zhongyao Zazhi* 34(10), 1235-1237.
- Häcker G. (2000) The morphology of apoptosis. *Cell Tissue Research* 301, 5-17.
- Ham S.B., Kim Y.I., Kwon Y.S., Kim C.M. (1999) Compounds of the stem of *Clematis trichotoma*. *Saengyak Hakhoechi* 30(3), 301-305.
- Hanahan D. and Weinberg R.A. (2000) The hallmarks of cancer. *Cell* 100, 57-70.
- Harvey A. (2000) Strategies for discovering drugs from previously unexplored natural products. *DDT* 5, 294-300.
- Hemaiswarya S. and Doble M. (2006) Potential synergism of natural products in the treatment of cancer. *Phytotherapy Research* 20, 239-249.
- Hisamuddin I.M. and Yang V.W. (2004) Genetics of colorectal cancer. *Med Gen Med* 6(3), 13.
- Ho L.H., Taylor R., Dorstyn L. (2009) A tumor suppressor function for caspase 2. *Proc Natl Acad Sci* 106, 5336-5341.
- Hopkinscoloncancercenter - <http://hopkinscoloncancercenter.org> : 28.7.2011 (19.15h)
- <http://www.sigmaaldrich.com/life-science/your-favorite-gene-search/pathwayoverviews/cyclins-and-cell-cycle-regulation.html> 19.7.2011 (14.25h)
- http://www.biotium.com/product/product_info/Protocol/30001.pdf 21.7.2011 (9.10h)
- <http://www.hakeem-sy.com> 28.7.2011 (20.00h)
- Huang X., Tran T., Zhang L., Hatcher R., Zhang P. (2005) DNA damage induced MC is mediated by the Chk1 dependent mitotic exit DNA damage checkpoint. *Natl Acad Sci*. 102, 1065-1070.
- Hui S., Zhang X., Cai Y., Han W.L., Wang Y., Ye W. (2009) Study on chemical constituents of *Ilex rotunda* Thunb. *Linchan Huaxue Yu Gongye* 29(1), 111-114.
- Hyzy M., Bozko P., Konopa J., Skladanowski A. (2005) Antitumour imidazoacridone C-1311 induces cell death by mitotic catastrophe in human colon carcinoma cells. *Biochemical Pharmacology* 69, 801-809.
- IARC: <http://www.iarc.fr/> 25.7.2011 (12.45h)
- Ianzini F., Bertoldo A., Kosmacek E.A., Phillips S.L., Mackey M.A. (2006) Lack of p53 function promotes radiation-induced mitotic catastrophe in mouse embryonic fibroblast cells. *Cancer Cell Int* 6(11), 1-8.

Ianzini F., Domann F.E., Kosmacek E.A., Phillips S.L., Mackey M.A. (2007) Human glioblastoma U87MG cells transduced with a dominant negative p53 (TP53) adenovirus construct undergo radiation-induced mitotic catastrophe. *Radiat Res* 168, 183-192.

Ilyas M., Straub J., Tomlinson I.P., Bodmer W.F. (1999) Genetic pathways in colorectal and other cancers. *Eur J Cancer*, 35(14), 1986-2002.

Janumyan Y.M., Sansam C.G., Chattopadhyay A., Cheng N., Soucie E.L., Penn L.Z., Andrews D., Knudson C.M., Yang E. (2003) BCL XL and BCL 2 coordinately regulates apoptosis, cell cycle arrest and cell cycle entry. *EMBO J.* 22(20), 5459–5470.

Jass J.R. (2005) What's new in colorectal cancer. *Arch Pathol Lab Med* 129, 1380-1384.

Jemal A., Bray F., Center M.M., Ferlay J., Ward E., Forman D. (2011) Global Cancer Statistics. *Ca Cancer J Clin* 61, 69-90.

Jiang H., Reinhardt H.C., Bartkova J., Tommiska J., Blomqvist C., Nevanlinna H., Bartek J., Yaffe M.B., Hemann M.T. (2009) The combined status of ATM and p53 link tumor development with therapeutic response. *Genes & Development* 23, 1895-1909.

Johnsson P., Peerlkamp N., Kamal-Eldin A., Andersson R.E., Andersson R., Lundgren L.N., Aman P. (2002) Polymeric fractions containing phenol glucosides in flaxseed. *Food Chemistry* 76(2), 207-212.

Jun K.Y., Lee E.Y., Jung M.J., Lee O.H., Lee E.S., Choo H.Y.P., Na Y., Kwon Y. (2011) Synthesis, biological evaluation, and molecular docking study of 3-(3'-heteroatom substituted-2'-hydroxy-1'-propyloxy) xanthone analogues as novel topoisomerase II α catalytic inhibitor. *European Journal of Medicinal Chemistry* 46, 1964-1971.

Jung G.R., Kim K.J., Choi C.H., Lee T.B., Han S.I., Han H.K., Lim S.C. (2007) Effect of Betulinic acid on anticancer drug-resistant colon cancer cells. *Basic & Clinical Pharmacology & Toxicology* 101, 277-285.

Jurek D., Udilova N., Jozkowicz A., Nohl H., Marian B., Schulte-Hermann R. (2005) Dietary lipid hydroperoxides induce expression of vascular endothelial growth factor (VEGF) in human colorectal tumor cells. *Faseb J*, 19(1), 97-99.

Kaindl U., Eyberg I., Rohr-Udilova N., Heinzle C., Marian B. (2008) The dietary antioxidants resveratrol and quercetin protect cells from exogenous prooxidative damage. *Food Chem. Toxicol.* 46, 1320–1326.

Kainz K., Virtbauer J., Kählig H., Arion V., Donath O., Reznicek G., Marian B., Krenn L. (2001) Two unusual methylcyclopropane glucosides from *Metaxya rostrata*. *Helvetica Chimica Acta*, submitted.

Kaufmann S.H., Desnoyers S., Ottaviano Y., Davidson N.E., Poirier G.G. (1993). Specific proteolytic cleavage of poly (ADP-ribose) polymerase: an early marker of chemotherapy- induced apoptosis. *Cancer Res.* 53, 3976-3985.

Khamidullina E.A., Fedorov S.V., Medvedeva S.A. Low-molecular phenolic compounds from *Pinus sibirica* Du Tour. *Rastitel'nye Resursy* 40(2), 73-79.

Khan I.A., Erdelmeier C.A.J., Sticher O., Rali T. (1992) New phenolic glucosides from the leaves of *Eurya tigan*. *Journal of Natural Products* 55, 1270-1274.

Kiang L.C., Tho L.Y., Lim C.H., Lim Y.M., Shah S.A., Weber J.F. (2011) Synthesis and SAR study of prenylated xanthone analogues as HeLa and MDA-MB-231 cancer cell inhibitors. *Letters in Drug Design & Discovery* 8(6), 523-528.

Kim R. (2005) Unknotting the roles of BCL 2 and BCL XL in cell death. *Biochemical and Biophysical Research Communication* 333, 336-343.

Kinghorn A.D., Fransworth N.R., Soejarto D.D., Cordell G.A., Swanson S.T., Pezzuto J.M., Wani M.C., Wall M.E., Oberlies N.H., Kroll D.J., Kramer R.A., Rose W.C., Vite G.D., Fairchild C.R., Peterson R.W., Wild R. (2003) Novel strategies for the discovery of plant-derived anticancer agents. *Pharmaceutical Biology* 41, 53-67.

Kinzler K.W. and Vogelstein B. (1996) Lessons from hereditary colorectal cancer. *Cell* 87(2), 159-170.

Koehn F.E. and Carter G.T. (2005) The evolving role of natural products in drug discovery. *Nature Reviews* 4, 206-220.

Kufe D.W., Pollock R.E., Weichselbaum R.R. (2003) Oncogenes in the initiation and progression of neoplasia. *Holland-Frei Cancer Medicine*. 6th edition. Hamilton (ON): BC Decker.

Kurosaka K., Takahashi M., Watanabe N. and Kobayashi Y. (2003) Silent cleanup of very early apoptotic cells by macrophages. *Journal of Immunology* 171, 4672-4679.

Laoukili J., Alvarez M., Meijer L.A.T., Stahl M., Mohammed S., Kleij L., Heck A.J.R., Medema R.H. (2008) Activation of FoxM1 during G2 requires cyclin A/cdk-dependent relief of autoexpression by the FoxM1 N-terminal domain. *Molecular and cellular biology* 28, 3076-3087.

Laoukili J., Kooistra M.R.H., Bras A., Kauw J., Kerhoven R.M., Morrison A., Clevers H., Medema R.H. (2005) FoxM1 is required for execution of the mitotic programme and chromosome stability. *Nature Cell Biology* 7, 126-136.

Larsson S.C. and Wolk A. (2006) Meat consumption and risk of colorectal cancer: a meta-analysis of prospective studies. *Int J Cancer* 119(11), 2657-2664.

Lassus P., Opitz-Araya X., Lazebnik Y. (2002) Requirement for caspase-2 in stress-induced apoptosis before mitochondrial permeabilization. *Science* 297, 1352-1354.

Lee W.Y., Park J.H., Kim B.S., Han M.J. (1990) Chlorophyll derivatives extracted from silkworm excreta are specifically cytotoxic to tumor cells in vitro. *Yonsei Med J.* 31(3), 225-233.

Lens S.M.A., Wolthuis R.M.F., Klompma R., Kauw J., Agami R., Brummelkamp T., Kops K., Medema R.H. (2003) Survivin is required for a sustained spindle checkpoint arrest in response to lack of tension *The EMBO Journal* 22, 2934 – 2947.

Leist M. and Jaattela M. (2001) Four deaths and a funeral: from caspases to alternative mechanisms. *Nat. Rev. Mol. Cell Biol.* 2(8), 589-598.

Levesque A.A. and Eastman A. (2007) p53-based cancer therapies: Is defective p53 the Achilles heel of the tumor? *Carcinogenesis* 28, 13-20.

Li X., Xiong Z., Yu M., Lu X., Li F. (2009) High performance liquid chromatographic fingerprints of ethanol and cyclohexane extracts of *Rhizoma Drynariae* and quantitative analysis of index components based on principal component analysis. *Sepu* 27(4), 453-457.

Li N., Li X., Yang S. (2006) Chemical constituents of organic acid part from *Camptosorus sibiricus* Rupr. *Shenyang Yaoke Daxue Xuebao* 23(7), 427-429.

Li G., Chen Y. (1997) Study on the chemical constituents of *Cuscuta australis* R.Br. *Zhongguo Zhongyao Zazhi* 22(9), 548-550.

Lipton L. and Tomlinson I. (2006) The genetics of FAP and FAP-like syndromes. *Fam Cancer*, 5(3), 221-226.

- Liu S., Xiao Z., Feng R. (1992) Chemical constituents of *Drynaria propinqua* (Wall) J. Sm. *Zhongguo Zhongyao Zazhi* 17(12), 737-739.
- Lock R.B. and Stribinskiene L. (1996) Dual Modes of Death Induced by Etoposide in Human Epithelial Tumor Cells Allow Bcl-2 to Inhibit Apoptosis without Affecting Clonogenic Survival. *Cancer Research* 56, 4006-4012.
- Long Z.M., Wu L.J., Sun B.H., Huang J., Gao H.J. (2009) Chemical constituents from rernel of *Castanea mollissima* Blume (IV). *Shenyang Yaoke Daxue Xuebao* 26(8), 614-616.
- Lukas C., Bartkova J., Latella L., Falck J., Mailand N., Schroeder T., Sehested M., Lukas J., Bartek J. (2001) DNA damage-activated kinase Chk2 is independent of proliferation or differentiation yet correlates with tissue biology. *Cancer Res* 61, 4990-4993.
- Lynch H.T., Smyrk T., Lynch J.F. (1996) Overview of natural history, pathology, molecular genetics and management of HNPCC (Lynch Syndrome). *Int J Cancer* 69(1), 38-43.
- Mahabussarakam W., Kuaha K., Wilairat P., Taylor W.C. (2006) Prenylated Xanthoness as potential antiplasmodial substances. *Planta Medica* 72, 912-916.
- Makherjee A.K., Basu S., Sarkar N., Ghosh A.C. (2001) Advances in cancer therapy with plant based natural products. *Current Medicinal Chemistry* 8, 1467-1486.
- Mann J. (2002) Natural products in cancer chemotherapy: past, present and future. *Nature reviews* 2, 143-148.
- Mansilla S., Priebe W., Portugal J. (2006) Mitotic catastrophe results in cell death by caspase-dependent and caspase-independent mechanisms. *Cell Cycle* 5, 53-60.
- Markowitz S.D. and Bertagnolli M.M. (2009) Molecular basis of colorectal cancer. *N. Engl. J. Med* 361, 2449-2460.
- Markowitz S.D. and Roberts A.B. (1996) Tumor suppressor activity of the TGF-beta pathway in human cancers. *Cytokine Growth Factor Rev* 7(1), 93-102.
- Matsumoto K., Akao Y., Ohguchi K., Ito T., Tanaka T., Iinuma M., Nozawa Y. (2005) Xanthoness induce cell-cycle arrest and apoptosis in human colon cancer DLD-1 cells. *Bioorganic & Medicinal Chemistry* 13, 6064-6069.
- Matsuzaki Y., Kurokawa N., Terai S., Matsumura Y., Kobayashi N., Okita K. (1996) Inhibitory effects of the herbal medicine Sho-saiko-to (TJ-9) on cell proliferation and procollagen gene expressions in cultured rat hepatic stellate cells. *Jpn. J. Cancer Res.* 87, 170-177.
- McDonald E.R.III and Deiry W.S. (2000) Cell cycle control as a basis for cancer drug development. *Int. J. Oncol.* 84, 871.
- McTiernan A., Ulrich C., Slate S., Potter J. (1998) Physical activity and cancer etiology: associations and mechanisms. *Cancer Causes Control* 9(5), 487-509.
- Melino G., Knight R.A., Nicotera P. (2005) How many ways to die? How many different models of cell death? *Cell Death and Differentiation* 12, 1457-1462.
- Mimaki Y., Ishibashi N., Komatsu M., Sashida Y. (1991) Studies on the chemical constituents of *Gloriosa rothschildiana* and *Colchicum autumnale*. *Shoyakugaku Zasshi* 45(3), 255-260.
- Miyaki M., Seki M., Okamoto M. (1990) Genetic changes and histopathological types in colorectal tumors from patients with familial adenomatous polyposis. *Cancer Res* 50(22), 7166-7173.

- Miyashita T., Krajewski S., Krajewska M., Wang H.G., Lin H.K., Liebermann D.A. (1994) Tumor suppressor p53 is a regulator of bcl-2 and bax gene expression in vitro and in vivo. *Oncogene*, 9(6), 1799-1805.
- Molinar-Toribio E., Gonzalez J., Ortega-Barria E., Capson T.L., Coley P.D., Kursar T.A., McPhail K., Cubilla-Rios L. (2006) Antiprotozoal activity against *Plasmodium falciparum* and *Trypanosoma cruzi* of xanthenes isolated from *Chrysochlamys tenuis*. *Pharmaceutical Biology* 44(7), 550-553.
- Monache F.D., Botta B., Nicoletti M., de Barros Coelho J.S., de Andrade Lyra F.D. (1981) Three New Xanthenes and Macluraxanthone from *Rheedia benthamiana* Pl. Triana (Guttiferae). *J. Chem. Soc.* 1, 484-488.
- Morimoto S., Nonaka G.I., Nishioka I. (1987) Tannins and related compounds. Aesulitannins, novel proanthocyanidins with doubly-bonded structures from *Aesulus hippocastanum* L. *Chem. Pharm. Bull.* 35, 4717-4729.
- Mullauer F.B., Kessler J.H., Medema J.P. (2009) Betulinic acid induces cytochrome c release and apoptosis in a Bax/Bak-independent, permeability transition pore dependent fashion. *Apoptosis* 14, 191-202.
- Na Y. (2009) Recent cancer drug development with xanthone structures. *J. Pharm. Pharmacol.* 61, 707-712.
- Nagase H. and Nakamura Y. (1993) Mutations of the APC gene. *Hum Mutat* 2, 425-434.
- Nagy J.A., Chang S.H., Shih S.C., Dvorak A.M., Dvorak, H.F. (2010) Heterogeneity of the tumor vasculature. *Semin. Thromb. Hemost.* 36, 321-331.
- Nakagawa Y., Iinuma M., Naoe T., Nozawa Y., Akao Y. (2007) Characterized mechanism of α -mangostin-induced cell death: caspase-independent apoptosis with release of endonuclease-G from mitochondria and increased miR-143 expression in human colorectal cancer DLD-1 cells. *Bioorganic & Medicinal Chemistry* 15, 5620-5628.
- Narita M., Shimizu S., Ito T., Chittenden T., Lutz R. J., Matsuda H., Tsujimoto Y. (1998) Bax interacts with the permeability transition pore to induce permeability transition and cytochrome c release in isolated mitochondria. *Proc. Natl. Acad. Sci.* 95, 14681-14686.
- National Cancer Institute: <http://www.cancer.gov/> 25.7.2011 (19.15h)
- NDDIC (National digestive diseases information clearinghouse): <http://digestive.niddk.nih.gov/diseases/pubs/colitis/> 3.8.2011 (8.10h)
- Newman D.J., Cragg G.M., Snader K.M. (2003) Natural products as sources of new drugs over the period 1981-2002. *J. Nat. Prod.* 66, 1022-1037.
- Newman D.J., Cragg G.M., Snader K.M. (2000) The influence of natural products upon drug discovery. *Nat. Prod. Rep.* 17, 215-234.
- Newman D.J. and Cragg G.M. (2006) Natural products as sources of new drugs over the last 25 years. *J. Nat. Prod.* 70, 461-477.
- Ngan C.Y., Yamamoto H., Tagaki A., Fujie Y., Takemasa I., Ikeda M. (2008) Oxaliplatin induces mitotic catastrophe and apoptosis in esophageal cancer cells. *Cancer Sci* 99, 129-139.
- Ngoupayo J., Tabopda T.K., Ali M.S. (2009) Antimicrobial and immunomodulatory properties of prenylated xanthenes from twigs of *Garcinia staudtii*. *Bioorganic & Medicinal Chemistry* 17(15), 5688-5695.

Nguyen H., Lallemand M.C., Bouteffouchet S., Michel S., Tillequin F. (2009) Antitumor Psoropermum xanthones and Sarcomelicope acridones: privileged structures implied in DNA alkylation. *J. Nat. Prod.* 72, 527-539.

Nicholson D.W., All A., Thomberly N.A., Vaillancourt J.P., Ding C.K., Gallant M., Gareau Y., Griffin P.R., Labelle M., Lazebnik Y.A. (1995). Identification and inhibition of the ICE/CED-3 protease necessary for mammalian apoptosis. *Nature* 376, 37-43.

Nigg E.A. (1995) Cyclin-dependent protein kinases: key regulators of the eukaryotic cell cycle. *Bioessays* 17(6), 471–480.

Ning L., Xian L., Shilin Y. (2006) Chemical constituents of organic acid part from *Camptosorus sibiricus* Rupr. *Shenyang Yaoke Daxue Xuebao* 23(7), 427-429.

Niida H., Tsuge S., Katsuno Y., Konishi A., Takeda N., Nakanishi N. (2005) Depletion of Chk1 leads to premature activation of cdc2-cyclin B and mitotic catastrophe. *J. Biol. Chem* 280, 39246-39252.

Norbury C.J. and Hickson I.D. (2001) Cellular responses to DNA damage. *Annual Review of Pharmacology and Toxicology* 41, 367-401.

Nyandat E., Rwekika E., Galeffi C., Palazzino G., Nicoletti M.(1993) Olinioside, 5-(4'-O- α -D-glucopyranosyl)-caffeoxyloxy-5,6-dihydro-4-methyl-(2H)-pyran-2-one from *Olinia usambarensis*. *Phytochemistry* 33(6), 1493-1496.

Oltvai Z.N., Milliman C.L., Korsmeyer S.J. (1993) Bcl-2 heterodimerizes in vivo with a conserved homolog, Bax, that accelerates programmed cell death. *Cell*. 74, 609–619.

Pagano M, Pepperkok R, Verde F, Ansorge W & Draetta G (1992) Cyclin A is required at two pints in the human cell cycle. *EMBO Journal* 11, 961 - 971.

Pai S.I., Lin Y.Y., Macaes B., Meneshian A., Hung C.F.,Wu T.C. (2006) Prospects of RNA interference therapy for cancer. *Gene Therapy* 13, 464–477.

Patwardhan B. Drug Discovery and Development: Traditional Medicine and Ethnopharmacology Perspectives. *Ethnopharmacology and Traditional Medicine*: http://www.scitopics.com/Drug_Discovery_and_Development_Traditional_Medicine_and_Ethnopharmacology_Perspectives.html : 28.7.2011 (21.00h)

Peart M.J., Tainton K.M., Ruefli A.A., Dear A.E., Sedelies K.A., O'Reilly L.A., Waterhouse N.J., Trapani J.A., Johnstone R.W. (2003) Novel Mechanisms of Apoptosis Induced by Histone Deacetylase Inhibitors. *Cancer Research* 63, 4460 – 4471.

Pekarek B. (2003) Die Heilpflanzen in den Hausgärten von La Gamba. Diplomarbeit an der Universität für Bodenkultur.

Peng L., Nijhawan D., Wang X. (2004) Mitochondrial Activation of Apoptosis. *Commentary Cell* 116, 57-59.

Pizzolatti M.G., Brighente I.M.C., Bortoluzzi A.J., Schripsema J., Verdi L.G. (2007) Cyathenosin A, a spiropyranosyl derivative of protocathechuic acid from *Cyathea phalerata*. *Phytochemistry* 68(9), 1327-1330.

Portugal J., Mansilla S., Bataller M. (2010) Mechanisms of drug-induced mitotic catastrophe in cancer cells. *Current Pharmaceutical Design* 16, 69-78.

Qui Y.L., Ksebaty M.B., Ptak R.G., Fan B.Y., Breitenbach J.M., Lin J.S., Cheng Y.C., Kern E.R., Drach J.C., Zemlicka J. (1998) (Z)- and (E)-2-((Hydroxymethyl) cyclopropylidene) methyladenine

and –guanine. New nucleoside analogues with a broad-spectrum antiviral activity. *J. Med. Chem.* 41, 10-23.

Rath G., Potterat O., Mavi S., Hostettmann K. (1996) Xanthones from *Hypericum roeperanum*. *Phytochemistry* 43, 513-520.

Ragnhammar P., Hafström L., Nygren P., Glimelius B. (2001) A systematic overview of chemotherapy effects in colorectal cancer. *Acta Oncologica* 40, 282-308.

Rahier N.J., Thomas C.J., Hecht S.M. (2005) Camptothecin and its analogs. In: Cragg G.M., Kingston D.G.I., Newman D.J. Chapter 2 of: *Anticancer Agents from Natural Products*. Brunner-Routledge Psychology Press, Taylor & Francis Group, Boca Raton, FL, 5–22.

Rajamanickam S. and Agarwal R. (2008) Natural products and colon cancer: current status and future prospects. *Drug Development Research* 69, 460-471.

Raju U., Nakata E., Mason K.A., Kian Ang K., Milas L. (2003) Flavopiridol, a cyclin-dependent kinase inhibitor, enhances radiosensitivity of ovarian carcinoma cells. *Cancer Research* 63, 3263 - 3267.

Raquel A., Castanheiro A., Silva M., Campos N.A., Nascimento M.S., Pinto M.M. (2009) Antitumor Activity of Some Prenylated Xanthones. *Pharmaceuticals* 2, 33-43.

Reddy L., Odhav B., Bhoola K.D. (2003) Natural products for cancer prevention: a global perspective. *Pharmacology & Therapeutics* 99, 1-13.

Ren W., Qin L., Xu Y., Cheng N. (2010) Inhibition of betulinic acid to growth and angiogenesis of human colorectal cancer cell in nude mice. *Chinese-German Journal of Clinical Oncology* 9, 153-157.

Renzi L., Gersch M.S., Campell M.S., Wu L., Osmani S.A., Gorbsky G.J. (1997) MPM-2 antibody-reactive phosphorylations can be created in detergent-extracted cells by kinetochore-bound and soluble kinases. *Journal of Cell Science* 110, 2013-2025.

Richter M., Ebermann R., Marian B. (1999) Quercetin-induced apoptosis in colorectal tumor cells : possible role of EGF receptor signaling. *Nutrition and Cancer* 34 (1), 88-99.

Rivier L., Bruhn J. (1979) Editorial. *J Ethnopharmacol* 1 (1979).

Roninson I.B., Broude E.V., Chang B.D. (2001) If not apoptosis, then what? Treatment-induced senescence and mitotic catastrophe in tumor cells. *Drug Resist Updat* 4, 303 – 313.

Ross P.J., George M., Cunningham D., DiStefano F., Jervoise H., Andreyev N., Workman P., Clarke P.A. (2001) Inhibition of Kirsten-ras Expression in Human Colorectal Cancer Using Rationally Selected Kirsten-ras Antisense Oligonucleotides. *Molecular Cancer Therapeutics* 1, 29-41.

Ruth A.C. and Roninson I.B. (2000) Effects of the Multidrug Transporter P-Glycoprotein on Cellular Responses ionizing Radiation. *Cancer Research* 60, 2576 –2578.

Rybak R.J., Hartline C.B., Qui Y.L., Zemlicka J., Harden E., Marshall G., Sommadossi J.P., Kern E.R. (2000) In vitro activities of methylenecyclopropane analogues of nucleosides and their phosphoalaninate prodrugs against cytomegalovirus and other herpesvirus infections. *Antimicrobial Agents and Chemotherapy* 44, 1506-1511.

Sakai S., Kawaguchi K., Kamakura H., Kawahara N., Goda Y. (2007) Characterization of major components in *Crataegus oxyacantha* L. leaves and analyses of the leaves and commercial hawthorn leave products. *Nippon Shokuhin Kagaku Gakkaishi* 14(2), 56-62.

Sanchez I. and Dynlacht B.D. (2005) New insights into cyclins, CDKs, and cell cycle control. *Seminars in Cell and Developmental Biology* 16, 311 - 321.

Sanchez Y., Wong C., Thoma R.S., Richman R., Wu Z., Piwnica-Worms H., Elledge S.J. (1997) Conservation of the Chk1 Checkpoint Pathway in Mammals: Linkage of DNA Damage to Cdk Regulation Through Cdc25. *Science* 277, 1497-1501.

Saraste A. and Pulkki K. (2000) Morphologic and biochemical hallmarks of apoptosis. *Cardiovasc Res* 45(3), 528-537.

Schölmerich J.S.W. (2005) Leitfaden kolorektales Karzinom - Prophylaxe, Diagnostik, Therapie. 2. Auflage ed. Bremen, UNI-MED Verlag AG.

Schreibman I.R. and Baker M. The hamartomatous polyposis syndroms : a clinical and molecular review. *Am J Gastroenterol* 100, 476-490.

Schulte-Hermann R.P.W. (2004) Mehrstufenprozess der Kanzerogenese und chemische Kanzerogenese. In: Hiddemann W.H.H, Bartram C., Die Onkologie. Heidelberg: Springer-Verlag 193-240.

Schwartz K. and Shah M.A. (2005) Targeting the cell cycle: a new approach to cancer therapy. *Journal of Clinical Oncology* 23, 9408 - 9421.

Shin S., Sung B.J., Cho Y.S., Kim H.J., Ha N.C., Hwang J.I., Chung C.W., Jung Y.K., Oh B.H. (2001) An anti-apoptotic protein human survivin is a direct inhibitor of caspase 3 and 7. *Biochemistry* 40, 1117-1123.

Shang X., Li C., Zhang C., Yang Y., Shi J. (2006) Non-alkaloid constituents from a Tibetan medicine *Meconopsis quintuplinervia*. *Zhongguo Zhongyao Zazhi* 31(6), 468-471.

Shaw R.J. and Cantley L.C. (2006) Ras, PI(3)K and mTOR signalling controls tumour cell growth. *Nature* 441,424-430.

Shen R., Wang P., Tang N. (2010) Cytotoxic activity and DNA-binding properties of xanthone derivatives. *J. Fluoresc.* 20, 1287-1297.

Shu Y.Z. (1998) Recent natural product based drug development: a pharmaceutical industry perspective. *J. Nat. Prod.* 61, 1053-1071.

Sidi S., Sanda T., Kennedy R.D. (2008) Chk1 suppresses a caspase 2 apoptotic response to DNA damage that bypasses p53, BCL 2 and caspase 3. *Cell* 133, 864-877.

Silva G.L., Lee I.S., Kinghorn A.D. (1998) Special problems with the extraction of plants. *Methods Biotechnol.* 4, 343-363.

Simpson S.H. (1988) Some preliminary considerations on the sobada: a traditional treatment for gastrointestinal illness in Costa Rica. *Social Science & Medicine* 27, 69-73.

Sinha R., Rothman N., Brown E.D. (1995) High concentrations of the carcinogen 2-amino-1-methyl-6-phenylimidazo-[4,5-b]pyridine (PhIP) occur in chicken but are dependent on the cooking method. *Cancer Res* 55, 4516-4519.

Sinha R., Rothman N., Salmon C.P. (1998) Heterocyclic amine content in beef cooked by different methods to varying degrees of doneness and gravy made from meat drippings. *Food Chem Toxicol* 36, 279-287.

Sinha R., Peters U., Cross A.J. (2005) Meat, Meat Cooking Methods and Preservation, and Risk for Colorectal Adenoma. *Cancer Res* 65, 8034-8041.

Singh R., George J., Shukla Y. (2010) Role of senescence and mitotic catastrophe in cancer therapy. *Cell Division* 5:4.

- Skog K. (1993) Cooking procedures and food mutagens: a literature review. *Food Chem Toxicol* 31, 655–675.
- Smiley S.T., Reers M., Mottola-Hartshorn C., Lin M., Chen A., Smith T.W., Steele G.D., Chen L. B. (1991) Intracellular heterogeneity in mitochondrial membrane potentials. *Proc. Natl. Acad. Sci.* 88, 3671-3675.
- Solecki R. and Shanidar I.V. (1975) A Neanderthal flower burial in northern Iraq. *Science* 190, 880–881.
- Son S., Lewis B. (2001) Free radical scavenging and antioxidative activity of caffeic acid and its derivatives. Abstracts of Papers, 221st American Chemical Society National Meeting, San Diego, United States, April 1-5, 2001
- Sook K.H., Hyun A.J., Min B.S., Jung J.H., Choi J.S. (2010) Isolation of Phenolics, Nucleosides, Saccharides and an Alkaloid from the root of *Aralia cordata*. *Natural Product Sciences* 16(1), 20-25.
- Soriano M.E. and Scorrano L. (2011) Traveling BAX and Forth from mitochondria to control apoptosis. *Cell* 145, 15-17.
- Sporn M.B. (1996) The war on cancer. *Lancet* 347, 1377-1381.
- Statistik Austria: http://www.statistik.at/web_de/statistiken/gesundheit/todesursachen/-todes ursachen_im_ueberblick/index.html 27.7.2011 (12.15h)
- Stratton M.R., Campbell P.J. and Futreal P.A. (2009) The cancer genome. *Nature* 458, 719-724.
- Stracker T.H., Usui T., Petrini J.H.J. (2009) Taking the time to make important decisions: the checkpoint effector kinases Chk1 and Chk2 and the DNA-damage response. *DNA repair* 8, 1047-1054.
- Su B.N., Pawlus A.D., Jung H.A., Keller W.J., McLaughlin J.L., Kinghorn A.D. (2005) Chemical Constituents of the Fruits of *Morinda citrifolia* (Noni) and Their Antioxidant Activity. *Journal of Natural Products* 68, 592-595.
- Suksamrarn S., Suwannapoch N., Phakhodee W., Thanuhiranlert J., Ratananukul P., Chimnoi N., Suksamrarn A. (2003) Antimycobacterial activity of prenylated xanthenes from the fruits of *Garcinia mangostana*. *Chem Pharm Bull* 51, 857-859.
- Takayama T., Miyanishi K., Hayashi T., Sato Y., Niitsu Y. (2006) Colorectal cancer: genetics of development and metastasis. *J. Gastroenterol* 41, 185–192.
- Tao W. (2005) The Mitotic Checkpoint in Cancer Therapy. *Cell Cycle* 4, 1495-1499.
- Tapia-Alveal C., Calonge T.M., O’Connell M.J. (2009) Regulation of Chk 1. *Cell Div.* 4, 1-7.
- Taraphdar A.K., Roy M., Bhattacharya R.K. (2001) Natural products as inducers of apoptosis: implication for cancer therapy and prevention. *Current Science* 80, 1387-1396.
- Terahara N., Saito N., Honda T., Toki K., Osajima Y. (1990) Acylated anthocyanins of *Clitoria ternatea* flowers and their acyl moieties. *Phytochemistry* 29(3), 949-953.
- Thomsom A.B.R. and Shaffer E.A. editors. (1994) First principles of gastroenterology. Janssen-Ortho, 5th edition.
- Tian J.K., Sun F., Cheng Y.Y. (2005) Chemical constituents from the roots of *Ranunculus ternatus*. *Journal of Asian Natural Products Research* 8(1-2), 35-39.

Tshikalange T.E., Meyer J.J.M., Lall N., Munoz E., Sancho R., Van de Venter M., oosthuizen V. (2008) In vitro anti-HIV-1 properties of ethnobotanically selected South African plants used in the treatment of sexually transmitted diseases. *Journal of Ethnopharmacology* 119, 478-481.

Uchida H., Kodama E.N., Yoshimura K., Maeda Y., Kosalaraska P., Maroun V., Qui Y.L., Zemlicka J., Mitsuya H. (1999) In vitro anti-human immunodeficiency virus activities of Z- and E-methylenecyclopropane nucleoside analogues and their phospho-L-Alaninate Diesters. *Antimicrobial Agents and Chemotherapy* 43, 1487-1490.

Ueda M. and Takada A. (2003) Preparation of β -D-pyranosyl-trans-p-coumaric acid derivatives as herbicides and intermediates thereof and method for their preparation. Kokai Tokyo Koho, Patent written in Japanese.

Yam C.H., Fung T.K., Poon R.Y.C. (2002) Cyclin A in cell cycle control and cancer. *Cell. Mol. Life Sci.* 59, 1317-1326.

Yamane K., Schupp J.E., Kinsella T.J. (2007) BRCA1 activates a G2/M cell cycle checkpoint following 6-thioguanine induced DNA mismatch damage. *Cancer Res.* 67, 6286-6292.

Yang L., Wang M., Zhao Y., Tu Y. (2004) Studies on chemical constituents in rhizome of *Matteuccia struthiopteris*. *Zhongguo Zhongyao Zazhi* 29(7), 647-649.

Yin H., Fu H., Hua H., Pei Y. (2006) Chemical constituents of *Saussurea lappa* C.B Clarke. *Shenyang Yaoke Daxue Xuebao* 23(10), 641-645.

Yingxue L., Zhonggang L., Lan S., Ruiping Y., Dongfang H., Yuehu P. (2009) Chemical constituents from *Scutellaria baicalensis* Georgi. *Zhongguo Yaowu Huaxue Zazhi* 19(1), 59-62.

Yogeewari P. and Sriram D. (2005) Betulinic Acid and Its Derivatives: A Review on their Biological Properties. *Current Medicinal Chemistry* 12, 657- 666.

Yuan J., Yan R., Krämer A., Eckerdt F., Roller M., Kaufmann M., Strebhardt K. (2004) Cyclin B1 depletion inhibits proliferation and induces apoptosis in human tumor cells. *Oncogene* 23, 5843-5852.

Zaffaroni N., Pannati M., Diadone M.G. (2005) Survivin as a target for new anticancer interventions. *Journal of Cellular and Molecular Medicine* 9, 360-372

Zhang H.Y., Gu Y.Y., Li Z.G., Jia Y.H., Yuan L., Li S.H., An G.S., Ni J.H., Jia H.T. (2004) Exposure of Human Lung Cancer Cells to 8-Chloro-Adenosine Induces G2/M Arrest and Mitotic Catastrophe. *Neoplasia* 1-11.

Zhao J., Pawar R.S., Ali Z., Khan I.A. (2007) Phytochemical Investigation of *Turnera diffusa*. *J. Nat. Prod.* 70(2), 289-292.

Zhen H.N., Li L.W., Zhang W., Fei Z., Shi C.H., Yang T.T. (2007) Short hairpin RNA targeting survivin inhibits growth and angiogenesis of glioma U251 cells. *Int J Oncol.* 31, 1111-1117.

Zhou Y.Z., Chen H., Qiao L., Xu N., Cao J.Q., Pei Y.H. (2008) Two new compounds from *Carthamus tinctorius*. *Journal of Asian Natural Products Research* 10(5), 429-433.

Zhu T.F., Huang K.Y., Deng X.M., Zhang Y., Xiang H., Gao H.Y., Wang D.C. (2008) Three new caffeoyl glycosides from the roots of *Picrorhiza scrophulariiflora*. *Molecules* 13(4), 729-735.

Zhu W., Yin C., Wang S., Zuo G., Hao X. (2001) Chemical constituents of *Porana spectabilis* Kurz. *Tianran Chanwu Yanjiu Yu Kaifa* 13(5), 1-4.

Zou X., Liang J., Ding L., Peng S. (2006) Studies on chemical constituents of *paederia scandense*. *Zhongguo Zhongyao Zazhi* 31(17), 1436-1441.

- Zuco V., Supino R., Righetti S.C., Cleris L., Marchesi E., Gambacorti-Passerini C., Formelli F. (2001) Selective cytotoxicity of betulinic acid on tumor cell lines, but not on normal cells. *Cancer Letters* 175, 17-25.
- Vakifahmetoglu H., Olsson M., Zhivotovsky B. (2008) Death through a tragedy: mitotic catastrophe. *Cell Death and Differentiation* 15, 1153-1162.
- Vakifahmetoglu-Norberg H. and Zhivotovsky B. (2010) The unpredictable caspase 2: what can it do? *Trends in Cell Biology* 20(3), 150-159.
- Van Cruchten S. and Van Den Broeck W. (2002) Morphological and biochemical aspects of apoptosis, oncosis and necrosis. *Anat Histol Embryol* 31(4), 214-223.
- Vermeulen K., Van Bockstaele D.R., Berneman Z.N. (2003) The cell cycle: a review of regulation, deregulation and therapeutic targets in cancer. *Cell Prolif.* 36, 131-149.
- Virtbauer J. (2007) Bioassay-guided chemische Untersuchungen von tropischen Arzneipflanzen. Dissertation an der Universität Wien.
- Virtbauer J., Krenn L., Kählig H., Hüfner A., Donath O., Marian B. (2008) Chemical and pharmacological investigation of *Metaxya rostrata*. *Zeitschrift für Naturforschung* 63c, 469-475.
- Vogelstein B., Fearon E.R., Hamilton S.R., Kern S.E., Preisinger A.C., Leppert M., Nakamura Y., White R., Smits A.M., Bos J.L. (1988) Genetic alterations during colorectal-tumor development. *N Engl J Med* 319(9),525-532.
- Wall M.E., Wani M.C., Brown D.M., Fullas F., Olwald J.B., Josephson F.F. (1996) Effect of tannins on screening of plant extracts for enzyme inhibitory activity and techniques for their removal. *Phytomedicine* 3, 281-285.
- Walworth N., Davey S., Beach D. (1993) Fission yeast chk 1 protein kinase links the rad checkpoint pathway to cdc2. *Nature* 363, 368-371.
- Watanapokasin R., Jarinthan F., Jerusalmi A., Suksamrarn S., Nakamura Y., Sukserree S., Uthaisang-Tanethpongtham W., Ratananukul P., Sano T. (2010) Potential of xanthenes from tropical fruit mangosteen as anti-cancer agents: caspase-dependent apoptosis induction in vitro and in mice. *Appl. Biochem. Biotechnol.* 162, 1080-1094.
- Wei Y., Yu L., Bowen J., Gorovsky M.A., Allis C.D. (1999) Phosphorylation of histone H3 is required for proper chromosome condensation and segregation. *Cell* 97, 99–109.
- Weinberg R.A. (2007) The biology of cancer. New York, Garland Science.
- Weitz J.S.A., Kadmon M., Eble M.J., Herfarth C. (2004) Kolon- und Rektumkarzinoma. In: Hiddemann W.H.H, Bartram C. Die Onkologie. Heidelberg, Springer Verlag.
- White R.L. (1998) Tumor suppressing pathways. *Cell* 92(5), 591-592.
- WHO: <http://www.who.int/cancer/> 25.7.2011 (15.00h)
- Williams D.H., Stone M.J., Hauck P.R., Rahman S.K. (1989) Why are secondary metabolites (natural products) biosynthesized? *J. Nat. Prod.* 52, 1189-1208.
- Winter M., Herrmann K. (1984) Analysis of hydroxycinnamic acid esters and their glucosides by reversed-phase high-performance liquid chromatography after polyamide separation. *Journal of Chromatography* 315, 243-51.
- Wonsey D.R. and Follettie M.T. (2005) Loss of the forkhead transcription factor Fox M1 causes centrosome amplification and mitotic catastrophe. *Cancer Research* 65, 5181-5189.

Bibliography

Wu X., Cao S., Goh S., Hsu A., Tan B.K.H. (2001) Mitochondrial destabilisation and caspase-3 activation are involved in the apoptosis of jurkat cells induced by Gaudichaudiaone A, a cytotoxic xanthone. *Planta Med.* 68, 198-203.

Zbuk K.M. and Eng C. (2007) Hamartomatous Polyposis Syndromes. *Nat Clin Pract Gastroenterol Hepatol* 4(9), 492-502.

Zielonke N. (2010) Krebsinzidenz und Krebsmortalität in Österreich. Statistik Austria.

URHEBERRECHT

Ich habe mich bemüht, sämtliche Inhaber der Bildrechte ausfindig zu machen und ihre Zustimmung zur Verwendung der Bilder in dieser Arbeit eingeholt. Sollte dennoch eine Urheberrechtsverletzung bekannt werden, ersuche ich um Meldung bei mir.

Kerstin Kainz

10 Supplementary Information

Content	Page
<i>Compound KK1</i> : (1R,2E)-2-(6-hydroxyhexyliden)cyclopropyl- β -D-glucopyranoside – X-ray	S2
Figure S1 : ORTEP plot of compound KK1 (50% probability ellipsoids)	S2
Table S1 : Atomic coordinates for non-hydrogen atoms of compound KK1	S3
Table S2 : Bond lengths for compound KK1 (Å)	S3
Table S3 : Bond angles for compound KK1 (°)	S4
Table S4 : Torsion angles for compound KK1 (Å)	S6
Figure S2 : ^1H NMR spectrum of compound KK1 (CD_3OD , 600.13 MHz)	S8
Figure S3 : ^{13}C NMR spectrum (ATP) of compound KK1 (CD_3OD , 150.92 MHz)	S9
Figure S4 : (ge)-DQF-COSY spectrum of compound KK1 (CD_3OD)	S10
Figure S5 : TOCSY spectrum (100 ms MLEV-17 spinlock) of compound KK1 (CD_3OD)	S10
Figure S6 : (ge)-HSQC spectrum (multiplicity edited) of compound KK1 (CD_3OD)	S11
Figure S7 : (ge)-HMBC spectrum of compound KK1 (CD_3OD)	S11
Figure S8 : NOESY spectrum (800 ms mixing time) of compound KK1 (CD_3OD)	S12
Figure S9 : Experimental and calculated ^1H NMR spectra of compound KK1	S11
<i>Compound KK5</i> : (6E)-6[(2R)-2-(β -D-glucopyranosyloxy)cyclopropylidene]hexanoic acid	S13
Figure S10 : ^1H NMR spectrum of compound KK5 (CD_3OD , 600.13 MHz)	S14
Figure S11 : Overlay ^1H NMR spectra of compounds KK1 and KK5	S15
Figure S12 : ^{13}C NMR spectrum (ATP) of compound KK5 (CD_3OD , 150.92 MHz)	S16
Figure S13 : (ge)-DQF-COSY spectrum of compound KK5 (CD_3OD)	S17
Figure S14 : (ge)-HSQC spectrum (multiplicity edited) of compound KK5 (CD_3OD)	S17
Figure S15 : (ge)-HMBC spectrum of compound KK5 (CD_3OD)	S18
Figure S16 : NOESY spectrum (800 ms mixing time) of compound KK5 (CD_3OD)	S18
Figure S17 : Structures of compounds KK3 , KK6 and KK7	S19
Table S5 : ^1H NMR (600.13 MHz) and ^{13}C NMR (150.92 MHz) Data of KK3 , KK6 and KK7	S19
Figure S18 : (ge)-HSQC spectrum (multiplicity edited) of compound KK3 (CD_3OD)	S20
Figure S19 : (ge)-HSQC spectrum of compound KK6 (sample not pure; CD_3OD)	S20
Figure S20 : (ge)-HSQC spectrum (multiplicity edited) of compound KK7	S21
<i>Structures of compound XB – 2-deprenyl-rheediaxanthone B</i>	S21
MS-analysis of compound XB	S21
Figure S21 : ^{13}C NMR spectrum (ATP) of compound XB (CD_3OD , 150.92 MHz)	S23
Figure S22 : ^1H NMR spectrum of compound XB (CD_3OD , 600.13 MHz)	S24
Figure S23 : (ge)-HSQC spectrum (multiplicity edited) of compound XB (CD_3OD)	S25
Figure S24 : (ge)-HMBC spectrum of compound XB (CD_3OD)	S25
Figure S25 : (ge)-DQF-COSY spectrum of compound XB (CD_3OD)	S26
Figure S26 : NOESY spectrum (800 ms mixing time) of compound XB (CD_3OD)	S26
	S1

Experimental Procedures

All NMR spectra were recorded on a Bruker Avance DRX 600 NMR spectrometer using a 5 mm switchable quadrupole probe (QNP, ^1H , ^{13}C , ^{19}F , ^{31}P) with z axis gradients and automatic tuning and matching accessory. The resonance frequency for ^1H NMR was 600.13 MHz, for ^{13}C NMR 150.92 MHz. All measurements were performed for a solution in fully deuterated methanol at 298 K. Standard 1D and gradient-enhanced (ge) 2D experiments, like double quantum filtered (DQF) COSY, TOCSY, NOESY, HSQC, and HMBC, were used as supplied by the manufacturer. Chemical shifts are referenced internally to the residual, non-deuterated solvent signal for ^1H ($\delta = 3.31$ ppm) or to the carbon signal of the solvent for ^{13}C ($\delta = 49.00$ ppm). The analysis of the ^1H – ^1H coupling constants (given in Hertz) were supported by the program Spin-Works (provided by Kirk Marat, University of Manitoba, Canada).

Single crystal X-ray structure analysis was performed on a Bruker X8 APEXII CCD diffractometer with graphite-monochromated $\text{MoK}\alpha$ radiation, $\lambda = 0.71073$ Å.

Compound KK1: (1R,2E)-2-(6-hydroxyhexyliden)cyclopropyl- β -D-glucopyranoside

X-ray: $\text{C}_{15}\text{H}_{26}\text{O}_7$, $M_r = 318.36$, monoclinic, space group $P2_1$ (no.4), $a = 9.5033(10)$, $b = 8.4361(13)$, $c = 20.625(3)$ Å, $V = 1631.5(4)$ Å³, $Z = 4$, $\rho_{\text{calc}} = 1.296$ g/cm³, $\mu = 0.102$ mm⁻¹

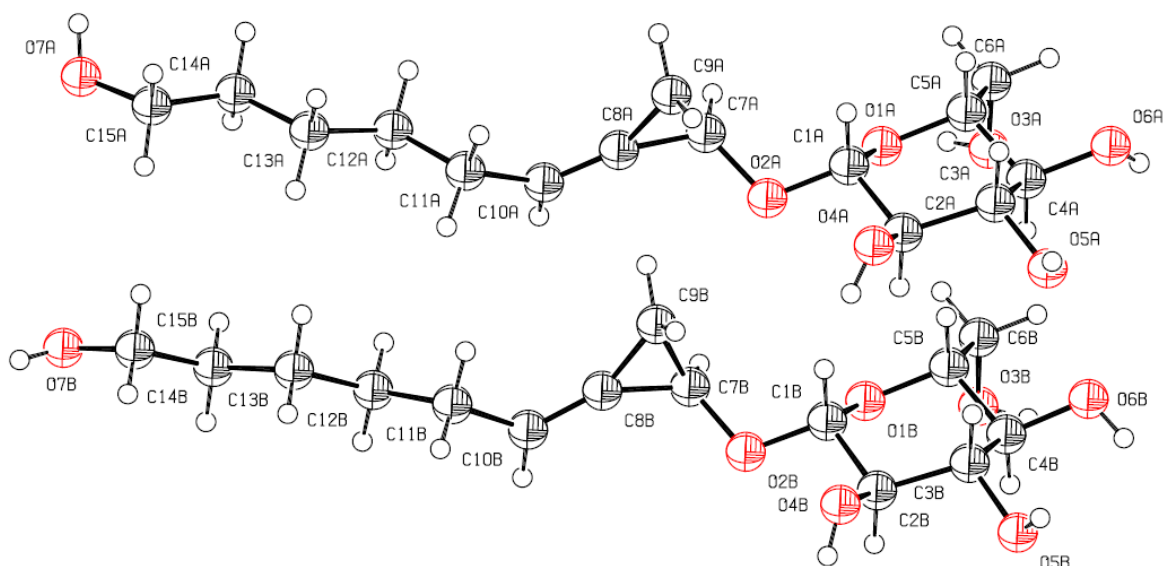


Figure S1: ORTEP plot of compound KK1 (50% probability ellipsoids)

Table S1: Atomic coordinates for non-hydrogen atoms of compound **KK1**

Atom	x	y	z	Atom	x	y	z
O1A	0.58862	0.65502	0.82777	O1B	1.07454	0.60611	0.82215
O2A	0.56711	0.48067	0.74237	O2B	1.05703	0.44365	0.73272
O3A	0.75310	0.88307	0.90807	O3B	1.23613	0.82009	0.90726
O4A	0.52487	0.22582	0.82940	O4B	1.01612	0.17673	0.81073
O5A	0.63917	0.28790	0.96403	O5B	1.13081	0.22115	0.94854
O6A	0.59558	0.60311	1.00604	O6B	1.06551	0.53600	0.99626
O7A	0.24219	0.54544	0.20564	O7B	0.76214	0.49866	0.19955
C1A	0.53009	0.50609	0.80457	C1B	1.01767	0.45898	0.79491
C2A	0.59325	0.37170	0.84982	C2B	1.08204	0.32017	0.83707
C3A	0.56980	0.40628	0.92038	C3B	1.05615	0.34309	0.90798
C4A	0.62744	0.56906	0.94172	C4B	1.10581	0.50730	0.93363
C5A	0.55695	0.69308	0.89196	C5B	1.03768	0.63527	0.88592
C6A	0.60371	0.86117	0.90854	C6B	1.08558	0.80187	0.90626
C7A	0.47106	0.55643	0.69196	C7B	0.98088	0.54991	0.68635
C8A	0.44815	0.48762	0.62586	C8B	0.93853	0.49324	0.61913
C9A	0.33337	0.46897	0.66537	C9B	0.82481	0.51268	0.65918
C10A	0.49120	0.47147	0.56871	C10B	0.97676	0.44693	0.56309
C11A	0.40738	0.39557	0.50841	C11B	0.87602	0.38886	0.50431
C12A	0.38125	0.50916	0.44971	C12B	0.88949	0.47948	0.44148
C13A	0.31746	0.42537	0.38579	C13B	0.79374	0.41242	0.38028
C14A	0.29584	0.53501	0.32601	C14B	0.82110	0.48914	0.31656
C15A	0.25054	0.44436	0.26260	C15B	0.72917	0.42027	0.25611

Table S2: Bond lengths for compound **KK1** (Å)

Bond	Length	Bond	Length
O1A-C1A	1.4249	O1B-C1B	1.4316
O1A-C5A	1.4409	O1B-C5B	1.4363
O2A-C1A	1.4008	O2B-C7B	1.4201
O2A-C7A	1.4191	O2B-C1B	1.3993
O3A-C6A	1.4333	O3B-C6B	1.4358
O4A-C2A	1.4231	O4B-C2B	1.4287
O5A-C3A	1.4316	O5B-C3B	1.4382
O6A-C4A	1.4369	O6B-C4B	1.4265
O7A-C15A	1.4433	O7B-C15B	1.4196
O3A-H3A	0.8400	O3B-H3B	0.8400
O4A-H4A	0.8400	O4B-H4B	0.8400
O5A-H5A	0.8400	O5B-H5B	0.8400
O6A-H6A	0.8400	O6B-H6B	0.8400
O7A-H7A	0.8400	O7B-H7B	0.8400
C1A-C2A	1.5279	C1B-C2B	1.5260
C2A-C3A	1.5356	C2B-C3B	1.5343
C3A-C4A	1.5169	C3B-C4B	1.5298
C4A-C5A	1.5405	C4B-C5B	1.5316
C5A-C6A	1.5086	C5B-C6B	1.5154
C7A-C9A	1.5244	C7B-C9B	1.5304
C7A-C8A	1.4651	C7B-C8B	1.4598

Supplementary Information

C8A-C10A	1.3161	C8B-C10B	1.3256
C8A-C9A	1.4724	C8B-C9B	1.4723
C10A-C11A	1.5063	C10B-C11B	1.4996
C11A-C12A	1.5323	C11B-C12B	1.5278
C12A-C13A	1.5314	C12B-C13B	1.5387
C13A-C14A	1.5282	C13B-C14B	1.5247
C14A-C15A	1.5157	C14B-C15B	1.5169
C1A-H1A	1.0000	C1B-H1B	1.0000
C2A-H2A	1.0000	C2B-H2B	1.0000
C3A-H3A	1.0000	C3B-H3B	1.0000
C4A-H4A	1.0000	C4B-H4B	1.0000
C5A-H5A	1.0000	C5B-H5B	1.0000
C6A-H6A1	0.9900	C6B-H6B1	0.9900
C6A-H6A2	0.9900	C6B-H6B2	0.9900
C7A-H7A	1.0000	C7B-H7B	1.0000
C9A-H9A1	0.9900	C9B-H9B1	0.9900
C9A-H9A2	0.9900	C9B-H9B2	0.9900
C10A-H10A	0.9500	C10B-H10B	0.9500
C11A-H11A1	0.9900	C11B-H11B1	0.9900
C11A-H11A2	0.9900	C11B-H11B2	0.9900
C12A-H12A1	0.9900	C12B-H12B1	0.9900
C12A-H12A2	0.9900	C12B-H12B2	0.9900
C13A-H13A1	0.9900	C13B-H13B1	0.9900
C13A-H13A2	0.9900	C13B-H13B2	0.9900
C14A-H14A1	0.9900	C14B-H14B1	0.9900
C14A-H14A2	0.9900	C14B-H14B2	0.9900
C15A-H15A1	0.9900	C15B-H15B1	0.9900
C15A-H15A2	0.9900	C15B-H15B2	0.9900

Table S3: Bond angles for compound **KK1** (°)

Atoms	Angle	Atoms	Angle
C1A-O1A-C5A	112.12	C1B-O1B-C5B	112.03
C1A-O2A-C7A	112.00	C1B-O2B-C7B	112.09
C6A-O3A-H3A	109.00	C6B-O3B-H3B	109.00
C2A-O4A-H4A	109.00	C2B-O4B-H4B	109.00
C3A-O5A-H5A	109.00	C3B-O5B-H5B	109.00
C4A-O6A-H6A	109.00	C4B-O6B-H6B	109.00
C15A-O7A-H7A	109.00	C15B-O7B-H7B	109.00
O2A-C1A-C2A	108.27	O2B-C1B-C2B	108.02
O1A-C1A-O2A	107.46	O1B-C1B-O2B	107.44
O1A-C1A-C2A	110.86	O1B-C1B-C2B	110.55
C1A-C2A-C3A	109.56	C1B-C2B-C3B	109.57
O4A-C2A-C1A	110.23	O4B-C2B-C1B	108.84
O4A-C2A-C3A	108.37	O4B-C2B-C3B	109.93
C2A-C3A-C4A	110.23	C2B-C3B-C4B	110.82
O5A-C3A-C2A	109.91	O5B-C3B-C2B	108.90
O5A-C3A-C4A	109.96	O5B-C3B-C4B	110.57
C3A-C4A-C5A	108.91	C3B-C4B-C5B	109.98
O6A-C4A-C3A	109.18	O6B-C4B-C3B	110.71

Supplementary Information

O6A-C4A-C5A	110.19	O6B-C4B-C5B	108.33
C4A-C5A-C6A	114.03	C4B-C5B-C6B	113.54
O1A-C5A-C4A	109.12	O1B-C5B-C4B	109.09
O1A-C5A-C6A	108.66	O1B-C5B-C6B	107.78
O3A-C6A-C5A	112.04	O3B-C6B-C5B	110.92
C8A-C7A-C9A	58.97	C8B-C7B-C9B	58.94
O2A-C7A-C9A	117.24	O2B-C7B-C9B	118.32
O2A-C7A-C8A	118.94	O2B-C7B-C8B	117.67
C7A-C8A-C10A	148.61	C7B-C8B-C10B	148.46
C7A-C8A-C9A	62.53	C7B-C8B-C9B	62.92
C9A-C8A-C10A	148.30	C9B-C8B-C10B	148.47
C7A-C9A-C8A	58.50	C7B-C9B-C8B	58.14
C8A-C10A-C11A	125.72	C8B-C10B-C11B	124.87
C10A-C11A-C12A	112.49	C10B-C11B-C12B	113.06
C11A-C12A-C13A	112.46	C11B-C12B-C13B	113.07
C12A-C13A-C14A	113.43	C12B-C13B-C14B	112.95
C13A-C14A-C15A	111.89	C13B-C14B-C15B	112.94
O7A-C15A-C14A	111.99	O7B-C15B-C14B	108.81
O1A-C1A-H1A	110.00	O1B-C1B-H1B	110.00
C2A-C1A-H1A	110.00	O2B-C1B-H1B	110.00
O2A-C1A-H1A	110.00	C2B-C1B-H1B	110.00
O4A-C2A-H2A	110.00	O4B-C2B-H2B	110.00
C3A-C2A-H2A	110.00	C1B-C2B-H2B	109.00
C1A-C2A-H2A	110.00	C3B-C2B-H2B	109.00
C2A-C3A-H3A	109.00	C2B-C3B-H3B	109.00
O5A-C3A-H3A	109.00	O5B-C3B-H3B	109.00
C4A-C3A-H3A	109.00	C4B-C3B-H3B	109.00
O6A-C4A-H4A	110.00	O6B-C4B-H4B	109.00
C3A-C4A-H4A	110.00	C3B-C4B-H4B	109.00
C5A-C4A-H4A	110.00	C5B-C4B-H4B	109.00
O1A-C5A-H5A	108.00	O1B-C5B-H5B	109.00
C6A-C5A-H5A	108.00	C6B-C5B-H5B	109.00
Atoms	Angle	Atoms	Angle
C4A-C5A-H5A	108.00	C4B-C5B-H5B	109.00
O3A-C6A-H6A1	109.00	O3B-C6B-H6B1	109.00
C5A-C6A-H6A1	109.00	C5B-C6B-H6B1	109.00
C5A-C6A-H6A2	109.00	C5B-C6B-H6B2	109.00
O3A-C6A-H6A2	109.00	O3B-C6B-H6B2	109.00
H6A1-C6A-H6A2	108.00	H6B1-C6B-H6B2	108.00
C9A-C7A-H7A	116.00	C9B-C7B-H7B	117.00
O2A-C7A-H7A	116.00	O2B-C7B-H7B	117.00
C8A-C7A-H7A	116.00	C8B-C7B-H7B	117.00
C8A-C9A-H9A2	118.00	C8B-C9B-H9B2	118.00
C8A-C9A-H9A1	118.00	C8B-C9B-H9B1	118.00
H9A1-C9A-H9A2	115.00	H9B1-C9B-H9B2	115.00
C7A-C9A-H9A2	118.00	C7B-C9B-H9B2	118.00
C7A-C9A-H9A1	118.00	C7B-C9B-H9B1	118.00
C11A-C10A-H10A1	117.00	C11B-C10B-H10B1	118.00
C8A-C10A-H10A1	117.00	C8B-C10B-H10B1	118.00
C12A-C11A-H11A1	109.00	C12B-C11B-H11B1	109.00

Supplementary Information

C10A-C11A-H11A2	109.00	C10B-C11B-H11B2	109.00
H11A1-C11A-H11A2	108.00	H11B1-C11B-H11B2	108.00
C10A-C11A-H11A1	109.00	C10B-C11B-H11B1	109.00
C12A-C11A-H11A2	109.00	C12B-C11B-H11B2	109.00
C13A-C12A-H12A2	109.00	C13B-C12B-H12B2	109.00
H12A1-C12A-H12A2	108.00	H12B1-C12B-H12B2	108.00
C13A-C12A-H12A1	109.00	C13B-C12B-H12B1	109.00
C11A-C12A-H12A1	109.00	C11B-C12B-H12B1	109.00
C11A-C12A-H12A2	109.00	C11B-C12B-H12B2	109.00
H13A1-C13A-H13A2	108.00	H13B1-C13B-H13B2	108.00
C12A-C13A-H13A1	109.00	C12B-C13B-H13B1	109.00
C14A-C13A-H13A1	109.00	C14B-C13B-H13B1	109.00
C14A-C13A-H13A2	109.00	C14B-C13B-H13B2	109.00
C12A-C13A-H13A2	109.00	C12B-C13B-H13B2	109.00
C15A-C14A-H14A1	109.00	C15B-C14B-H14B1	109.00
C13A-C14A-H14A2	109.00	C13B-C14B-H14B2	109.00
H14A1-C14A-H14A2	108.00	H14B1-C14B-H14B2	108.00
C13A-C14A-H14A1	109.00	C13B-C14B-H14B1	109.00
C15A-C14A-H14A2	109.00	C15B-C14B-H14B2	109.00
C14A-C15A-H15A1	109.00	C14B-C15B-H15B1	110.00
H15A1-C15A-H15A2	108.00	H15B1-C15B-H15B2	108.00
C14A-C15A-H15A1	109.00	C14B-C15B-H15B1	110.00
O7A-C15A-H15A1	109.00	O7B-C15B-H15B1	110.00
O7A-C15A-H15A2	109.00	O7B-C15B-H15B2	110.00

Table S4: Torsion angles for compound **KK1** (Å)

Atoms	Angle	Atoms	Angle
C5A-O1A-C1A-O2A	-179.87	C5B-O1B-C1B-O2B	178.85
C5A-O1A-C1A-C2A	-61.73	C5B-O1B-C1B-C2B	-63.51
C1A-O1A-C5A-C4A	63.19	C1B-O1B-C5B-C4B	63.67
C1A-O1A-C5A-C6A	-171.92	C1B-O1B-C5B-C6B	-172.64
C7A-O2A-C1A-O1A	-83.90	C7B-O2B-C1B-O1B	-71.72
C7A-O2A-C1A-C2A	156.31	C7B-O2B-C1B-C2B	169.00
C1A-O2A-C7A-C8A	-151.07	C1B-O2B-C7B-C8B	-142.69
C1A-O2A-C7A-C9A	-83.27	C1B-O2B-C7B-C9B	-74.98
O1A-C1A-C2A-C3A	55.71	O1B-C1B-C2B-C3B	56.11
O1A-C1A-C2A-O4A	174.88	O1B-C1B-C2B-O4B	176.34
O2A-C1A-C2A-O4A	-67.48	O2B-C1B-C2B-O4B	-66.38
O2A-C1A-C2A-C3A	173.36	O2B-C1B-C2B-C3B	173.39
C1A-C2A-C3A-C4A	-53.75	C1B-C2B-C3B-C4B	-51.82
O4A-C2A-C3A-O5A	64.58	O4B-C2B-C3B-O5B	66.78
O4A-C2A-C3A-C4A	-174.06	O4B-C2B-C3B-C4B	-171.39
C1A-C2A-C3A-O5A	-175.11	C1B-C2B-C3B-O5B	-173.66
O5A-C3A-C4A-C5A	177.04	O5B-C3B-C4B-C5B	173.86
C2A-C3A-C4A-O6A	176.08	C2B-C3B-C4B-O6B	172.69
C2A-C3A-C4A-C5A	55.72	C2B-C3B-C4B-C5B	53.01
O5A-C3A-C4A-O6A	-62.59	O5B-C3B-C4B-O6B	-66.45
O6A-C4A-C5A-C6A	59.17	O6B-C4B-C5B-C6B	61.08

Supplementary Information

C3A-C4A-C5A-O1A	-59.40	C3B-C4B-C5B-O1B	-57.59
O6A-C4A-C5A-O1A	-179.13	O6B-C4B-C5B-O1B	-178.71
C3A-C4A-C5A-C6A	178.91	C3B-C4B-C5B-C6B	-177.80
O1A-C5A-C6A-O3A	-58.97	O1B-C5B-C6B-O3B	-58.22
C4A-C5A-C6A-O3A	62.98	C4B-C5B-C6B-O3B	62.72
O2A-C7A-C8A-C9A	106.13	O2B-C7B-C8B-C9B	108.03
O2A-C7A-C8A-C10A	-82.43	O2B-C7B-C8B-C10B	-67.60
C9A-C7A-C8A-C10A	171.44	C9B-C7B-C8B-C10B	-175.62
O2A-C7A-C9A-C8A	-108.99	O2B-C7B-C9B-C8B	-106.93
C7A-C8A-C10A-C11A	-170.39	C7B-C8B-C10B-C11B	177.14
C9A-C8A-C10A-C11A	-4.94	C9B-C8B-C10B-C11B	4.61
C10A-C8A-C9A-C7A	-171.52	C10B-C8B-C9B-C7B	175.62
C8A-C10A-C11A-C12A	120.93	C8B-C10B-C11B-C12B	125.73
C10A-C11A-C12A-C13A	170.84	C10B-C11B-C12B-C13B	175.96
C11A-C12A-C13A-C14A	-177.75	C11B-C12B-C13B-C14B	-172.67
C12A-C13A-C14A-C15A	172.73	C12B-C13B-C14B-C15B	178.63
C13A-C14A-C15A-O7A	-174.92	C13B-C14B-C15B-O7B	-179.97

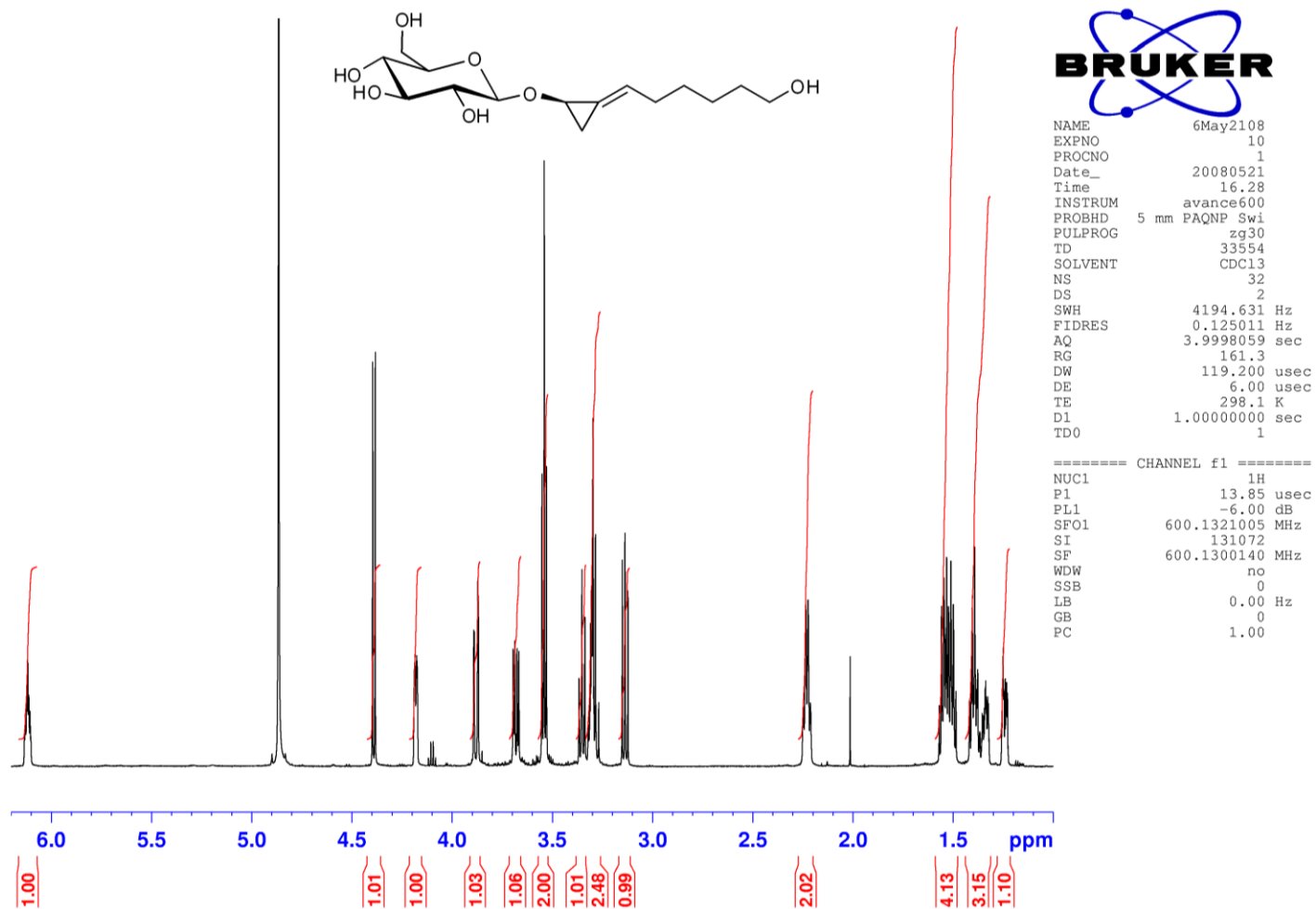
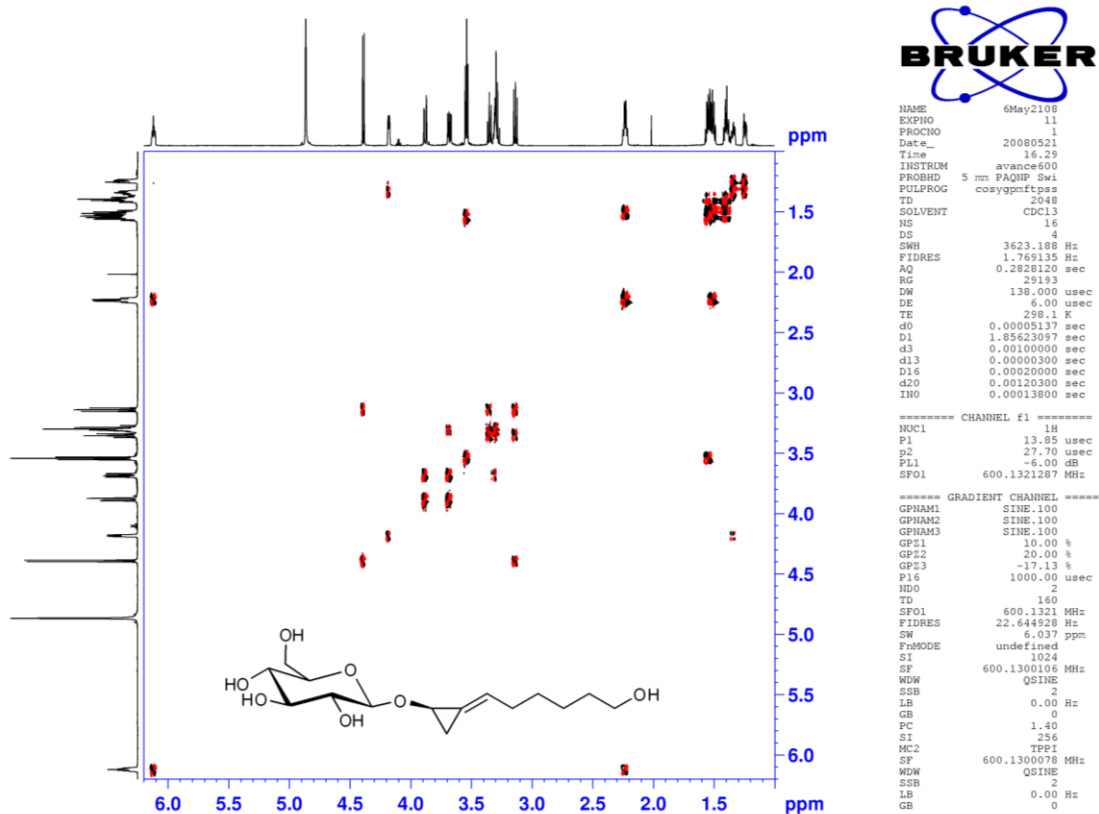
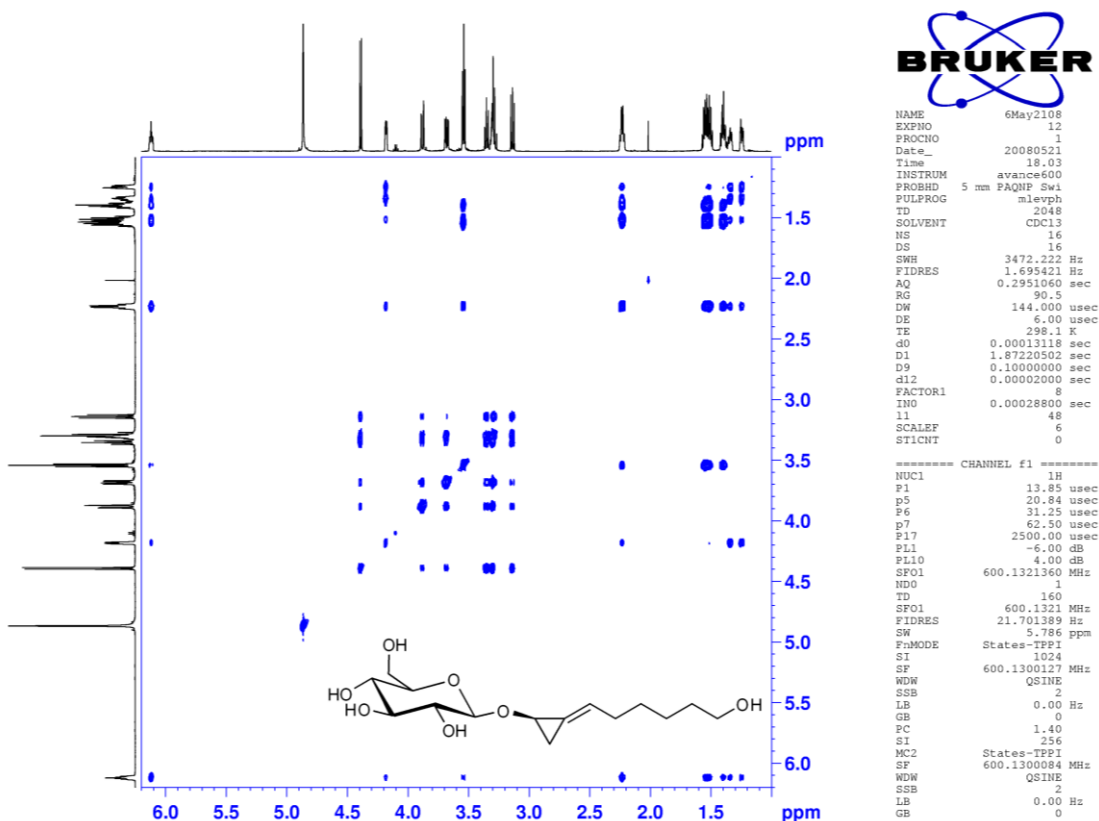
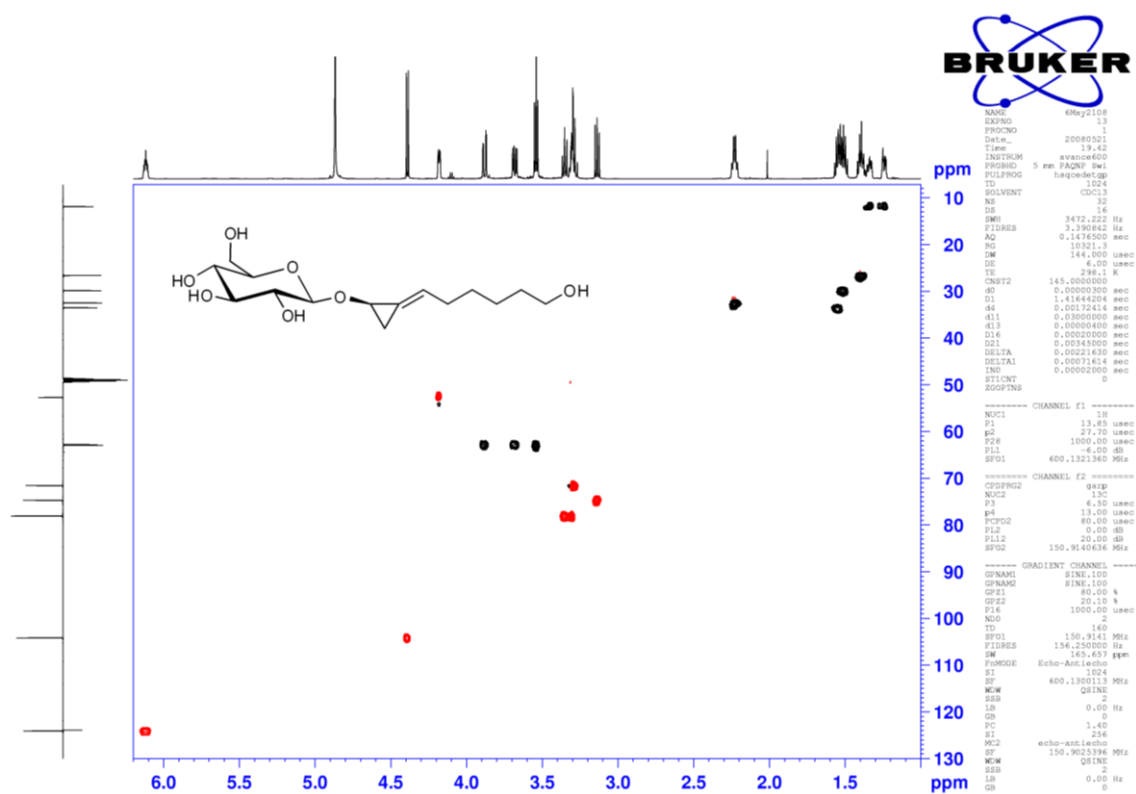
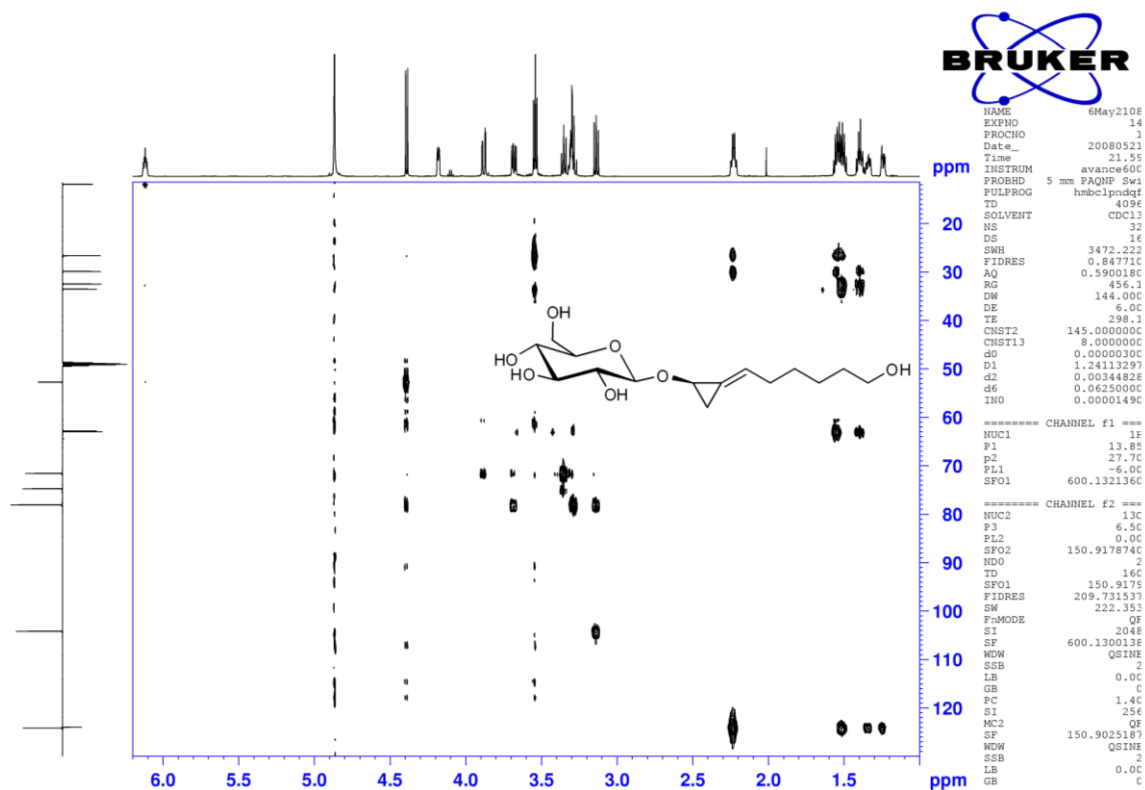


Figure S2: ^1H NMR spectrum of compound **KK1** (CD_3OD , 600.13 MHz)

Figure S4: (ge)-DQF-COSY spectrum of compound **KK1** (CD₃OD)Figure S5: TOCSY spectrum (100 ms MLEV-17 spinlock) of compound **KK1** (CD₃OD)

Figure S6: (ge)-HSQC spectrum (multiplicity edited) of compound **KK1** (CD₃OD)Figure S7: (ge)-HMBC spectrum of compound **KK1** (CD₃OD)

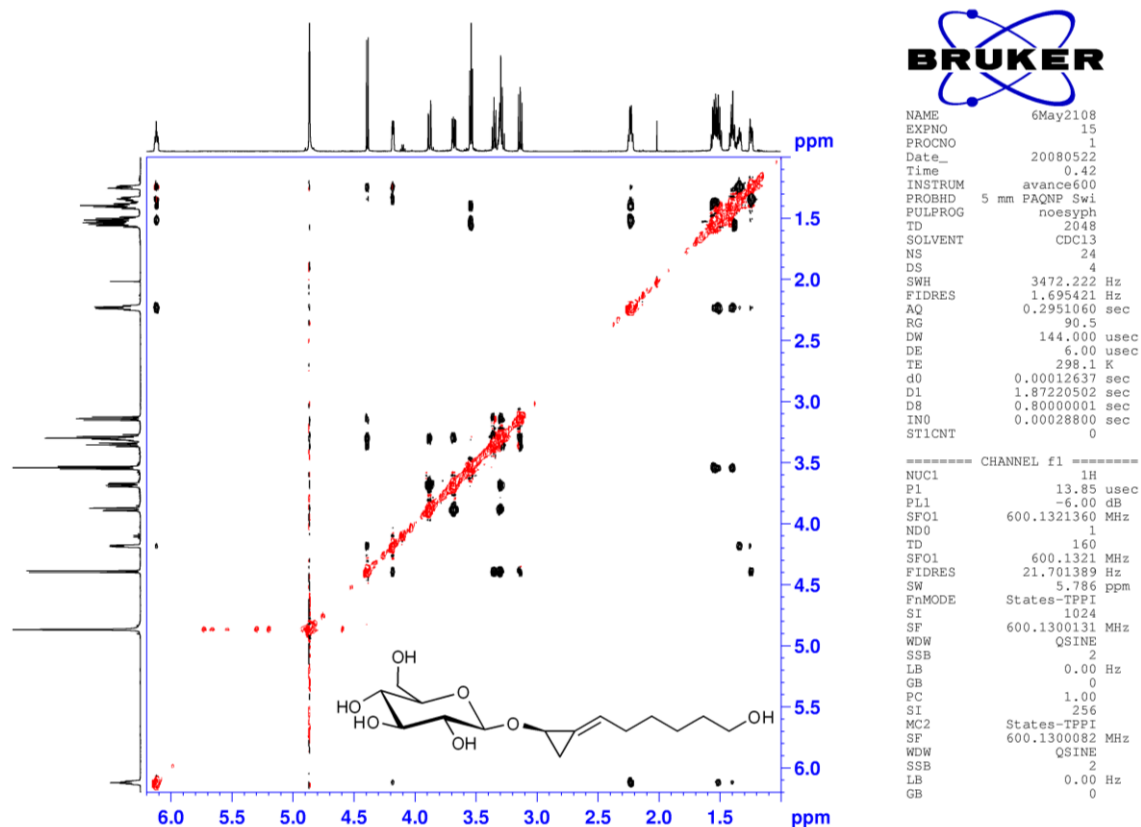


Figure S8: NOESY spectrum (800 ms mixing time) of compound **KK1** (CD_3OD)

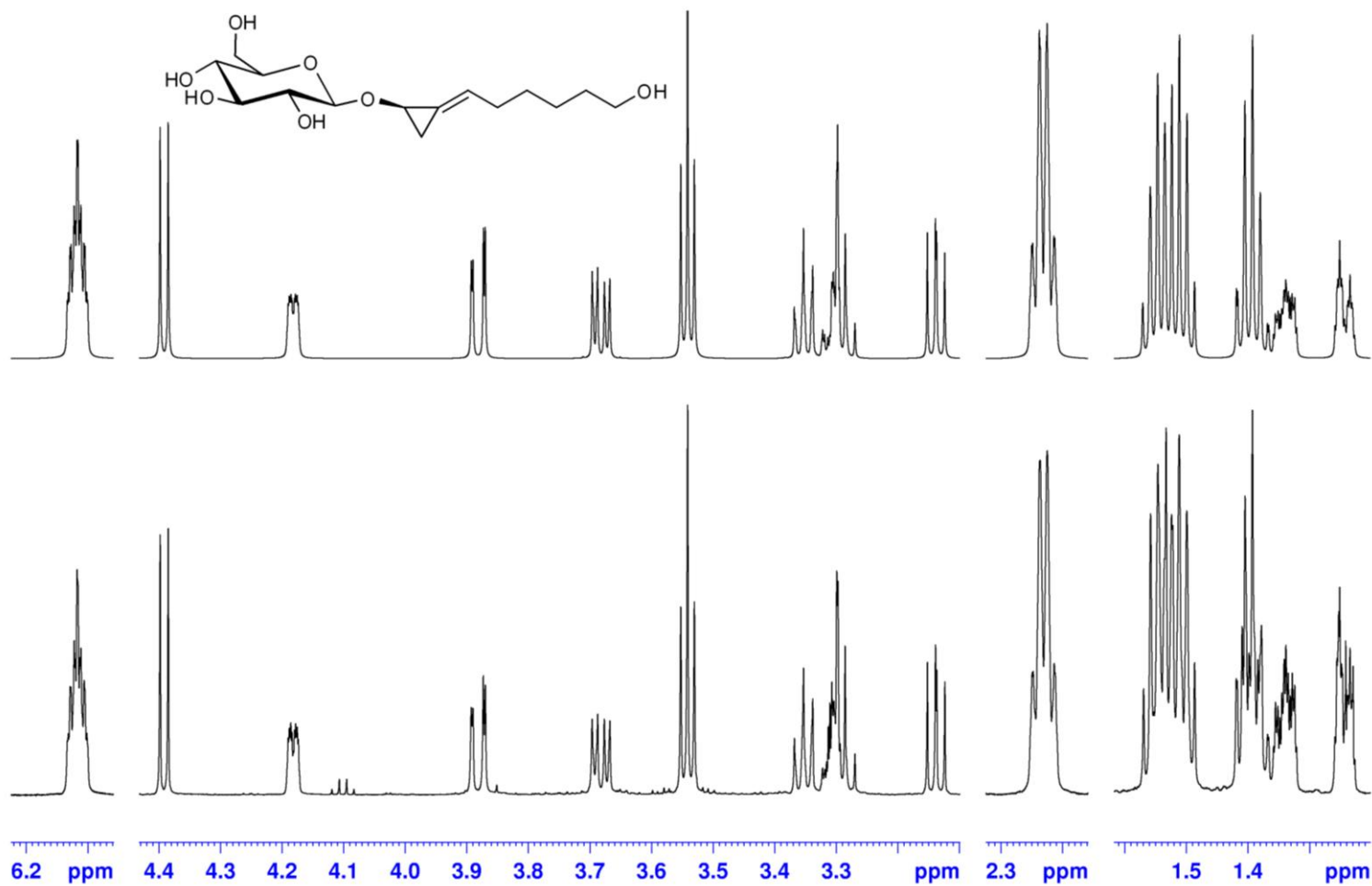


Figure S9: Experimental (lower trace) and calculated (upper trace) ^1H NMR spectra of compound **KK1**

KK5: (6E)-6[(2R)-2-(β-D-glucopyranosyloxy)cyclopropylidene]hexanoicacid
 (all NMR spectra show as impurity the plasticizer Di(2-ethylhexyl)-phthalate)

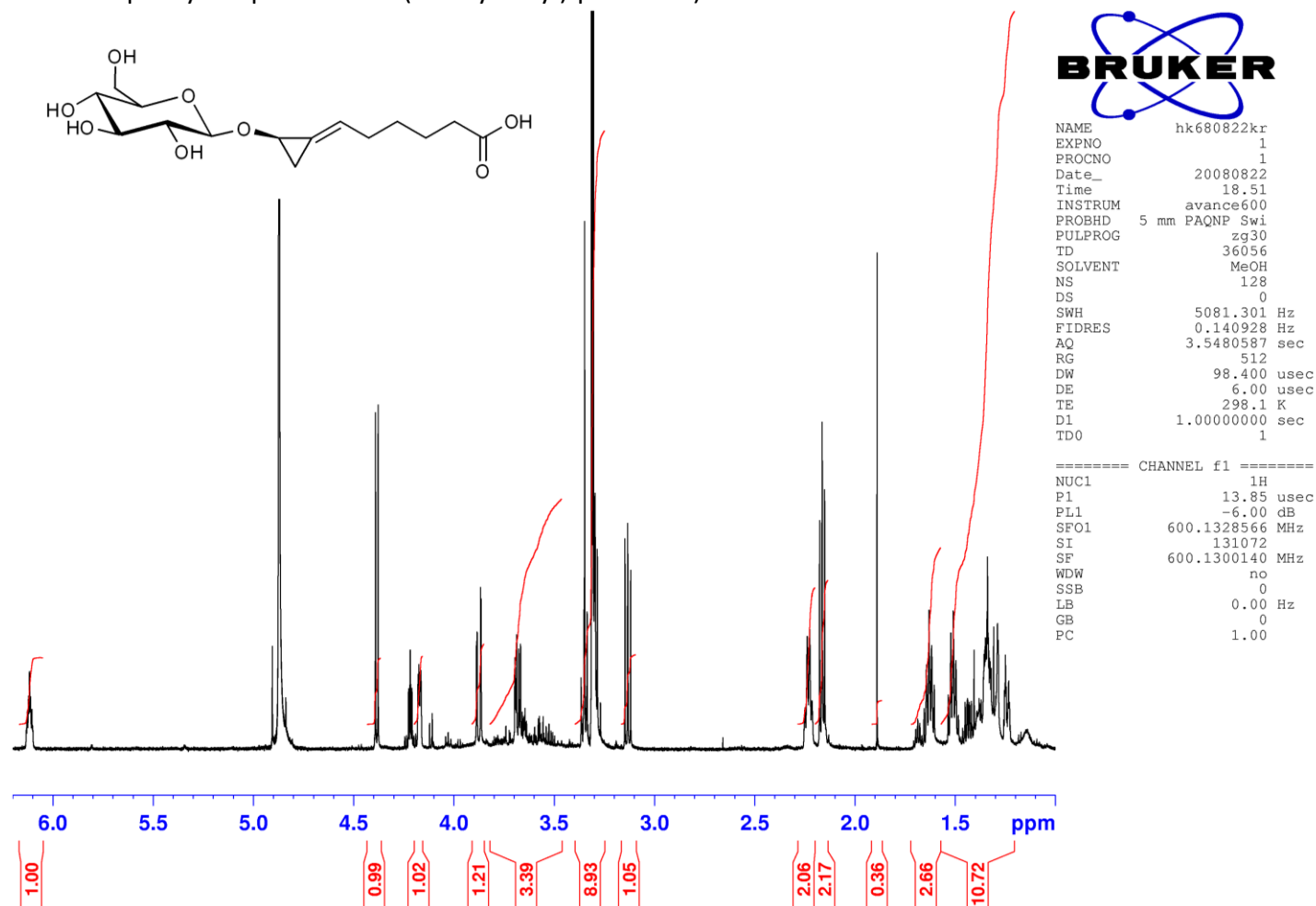


Figure S10: ^1H NMR spectrum of compound **KK5** (CD_3OD , 600.13 MHz)

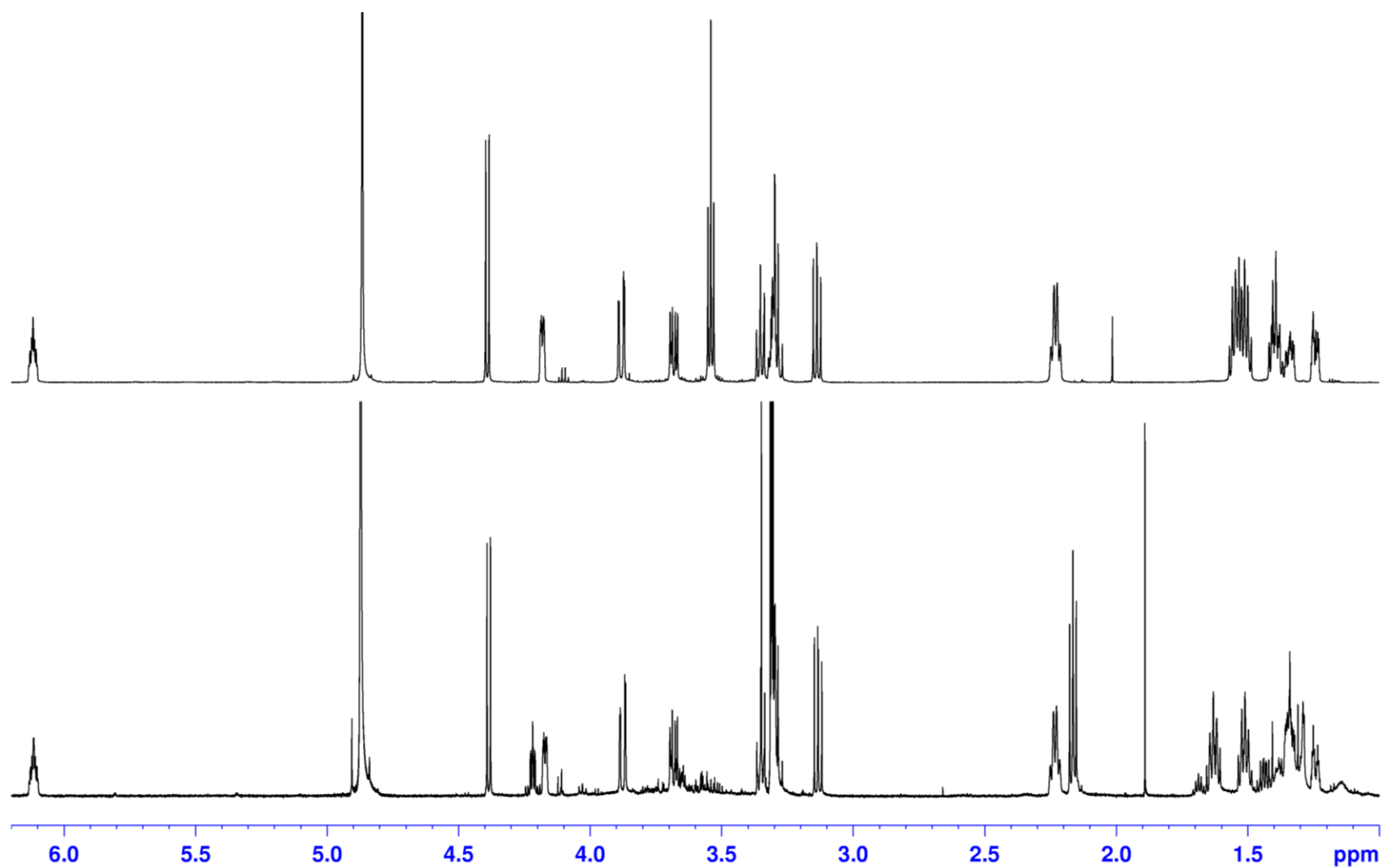


Figure S11: Overlay ^1H NMR spectra of compounds **KK1** (upper trace) and **KK5** (lower trace)

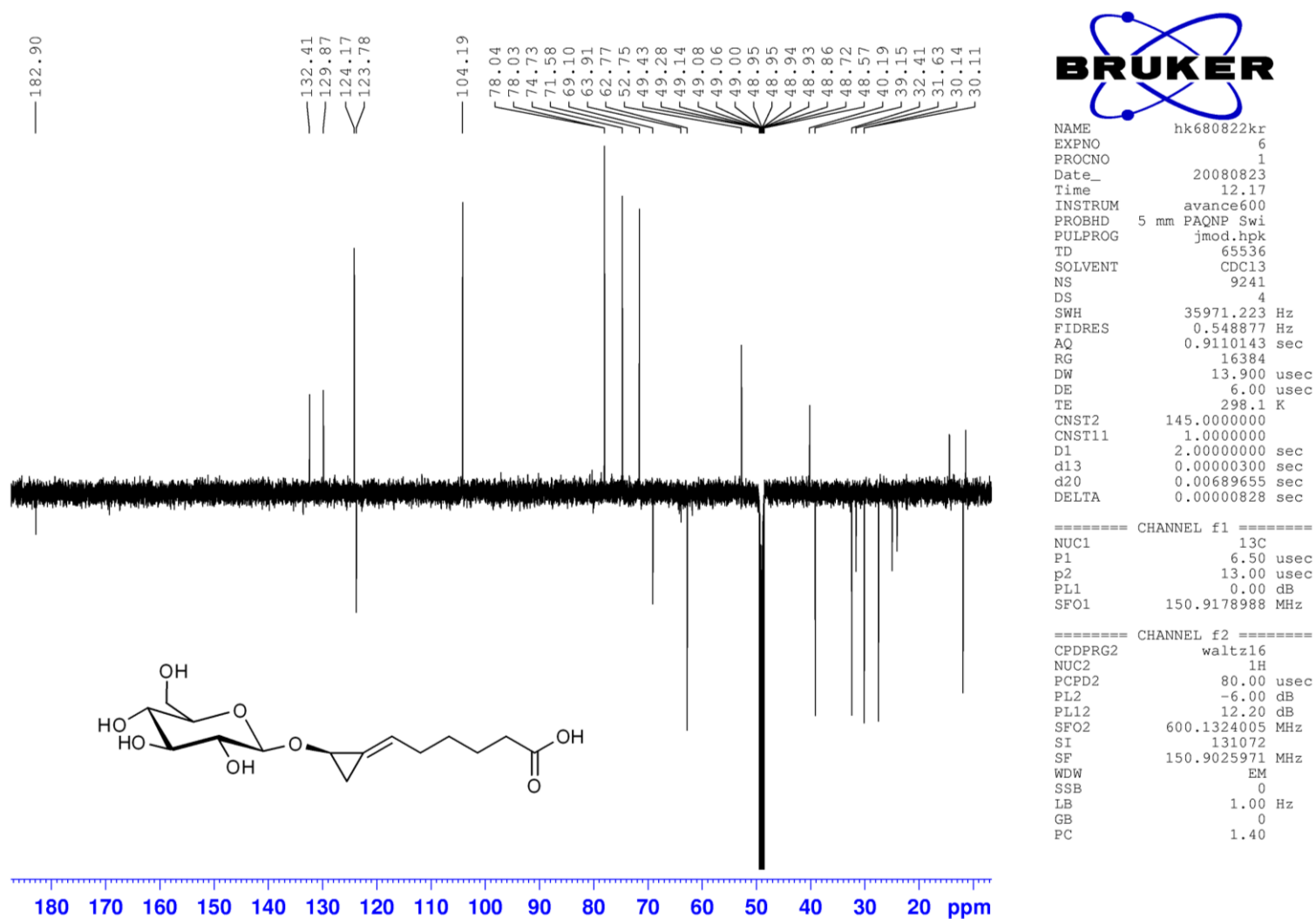
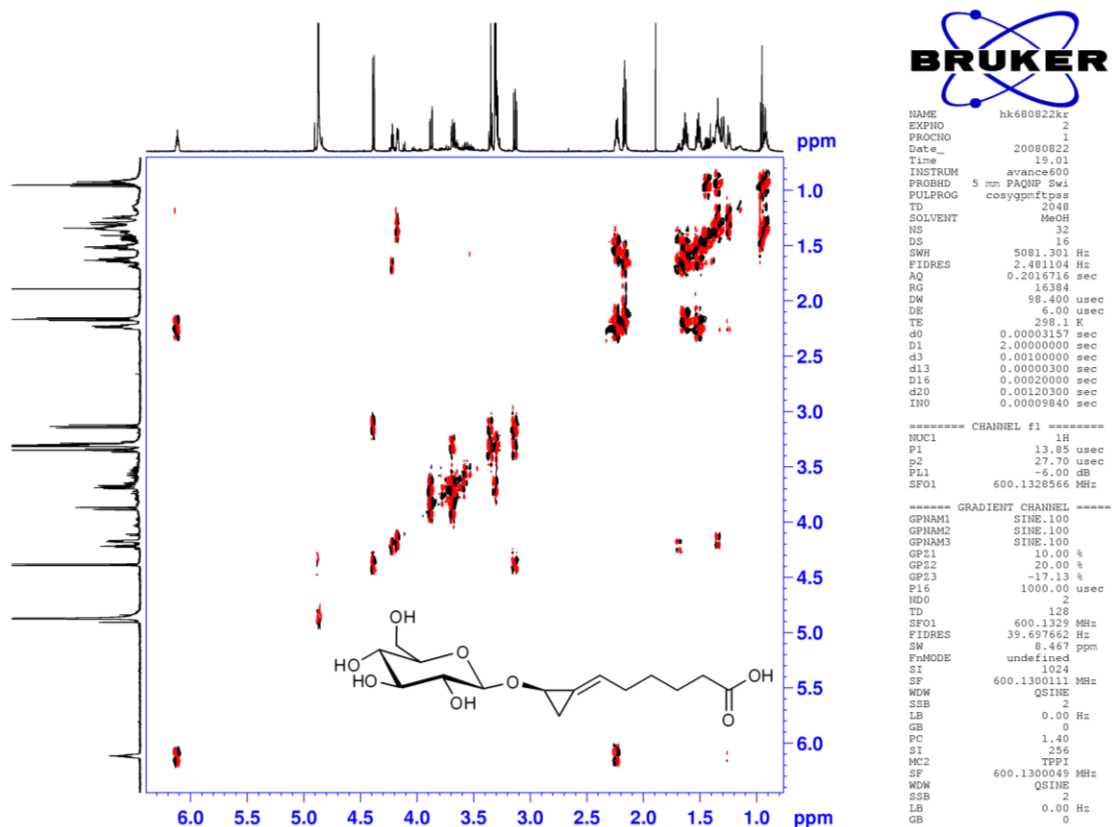
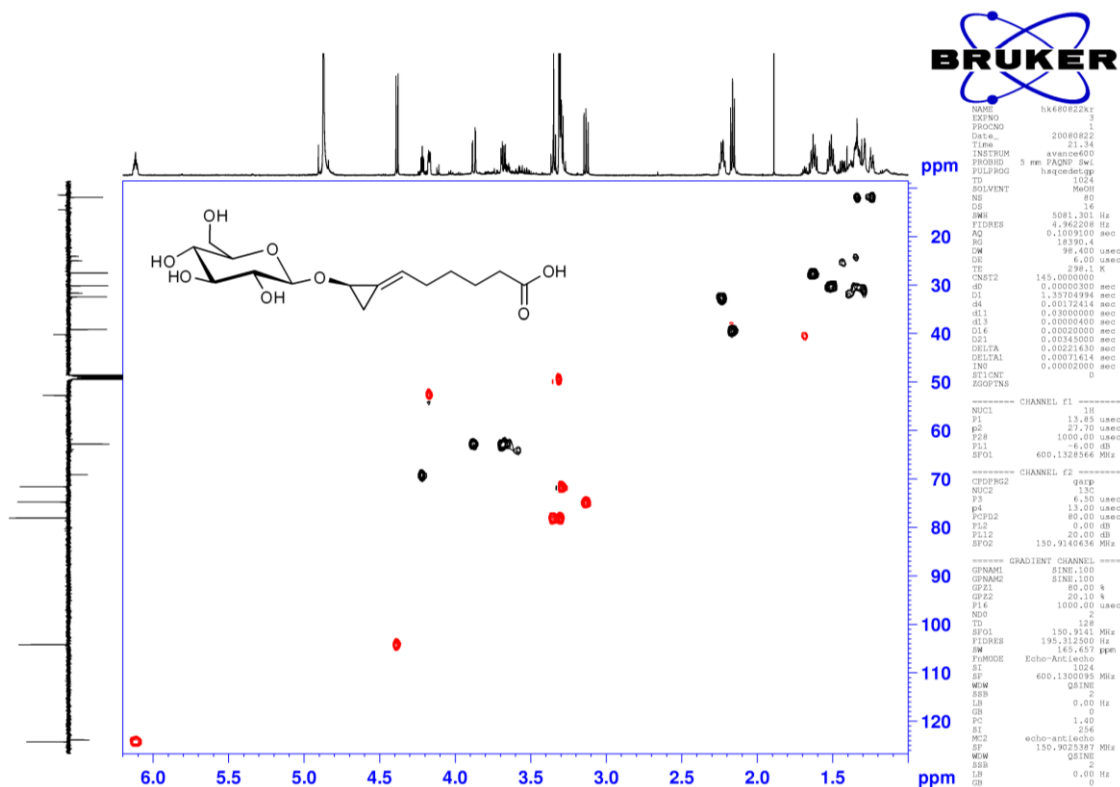
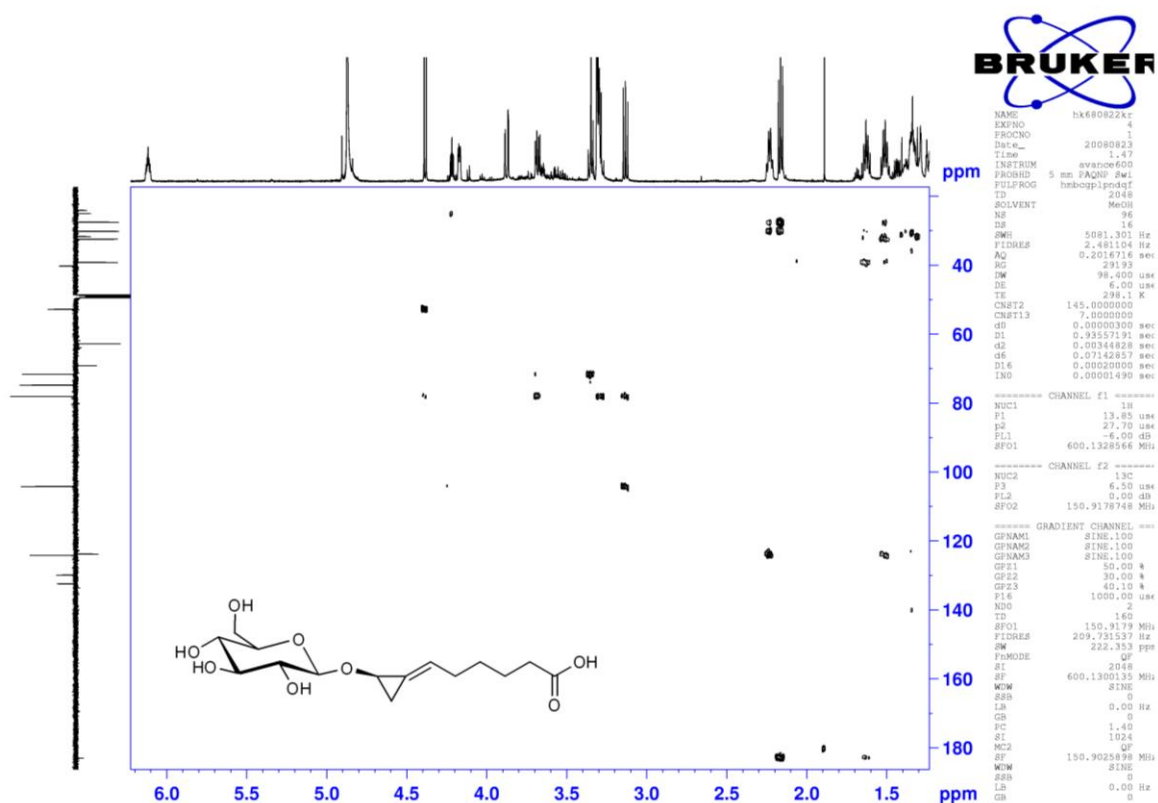
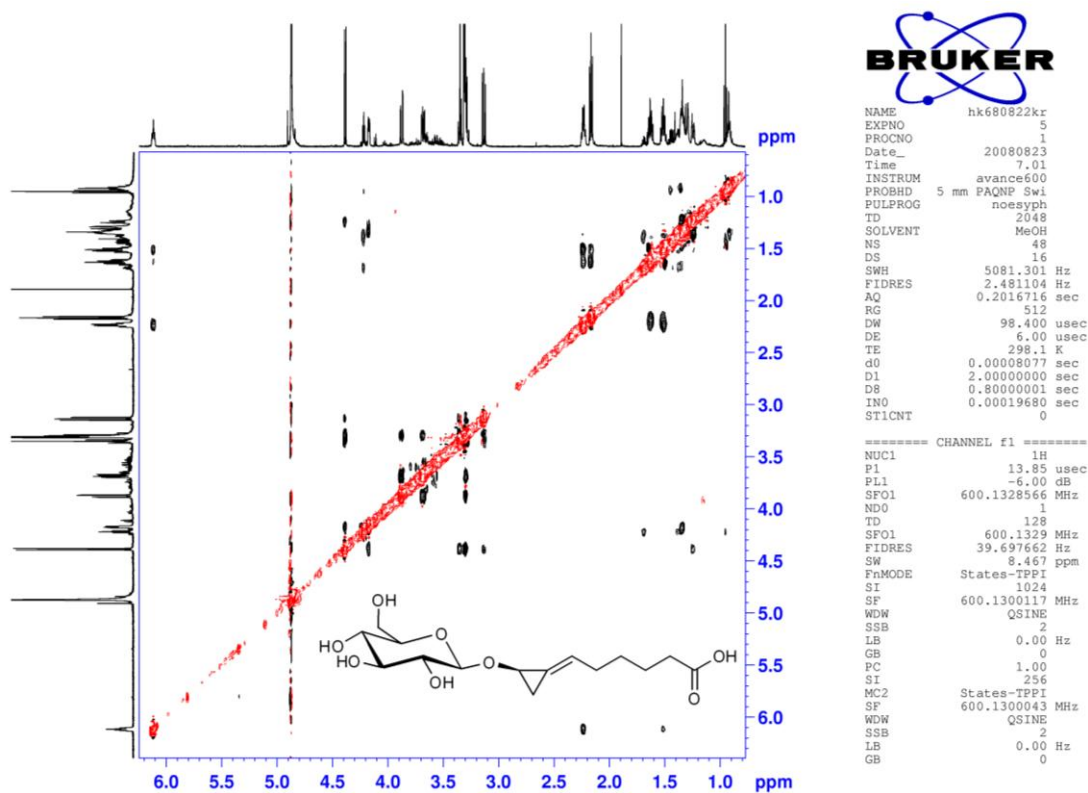
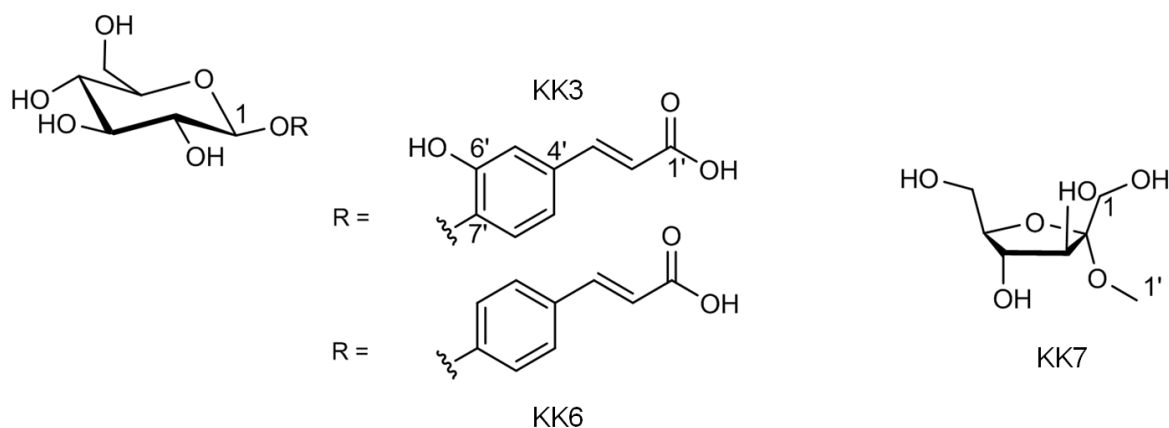


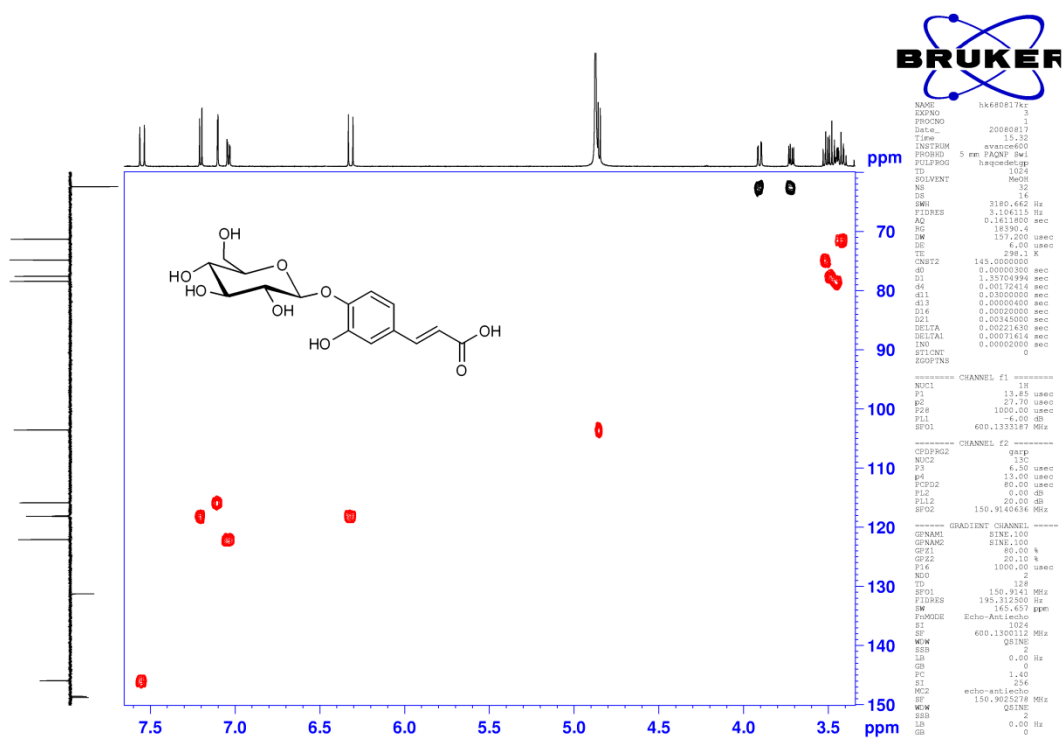
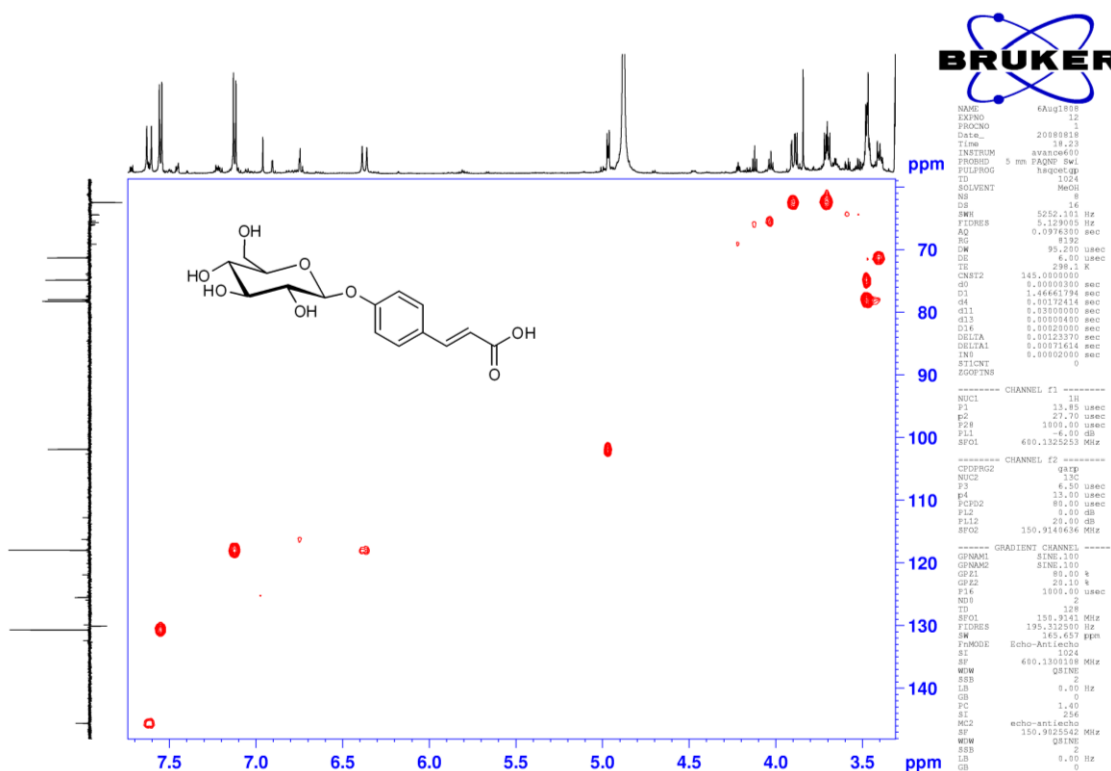
Figure S12: ¹³C NMR spectrum (ATP) of compound **KK5** (CD₃OD, 150.92 MHz)

Figure S13: (ge)-DQF-COSY spectrum of compound KK5 (CD₃OD)Figure S14: (ge)-HSQC spectrum (multiplicity edited) of compound KK5 (CD₃OD)

Figure S15: (ge)-HMBC spectrum of compound KK5 (CD₃OD)Figure S16: NOESY spectrum (800 ms mixing time) of compound KK5 (CD₃OD)

**Figure S17:** Structures of of compounds **KK3**, **KK6** and **KK7****KK3:** 4-O-β-D-glucopyranosyl-caffeic-acid**KK6:** 4-O-β-D-glucopyranosyl-p-trans-coumaric-acid**KK7:** methyl-α-fructofuranoside**Table S5:** ^1H NMR (600.13 MHz) and ^{13}C NMR (150.92 MHz) Data of **KK3** and **KK6** in CD_3OD , **KK7** in CD_3OD : $\text{CDCl}_3 = 1 : 1$ (δ in ppm; in parenthesis coupling constants in Hz)

	KK3		KK 6		KK7	
	δ_{H}	δ_{C}	δ_{H}	δ_{C}	δ_{H}	δ_{C}
1	4.853 d (7.5)	103.55	4.968 d (7.6)	101.86	3.718 d (12.1) 3.651 d (12.1)	60.04
2	3.516 dd (7.5, 9.2)	74.80	3.472 m	74.83		108.61
3	3.480 dd (9.2, 8.5)	77.55	3.472 m	77.94	4.024 d (4.0)	81.62
4	3.413 dd (8.5, 9.7)	71.28	3.400 m	71.30	3.939 dd (5.9, 4.0)	77.93
5	3.452 ddd (9.7, 2.2, 5.4)	78.41	3.472 m	78.23	3.879 ddd (5.9, 4.0, 2.9)	84.21
6a	3.906 dd (12.1, 2.2)	62.40	3.900 dd (12.1, 2.2)	62.45	3.768 dd (12.1, 2.9)	61.84
6b	3.720 dd (12.1, 5.4)		3.705 dd (12.1, 5.7)		3.641 dd (12.1, 4.0)	
1'		170.79		170.90	3.300 s	48.90
2'	6.319 d (15.9)	118.08	6.374 d (16.0)	117.96		
3'	7.549 d (15.9)	145.91	7.616 d (16.0)	145.58		
4'		131.25		130.07		
5'	7.103 d (2.1)	115.84	7.550 d (8.8)	130.68		
6'		148.54	7.122 d (8.8)	117.96		
7'		148.75		160.76		
8'	7.203 d (8.4)	118.14				
9'	7.039 dd (8.4, 2.1)	122.08				

Figure S18: (ge)-HSQC spectrum (multiplicity edited) of compound KK3 (CD₃OD)Figure S19: (ge)-HSQC spectrum of compound KK6 (sample not pure; CD₃OD)

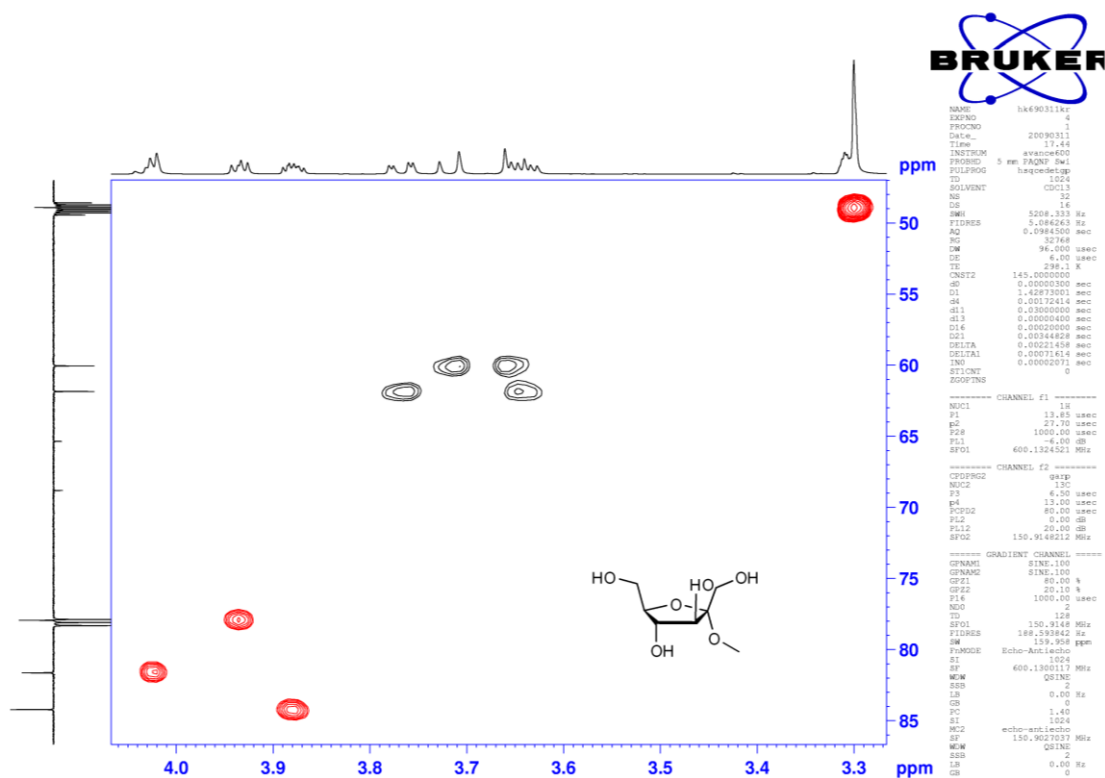
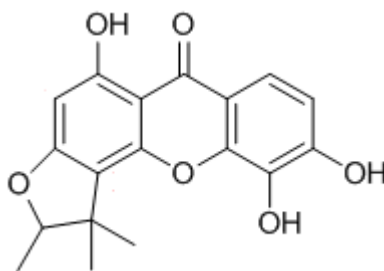


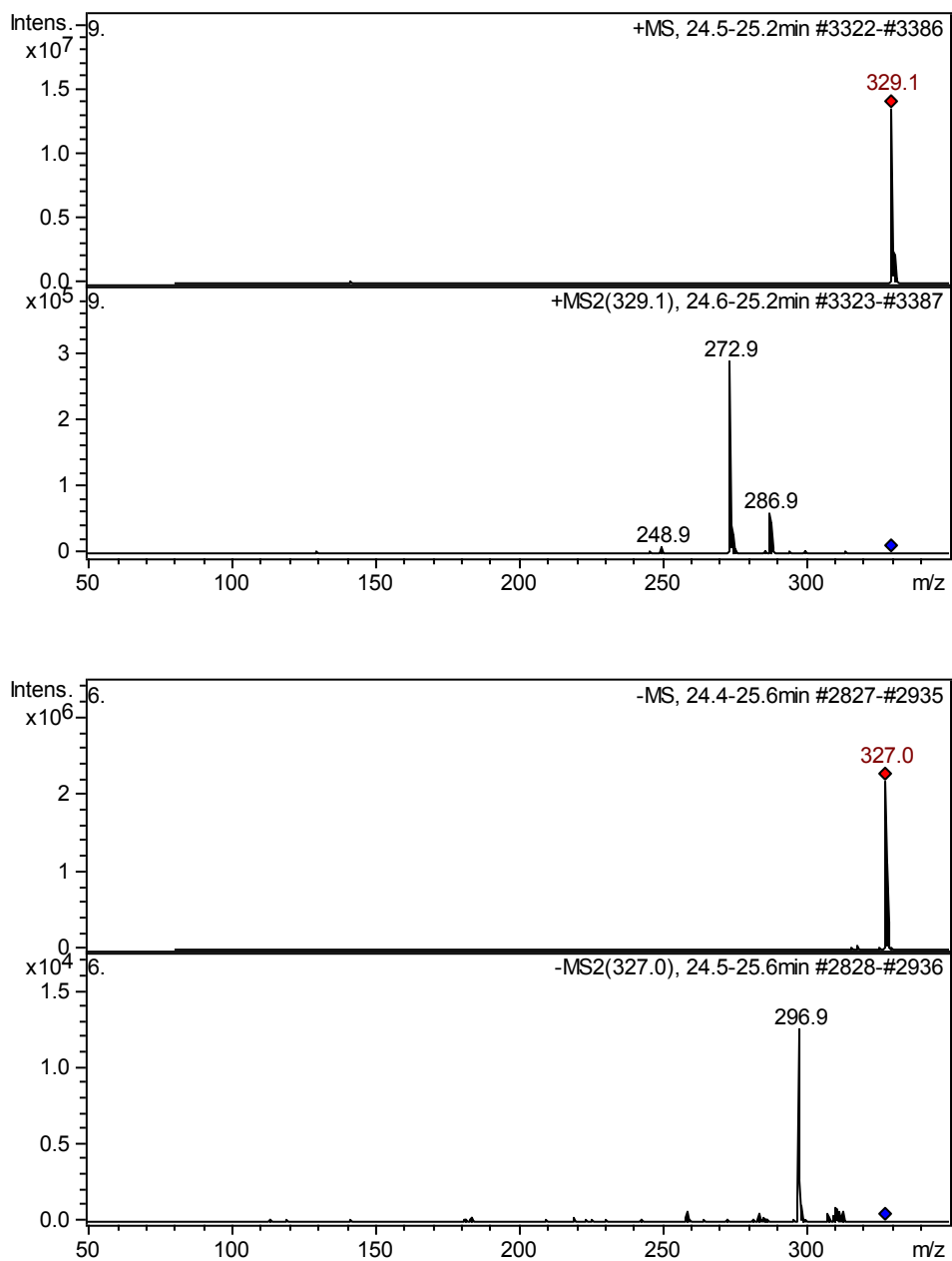
Figure S20: (ge)-HSQC spectrum (multiplicity edited) of compound **KK7** (sample not pure; CD₃OD : CDCl₃ = 1 : 1)

Structure of compound XB – 2-deprenyl-rheediaxanthone B



MS- analysis of compound **XB**:

ESIMS m/z 329.0 $[M + H]^+$; ESIMS² ($329.1 \rightarrow$) m/z 286.9 (21) $[M - C_3H_6 + H]^+$, 272.9 (100) $[M - C_4H_8 + H]^+$, 248.9 (3); ESIMS m/z 327.0 $[M - H]^-$; ESIMS² ($327.0 \rightarrow$) m/z 296.9 $[M - CH_2O - H]^-$ (100).



Multistage mass spectra (LC-ESI-IT-MSⁿ) of 2-deprenylrheedioxanthone B: (A) positive ion mode MS¹, (B) positive ion mode MS² (329.1 →), (C) negative ion mode MS¹, and (D) negative ion mode MS² (327.0 →).

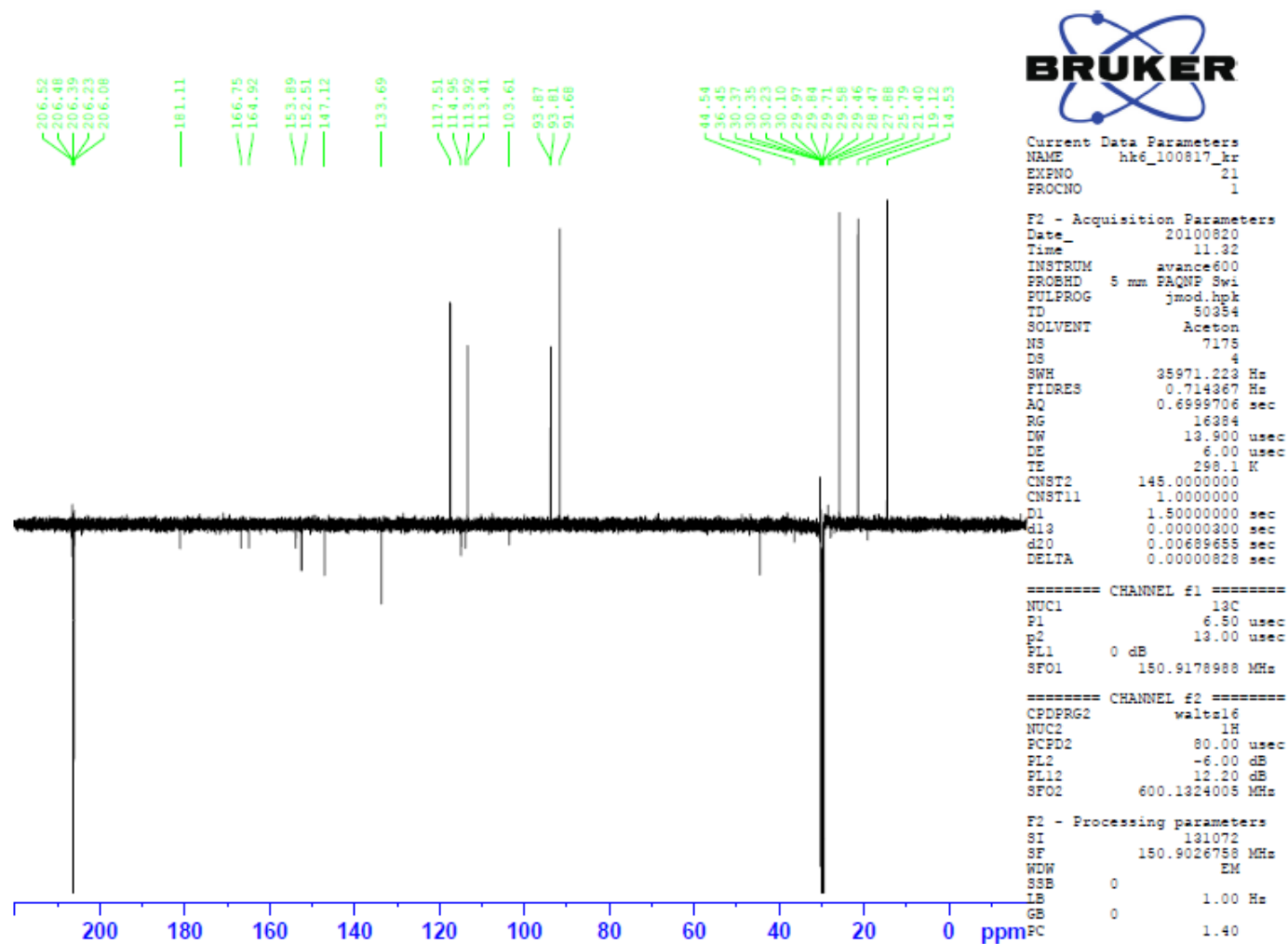


Figure S21: ^{13}C NMR spectrum (ATP) of compound **XB** (CD_3OD , 150.92 MHz)

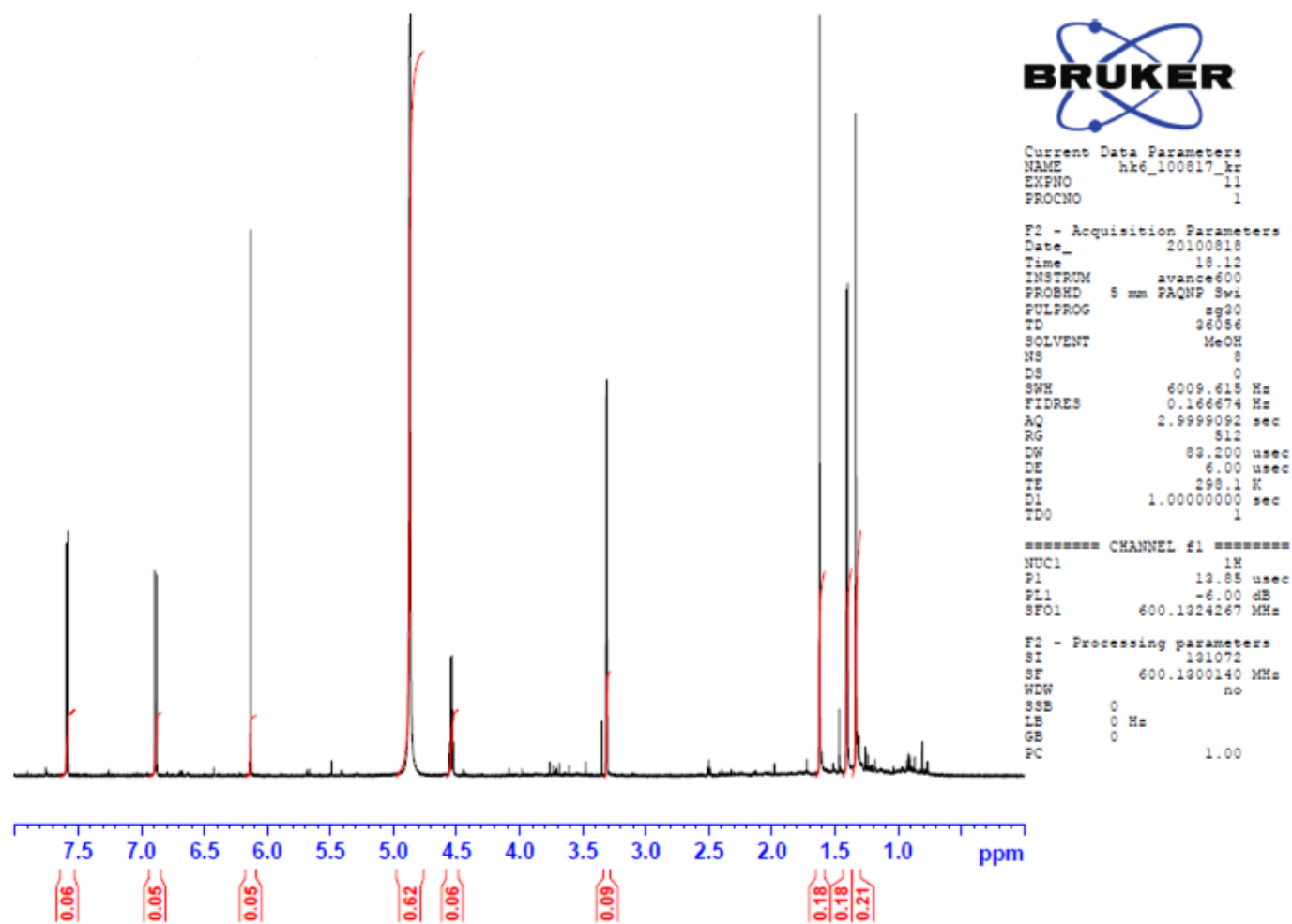
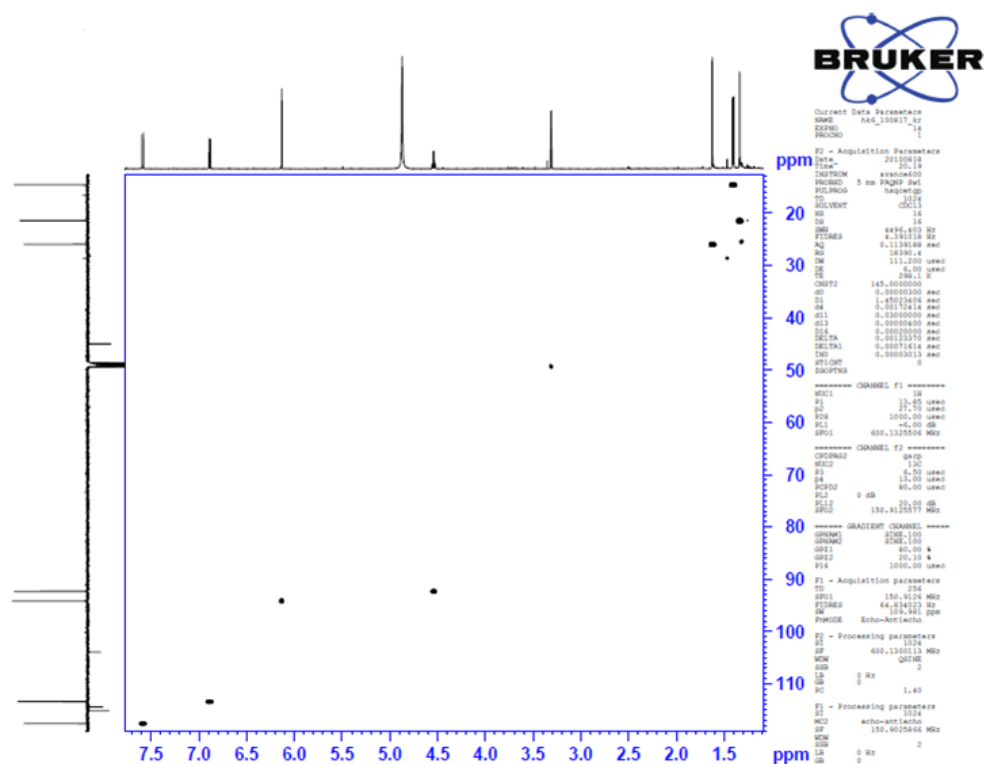
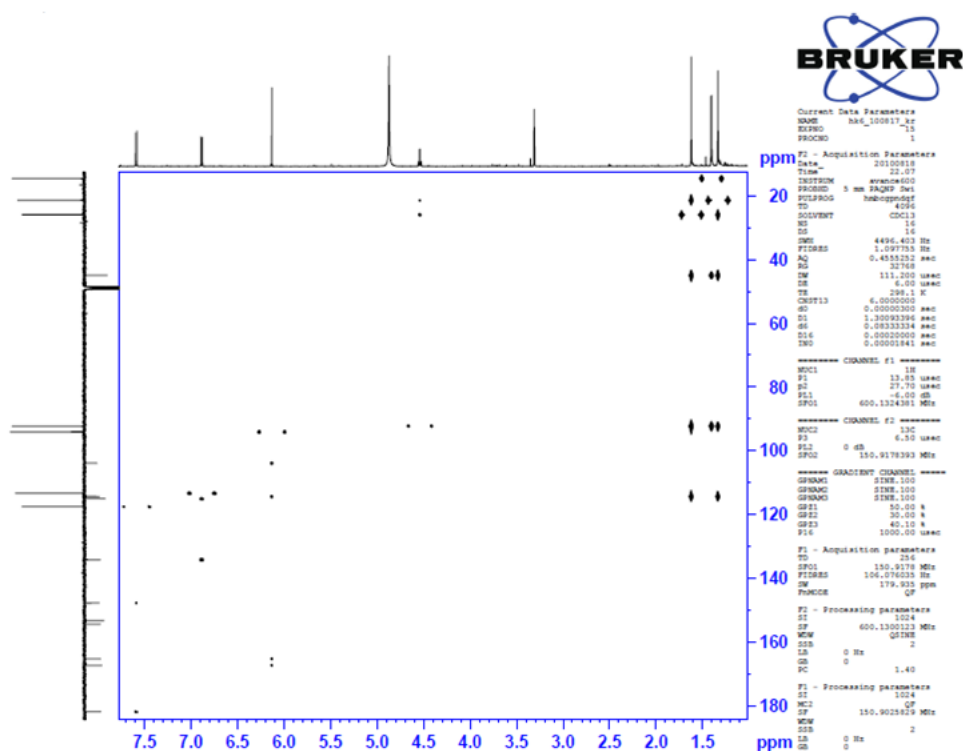


Figure S22: ^1H NMR spectrum of compound **XB** (CD_3OD , 600.13 MHz)

Figure S23: (ge)-HSQC spectrum (multiplicity edited) of compound **XB** (CD₃OD)Figure S24: (ge)-HMBC spectrum of compound **XB** (CD₃OD)

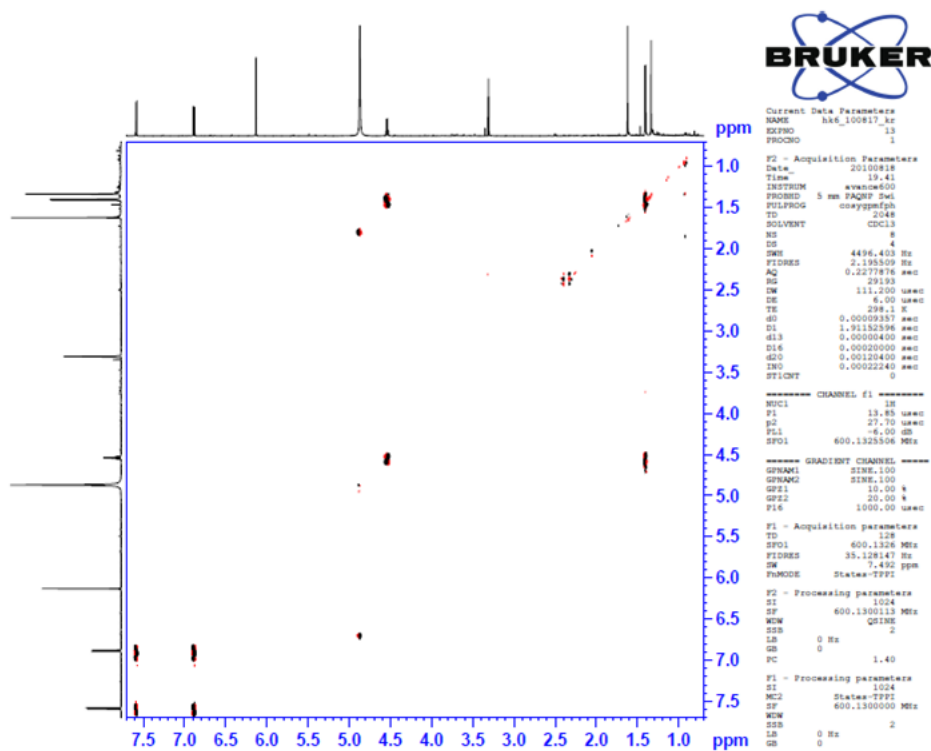


Figure S25: (ge)-DQF-COSY spectrum of compound **XB** (CD₃OD)

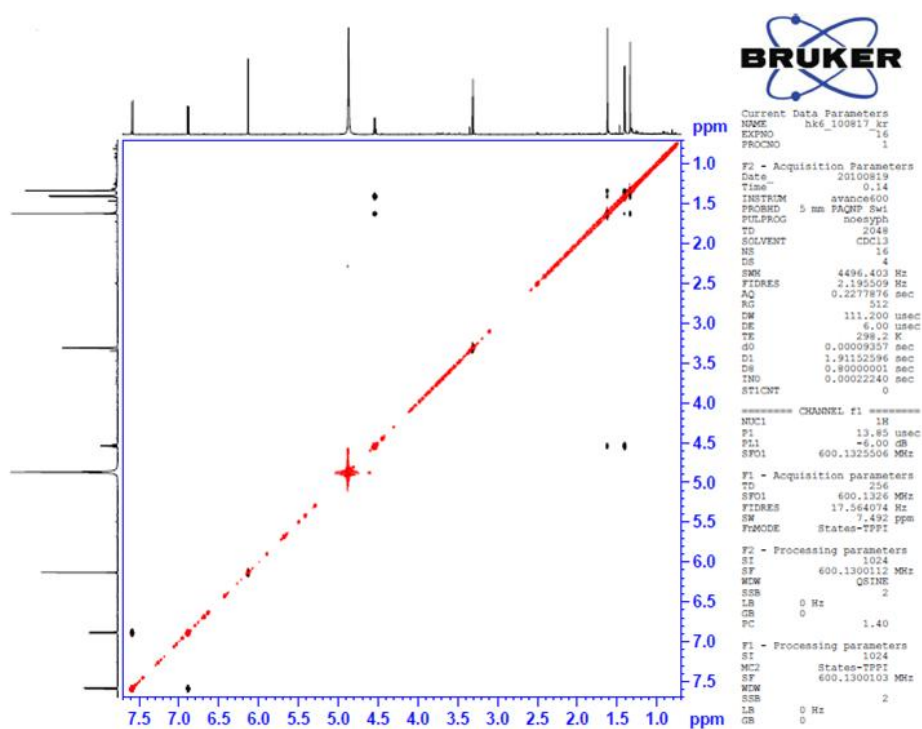


Figure S26: NOESY spectrum (800 ms mixing time) of compound **XB** (CD₃OD)

11 CURRICULUM VITAE

PERSONAL INFORMATION:

First name:	Kerstin Patricia	
Last name:	Kainz	
Title:	Mag. rer. nat.	
Date of birth:	22. 9. 1982	
E-mail address:	kerstin.kainz@univie.ac.at kerstin.kainz@gmx.at	
Address:	Thaliastr. 41 / 4 1160 Wien	Gottfried von Einem Str. 10 3874 Litschau
Nationality:	Austria	

EDUCATION AND TRAINING:

Since 2/2008	PhD student at the Department of Pharmacognosy, University of Vienna Project: „New Plant-Derived Lead Compounds against Colorectal Tumors“ in cooperation with the Institute of Cancer Research
Since 3/2007	University of Natural Resources and Applied Life Sciences, Vienna Diploma programme: Food Science und –technology Focus on Food Technology
8/2004 – 7/2005	2 semester ERASMUS in Montpellier, France Université Montpellier II – Sciences et Techniques du Languedoc Diploma programme: Sciences des Aliments
10/2001 – 11/2006	University of Vienna, Department of Nutritional Science Diploma programme: Nutritional Sciences Focus on Analytical Chemistry, Nutritional Economy and Ecology Diploma Thesis: Analysis and Evaluation of Sport Drinks
8/2000 – 8/2001	1 year au pair-girl in Galway, Ireland
9/1992 – 6/2000	Bundesgymnasium Waidhofen an der Thaya
9/1988 – 6/1992	Elementary school in Litschau

PERSONAL SKILLS AND COMPETENCES:

Tutor („Mikrobiologie und Hygiene“ – Nutritional Sciences)
Assistent („Prüfung und instrumentelle Analytik biogener Arzneimittel“ – Pharmacy)
Metabolomics Workshop in Leiden, Netherlands

SCIENTIFIC ACTIVITIES:

Poster presentations:

Kainz KP, Virtbauer J, Marian B, Kählig H, Donath O, Reznicek G, Krenn L. New compounds from *Metaxya rostrata* (Kunth C. Presl)" 57th International Congress and Annual Meeting of the Society for Medicinal Plant Research, 2009, Geneva (Switzerland)

Kainz KP, Virtbauer J, Kählig H, Krenn L. Phenolic Compounds from *Metaxya rostrata* (Kunth C. Presl). 5th PhD-Symposium, Young Scientist Association of the Medical University of Vienna, 2009, Vienna (Austria)

Kainz KP, Virtbauer J, Kählig H, Krenn L. Glycosides of phenolic acids from *Metaxya rostrata* (Kunth C. Presl). 21st Scientific Congress of the Austrian Pharmaceutical Society, 2009, Vienna (Austria)

Kainz KP, Schuster D, Krenn L. In silico guided search for anti-viral properties of a natural methylenecyclopropane glucoside. 58th International Congress and Annual Meeting of the Society for Medicinal Plant Research, 2010, Berlin (Germany)

Short lectures:

Kainz KP, Virtbauer J, Kählig H, Arion V, Donath O, Reznicek G, Huber W, Marian B, Krenn L. New compounds from *Metaxya rostrata* (Kunth C. Presl). Young Researchers' Workshop, 57th International Congress and Annual Meeting of the Society for Medicinal Plant Research, Geneva (Switzerland). *Awarded talk*.

Kainz KP, Kählig H, Zehl M, Marian B, Krenn L. Cytotoxic compounds from *Metaxya rostrata* (Kunth C. Presl). Trends in Natural Products Research: A PSE Young Scientists Meeting, Kolymyari, Crete (Greece)

Publications:

Kainz KP, Virtbauer J, Marian B, Kählig H, Donath O, Reznicek G, Krenn L. Two new unusual methylene-cyclopropane glucosides from *Metaxya rostrata*. *Helvetica Chimica Acta*, 2011, submitted.

Kainz KP, Kählig H, Huber W, Krenn L, Marian B. 2-deprenyl-rheediaxanthone B, isolated from *Metaxya rostrata*, induces mitotic catastrophe in colorectal cancer cells. *Int. Journal of Cancer*, 2011, in preparation.

Kainz KP, Zehl M, Kählig H, Bleier J, Schmidt N, Merlinger B, Pemmer T, Krenn L. Phytochemical Investigation of *Metaxya rostrata*, *Phytochemical Letters*, 2011, in preparation.

Awards:

2011: Harborne Prize Award of the Phytochemical Society of Europe at the Young Scientist meeting in Kolymyari, Crete (Greece)

2009: Awarded oral presentation at the GA Workshop Dedicated to Young Researchers. 57th International Congress and Annual Meeting of the Society for Medicinal Plant and Natural Product Research, Geneva (Switzerland)